

PARSONS

66282

NATIONAL AERONAUTICS AND SPACE ADMINISTRATION

NASA CONFERENCE ON SOME PROBLEMS RELATED TO AIRCRAFT OPERATION

A COMPILATION OF THE PAPERS PRESENTED

Langley Research Center
Langley Field, Va.

November 5-6, 1958

NASA

FACILITY FORM 602

N65-88161

(ACCESSION NUMBER)

(PAGES)

(NASA CR OR TMX OR AD NUMBER)

(THRU)

(CODE)

(CATEGORY)

NASA CONFERENCE ON
SOME PROBLEMS RELATED TO AIRCRAFT OPERATION

A Compilation of the Papers Presented

Langley Research Center
Langley Field, Va.

November 5 and 6, 1958

TABLE OF CONTENTS

	Page
INTRODUCTION	vii
LIST OF CONFEREES	ix

TECHNICAL PAPERS PRESENTED

Session Chairman: Philip Donely

TAKE-OFF, APPROACH, AND LANDING CHARACTERISTICS

1. Factors Which Influence Landing Approach Speeds . . . by Fred J. Drinkwater III, Maurice D. White, and George E. Cooper	1
2. Flight Investigation of an Automatic Throttle Control in Landing Approaches . . . by Lindsay J. Lina, Robert A. Champine, and Garland J. Morris	11
3. Controllable Thrust Reverser for Flight and Landing . . . by Seth B. Anderson and George E. Cooper	19
4. A Review of Statistics of Airplane Landing Contact Conditions . . . by Norman S. Silsby	29
5. Tire-to-Surface Friction Especially Under Wet Conditions . . . by Richard H. Sawyer, Sidney A. Batterson, and Eziaslav N. Harrin	37
6. Study of Taxiing Problems Associated With Runway Roughness . . . by Benjamin Milwitzky	51
7. Flight Studies of Problems Pertinent to Low-Speed Operation of Jet Transports . . . by Jack Fischel, Stanley P. Butchart, Glenn H. Robinson, and Robert A. Tremant	61

Session Chairman: Lawrence A. Clousing

FLYING AND HANDLING QUALITIES

8. Some Possible Developments in VTOL Transport Aircraft . . . by Marion O. McKinney, Jr.	83
9. Use of Flight Simulators for Pilot-Control Problems . . . by George A. Rathert, Jr., Brent Y. Creer, and Joseph G. Douvillier, Jr.	95
10. Flying Qualities Associated With Electronic Flight Control Systems . . . by S. A. Sjoberg	107
11. A Review of Atmospheric Turbulence and Its Significance to Jet Transport Operations . . . by Roy Steiner and Martin R. Copp	119
12. Pitch-Up Problem - A Criterion and Method of Evaluation . . . by Melvin Sadoff	129
13. Some Effects of Yaw Damping on Airplane Motions and Vertical- Tail Loads in Turbulent Air . . . by Jack Funk and T. V. Cooney	143
14. Flight Studies of Problems Pertinent to High-Speed Operations of Jet Transports . . . by Stanley P. Butchart, Jack Fischel, Robert A. Tremant, and Glenn H. Robinson	151

Session Chairman: Eugene J. Manganiello

FLIGHT SAFETY

15. A Compensated Static-Pressure Tube for Fuselage-Nose Installations . . . by William Gracey and Virgil S. Ritchie	169
16. Electrostatic Hazards During High-Speed Fueling . . . by I. Irving Pinkel	179

	Page
17. Jet-Fuel Jettisoning . . . by Herman H. Lowell	187
18. Crash-Fire-Prevention System for the T-56 Turbopropeller Engine . . . by Arthur M. Busch	199
19. Jet-Transport Ditching Characteristics . . . by Lloyd J. Fisher and William C. Thompson	207
20. Aircraft Maintenance as a Possible Factor in Some Types of Flutter . . . by Dennis J. Martin	219
21. Some Aspects of Compressor and Turbine Blading Reliability . . . by Richard H. Kemp and John W. Weeton	231

Session Chairman: Floyd L. Thompson

AIRCRAFT NOISE

22. Boundary-Layer Noise at Subsonic and Supersonic Speeds . . . by Gareth H. Jordan and Norman J. McLeod	247
23. Jet-Engine-Noise Reduction . . . by Warren J. North	257
24. Noise Problems Associated With Ground Operations of Jet Aircraft . . . by Harvey H. Hubbard	269
25. The Shock-Wave Noise Problem of Supersonic Aircraft in Steady Flight . . . by Domenic J. Maglieri and Harry W. Carlson	283

Session Chairman: Floyd L. Thompson

CHARACTERISTICS OF FUTURE TYPE TRANSPORT AIRCRAFT

26. Several Methods for Reducing the Drag of Transport Configurations at High Subsonic Speeds . . . by Richard T. Whitcomb and Atwood R. Heath, Jr.	299
---	-----

27. Powerplants for Supersonic Transport Airplanes . . .	
by Arthur V. Zimmerman	311
28. Some Considerations of Supersonic and Hypersonic Airplanes	
as Commercial Transports . . . by J. Lloyd Jones and	
David H. Dennis	321

INTRODUCTION

This volume contains copies of the technical papers presented at the NASA Conference on Some Problems Related to Aircraft Operation on November 5 and 6, 1958, at the Langley Research Center. A list of the conferees, who are members of the aircraft industry and the military services, is included.

The original presentation and this record are considered supplementary to, rather than substitutes for, the Administration's system of complete and formal reports.

LIST OF CONFEREES

The following were registered at the NASA Conference on Some Problems Related to Aircraft Operation, Langley Research Center, Langley Field, Va., November 5 and 6, 1958:

ANDERSON, Seth B.	NASA - Ames Research Center
AYDELOTTE, John H.	Boeing Airplane Co.
BAILEY, Frederick J., Jr.	NASA - Langley Research Center
BASNIGHT, Thomas A.	Airline Pilots Association
BATES, George P.	NASA Headquarters
BATTERSON, Sidney A.	NASA - Langley Research Center
BAYLESS, Ralph L.	NASA Committee on Aircraft Operating Problems
BEARD, M. G.	NASA Committee on Aircraft Operating Problems
BECHTOLD, Capt. Edward J.	Airline Pilots Association
BELSLEY, Steven E.	NASA - Ames Research Center
BERANEK, Leo L.	Subcommittee on Aircraft Noise
BILDERBACK, Gene W.	Temco Aircraft Corp.
BLAKE, Charles L.	Convair
BLAKESLEE, Lt. Donald J. M.	Flight Safety, Langley AFB
BOGEMA, Bernard L.	The Martin Co.
BONNER, Lt. Col. Joseph B., USAF	Air Research and Development Command
BORGER, J. G.	Pan-American World Airways System
BRAME, Charles B.	Pratt & Whitney Aircraft Div.
BREUHAUS, W. O.	NASA Subcommittee on Aerodynamic Stability and Control
BREWER, Jack D.	NASA Headquarters
BROCKWAY, D. J.	Bureau of Aeronautics
BROWN, Jay G.	United Air Lines, Inc.
BUSCH, Arthur M.	NASA - Lewis Research Center
BUSEMANN, Dr. Adolf	NASA - Langley Research Center
BUTCHART, Stanley P.	NASA High-Speed Flight Station
BUTLER, Robert H.	Boeing Airplane Co.
CADLE, Comdr. John W., Jr.	Naval Air Station, Johnsville, Penn.
CAHILL, Jones F.	Lockheed Aircraft Corp.
CAKE, Walter J.	Pratt & Whitney Aircraft Div.
CALLAGHAN, Edmund E.	NASA - Lewis Research Center
CARLSON, Harry W.	NASA - Langley Research Center
CARLSON, Raymond	Air Research and Development Command
CARPENTER, Randall H.	Flight Safety Foundation
CASE, Lt. Warren	Aberdeen Proving Ground
CASSIDY, Col. Robert F.	U. S. Continental Army Command

CATHAWAY, Russ G.
CHAMBERLAIN, Richard K.
CHAMPINE, Robert A.
CHARAK, Mason C.
CHENEY, Harold K.
CLARKE, Alan E.
CLOUSING, Lawrence A.
COLES, Willard D.
COLLINS, Lt. Comdr. Willard C.
COOK, Woodrow L.
COONEY, T. V.
COOPER, Maj. Dowd L.
COPP, Martin R.
COULTER, S. Leighton
CROWLEY, John W.

DALLAS, Allen W.
DARBY, Robert A.
DAUBERT, Henry C.
DECKER, James L.
DESMOND, G. L.

DICKERSON, William N.
DICKINSON, Warren T.

DIEHL, Capt. W. S., USN (Ret.)

DILLARD, Maj. William N.

DISLER, Maurice R.
DOBI, Nicholas
DOLSON, Charles H.
DONELY, Philip
DRALEY, Eugene C.
DRINKWATER, Fred J. III

EBERLE, Robert B.
ENGEN, Comdr. Donald

EVERETT, Maj. Phillip E.

FEDZIUK, Henry A.
FISCHEL, Jack
FISCHER, Lee J.
FISHER, Herbert O.
FISHER, Lloyd J.
FORTNER, Marion J.
FOULDS, Bert A.

Lockheed Aircraft Corp.
General Tire and Rubber Co.
NASA - Langley Research Center
NASA Headquarters
Convair
British Joint Services Mission
NASA - Ames Research Center
NASA - Lewis Research Center
Naval Air Material Center
NASA - Ames Research Center
NASA High-Speed Flight Station
Air Research and Development Command
NASA - Langley Research Center
Civil Aeronautics Administration
NASA Headquarters

NASA Subcommittee on Flight Safety
Fairchild Aircraft

Lear, Inc.

The Martin Co.

NASA Subcommittee on Low-Speed
Aerodynamics

B. F. Goodrich Co.

NASA Committee on Aircraft Operating
Problems

NASA Committee on Aircraft, Missile,
and Spacecraft Aerodynamics
Director of Safety and Flying Safety,
Langley AFB

Civil Aeronautics Administration

Civil Aeronautics Board

Delta Air Lines, Inc.

NASA - Langley Research Center

NASA - Langley Research Center

NASA - Ames Research Center

Chance Vought Aircraft, Inc.
Naval Air Test Center, Patuxent River,
Md.

Air Research and Development Command

NASA - Langley Research Center
NASA High-Speed Flight Station
General Electric Co.

The Port of New York Authority

NASA - Langley Research Center

Department of the Army

Douglas Aircraft Co.

FRIEND, Carl F.
FROESCH, Charles

FUNK, Jack

GEORGE, Joseph J.

GLENN, Clayton Holly
GLUYAS, George
GOODIER, Arthur A.
GORANSON, R. Fabian
GOUGH, William V.
GRACEY, William
GUSTAFSON, Robert

HALL, Charles F.
HALNON, William L.

HANEY, James E.
HANSBERRY, Harvey L.
HARRIN, Eziaslav N.
HARRIS, Thomas A.
HASSELTINE, Maj. Carroll L.
HEATH, Atwood R., Jr.
HEATH, Gloria W.
HELDENFELS, Richard R.
HERNDON, Donald
HIRSCHORN, Martin
HODSON, Edward C.
HOECKSTRA, H. D.
HOOVER, Isaac H.
HORTON, Cyril F.
HUBBARD, Harvey H.

IVEY, Reese

JACOBSON, Daniel H.

JOLINE, Everett
JONES, J. Lloyd
JORDAN, Gareth H.

KARANT, Max
KELLY, Raymond D.

KEMP, Richard H.
KING, Comdr. James P.

Ryan Aeronautical Co.
NASA Committee on Aircraft Operating
Problems
NASA - Langley Research Center

NASA Subcommittee on Meteorological
Problems
Trans-Canada Air Lines
Northrop Aircraft, Inc.
Department of Commerce
NASA Headquarters
NASA - Lewis Research Center
NASA - Langley Research Center
NASA Subcommittee on Low-Speed
Aerodynamics

NASA - Ames Research Center
NASA Subcommittee on Meteorological
Problems
Northrop Aircraft, Inc.
National Fire Protection Association
NASA - Langley Research Center
NASA - Langley Research Center
Air Weather Service, Scott AFB
NASA - Langley Research Center
Flight Safety Foundation
NASA - Langley Research Center
Civil Aeronautics Board
International Aerocoustics Corp.
Civil Aeronautics Board
Department of Commerce
Civil Aeronautics Board
Off. of Asst. Sec. of Defense
NASA - Langley Research Center

Tactical Air Command, Langley AFB

NASA Subcommittee on Low-Speed
Aerodynamics
Sperry Gyroscope Co.
NASA - Ames Research Center
NASA High-Speed Flight Station

Aircraft Owners and Pilots Association
NASA Committee on Aircraft Operating
Problems
NASA - Lewis Research Center
Navy Weather Research Facility,
Norfolk

KIRCHNER, Otto E.
KONECZNY, W. Edmund
KOVEN, William
KRENKEL, August
KRIEGER, William R.

LaFETRA, Capt. Vincent
LARRABEE, Elmer E.

LAUBMAN, Wing/Comdr. Donald
Currie
LAURENCE, James C.
LAWRENCE, Col. Rollo C., Jr.,
USAF
LEDERER, Jerome

LESLEY, Ralph
LEWIS, Lt. Col. William
LILLIENKAMP, Ralph H.
LINA, Lindsay J.
LITTLEWOOD, William

LOCKE, Frederick W. S., Jr.
LONDEAU, Wing/Comdr. Harold
Joseph, RCAF
LONGHURST, William S.
LOTHIAN, G. B.
LOVELL, P. M.
LOWE, A. W.
LOWELL, Herman H.

MADSEN, A. P.
MAGGIN, Bernard
MAGLIERI, Domenic J.
MANGANIELLO, Eugene J.
MARTIN, Dennis J.
MATTESON, Harry C.
McCRACKEN, Capt. Robert L.
McGUIRE, Terence Joseph, Jr.
McHUGH, James G.

McKINNEY, Marion O., Jr.
McMAKEN, Lt. Col. Edward, USA

MEYERHOFF, Dr. Leonard
MILLER, Chester William
MILLER, Comdr. Donald A.
MILWITZKY, Benjamin
MORRIS, Garland J.

NASA Subcommittee on Flight Safety
Civil Aeronautics Board
Bureau of Aeronautics
Republic Aviation Corp.
Department of Commerce

Flying Safety, Langley AFB
NASA Subcommittee on Aerodynamic
Stability and Control
Canadian Joint Staff, Washington, D. C.

NASA - Lewis Research Center
Directorate of Mnt.-Engineering

NASA Committee on Aircraft Operating
Problems
Republic Aviation Corp.
Directorate of Flight Safety Research
McDonnell Aircraft Corp.
NASA - Langley Research Center
NASA Committee on Aircraft Operating
Problems

Bureau of Aeronautics
Department of National Defence, Ottawa

Canadair Limited
Trans-Canada Air Lines
NASA Headquarters
McDonnell Aircraft Corp.
NASA - Lewis Research Center

Convair
NASA Headquarters
NASA - Langley Research Center
NASA - Lewis Research Center
NASA - Langley Research Center
Convair
Air Research and Development Command
Curtiss-Wright Corp.
U. S. Army Transportation Research
and Engineering Command, Fort Eustis
NASA - Langley Research Center
Office of Chief of Research and
Development
Eastern Research Group
McDonnell Aircraft Corp.
Office of Chief of Naval Operations
NASA - Langley Research Center
NASA - Langley Research Center

MORRISON, Robert A.
MYERS, Boyd C.

North American Companies
NASA Headquarters

NASH, William P.
NELSON, Lewis A.
NEWMAN, Comdr. Raymond C.
NOLAN, Donald J.
NOLLAN, John L.
NORTH, Warren J.
NUGENT, Lt. Comdr. Floyd C.

NUGENT, Lt. Col. Richard S.

Weather Bureau
Northrop Aircraft, Inc.
U. S. Naval Air Development Center
Division of General Motors Corp.
North American Aviation, Inc.
NASA - Lewis Research Center
Naval Air Test Center, Patuxent River,
Md.
Air Research and Development Command

OHLFEST, Donald
O'MALLEY, James A., Jr.

Riddle Airlines, Inc.
NASA Subcommittee on Low-Speed
Aerodynamics
Air Research and Development Command
Chief of Naval Operations, Safety Div.
Boeing Airplane Co.
U. S. Army Aviation School, Fort Rucker

OMOHUNDRO, Col. Thomas T.
ORTMAN, Comdr. Oliver
ORTON, Howard E.
OSWALT, Lt. Col. John W.

PALMER, Lt. Comdr. Melvin D.

Chief of Naval Operations, Air Warfare
Div.
U. S. Naval Research Laboratory

PAMP, Lt. Comdr. John D.
Brainard
PARKINSON, John B.
PARRACK, Dr. Horace O.
PATRILLO, Lt. Col. Leslie G., Jr.
PENNY, Maj. William W., Jr.
PENNELL, Maynard L.
PETERMAN, Capt. Don
PETERSON, Ivar C.
PIERCE, Ernest W.
PINKEL, I. Irving
PINKEL, L. C.
POLLOCK, Philip
PRESS, Harry
PRESTON, G. Merritt
PYLE, James T.

NASA - Langley Research Center
NASA Subcommittee on Aircraft Noise
Air Research and Development Command
NASA - Ames Research Center
Boeing Airplane Co.
Langley AFB
Aircraft Industries Association
Douglas Aircraft Co.
NASA - Lewis Research Center
Convair
OCAMA, Tinker AFB
NASA Headquarters
NASA - Lewis Research Center
NASA Committee on Aircraft Operating
Problems

RANKIN, Lt. Col. Warner F.
RATHERT, George A., Jr.
RHODE, Richard V.
RICE, George E.
RICHARDSON, Lt. Col. J. D., Jr.
RITCHIE, Virgil S.
ROBSON, Douglas A. L.

Directorate of Research and Development
NASA - Ames Research Center
NASA Headquarters
Aero-General Corp.
Naval Air Test Center
NASA - Langley Research Center
British Joint Services Mission

ROCHÉ, Jean A.
ROSENDAHL, Vice Adm. Charles E.,
USN (Ret.)

Air Research and Development Command
National Air Transport Coord.
Commission

SADOFF, Melvin
SAWYER, Richard H.
SCHAEFFER, Valentine H.
SCHUCK, George I.

NASA - Ames Research Center
NASA - Langley Research Center
Chance Vought Aircraft, Inc.
U. S. Army Transportation Research
and Engineering Command, Fort Eustis
Greer Hydraulics, Inc.
Capital Airlines
Federal Aviation Agency
Flight Safety, Langley AFB
NASA Subcommittee on Aerodynamic
Stability and Control

SCOTT, Edward J.
SEWALL, William R.
SHEFTTEL, David J.
SHERO, Maj. Victor K.
SHORR, Melvin

NASA - Langley Research Center
NASA - Langley Research Center
NASA - Langley Research Center
OCAMA, Tinker AFB
Curtiss-Wright Corp.
United Air Lines, Inc.
NASA - Langley Research Center
NASA Subcommittee on Aircraft Noise
Federal Aviation Agency
NASA Subcommittee on Flight Safety
McDonnell Aircraft Co.
NASA - Langley Research Center
Flight Safety, Fort Rucker
Federal Aviation Agency
AF Flight Test Center, Edwards AFB
NASA Committee on Aircraft Operating
Problems
The Port of New York Authority
Boeing Airplane Co.

SHORTAL, Joseph A.
SILSBY, Norman S.
SJOBERG, S. A.
SMITH, Lt. Col. S. R.
SOBEL, John A. III
SOMMERMEYER, Irving E.
SOULÉ, H. A.
SPANO, B. S.
STANTON, Charles I.
STAPP, Col. John P., USAF
STEELE, Fred I.
STEINER, Roy
STEWART, Capt. Thomas B.
STOCK, Clarence J.
STOLIKER, Frederick N.
STUART, Donald M.

SULLIVAN, Thomas M.
SUTTER, Joseph F.

TAYLOR, Harold
TEPLITZ, Jerome

British Joint Services Mission
NASA Subcommittee on Aerodynamic
Stability and Control
Flying Safety, Langley AFB
Civil Aeronautics Administration
NASA - Langley Research Center
NASA - Langley Research Center
NASA Subcommittee on Flight Safety
National Research Council
NASA Committee on Aircraft, Missile,
and Spacecraft Aerodynamics

THOMAS, Capt. David
THOMAS, E.
THOMPSON, Floyd L.
THOMPSON, William C.
THOREN, R. L.
THORNTON, Charles P.
TOFTOY, Maj. Gen. H. N., USA

VENNEL, Capt. Woodrow W.
VOHS, Maj. Lester J.

U. S. Coast Guard, Washington, D. C.
Federal Aviation Agency

VOLLMECKE, Albert A.

NASA Committee on Aircraft, Missile,
and Spacecraft Construction

WATTSON, Robert K.,

WEETON, John W.

WEIL, Joseph

WELLS, Col. James F.

University of Wichita

NASA - Lewis Research Center

NASA High-Speed Flight Station

U. S. Army Board for Aviation

Accident Research, Fort Rucker

NASA - Langley Research Center

NASA - Ames Research Center

Military Air Transport Service,

Scott AFB

The Port of New York Authority

North American Aviation, Inc.

U. S. Coast Guard, Washington, D. C.

Piedmont Airlines

Aviation Safety Center, Cornell

University

WHITCOMB, Richard T.

WHITE, Maurice D.

WILCOX, Col. Frank H.

WILEY, John R.

WILLIAMS, Edwin T.

WILLIAMS, Lt. Comdr. Milton B.

WOOD, James F.

WOODHAM, Ruland M.

YOUNG, H. Harold

NASA Subcommittee on Flight Safety

ZAMUDA, Joseph

ZIMMERMAN, Arthur V.

ZIMMERMAN, Glenn A.

Civil Aeronautics Board

NASA - Lewis Research Center

B. F. Goodrich Co.

FACTORS WHICH INFLUENCE LANDING APPROACH SPEEDS

By Fred J. Drinkwater III, Maurice D. White,
and George E. Cooper

Ames Research Center

INTRODUCTION

The landing of an airplane is one of the most critical phases of its operation and higher landing speeds have increased the need for practical solutions to landing problems. The National Aeronautics and Space Administration has, for some time, been conducting investigations directed toward reducing landing approach speeds, as, for example, by the use of boundary-layer control to increase the maximum lift. Flight tests have shown, however, that simply increasing the maximum lift coefficient does not assure that the approach speed will be reduced correspondingly. Consequently, a recent NASA study was undertaken to obtain a better understanding of the factors which influence the pilot's choice of an approach speed. The flight-test phase of this study consisted of landing-approach evaluations of a wide variety of airplanes.

In addition to determining the minimum comfortable approach speed of each airplane the pilots also recorded their reasons for not further reducing the speed. The purpose of this paper is to present an analysis of the factors which either influenced the pilot's choice of an approach speed or which affected the safety and precision of the landing.

RESULTS AND DISCUSSION

The first factor to be considered in an approach-speed evaluation is the type of approach which is used. The landing-approach patterns may be separated into two basic types: the tactical and the constant-angle, constant-airspeed approaches.

The tactical-approach pattern is illustrated in figure 1. It is executed in a race-track pattern, airspeed is decreased throughout the descent, and the approach-path angle is not held constant. This approach pattern gives the pilot a reference starting point over the runway and allows him to adjust the approach-path angle by varying his turn radius. Until recently most airplanes could complete this approach at idle power. It is an exacting task and pilots take pride in their ability to arrive at the end of the runway at the touchdown

speed. However, the excess airspeed often used to compensate for the difficulty in judging the approach creates additional problems.

Another type of approach is the constant-speed, constant-angle approach which is shown in figure 2. This approach pattern is used in airline operations, aircraft-carrier landings, and other situations where precision control of the landing is essential. The advantage of this approach is that the number of factors that the pilot must vary is reduced and, as a result, the approach is easier for the pilot to judge. However, it is often made at a minimum speed. Consequently, the airspeed indicator must be monitored closely to assure that the speed does not decrease to a dangerous level while flight-path-angle adjustments are made. This type of approach was used in the flight tests conducted in this investigation because it permitted more consistent evaluations of the approach speeds.

The predominant reason given for not further reducing speed was the loss of ability to control the flight-path angle. In reference 1 the major reason for limiting the approach speed is described as the deterioration in speed stability. In many of the cases studied in the NASA investigation, rapid changes in airspeed were associated with the development of unsatisfactory flight-path-angle controllability. It appears quite probable, therefore, that the pilots of both studies were describing the same type of situation.

The factors which determine the pilot's ability to control flight-path angle are indicated by the simplified equation developed in figure 3. Included in the figure is a diagram of the forces from which the equation was derived. The flight-path angle is seen to be determined by the lift-drag ratio, the thrust-weight ratio, and the rate of speed change. The equation indicates that the approach angle can be made independent of the engine if an appropriate rate-of-speed change is used. This will be recognized as the technique used in the tactical approach. At a constant speed the angle is primarily dependent on engine thrust and lift-drag ratio.

The throttle and the elevator are two controls with which the pilot can adjust the flight-path angle and airspeed. For the constant-speed, constant-angle approach the manner in which the pilot uses each control was found to be dependent on certain airplane characteristics.

For airplanes which had high lift-drag ratios the elevator was used to direct the flight-path angle and the engine power was adjusted to maintain a constant speed. With lower lift-drag ratios, of the order of 4 and below, the rate at which speed changed during maneuvers became large. The pilots then found that either they would have to maintain excess speed to allow for these speed changes or they would have to

make flight-path-angle adjustments with the throttle, with the elevator being used to maintain the desired speed.

The change in the total drag of the airplane with speed or the variation of L/D with C_L also influenced pilot technique. Figure 4 shows the L/D variation with C_L for several contemporary airplanes. In addition to the airplanes which have low lift-drag ratios there are designs for which the L/D decreases with increasing lift throughout the approach-speed range. The pilots noted that, for this latter class of airplane, increased use of thrust to change the flight-path angle was necessary. Flight in this region is commonly referred to as being on the "back side" of the drag curve and on older airplanes it occurred only at speeds very close to the stall speed. However, it includes the entire approach-speed range for many high-speed airplanes. In fact, service pilots are often not aware that they are making approaches in this condition for several types of airplanes now in operation. Although these curves represent fighter-type airplanes, those for the coming generation of transport airplanes appear to follow the same trend.

A generalized plot of drag and airspeed is shown in figure 5 which indicates the shape of the drag curve in more familiar terms. In this figure the back side is represented by the left-hand portion of the curves. The upper curve is characteristic of an airplane which has greater drag than that represented by the lower curve.

The pilots noted that flight on the back side of the drag curve was not unduly difficult. However, those pilots who relied most on engine thrust for flight-path-angle control consistently selected lower approach speeds. The increased reliance of the pilot on the throttle as a flight-path-angle control indicated that additional consideration must be given to engine response and the thrust-weight ratio available in the approach. Flight tests of fighter-type airplanes demonstrated that reductions in the margin of thrust-weight ratio to less than 0.12 represent a reason for limiting the approach speed. In figure 5 this limitation is shown as a horizontal boundary which intersects the upper drag curve.

Transport-type airplanes generally have lower thrust-weight ratios available for maneuvering than do fighter airplanes. Tests are needed to establish the effect that this thrust-margin requirement will have on transport operations.

Another adverse thrust-response condition occurs when landing a very low drag airplane. In this case very little thrust is required to maintain the approach angle and the engines are operated in the low range of rpm where the time constants for current engines are very long.

Because of the small variation of drag with airspeed which often occurs with a high lift-drag ratio and the poor engine response at low power settings, it is difficult to select the power setting which will maintain the desired glide angle. In addition, wave-off thrust may not be available for as much as 10 seconds after full power is selected. The drag-airspeed region where this tendency is noticed appears at the bottom of figure 5. The use of higher airspeed compensates for the slow engine response since the pilot can use up the excess airspeed while waiting for thrust to develop.

Jet-transport airplanes which have high lift-drag ratios in the landing configuration may be expected to have a problem due to poor engine response because of the low power which is required during the approach. One of the advantages of an inflight fully modulating type of thrust reverser is that it allows the pilot to modulate thrust at a rate which is independent of the basic engine response time. This characteristic of a thrust reverser was evaluated during landing approaches in addition to its use during high-speed flight and ground operation.

One other factor related to engine operation is the longitudinal trim changes due to changes in power. It appears that this factor in conjunction with longitudinal stability effects determines whether the effect of a thrust change appears predominantly as a speed change or flight-path-angle change. The most desirable initial response for a constant-speed approach was indicated to be that in which a thrust change produced a change in flight-path angle with no speed change at all. This produced what the pilots termed a "locked-in" feeling. Examples of undesirable thrust-produced pitching moments were also noted among the airplanes flown in this evaluation. This factor was conveniently varied on one airplane by simply placing thrust deflecting tabs in the tailpipe. However, quantitative results are yet to be obtained.

Static longitudinal stability was noted to contribute to the precision of constant-speed approaches, particularly when the airplane was operated on the back side of the drag curve. It is generally recognized that the back side of the drag curve represents a region of speed instability when longitudinal stability effects are neglected. If, however, the airplane has strong positive static stability, then the tendency of the airplane to diverge in speed after a disturbance is greatly reduced by the tendency of the airplane to return to its trim speed. Therefore, the amount of attention required of the pilot in monitoring airspeed is greatly reduced. The existence of positive static longitudinal stability appeared to be a necessary condition in order to achieve the locked-in feeling desired by the pilots. The limitations due to the lack of static longitudinal stability have not been clearly defined. It is noteworthy, however, that, while many statically unstable

airplanes have been flown and many are flown in approaches on the back side of the drag curve, there are no known instances of airplanes having been flown operationally with both of these characteristics in combination.

One other limitation to the approach speed is indicated by the vertical boundary in figure 5. If other factors did not limit the approach speed, the minimum speeds selected under ideal conditions in a constant-speed approach were 110 percent of the power-on stall speed. However, stall speeds have become more indeterminate and, therefore, this boundary is difficult to define. The stall of many airplanes that had highly swept and/or low-aspect-ratio wings tended to be characterized by a gradual onset of instability about one or more axes which contributed to the difficulty of defining the stall speed. The lack of a well-defined stall warning or the need for an unconventional technique to recover from an incipient stall often resulted in the use of higher speeds during the approach.

Further analysis of the flight data and of pilots' opinions obtained during the flight program indicates the reason "ability to control flight-path angle" requires a broader interpretation than is afforded by consideration only of the airplane's ability to change altitude. The pilot, himself, must be considered. In flying at the minimum comfortable approach speed the pilot must concentrate a great deal of his attention to the basic task of controlling altitude precisely while he must monitor airspeed closely. He must allow more speed margin to the extent that extraneous control problems divert him from this basic task. Thus, although secondary considerations, such as lateral and directional instability and control problems, may force him to approach at higher speeds, the pilot would still describe the limiting factor as ability to control flight-path angle.

There were cases where other factors which normally would be considered extraneous or secondary became of dominant importance as the reason for limiting the approach speed. For example, the reduction in forward visibility at high angles of attack and the marginal ground clearance at the tail were actually found to be limiting reasons for several of the airplanes evaluated.

The foregoing discussion has indicated the factors limiting the approach speed as determined under ideal test conditions. However, it should be recognized that under actual operating conditions additional distracting influences, such as traffic density, air turbulence, and low visibility, may force the pilot to use higher approach speeds.

CONCLUDING REMARKS

A wide variety of factors which influence the pilot's selection of an approach speed has been presented. It is apparent from this study that the low-speed handling qualities of the airplane as a whole should be considered in order to predict an approach speed. In addition, reductions in approach speed appear to be possible if the pilots adapt their control technique to the airplane characteristics.

Extensive work is continuing with both flight and ground simulator programs. Power-off landings in configurations with very low lift-drag ratio represent one of the important problems included in the program.

REFERENCE

1. Lean, D., and Eaton, R.: The Influence of Drag Characteristics on the Choice of Landing Approach Speeds. Rep. 122, AGARD, North Atlantic Treaty Organization (Paris), May 1957.

TACTICAL-APPROACH PATTERN

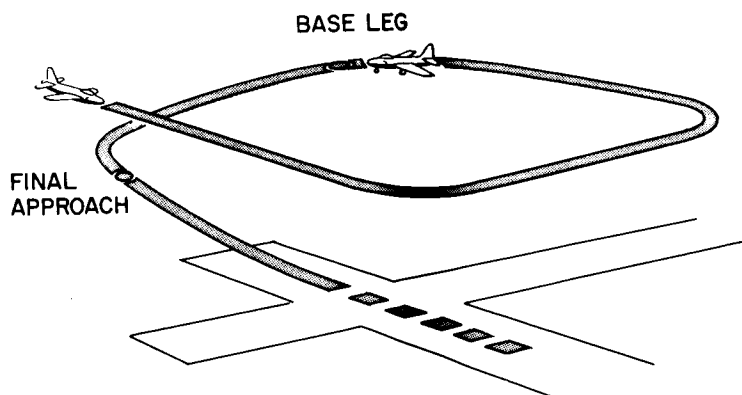


Figure 1

APPROACH WITH CONSTANT SPEED AND ANGLE

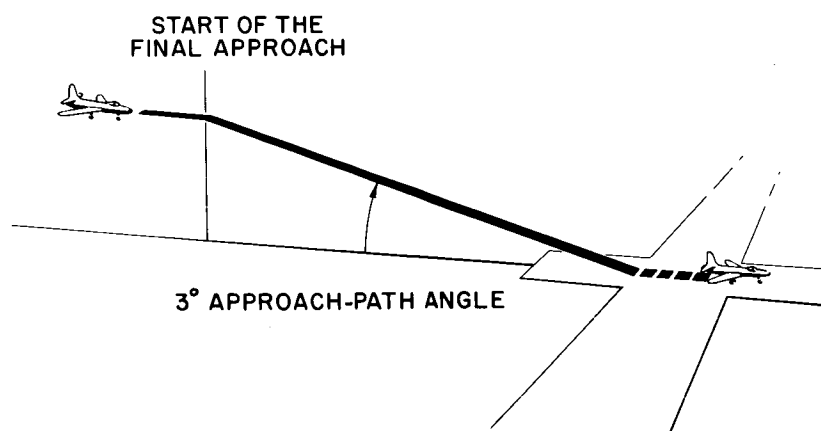
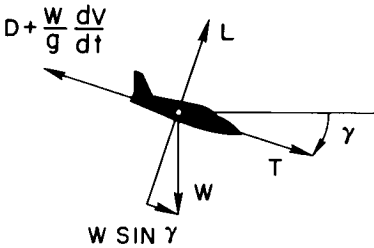


Figure 2

SIMPLIFIED FORCE EQUATION FOR THE LANDING APPROACH



(1) $D + \frac{W}{g} \frac{dv}{dt} = T + W \sin \gamma$

(2) $\sin \gamma = \frac{D}{W} - \frac{T}{W} + \frac{dv}{dt} \frac{1}{g}$

$L \approx W$

(3) $\gamma = \frac{D}{L} - \frac{T}{W} + \frac{dv}{dt} \frac{1}{g}$

Figure 3

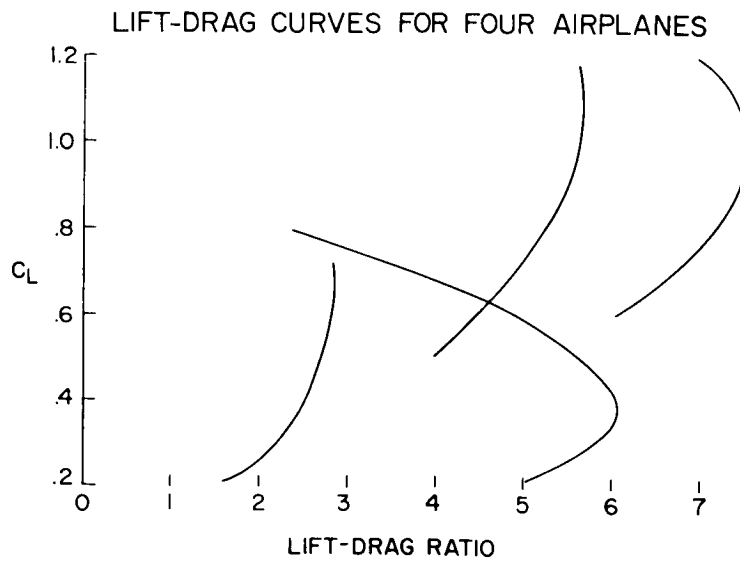


Figure 4

CONDITIONS WHICH LIMIT APPROACH SPEEDS

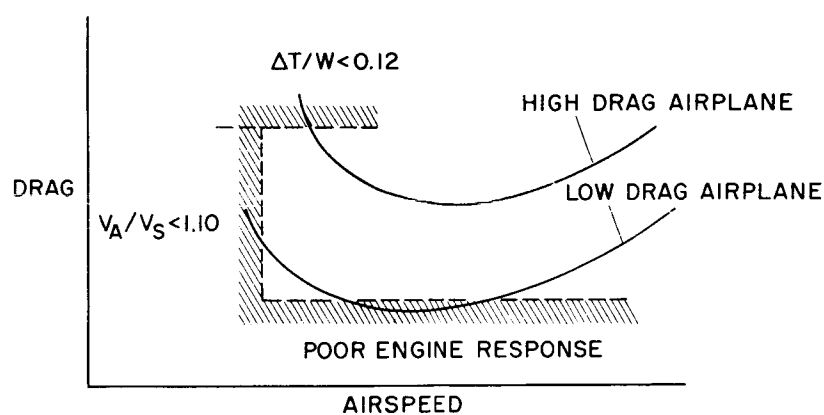


Figure 5

FLIGHT INVESTIGATION OF AN AUTOMATIC THROTTLE

CONTROL IN LANDING APPROACHES

By Lindsay J. Lina, Robert A. Champine,
and Garland J. Morris

Langley Research Center

SUMMARY

A flight investigation of an automatic throttle control in landing approaches has been made. It was found that airspeed could be maintained satisfactorily by the automatic throttle control. Turbulent air caused undesirably large variations of engine power which were uncomfortable and disconcerting; nevertheless, the pilot felt that he could make approaches 5 knots slower with equal assurance when the automatic control was in operation.

INTRODUCTION

Several previous flight investigations of landing approaches have been made in an effort to determine the factors influencing the pilot's choice of minimum approach speed. A number of factors affect this choice. The determining factors are not always the same. Inability to control altitude was, however, most often found to be the reason given by pilots for the choice of minimum approach speed. There are several aerodynamic characteristics of an airplane that influence this ability to control height, but one of the most important is the variation of drag with airspeed at a constant flight-path angle. In landing approaches, when the pilot is holding the airplane to a fixed glide slope, the airplane is unstable in speed if the approach is being made at a speed less than the minimum-drag speed. For example, if a disturbance causes a small decrease in speed, the drag will increase and the speed will continue to decrease until the pilot advances the throttle. At speeds higher than the minimum-drag speed, the drag slope is stable and the airplane, if disturbed in speed, will tend to return to the selected speed without corrective throttle application. Approaches for landing on short runways and aircraft carriers are usually made at the minimum speed compatible with good handling qualities of the airplane.

In an attempt to aid the pilot in these critical landing conditions, an automatic throttle control was designed and installed in a Navy swept-wing jet fighter in the belief that reducing the workload on the pilot might enable him to fly the airplane at a lower approach speed.

DESCRIPTION OF AUTOMATIC THROTTLE CONTROL

A block diagram of the throttle control is shown in figure 1. The throttle control provides automatic stabilization of speed for approaches on the back side of the drag curve. The control consists of an inner-loop servomechanism which positions the throttle and an outer loop which includes the engine, the airplane characteristics, and the airspeed pickup. Adjustment of the manual-throttle position, therefore, is, in effect, a speed-selection setting by virtue of the outer-loop feedback. A certain selected position of the manual throttle results in a particular electrical input signal. This signal is summed with the airspeed signal at the first summing point and will be canceled by only one particular value of airspeed. An error in airspeed from the selected value will result in a signal at the second summing point which will then command a new throttle position. This new throttle position will change the thrust and therefore the airspeed until the airplane is flying at the selected speed.

The airspeed-gain setting for the tests presented provides a stabilization of about 0.05g per knot of airspeed deviation. For the test airplane, the stabilization was about 740 pounds of thrust change per knot of airspeed error. A throttle limiter (see fig. 1) reduces the rate of throttle movement for rapid thrust changes greater than about 1,200 pounds of thrust on either side of the drag curve.

FLIGHT-TEST METHOD

Flight tests with the automatic throttle control were conducted using the Navy mirror landing system to provide a constant-angle glide slope. Figure 2 will aid in explaining the mirror landing system. In operation, the pilot looks at the light which appears in the mirror from the source lights. If the airplane is above the 4° glide slope, the image will appear above the reference lights. If the airplane is below the 4° glide slope, the image will appear below the reference lights.

RESULTS AND DISCUSSION

The variation of drag with airspeed for the airplane has been determined in a flight investigation at the Langley Research Center. This plot is presented in figure 3 to show the slope of the drag curve for each landing approach that will be presented. Mirror landing approaches using manual throttle control are marked "A" and "B" and approaches with the automatic throttle control are marked "C" and "D."

A comparison will first be made of the two approaches in which manual throttle control is used. Approach A was made at a speed about normal for the test airplane, whereas approach B was at a speed less than normal. It should be noted that the slope of the drag curve is positive for approach A and negative for approach B. Figures 4 and 5 are time histories of these two approaches. The measurements shown are elevator deflection δ_e , engine thrust F_n , airspeed corrected to a constant weight V_e , and altitude h . The time scale is in seconds before touchdown. Although the pilot was able to maintain speed and flight-path angle almost equally well for both approaches, the greater difficulty of making the lower speed approach is apparent from the larger amount of throttle movement and elevator movement required.

The effectiveness of the automatic throttle control in relieving the pilot of the task of maintaining a selected speed is shown by comparing the time histories of approach B (fig. 5) and approach C (fig. 6). It can be seen in figure 3 that approach C is at a lower airspeed and has a more negative slope than approach B. The comparison shows that the pilot was able to maintain the proper flight path about as well with the manual throttle control (fig. 5) as with the automatic throttle control (fig. 6) and the speed was kept constant within about the same limits. However, the automatic control relieved the pilot of the task of keeping the speed constant and he was able to make the approach at a lower speed. It should be noted that the automatic control made more frequent throttle adjustments than the pilot. Combined effects of other factors such as buffeting, lateral control, longitudinal stability, and attitude angle prevented further reduction of the approach speed. In the pilot's opinion, landing approaches with the automatic throttle control at low speeds were easier and were made with less apprehension than those made with the manual throttle control at the same speed.

The approaches shown so far were in relatively smooth air. Approaches were also made in very turbulent air. One of these approaches is presented and is shown at point D on the drag curve (fig. 3). A comparison of this approach with approach C shows that it was made at a higher speed with less airspeed instability. The time histories of these two approaches (figs. 6 and 7) show a comparison of the operation of the automatic throttle control in smooth air and in very turbulent

air. It can be seen that again the flight path was flown about equally well and the speed was held nearly constant for both approaches, but large and frequent throttle adjustments were made by the automatic control in response to the gusts. The pilot found that engine surging was very uncomfortable and disconcerting, but preferred to make approaches, even in rough air, with the automatic throttle control operating. The pilot felt that he could make approaches 5 knots slower with equal assurance when the automatic control was in operation.

CONCLUDING REMARKS

A flight investigation of an automatic throttle control in landing approaches showed that airspeed could be maintained satisfactorily. Turbulent air caused undesirably large variations of engine power which were uncomfortable and disconcerting; nevertheless, the pilot felt that he could make approaches 5 knots slower with equal assurance when the automatic control was in operation. Some additional flight tests will be made in an effort to determine the airspeed-gain settings and throttle-limiter characteristics for desirable operation in both smooth and turbulent air.

AUTOMATIC THROTTLE CONTROL

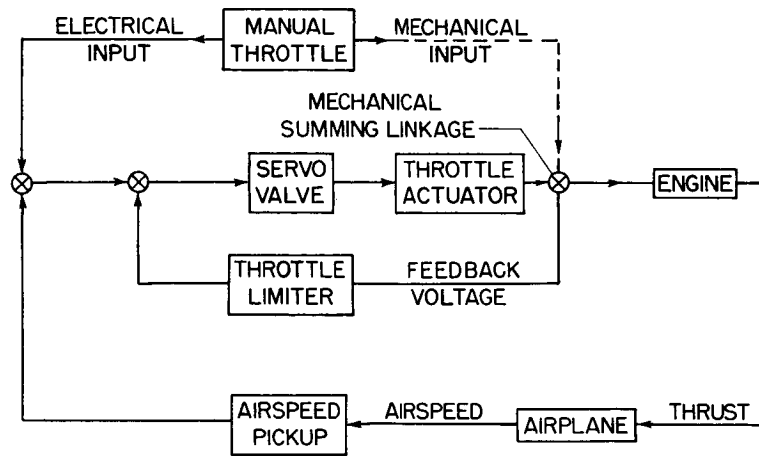


Figure 1

SKETCH OF NAVY MIRROR LANDING SYSTEM

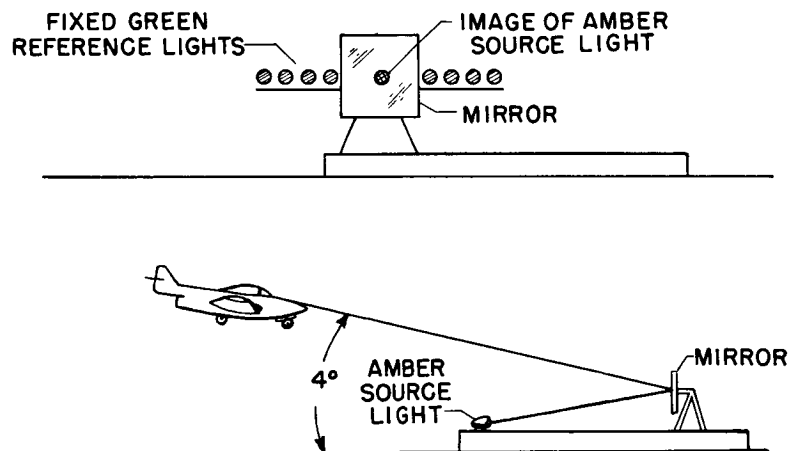


Figure 2

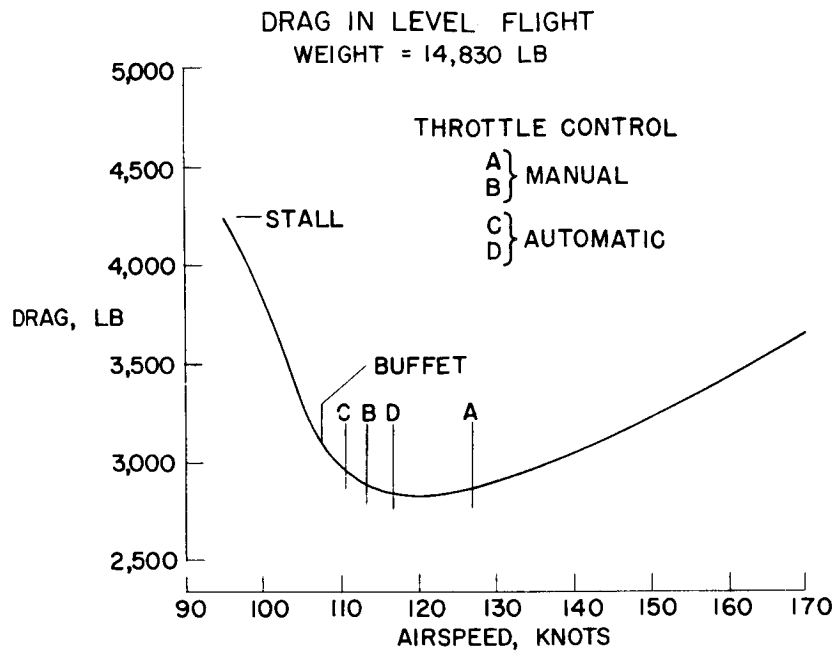


Figure 3

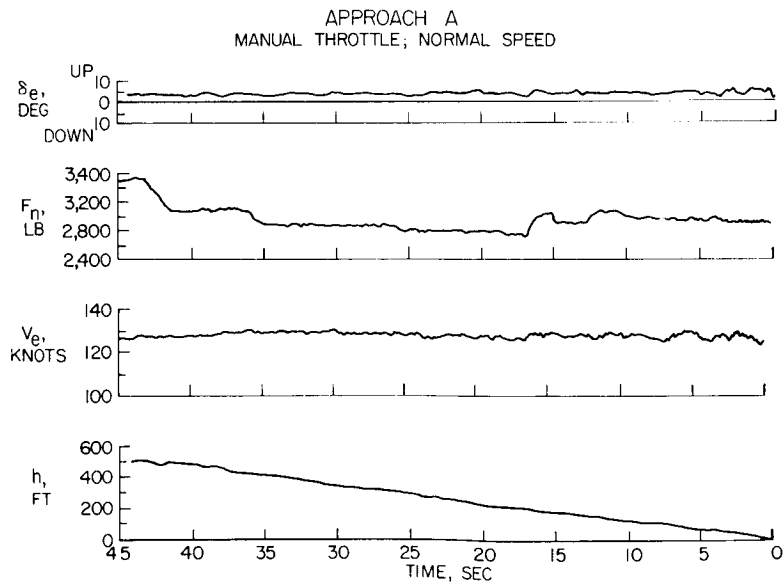


Figure 4

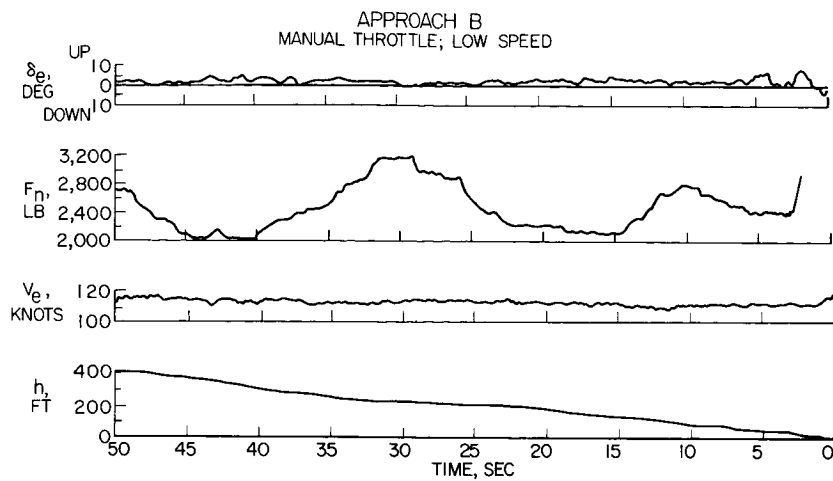


Figure 5

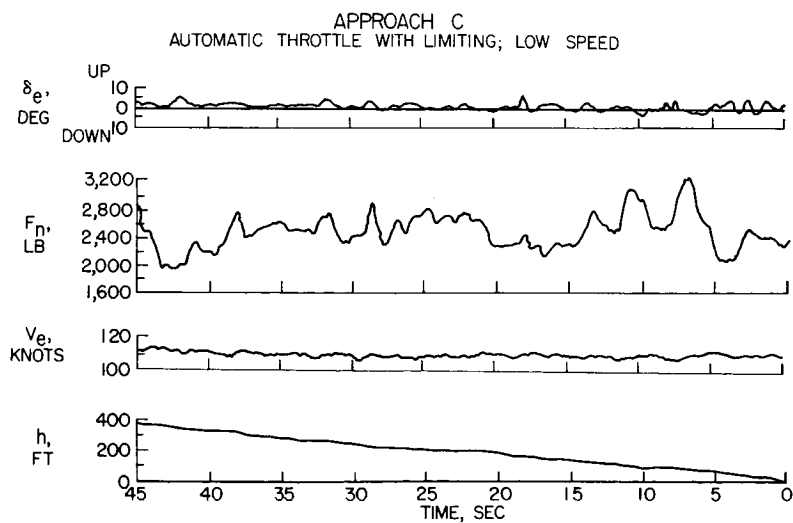


Figure 6

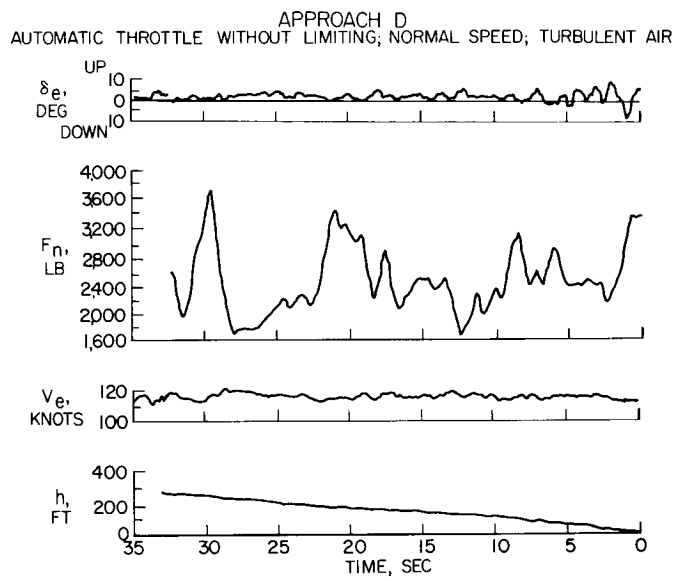


Figure 7

CONTROLLABLE THRUST REVERSER FOR FLIGHT AND LANDING

By Seth B. Anderson and George E. Cooper

Ames Research Center

INTRODUCTION

It is a known fact that increased approach speeds result in an increase in accidents of the overshoot type. One factor affecting approach speeds noted by Fred J. Drinkwater III in a previous paper was thrust response. Recent experience obtained during landings of a wide variety of jet airplanes has indicated that pilots tend to compensate for poor thrust response by increasing approach speeds.

Rapid thrust response and increased control over the level of thrust can be provided by a thrust reverser which is fully controllable by the pilot. By virtue of its ability to change the effective ratio of lift to drag, the reverser can be used to control the glide path over a wide range.

The feasibility of several thrust-reversing principles has been demonstrated during taxiing tests at the Lewis Research Center (refs. 1 and 2). The results of an earlier attempt to use in-flight thrust modulation are given in reference 3. In order to investigate further the in-flight and ground use of a modulating thrust reverser, the Ames Research Center installed a reverser on a Lockheed F-94C. The results of 80 flights in which the reverser was used during high-speed, landing-approach, and ground operation are discussed.

DESCRIPTION OF REVERSER

The reverser was of the cylindrical target type, actuated hydraulically, and controlled by means of a "beep switch" mounted on the throttle. The reverser installed on the Lockheed F-94C airplane is shown in figure 1. As may be seen, the reverser was rugged and was suitable for research purposes only. Fail-safe features allowed the exhaust gases to open the reverser in case of an electrical or hydraulic failure. In addition, a hydraulic accumulator insured rapid opening of the reverser in an emergency.

OPERATIONAL USE OF REVERSER

Although the reverser location on the Lockheed F-94C is different from that contemplated for jet transports, some of the benefits and problems in the operational use of the reverser may be common to both applications.

Landing Procedure With Reverser

In using the reverser during a landing approach where speed and flight-path angle remain relatively constant, such as in an instrument approach, engine speed N is set and maintained constant at 85 percent (slightly more than thrust for level flight at the approach speed). The reverser is deflected, first to decelerate the airplane to the gear-down speed, then to the flap-down speed, and then to the desired approach speed V_1 of, for example, 140 knots. With the airplane trimmed at the approach speed, flight-path adjustments are made by positioning the reverser. Speed adjustments, if necessary, can be obtained quickly by reverser positioning together with angle-of-attack changes by means of the elevator. As soon as all wheels are on the runway, reverser deflection is increased from 0.4 (that used to maintain the desired approach angle) to full reverse position, and the engine speed is advanced to 100 percent. The point to remember is that maximum braking can be obtained immediately, in contrast to the proposed operation for jet transports where engine speed is reduced to idle, reversers are deflected, and then engine speed is advanced.

It was found that use of the reverser resulted in a number of benefits, some of which are directly applicable to the jet transport. For one thing, pilots reported an improvement in control of airspeed and control of location of touchdown point. The factors responsible for this improvement were the thrust response characteristics of the reverser in conjunction with the wide range of approach angles made available. A comparison of the thrust response with and without the reverser is shown in figure 2. The variation of the change in flight-path angle with reverser position is shown in figure 3. Note that a 3° approach requires only a small reverser deflection.

The advantages of reverser control over throttle control were found to become more pronounced with increases in deviations or corrections required in either flight-path angle or airspeed. This fact was brought out in GCA, ILS, and mirror approaches in which the glide path was intercepted with 15 knots of excess airspeed. By using the reverser, the airspeed was reduced rapidly from 155 knots to 140 knots, and the pilot was free to devote his attention as desired during the rest of the approach. When using the throttle, particularly in mirror and ILS

approaches where the time element is shorter, it was necessary to retard the throttle to idle in order to decelerate to 140 knots prior to touchdown. Because of the poor thrust response in the low engine-speed range, the pilot was reluctant to retard the throttle to idle; consequently, touchdown was made at a higher speed than desired, and an undue amount of attention was required to monitor airspeed during the long speed-transition period.

Effect of Reverser Use on Approach Speed

As indicated previously, thrust response was one of the factors influencing the choice of minimum approach speed. It would be expected that where thrust response when using the reverser was greater than that when using the throttle, reductions in approach speed would occur. This expectation was found to be the case, as indicated by the data shown in figure 4 in which the variation of flight-path angle with selected approach speed is presented for approaches made with reverser and with throttle. It can be seen that the magnitude of the reduction in approach speed due to the reverser varied with the steepness of the flight-path angle. Normally, any increase in approach angle will be accompanied by some increase in approach speed in order to maintain a safe margin for flare. It is seen, however, that with the reverser it was possible to approach at angles up to 10° with only small increases in approach speed. These steeper approach angles were possible only because the thrust could be increased rapidly by using the reverser to offset the airspeed decrease during the flare. Such steep approaches were not considered possible by the pilots without the positive rapid thrust control provided by the reverser. Although no reductions in approach speed were realized at low angles, there was, however, an improvement in flight-path control which resulted in an advantage in controlling the tendency to float after the flare by reducing the residual thrust.

Effect on Wave-Off Characteristics

One of the most impressive improvements obtained through use of the reverser was in wave-off. This improvement resulted from the rapid thrust response and a longitudinal-trim change with reverser deflection which served to rotate the airplane immediately to the climb-out flight-path angle.

Use of Reverser For In-Flight Deceleration and Emergency Descent

The reverser was particularly useful for in-flight deceleration and emergency descent where it is necessary to lose altitude rapidly

without exceeding a limit airspeed. For this purpose the reverser was found to be superior to aerodynamic speed brakes both from the deceleration and buffet aspects.

Effect of Trim Change

Some of the actual and potential problem areas were disclosed by the reverser tests. For the installation tested, a longitudinal-trim change with reverser deflection was the most serious aerodynamic problem arising. The trim change became more severe with increasing amounts of engine power and lower values of airspeed. The effect of reverser modifications on the longitudinal trim is shown in figure 5. For both configurations (designated A and B) it can be seen that the elevator angle required for trim at the larger reverser deflections exceeds that which is available. Configuration B, although providing an increase in the usable range of reverser deflection, was unsatisfactory because of the inflection occurring at 0.4 deflection. It should be noted that the severity of the trim change increased with an increase in reverse effectiveness. For example, this large trim change corresponds to a reverse-thrust ratio of 80 percent. With a lower effectiveness of, for example, 40 percent, ample elevator control was available over the full reverser range. In addition, tests conducted at the Ames Research Center have disclosed that a certain amount of trim change (nose-up with increasing thrust) may be desirable since it gives the pilot an immediate indication of a change in flight-path angle. It would be expected that the trim-change type of disturbance would be less serious on the jet transport since the reverser location would not have as pronounced an effect on the flow in the vicinity of the horizontal tail. For the reverser positions used in a landing approach at 150 knots, the exhaust wake was not widened essentially from that of the normal engine-exhaust wake at 3.5-wing-chord lengths in the rearward direction, which is representative of the tail distance from the inboard engine pod of a jet transport. At a deflection of 0.8 the wake was doubled in width and, with some engine locations, may buffet the tail. In addition, because of the flow of exhaust gases near the wing, there would be more reason to expect greater disturbing effects on other items such as stalling, lateral stability and control, and buffeting.

EFFECT OF REVERSER ON MISCELLANEOUS CHARACTERISTICS

Tests showed that deflection of the reverser had no marked effect on the lateral directional dynamic stability or damping, the static directional stability, and the pitching moment due to sideslip. Although the stalling characteristics were not altered, the apparent

stalling speed or minimum flight speed (determined by maximum elevator deflection) was increased because of the trim change mentioned previously.

Buffet induced by the reversed exhaust gases was considered mild; the greatest intensity occurred in the intermediate reverser deflection range where tuft studies showed exhaust-flow attachment to the fuselage skin ahead of the reverser. Certain problems inherent in the use of the reverser, such as a longitudinal-trim change, buffeting, and heating effects, became less serious as the airspeed increased. It would be expected that a similar effect would be experienced with a wing-pod mounted installation.

Deceleration values of approximately $1/3g$ were obtained with full-reverse thrust during the landing roll, and reductions resulted in landing roll of the order of one-half that of using brakes alone.

Structural heating of the blunt rear fuselage fairing restricted reverser use at full engine power to speeds greater than 50 knots. There was no increase in engine-inlet temperature at speeds greater than 50 knots when using full-reverse thrust.

The "beep control" was a satisfactory method of controlling the reverser for the tests conducted, but several limitations were noted which indicate that a proportional type of control would be desirable for operational use.

CONCLUSIONS

The following conclusions have been made from the investigation of a modulating thrust reverser on the Lockheed F-94C airplane.

1. Use of the reverser in landing approach resulted in improved control over a relatively large range of flight-path angles for a given approach speed. Large reductions in approach speed were realized by using the reverser rather than the throttle for steep approaches.

2. Improved control of flight-path angle was made possible by the rapidity with which large thrust changes could be made; this improvement resulted in improved accuracy in selecting the touchdown point with the use of the reverser. Some of the improved flight-path control resulted from a nose-down trim change with decreasing thrust induced by the reverser.

3. The longitudinal-trim change induced by the reverser compromised its use in landing approach by restricting the usable deflection range.

Improvements were noted in the use of the reverser for deceleration at high speeds or as an emergency letdown device.

4. The wave-off characteristics of the airplane were improved by rapid thrust response and the nose-up trim change produced by the reverser.

5. Deceleration values of approximately $1/3g$ were obtained with full-reverse thrust during the landing roll and reductions resulted in landing roll of the order of one-half that of using brakes alone.

6. There were no marked changes in the lateral directional dynamic stability characteristics, the static directional stability, or the pitching moment due to sideslip because of the use of the reverser.

7. The reversed flow resulted in mild buffet of the airplane and controls.

8. Structural heating of the blunt rear fuselage fairing restricted reverser use at full engine power to speeds greater than 50 knots, but did not result in an increase in engine-inlet temperature.

9. The "beep control" was a satisfactory method of controlling the reverser for the tests conducted; however, a proportional type of control would be desirable for operational use.

REFERENCES

1. Kohl, Robert C.: Performance and Operational Studies of a Full-Scale Jet-Engine Thrust Reverser. NACA TN 3665, 1956.
2. Kohl, Robert C., and Algranti, Joseph S.: Investigation of a Full-Scale, Cascade-Type Thrust Reverser. NACA TN 3975, 1957.
3. Polak, I. P.: Development of Turbo-Jet Engine Thrust Destroying and Reversing Nozzle, No. AEL 102. Rep. No. AEL-1108 (Project TED Nos. NAM-PP-375 and NAM-04614), Naval Air Material Center, NAES (Philadelphia), Jan. 13, 1950.

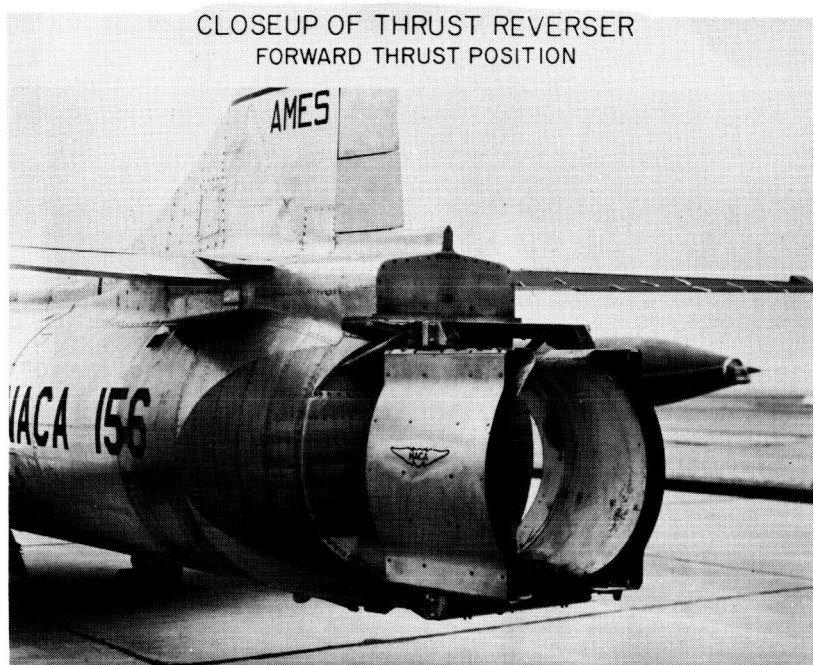


Figure 1(a)

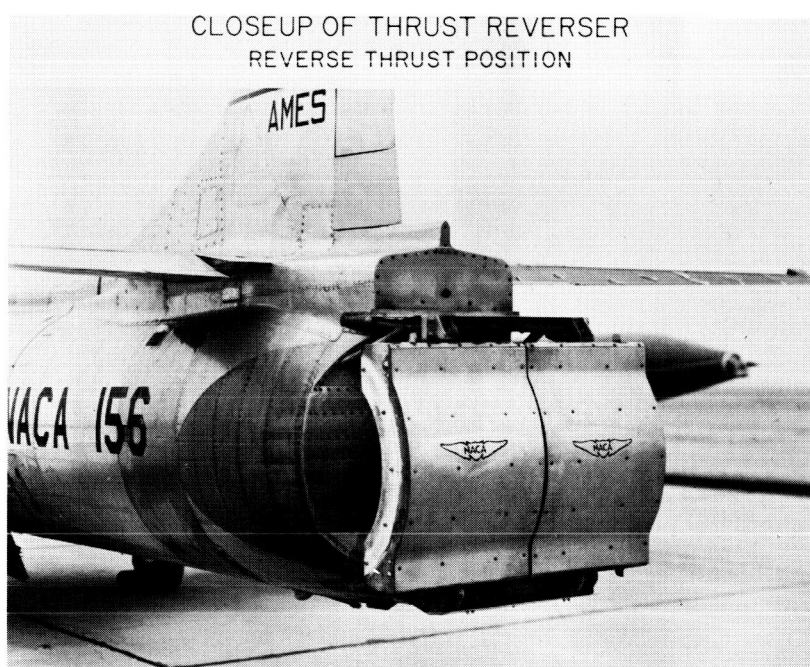


Figure 1(b)

THRUST RESPONSE USING REVERSER AND THROTTLE

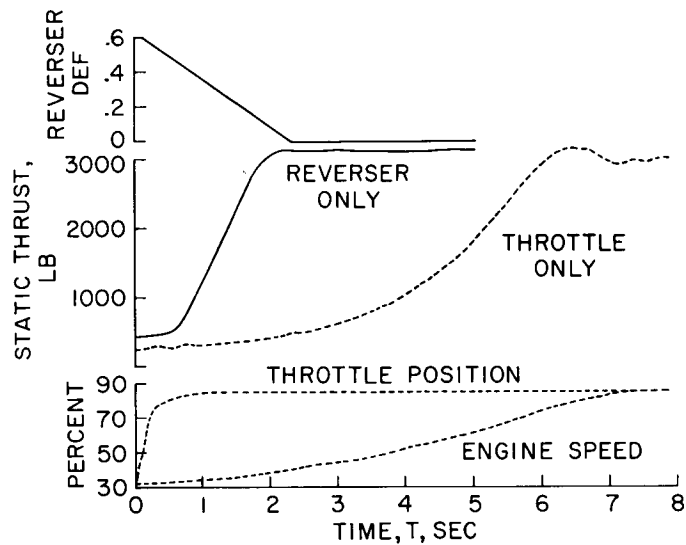


Figure 2

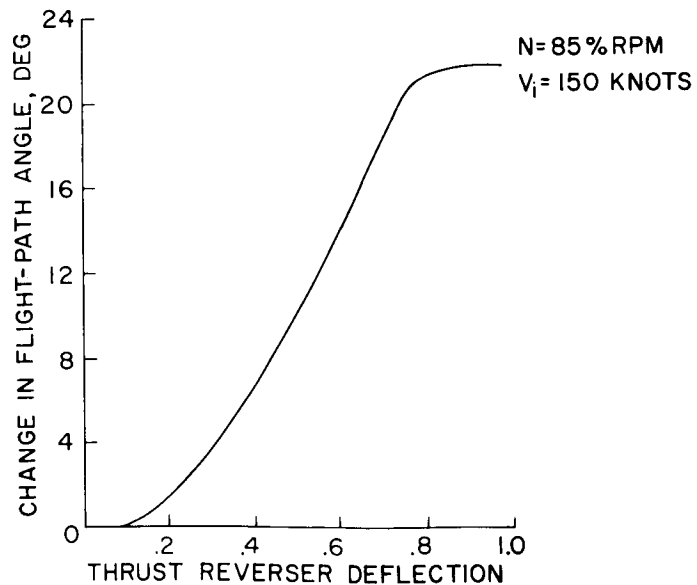
EFFECT OF REVERSER ON FLIGHT-PATH ANGLE
LANDING APPROACH CONFIGURATION

Figure 3

EFFECT OF FLIGHT-PATH ANGLE ON APPROACH SPEED

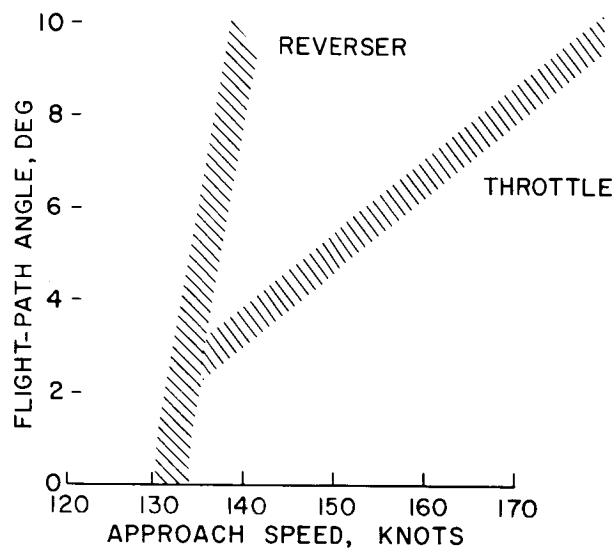


Figure 4

EFFECT OF REVERSER CONFIGURATION ON TRIM

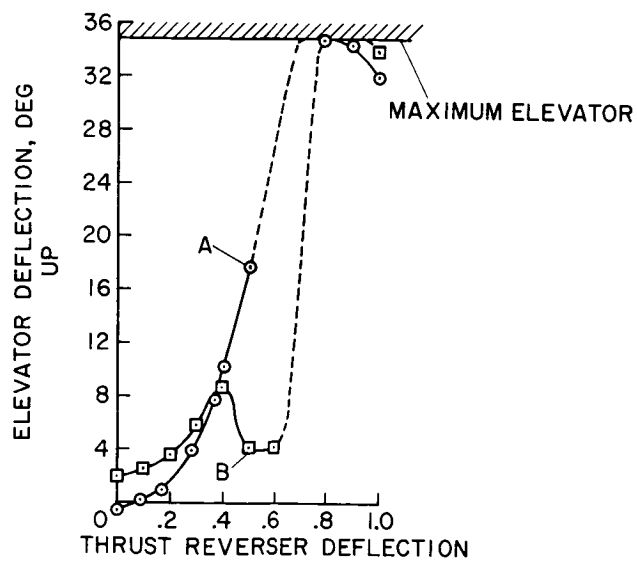


Figure 5

A REVIEW OF STATISTICS OF AIRPLANE LANDING CONTACT CONDITIONS

By Norman S. Silsby

Langley Research Center

INTRODUCTION

The manner in which airplanes are landed in routine operations is of primary concern in setting limitations on the operation of airplanes on existing runways, in the design of new runways, in the design of the airplanes themselves, and to some extent in the overall safety of flight operations. For several years, a continuing program has been in progress at Langley to obtain a large number of measurements of landings of various types of land-based commercial and military airplanes in order to obtain statistical descriptions of the contact conditions at touchdown (refs. 1 to 6). The present paper gives a brief summary of data obtained in this program and includes a recent evaluation of the effect of airport altitude on landing contact conditions.

DISCUSSION

Three of the more important contact conditions which have been under investigation are shown schematically in figure 1. This sketch represents an airplane approach and landing on a runway with contact at a distance l from the runway threshold. The contact conditions measured were the vertical velocity (obtained for each of the main landing-gear wheels, the average of which is considered to be the center-of-gravity vertical velocity V_v of the airplane), the horizontal velocity V_h , and the distance l . Measurements of these quantities are obtained by a specially developed photographic technique described in reference 7.

Although the horizontal velocity V_h that is measured with the camera setup is the ground speed, for purposes of analysis the measured values are converted to true airspeed V_t and expressed as a percentage above the estimated stalling speed.

Most of the published data to date (refs. 1 to 6) relate essentially to sea-level airports. A question was raised as to a possible effect of altitude on the contact conditions. Consideration of the lower density at altitude suggested that the contact conditions might be somewhat more severe, on the average, in landings on terrain above sea level. Therefore, a recent investigation was undertaken to obtain comparable

measurements at a mile-high airport (Stapleton Airfield in Denver, Colorado), and at a sea-level airport (International Airport, San Francisco, California). Several airlines serve each airport in sufficient volume of the various current transport airplanes to permit a substantial amount of statistical data to be obtained in a relatively short time. About 185 routine operational landings were obtained at Denver and about 670 routine landings at San Francisco. The effect of altitude has been examined by comparing a sample of the landing measurements taken at Denver with a comparable sample having the same distribution with regard to airplane types (selected at random from the San Francisco landings). Thus, a statistical sample of 170 landings at each airport was obtained for comparison and analysis.

A comparison of the statistical distributions of vertical velocity is shown in figure 2. In this bar graph, the vertical height of each bar represents the number of landings, or frequency, in percent of the total landings of the occurrence of values of vertical velocities in various 0.5 ft/sec intervals from 0 to 0.5, 0.5 to 1.0, 1.0 to 1.5, The solid bars represent San Francisco data and the hatched bars represent Denver data. The plot shows a marked difference in the distributions for the two airports, with the highest frequency occurring in the 0 to 0.5 ft/sec interval at Denver, whereas the highest frequency at San Francisco occurs in the 1.0 to 1.5 ft/sec interval.

This difference in distribution, that is, a larger number of landings at Denver in the lower vertical-velocity intervals results in a statistically significant lower mean velocity \bar{V}_v of 0.92 ft/sec for Denver compared with the mean value of 1.27 ft/sec for San Francisco. It thus appears that for an airport at high altitude the effect on vertical velocity of airplane landings is to reduce the severity, on the average. The distribution indicates that at each airport the maximum vertical velocity occurred in the same interval (3.5 to 4 ft/sec).

Figure 3 shows a similar bar graph for the location of the contact points down the runway, where the vertical scale is again frequency of landings, percent total, occurring in the various 400-foot intervals of l (0 to 400, 400 to 800, . . . , 2,400 to 2,800). Both distributions indicate that the maximum frequency (something over 40 percent of the airplane landings) of contact points were in the 800- to 1,200-foot interval. The mean distance \bar{l} was 1,058 feet at San Francisco and 1,151 feet at Denver, differing by only 100 feet. The mean contact point \bar{l} occurring at about 1,000 feet has been the value obtained for all airports and for all airplane types investigated so far, regardless of the lengths of runways, which have varied between about 6,500 feet to close to 9,000 feet. An analysis of the landing-contact points on two parallel runways identified at San Francisco as runways 28L and 28R (6,500 feet and 8,870 feet, respectively) indicated no significant differences in

contact-point distributions. It consequently appears that, where runway length is more than adequate, some other factor or factors must influence touchdown point, possibly a natural target, such as runway or taxiway intersections, or possibly a desired turnoff point.

The bar graph of figure 4 shows a comparison of the frequency distributions of the airspeed at contact V_t (expressed in percent above the stall) occurring in various intervals 0 to 10, 10 to 20, These velocity distributions for the two airports are very similar, with the maximum frequency occurring in the same range 20 to 30 percent above the stalling speed and the mean true airspeeds \bar{V}_t being virtually the same (24 and 25 percent above stalling speed). There was also about the same percentage of landings occurring in the same highest bracket (50 to 60 percent above the stalling speed) for the two airports. It should be mentioned that although the percentages above the stalling speed are about the same, the true airspeeds and the stalling speeds are about 10 percent higher for Denver than for San Francisco because of the relative air densities.

These recent results have indicated that the effect of altitude was to reduce the severity of the vertical velocity somewhat but to increase slightly the probability of touching down a little farther down the runway, whereas essentially no difference was noted in the percentage of true airspeed above the stalling speed. An up-to-date summary of data on landing contact conditions available from the present investigation and from references 1 to 6 is given in the following table:

Type of operation	Number of landings	V_v , ft/sec		V_t , percent above stall		l , ft	
		Mean	Maximum	Mean	Maximum	Mean	Maximum
Commercial	1,333	1.3	5	25	59	1,080	2,450
Military							
Jet fighters	771	1.4	10.8	23	62	960	2,800
Large bombers							
Propeller	144	2.3	7	19	41	-----	-----
Jet	222	2	6.3	23	68	-----	-----

The results are broken down according to types of airplane operation, the two main types being the commercial and military. The military operations are further divided into jet-fighter and large-bomber types, and the large bombers are subdivided into propeller and jet types.

The data summary consists of mean and maximum values for the three contact conditions already discussed, namely, vertical velocity V_v , true airspeed V_t in percent above the stalling speed, and distance l of the touchdown point from the runway threshold. The mean values of vertical velocity for the military airplanes are somewhat larger than for the commercial airplanes, as are also the maximum values. A maximum value of 10.8 ft/sec was obtained in one landing of a jet fighter, the next lower values being about 7 ft/sec, for which there were three occurrences. With regard to airspeeds V_t at touchdown, the mean values in percent above stall for the military operations were slightly smaller than for the commercial airplanes while the maximums in general were greater. These comparisons also hold for the distance down the runway; that is, mean distances were smaller and maximums larger for military operations than for commercial operations.

One explanation for the somewhat more severe contact conditions obtained in military operations is that a substantial proportion of the military landing data was obtained during operational and transitional training, which has been found to result, on the average, in somewhat more severe contact conditions. Although no statistical data are yet available on jet transports, the comparison in the military category between propeller-driven and jet-propelled large airplanes indicates no significant differences between the landing contact conditions of the two types.

REFERENCES

1. Silsby, Norman S., Rind, Emanuel, and Morris, Garland J.: Some Measurements of Landing Contact Conditions of Transport Airplanes in Routine Operations. NACA RM L53E05a, 1953.
2. Silsby, Norman S.: Statistical Measurements of Contact Conditions of 478 Transport-Airplane Landings During Routine Daytime Operations. NACA Rep. 1214, 1955. (Supersedes TN 3194.)
3. Silsby, Norman S., and Harrin, Eziaslav N.: Statistical Measurements of Landing-Contact Conditions of a Heavy Bomber. NACA RM L55E03, 1955.
4. Kolnick, Joseph J., and Morris, Garland J.: Statistical Measurements of Landing Contact Conditions of the Boeing B-47 Airplane. NACA RM L55H24, 1955.
5. Silsby, Norman S., and Harrin, Eziaslav N.: Landing Conditions for Large Airplanes in Routine Operations. NACA RM L55E18c, 1955.
6. Silsby, Norman S.: Statistical Measurements of Landing Contact Conditions of Five Military Airplanes During Routine Daytime Operations. NACA RM L56F21a, 1956.
7. Rind, Emanuel: A Photographic Method for Determining Vertical Velocities of Aircraft Immediately Prior to Landing. NACA TN 3050, 1954.

SKETCH SHOWING QUANTITIES MEASURED

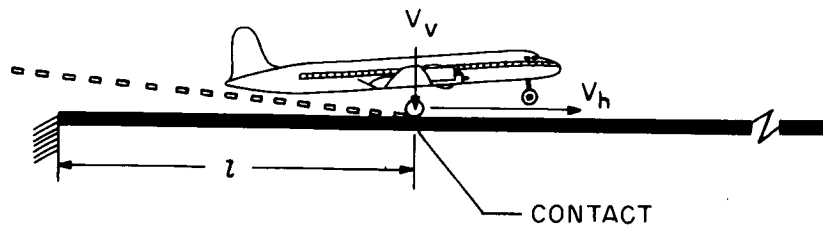


Figure 1

VERTICAL VELOCITY AT CONTACT FOR TWO AIRPORTS

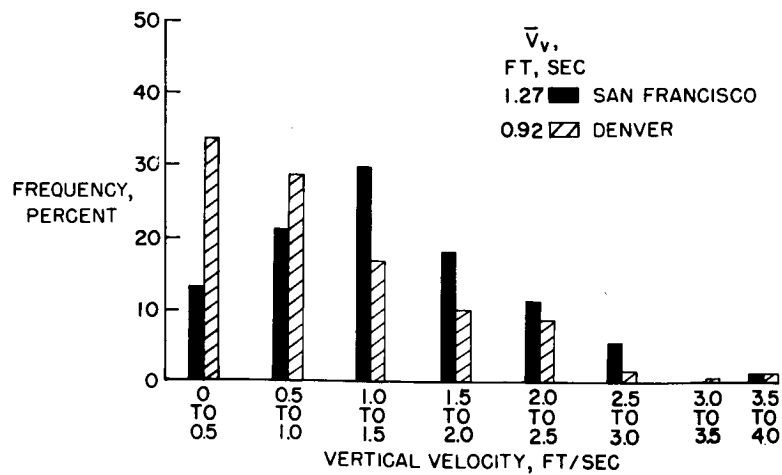


Figure 2

DISTANCE DOWN RUNWAY AT CONTACT FOR TWO AIRPORTS

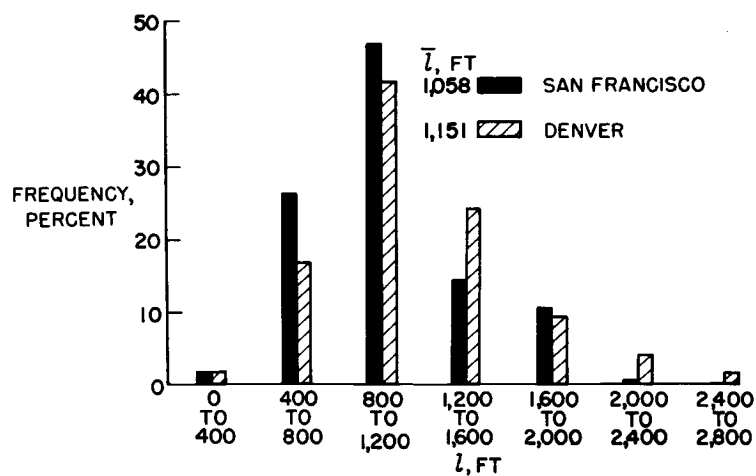


Figure 3

AIRSPEED AT CONTACT FOR TWO AIRPORTS

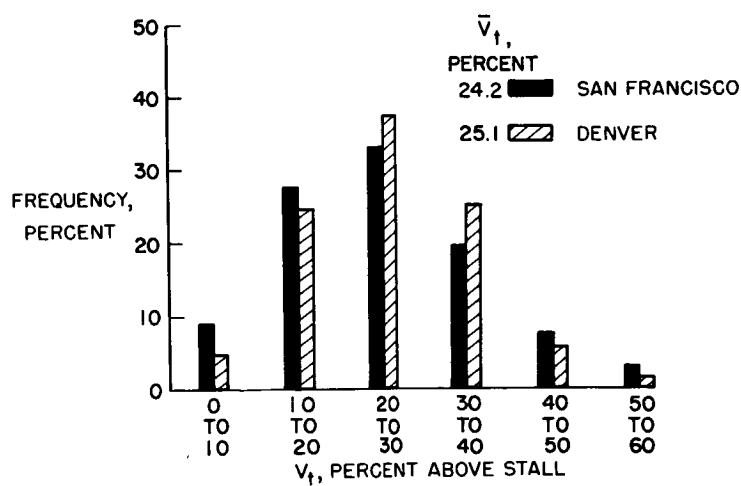


Figure 4

TIRE-TO-SURFACE FRICTION ESPECIALLY UNDER WET CONDITIONS

By Richard H. Sawyer, Sidney A. Batterson,
and Eziaslav N. Harrin

Langley Research Center

SUMMARY

The results of measurements of the maximum friction available in braking on various runway surfaces under various conditions is shown for a C-123B airplane and comparisons of measurements with a tire-friction cart on the same runways are made. The results of studies of wet-surface friction made with a 12-inch-diameter low-pressure tire on a tire-friction treadmill, with an automobile tire on the tire-friction cart, and with a 44 x 13 extra-high-pressure type VII aircraft tire at the Langley landing-loads track are compared. Preliminary results of tests on the tire-friction treadmill under wet-surface conditions to determine the effect of the wiping action of the front wheel of a tandem-wheel arrangement on the friction available in braking for the rear wheel are given.

INTRODUCTION

The coefficient of friction which can be developed between an airplane's tires and the runway surface is, in many cases, a primary factor in determining whether the airplane can make a safe stop in a landing on a given runway. Since most of the information available on tire-to-surface friction in braking is limited to measurements made at low speeds with automobile tires for the full-skid (that is locked wheel) condition, investigations have been undertaken by the Langley Research Center to provide information on tire-to-surface friction more directly applicable to aircraft braking. In these investigations, because of the increasing use on aircraft of automatic braking devices which attempt to prevent locking of the wheels and at the same time attempt to take advantage of the greater friction-coefficient values obtainable for the wheel in the incipient-skidding condition, particular attention has been paid to measuring the incipient-skidding (that is, maximum) value of the friction coefficient.

MEASUREMENTS ON ACTUAL RUNWAYS UNDER VARIOUS CONDITIONS

The first investigation was made in actual landing runs of a C-123B airplane (fig. 1) on various runways under various conditions. The main gear of this airplane was equipped with 49-inch-diameter (type III, 17.00-20, 16 ply rating) low-pressure tires which were inflated to a pressure of 65 lb/sq in. The airplane was equipped with an antiskid braking system which cycled the brakes on and off at a rate of about 2 cycles per second, producing traverses of the wheel slip ratio through the incipient-skidding condition and thereby allowing measurements of the maximum friction coefficient to be made frequently during the braked portion of the landing run.

Tire-to-surface friction measurements have also been made with the friction cart shown in figure 2. This cart, which is equipped with two 4-ply 6.70-15 automobile tires, was developed as a possible operational device for measuring the available friction on the runway. The two wheels of the cart are geared with a gear ratio less than 1.0 so that one wheel is forced to operate near the incipient-skidding condition. Figure 3 presents mean values of the maximum friction coefficient obtained over a speed range of about 15 to 115 knots for the airplane and up to about 50 knots with the cart on the same surfaces.

The agreement of the airplane and cart results for the surfaces shown is seen to be good. For dry surfaces, values of maximum friction coefficient of about 0.8 were obtained. On snow-covered surfaces, values of maximum friction coefficient ranging from about 0.24 to 0.37 were found, with the value apparently dependent on the subsurface. On ice, values of maximum friction coefficient of 0.18 to 0.20 were obtained, with no effect of temperature noted at the two temperatures of the investigation.

For wet surfaces, an example of comparative results with the airplane and cart is shown in the lower part of figure 4. It can be seen that the apparent decrease in maximum friction coefficient with speed and the large variations in maximum friction coefficient, which are attributed to the effect of differences in depth of water along the runway, made correlation of the results difficult. The apparent decrease in maximum friction coefficient with speed is believed to be associated with a gradual penetration by a film of water under the tire. This gradual penetration occurs because as speed is increased the tire has less time to overcome the inertia and viscous effects of the water in displacing the water from the path of the tire. Therefore, with increasing speed, the water penetrates farther and farther under the tire until the whole footprint is supported on a film of water and the tire is in effect "aquaplaning." The extremely low values of maximum

friction coefficient obtained with the airplane, which are especially apparent at the high speeds, in the heavy rain condition shown in the upper part of figure 4 are believed to be associated with a considerable penetration by a film of water under the tire.

An elementary analysis of this wet-surface phenomenon, based only on pressure and inertia-force considerations, indicates that the friction available should decrease with increase in the dynamic pressure exerted by the water on the tire, decrease with decrease in the tire footprint bearing pressure, and decrease with increase in the depth of water. Other factors such as footprint shape and tread design also influence the friction coefficient.

WET-SURFACE MEASUREMENTS BY VARIOUS METHODS

To study this low-friction wet-surface phenomenon under controlled conditions, the apparatus shown in figure 5 was built. In testing, a sheet of water is flowed onto the endless belt from the nozzle at the same speed as the belt while the 12-inch-diameter low-pressure tire is braked.

Some illustrative results of friction-coefficient measurements with the treadmill taken from reference 1 are shown in figure 6. The losses in maximum and full-skid values of friction coefficient with increase in speed are as predicted by the elementary analysis of the effect of the dynamic pressure of the water. For speeds in the equilibrium region indicated in figure 6, the wheel tends to stop with no braking applied, reaching a condition of stable equilibrium in the stopped position. At these speeds it can be seen that the free-roll friction coefficient has increased to a value as great as or greater than the full-skid value. Apparently, in this condition the pressure, inertia, and viscous forces of the water create a torque on the wheel which is equal and opposite to the torque from the frictional force.

Studies of wet-surface friction have also been made by towing the friction cart at various speeds through a water trough. The trough testing method was originated and developed by James P. Trant, Jr., at the Langley Research Center. The trough was constructed by simply erecting two low parallel walls on a concrete road surface. Some of the results of these measurements are given in figures 7 and 8. Figure 7 shows the effect of the depth of water and, as predicted by the elementary theory, the maximum friction decreases with increase in depth. It is interesting to note the large losses at the higher speeds, even for the thinnest depth of water. In figure 8, the predicted favorable effect of increasing the tire footprint bearing pressure is borne out

by the increase in the maximum friction coefficient with inflation pressure.

To study wet-surface friction at speeds and tire pressures more representative of aircraft operation, some tests have been made of a 44 x 13 extra-high-pressure, 26 ply rating, type VII tire at the Langley landing-loads track. For this purpose a water trough was constructed on the track roadbed. Preliminary results from these measurements are shown in figures 9 and 10.

Figure 9 shows that the maximum friction coefficient for this aircraft tire decreased rapidly as water depth increased in a similar fashion to the results obtained with the friction cart. The large decrease in friction from the dry-surface value (maximum friction coefficient of the order of 0.7 to 0.8) for the thinnest depth is also similar to the cart results.

Measurements on the local runways indicated that in a moderate rain depths of water up to 0.35 inch existed in puddles several hundred feet long and that 90 percent of the surface was covered with a minimum depth of water of 0.03 inch. A depth of water of 0.1 inch was accordingly selected for the tests at several tire pressures and speeds, and the results of these tests are shown in figure 10.

The μ_{MAX} values are seen to drop rapidly with increase in speed, values equal to about zero occurring at a little over 100 knots. The influence of inflation pressure is somewhat difficult to see, but there is some indication that at speeds below 80 knots the lowest tire pressure gives somewhat higher values of μ_{MAX} , whereas at speeds above 80 knots the highest tire pressure gives somewhat higher friction.

Since the elementary analysis indicated that the friction would be a function of the dynamic pressure of the water and the tire footprint bearing pressure, the results from the treadmill, friction cart, and landing-loads track are compared for one depth in figure 11 on the basis of the ratio of the dynamic pressure q to the gross footprint bearing pressure p_g . The results for the treadmill are for 0.09 inch of water, while the results for the friction cart and landing-loads track are for 0.1 inch of water. The treadmill and friction-cart results are for the recommended tire inflation pressure for the wheel loading used in each case. The recommended inflation pressure for the aircraft tire as loaded is 150 lb/sq in. The measured rolling friction has been subtracted from the treadmill results as the friction-cart and landing-loads-track measurements do not include rolling friction. The agreement of the results from the three methods, compared on the basis of q/p_g , is seen to be fairly good. In general it appears that prediction of

the friction for the aircraft tire from either the treadmill or cart results on this basis would lead to somewhat unconservative results, with the predicted friction coefficient being somewhat high. Attempts to strengthen the agreement of these results by involving other parameters such as footprint shape, tread design and wheel size have not yet proved successful.

The problem of low friction on wet surfaces can be alleviated, of course, by providing better drainage; perhaps through more crown on the runways, or creating escape paths for the water by better tread design or through use of a knobby surface. Higher bearing pressures attained through use of higher inflation pressures, tread design, or use of sharp angular-textured aggregates in the surface which give local bearing pressures of 2,000 to 8,000 lb/sq in. can all increase the friction available.

Another possibility, removal of the water by wiping action, has been tried on the treadmill with the tandem-wheel arrangement shown in figure 12. The wheel on the right in the figure wipes a path for the other wheel which is braked. Tests were made with the wheels as shown and also with the wiper wheel lifted out of the way. Results of these measurements are given in figure 13.

The favorable increase in the maximum and full-skid friction coefficients for the tandem arrangement at the higher speeds is quite evident. Considering the maximum friction values for both the tandem- and single-wheel arrangements, for a bogie gear with equal loads carried on the front and rear wheels and both wheels braked the effective maximum friction coefficient would be about 0.3 at the highest speed, an increase of 50 percent over the single-wheel value or the mean of two single-wheel values. Actually, in these tests only about 20 percent of the total weight was carried on the front wheel, and for such a weight distribution a gain of about 80 percent in the effective friction coefficient can apparently be realized. For the tandem arrangement, the full-skid and free-roll curves appear to indicate that the speed at which difficulty would be experienced in having the wheel attain the condition of equilibrium would be extended considerably.

CONCLUDING REMARKS

The effect of runway surface on the maximum friction coefficient has been shown for actual landings of a C-123B airplane on various surfaces under various conditions. Results of measurements made with a friction cart were found to agree with the airplane results for dry, snow-covered, and icy surfaces, but correlation of airplane and cart

results for wet surfaces was found to be very difficult. Study of wet-surface friction indicated that the loss of adhesion is related to the dynamic pressure of the water, the tire footprint bearing pressure, and the depth of water. Measurements of friction obtained by three methods for one depth of water agreed fairly well when compared on the basis of the ratio of the dynamic pressure of the water to the gross footprint bearing pressure. The wiping action of the front wheel of a tandem-wheel arrangement was shown to increase considerably the friction available on the rear tire.

REFERENCE

1. Harrin, Eziaslav N.: Low Tire Friction and Cornering Forces on a Wet Surface. NACA TN 4406, 1958.



Figure 1

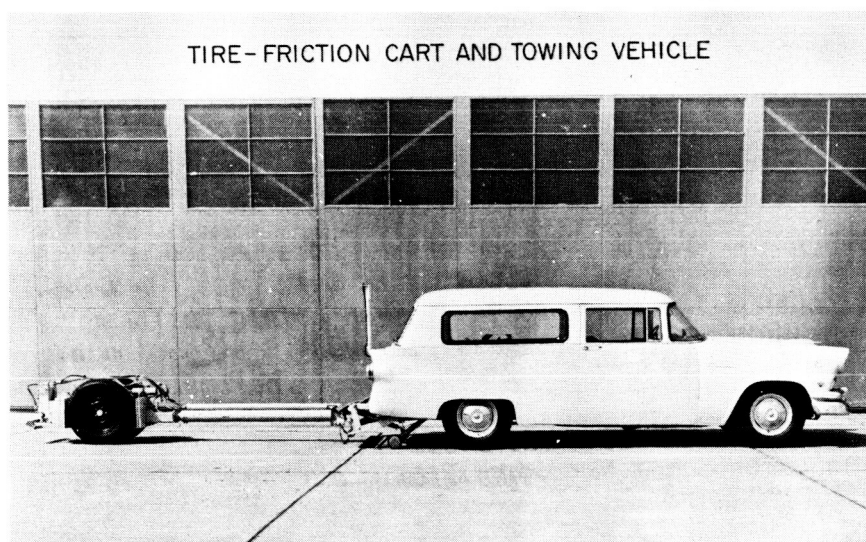


Figure 2

EFFECT OF SURFACE C-123B AIRPLANE AND FRICTION CART

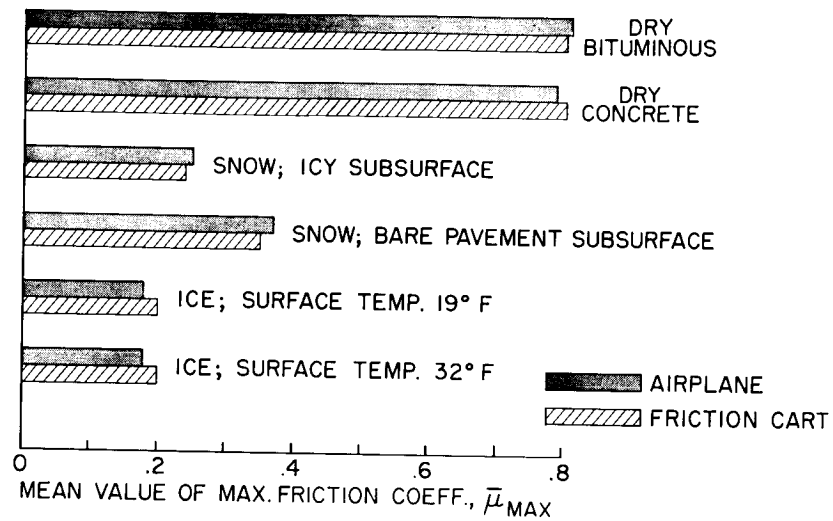


Figure 3

MAXIMUM FRICTION ON WET RUNWAYS C-123B AIRPLANE AND FRICTION CART

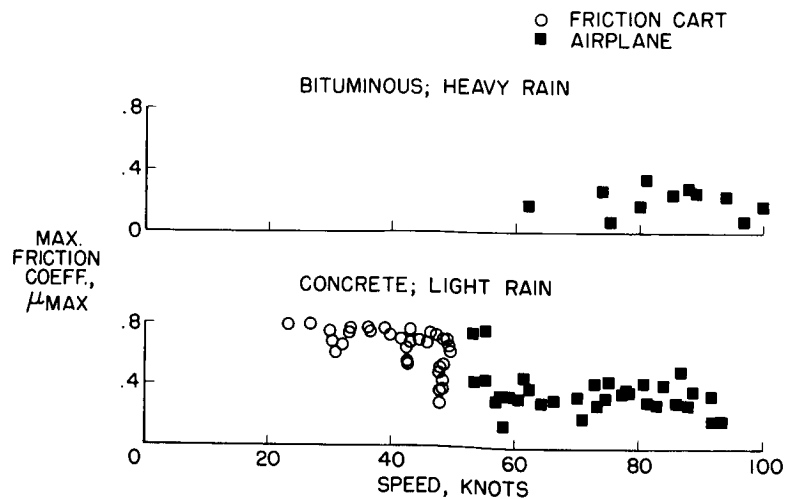


Figure 4

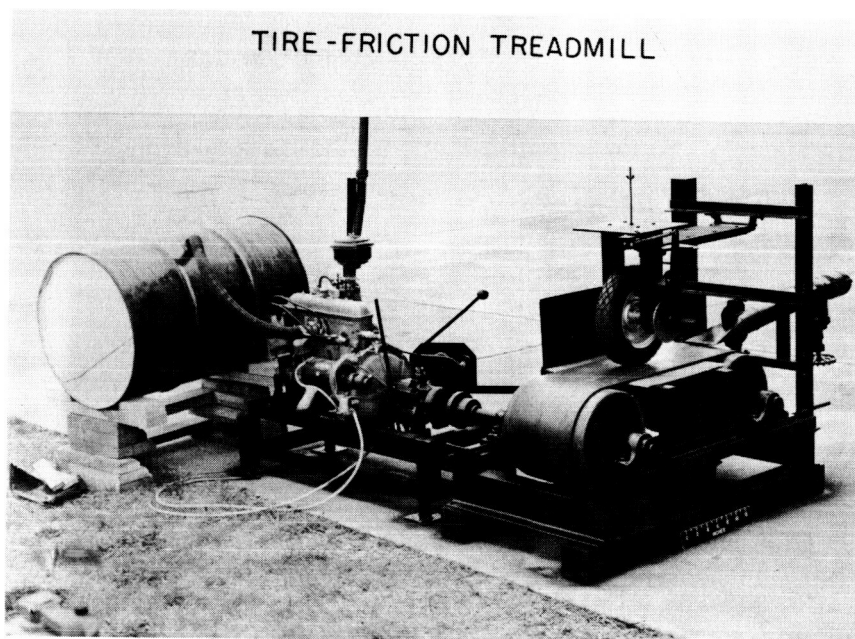


Figure 5

EFFECT OF SPEED
TREADMILL; SMOOTH TIRE; 13 LB/SQ IN.; 0.02-IN. WATER

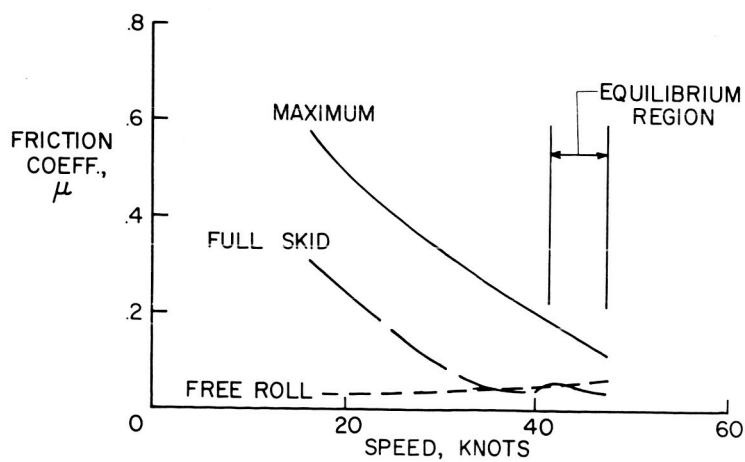


Figure 6

EFFECT OF WATER DEPTH
FRICTION CART; RIB TREAD; 40 LB/SQ IN.

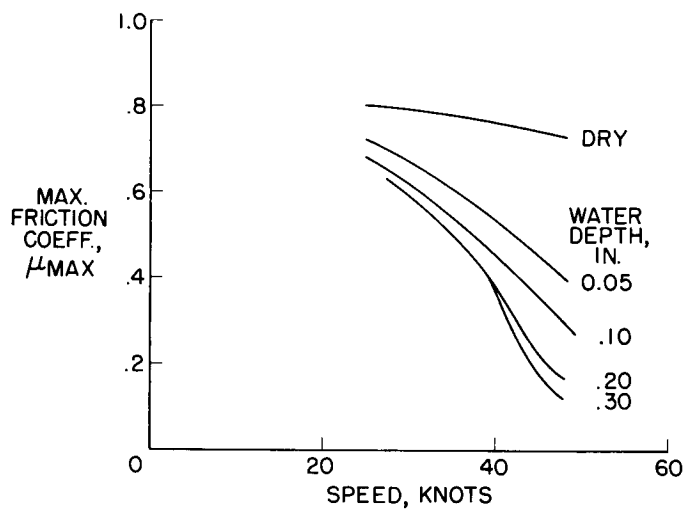


Figure 7

EFFECT OF INFLATION PRESSURE
FRICTION CART; RIB TREAD

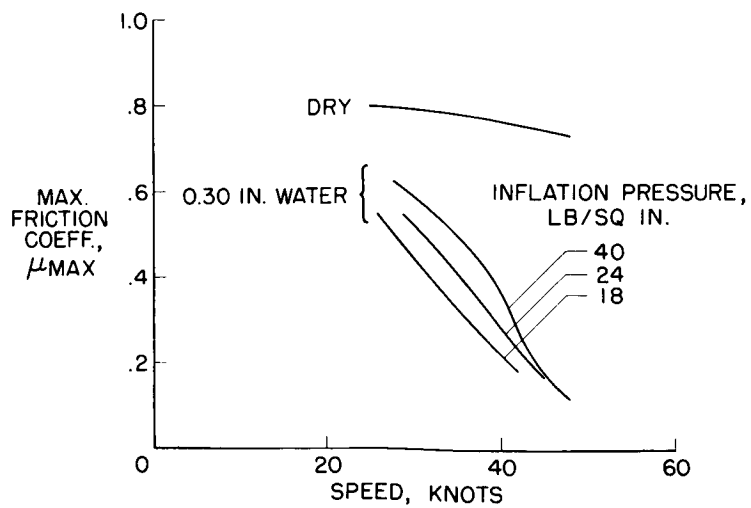


Figure 8

EFFECT OF WATER DEPTH
LANDING-LOADS TRACK; RIB TREAD; 150 LB/SQ IN.; 89 KNOTS

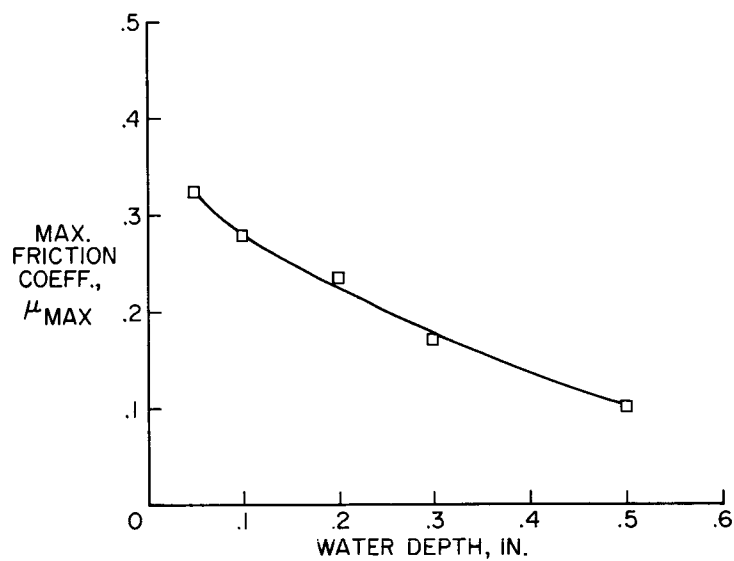


Figure 9

EFFECT OF SPEED AND INFLATION PRESSURE
ON WET-SURFACE FRICTION
LANDING-LOADS TRACK; RIB TREAD; 0.1 - IN. WATER

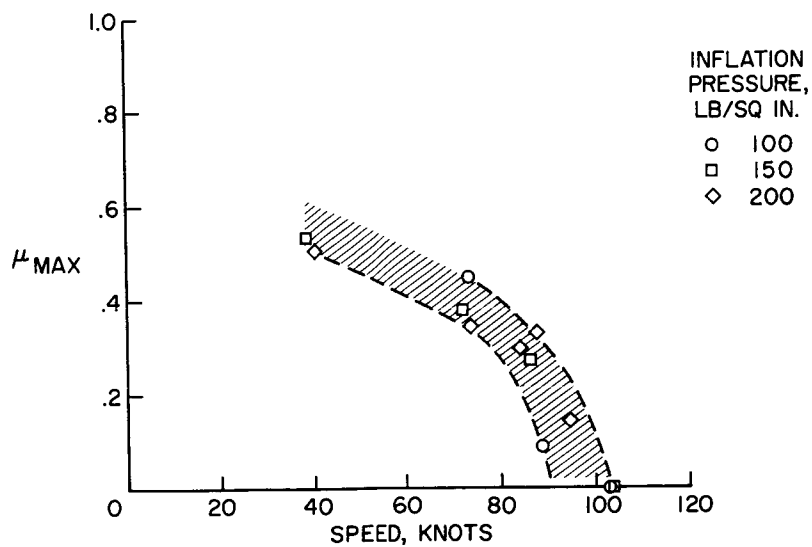


Figure 10

COMPARISON OF WET-SURFACE FRICTION RESULTS FROM
TREADMILL, FRICTION CART, AND LANDING-LOADS TRACK

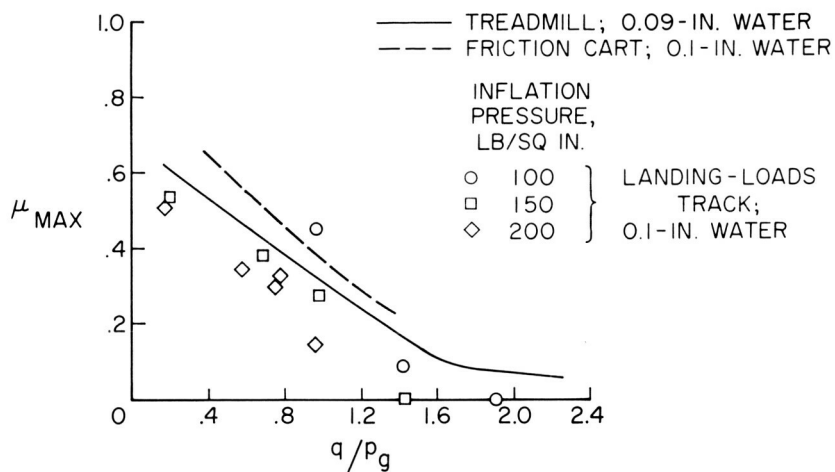


Figure 11

TANDEM WHEEL ARRANGEMENT ON TIRE-FRICTION TREADMILL

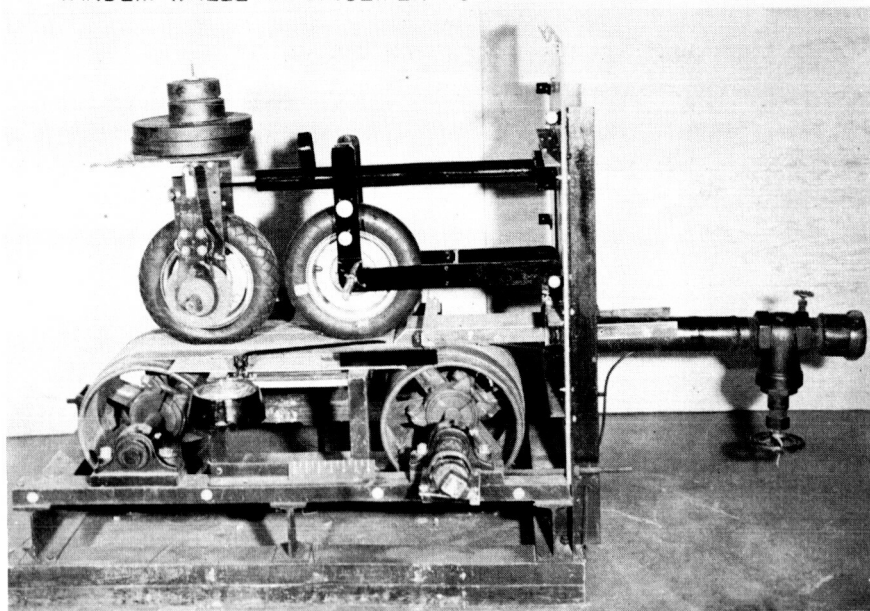


Figure 12

EFFECT OF WHEELS IN TANDEM
TREADMILL; TREADED TIRE; 13 LB/SQ IN.; 0.09-IN. WATER

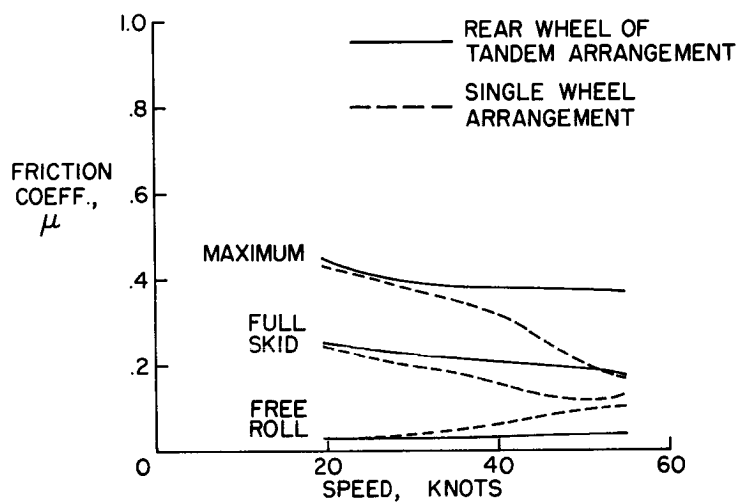


Figure 13

STUDY OF TAXIING PROBLEMS ASSOCIATED
WITH RUNWAY ROUGHNESS

By Benjamin Milwitzky

Langley Research Center

SUMMARY

This paper briefly reviews available statistical data on airplane taxi operations, examines the profiles and power spectra of four runways and taxiways covering a wide range of surface roughness, considers (on the basis of theoretical and experimental results) the loads resulting from taxiing on such runways over a range of speeds and, by synthesis of the aforementioned results, proposes new criteria for runway and taxiway smoothness which are applicable to new construction and may be used as a guide for determining when repairs are necessary.

INTRODUCTION

The motions and loads caused by runway and taxiway irregularities can produce a broad spectrum of operating difficulties, ranging from fatigue damage and structural failures to pilots' complaints. Recent trends in airplane design, such as increased structural flexibility and the use of large external stores, have served to aggravate the situation.

For some time, a research program has been in progress for the study of various aspects of the runway-roughness problem, such as the statistics of taxiing operations, the dynamics of the landing gear in taxiing, and the roughness characteristics of many runways in this country and abroad, the latter with the aid of surveys provided by countries of the North Atlantic Treaty Organization through the Advisory Group for Aeronautical Research and Development.

Because existing criteria for runway surface smoothness are largely subjective, much attention is being given to the development of improved criteria on a more rational engineering basis. Three questions that require answers are:

- (1) At what level does roughness become a problem?
- (2) How should runway surfaces be specified?
- (3) Is there anything the pilot can do to minimize the effects of roughness?

Recent research has provided information which may be used to answer these questions and the present paper attempts to summarize current thinking on the subject.

RESULTS AND DISCUSSION

VGH Data

To begin with, a few simple statistical results are presented in the following table:

AIRLINE EXPERIENCE

(Based on VGH-Recorder Data)

Taxiing time	Approximately 5 minutes
Time on taxiways	80 percent
Primary response	1.5 to 2 cps

Study of many VGH records from airline operations shows that the amount of time spent in taxiing is remarkably constant, approximately 5 minutes per flight (the word "flight" including one departure and one arrival). Very significantly, about 80 percent of this 5 minutes of taxiing is done on taxiways. Available flight records also show that for a wide range of airplanes, regardless of size and mission, the predominant response of the landing gear occurs in a very narrow frequency range, between 1.5 and 2 cycles per second; and this includes data from fighters, transports, and heavy bombers. Theoretical studies of landing-gear dynamics also show the same narrow sensitivity band. For frequencies outside this band, the landing gear provides relatively good isolation of the airplane from ground disturbances. The fact that the sensitive range is virtually always between 1.5 and 2 cycles per second is due to the standardized way in which tires are specified and shock-strut compression ratios are normally chosen.

Runway Profiles

Some idea of the roughness which may be encountered by airplanes can be gained by examining some typical runway profiles (fig. 1). For clarity the elevations are greatly magnified with respect to the horizontal distance, adjacent ticks representing an increment in elevation of 0.05 foot or 0.6 inch. The uppermost profile is a section from a former runway, now inactive as a runway but used as a taxiway. This particular taxiway is the worst of the 50 or so profiles that have been analyzed to date. Next is a profile from a runway which shall be called "runway X." Runway X is an active operational runway that is supposed to be good from an engineering standpoint but has caused pilots' complaints. The third plot shows a length of a very good commercial runway at a large international airport. Finally, a profile is shown of the pavement of the landing loads track at the Langley Research Center, which had to be very smooth for use in research.

The wide range of roughness from top to bottom of figure 1 is immediately evident. Closer inspection shows that each profile is composed of a jumble of superimposed waves of different wave lengths, the amplitudes generally becoming larger as the wave lengths increase.

These elevation profiles give a qualitative idea of the surface roughness but for technical analysis quantitative information regarding the variation of the amplitude of the waves with the wave length is needed. One way of showing this relationship is by means of the power spectrum, a form of which is presented in figure 2. For the present purposes, the ordinate Φ can be considered simply as an index of the relative amplitudes corresponding to the wave lengths shown on the abscissa. As expected, the uppermost curve is for the rough taxiway, whereas the spectra for the Langley landing loads track and the commercial runway fall considerably lower. Runway X, although better than the commercial runway at long wave lengths, appears to be almost as bad as the rough taxiway at intermediate wave lengths where the data end.

Since landing gears transmit the greatest loads when the impressed frequencies are between 1.5 and 2 cycles per second, the critical runway wave length corresponding to any given taxi speed can now be defined. If the speed range from 20 to 130 knots is considered, the critical wave lengths are found to lie between 17 and 150 feet. This region is of greatest concern, since the landing-gear response will be much reduced outside this range.

Taxi Loads

Figure 3 is a statistical presentation showing the frequency of occurrence of the loads that an airplane might experience in taxiing over the different types of runway in, for instance, 1,000 flights. The ordinate is the cumulative frequency of occurrence; that is, the number of acceleration peaks, both plus and minus, that will reach or exceed a given level in 1,000 flights. The solid-line curve is based on an analysis of a large amount of VGH data obtained in airline operations and might be considered as a national average. The other curves were derived from theoretical studies of taxiing on the four runways previously discussed and are based on a taxi speed of 30 knots. The end point at the zero-g level represents the total number of acceleration peaks experienced during the exposure time involved.

If all the taxiing were done on the rough taxiway, the loads would be about 3 times as high as the national average. Runway X, which has produced some complaints, appears to be comparable to the national average, whereas the good commercial runway and the Langley landing loads track would impose considerably smaller loads on the airplane. The implications regarding fatigue problems which may be caused by the different levels of roughness are self evident.

The effect of airplane taxi speed on the loads is illustrated in figure 4. The ordinate is the average acceleration amplitude resulting from traversing a given runway at a particular speed. The curves, again, are based on theoretical studies of taxiing over the four runways under consideration. The three experimental points shown were obtained from acceleration records of taxi tests of an F-100 airplane over runway X and give some confidence in the theoretical results. For reference, the straight line on the left represents the average acceleration amplitude from the VGH records of airline operations. Again, the rough taxiway is seen to be very rough. The accelerations for runway X are slightly above the national average throughout most of the speed range. The good commercial runway may begin to cause trouble at very high speeds. It is evident from these results that the variation of the acceleration with speed is closely dependent on the detailed characteristics of the runway. Thus, to answer one of our questions, there isn't much the pilot can do about reducing the loads on a rough runway except to taxi at very low speeds.

From the fact that runway X has caused complaints and also lies close to the national average, the airline data can be used to derive some rough inferences regarding the levels of acceleration that might be considered as limits for a satisfactory runway; on this basis, the average acceleration amplitudes for the usual range of operating speeds

should not exceed about $\frac{1}{8}g$ (fig. 4), and the maximum acceleration at speeds around 30 knots should not exceed about $\frac{1}{2}g$ (fig. 3).

Specification of Surface Smoothness

In the specification of runway-surface smoothness, current practice generally requires that the maximum deviation from a 10-foot straight edge shall not exceed $\frac{1}{8}$ inch. Frequently, a second requirement is specified - the deviation from the theoretical grade line shall not be more than ± 0.04 foot; that is, about $\pm \frac{1}{2}$ inch. A better way of specifying a runway can be suggested, and for this purpose, figure 5 is presented. By mathematical manipulation of the power spectra shown previously, the average peak amplitude σ' of the roughness within any given horizontal distance l can be determined. Such calculations have been made for three of the runways previously discussed. Unfortunately, this type of calculation was not possible for runway X because of certain limitations in the available data.

The derived curves for the commercial runway and the Langley landing-loads track are in close agreement with the actual specifications used for their construction. In the case of the commercial runway the calculated peak amplitude over 10 feet is 0.005 foot, which corresponds very closely with the $\frac{1}{8}$ -inch deviation from a 10-foot straight edge which was specified. In the case of the landing loads track, the calculated peak amplitude is practically constant and corresponds closely with the construction specification which limited the deviations to $\pm \frac{1}{8}$ inch from a given level surface throughout the entire length of the pavement.

The foregoing results suggest some new criteria for runway smoothness. Since a well-defined band of critical wave lengths exists, it must be taken into account by the specifications. Thus, deviations from a straight line must be limited over a length of 17 feet and over a length of 150 feet. In order to maintain control over the intermediate wave lengths, deviations over a length of 80 feet are also specified. As a specification for new construction, the commercial runway can be used as a guide, at least up to a length of 80 feet. At 150 feet a greater degree of smoothness should be obtainable so that a value closer to that of the Langley landing-loads track is specified. The values chosen for new construction are shown in figure 5 by the circles and are tabulated in terms of maximum deviation from a straight edge, in fractions of an inch. Over a 17-foot length, the maximum deviation $2\sigma'$ should not exceed $\frac{5}{32}$ inch; over an 80-foot length, the limit is

9/32 inch; and over a 150-foot length, the deviation should not exceed 11/32 inch.

Also needed is a guide to determine when a runway should be repaired. Working back from the airline data and the complaints regarding runway X has led to the conclusion that repairs are indicated when the deviations become about twice as large as those specified for new construction. The power spectra corresponding to these requirements are indicated by the two dotted lines superimposed on the spectra shown previously (fig. 6).

One last point should not be overlooked. Since airplanes spend about 80 percent of their taxi time on taxiways, it will be of little help to improve runways unless taxiways are similarly improved. It is therefore suggested that taxiways be built and maintained to the aforementioned specifications, with one exception. Since operation on taxiways will generally not be at the high speeds used on runways, the 150-foot requirement may be waived without detriment.

It goes without saying that the practice of using old abandoned rough runways as taxiways should be discouraged.

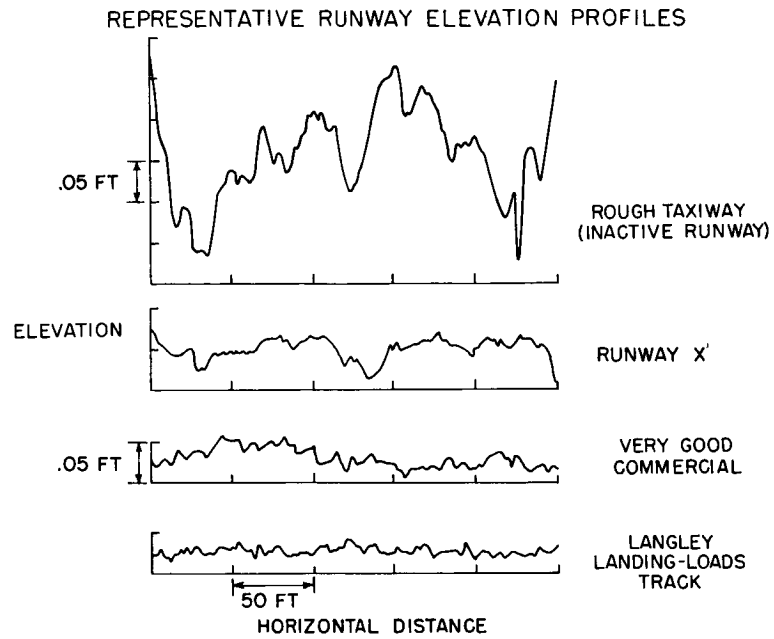


Figure 1

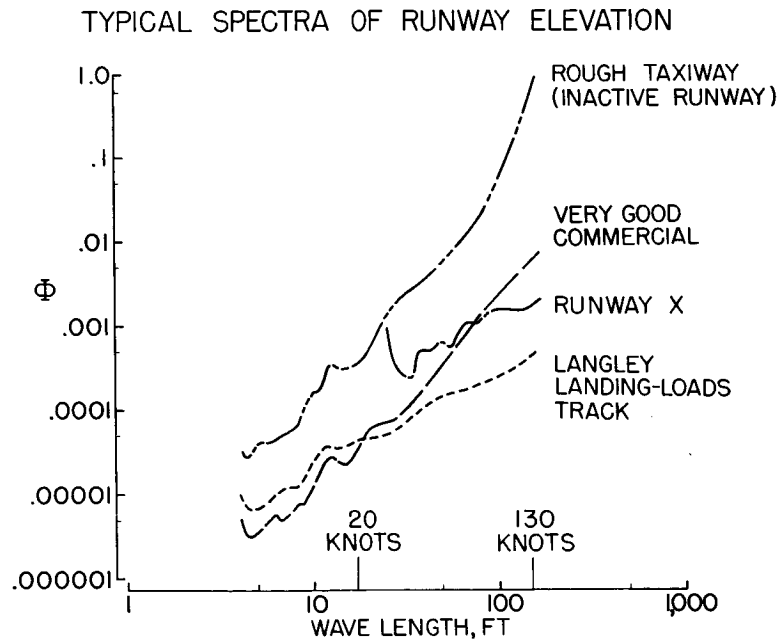


Figure 2

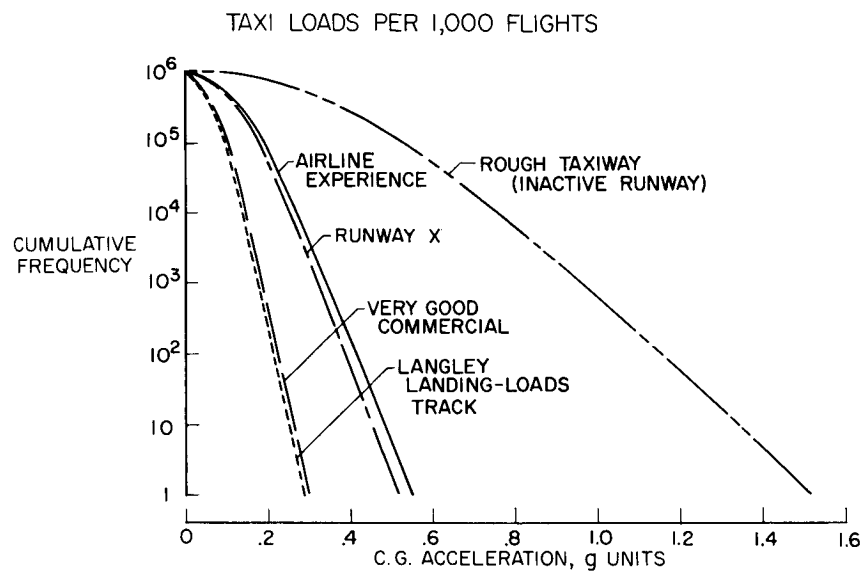


Figure 3

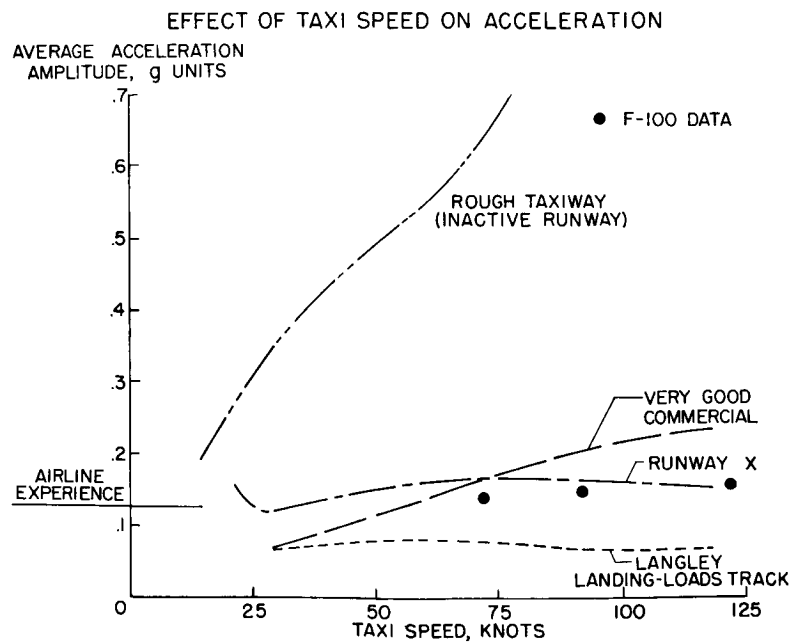


Figure 4

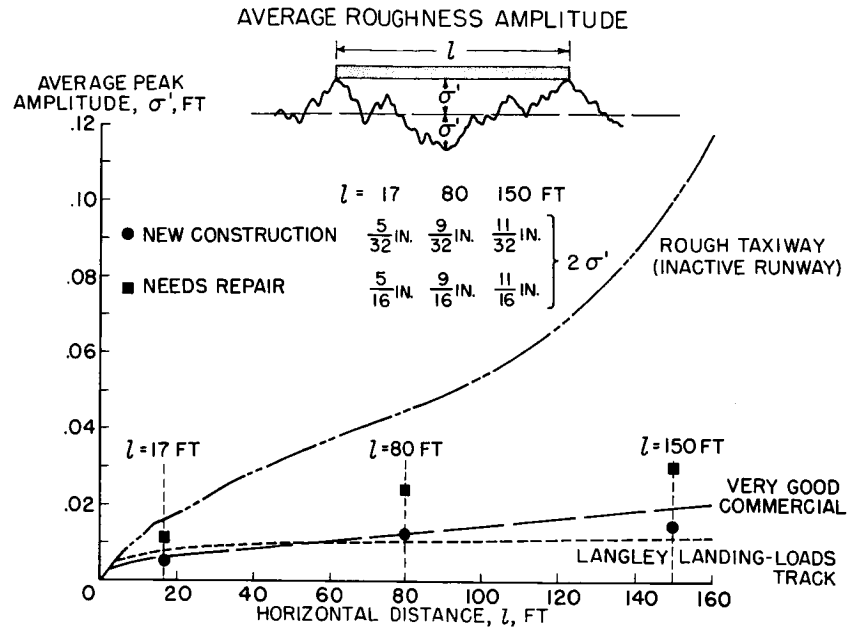


Figure 5

TYPICAL SPECTRA OF RUNWAY ELEVATION

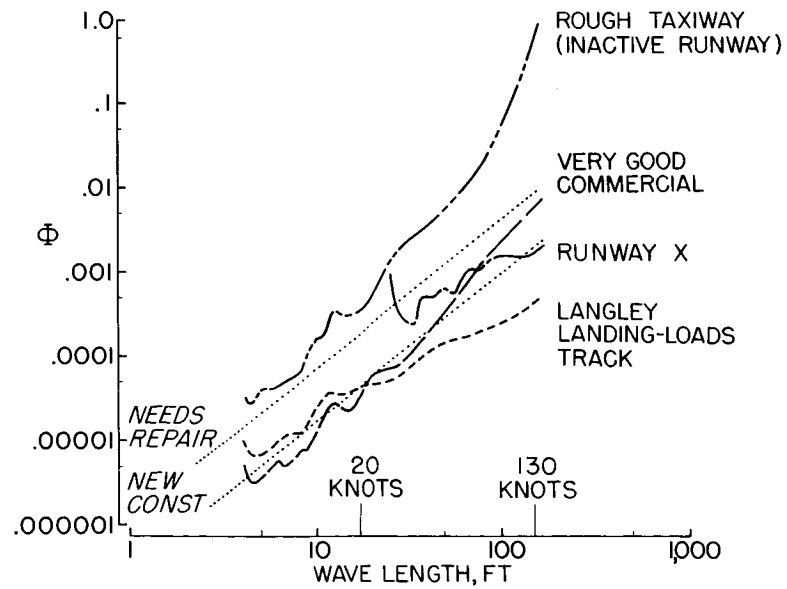


Figure 6

FLIGHT STUDIES OF PROBLEMS PERTINENT TO LOW-SPEED

OPERATION OF JET TRANSPORTS

By Jack Fischel, Stanley P. Butchart, Glenn H. Robinson,
and Robert A. Tremant

NASA High-Speed Flight Station

SUMMARY

Flight studies have been made of the low-speed operational regime of jet transports in order to assess potential operating problems. The study was performed utilizing a large multiengine jet airplane having geometric characteristics fairly representative of the jet transports; however, to insure general applicability of the results, the aerodynamic characteristics of the test airplane were varied to simulate a variety of jet-transport airplanes.

The specific areas investigated include those of the take-off and landing, and the relation of these maneuvers to the 1 g stall speed and stalling characteristics. The take-off studies included evaluation of the factors affecting the take-off speed and attitude, including the effects of premature rotation and of over-rotation on ground run required. The approach and landing studies pertained to such factors as: desirable lateral-directional damping characteristics; lateral-control requirements; space-positioning limitations during approach under VFR or IFR conditions and requirements for glide-path controls; and evaluation of factors affecting the pilot's choice of landing speeds.

Specific recommendations and some indication of desirable characteristics for the jet transports are advanced to alleviate possible operational difficulties or to improve operational performance in the low-speed range.

INTRODUCTION

There has been considerable speculation on the feasibility of extending current piston-engine transport operating techniques to the jet transport, both in the low- and the high-speed range. An investigation of the high-speed flight regime is reported in reference 1. In the low-speed flight regime, the specific areas of interest have pertained to take-off and landing, as outlined in table I. With regard to

the first item listed, some questions have been raised concerning the magnitude of take-off speed as related to the stall speed, the length of take-off run normally required for various loading conditions, and the effects of early rotation or over-rotation on the take-off run. The questions regarding the second item listed, airplane approach and landing characteristics, involve several factors pertaining to aircraft requirements and limitations, such as: lateral-directional damping requirements; lateral-control requirements; limitations on space-positioning during the landing approach under either VFR (visual flight rules) or IFR (instrument flight rules) conditions; requirements for use of glide-path controls; approach and landing speeds, and the factors affecting the pilot's choice of these speeds.

To investigate these aspects of take-off and landing, a flight study was performed at the NASA High-Speed Flight Station, utilizing a large multiengine jet airplane having geometric characteristics fairly representative of the jet transports. The test airplane had 35° swept wings of aspect ratio 7.1 and swept tail surfaces (fig. 1). For test purposes the airplane was equipped with a nose boom to measure airspeed, altitude, and directional flow angles. To simulate the aerodynamic characteristics of a variety of jet transport airplanes, various amounts of lateral-control power, glide-path control, and lateral-directional damping were utilized under conditions that might be encountered during transport operation in the low-speed flight regime.

SYMBOLS

a_n	normal acceleration, g units
b	wing span, ft
C_D	drag coefficient
C_m	pitching-moment coefficient
C_N	normal-force coefficient, $a_n W / qS$
F_a	lateral-control force, lb
F_e	longitudinal-control force, lb
F_r	rudder-pedal force, lb

Δh	height above runway, ft
h_p	pressure altitude, ft
i_t	stabilizer deflection, deg
P	period of lateral-directional oscillation, sec
p	roll rate, deg/sec or radians/sec
$pb/2V$	wing-tip helix angle, or lateral-control parameter, radians
q	dynamic pressure, lb/sq ft; pitching velocity, radians/sec
r	yawing velocity, radians/sec
S	airplane wing area, sq ft
$T_{1/2}$	time for lateral-directional oscillation to damp to 1/2 amplitude, sec
T_2	time for lateral-directional oscillation to double amplitude, sec
$T_{\phi=10^\circ}$	time to change bank angle 10° , sec
V	true velocity (except in ratio V/V_s), ft/sec
V_i	indicated calibrated airspeed, knots
V_s	indicated stall speed (from manufacturer's flight handbook), knots
V/V_s	ratio of indicated airspeed to indicated stall speed
W	airplane weight, lb
Y'	horizontal displacement of airplane from runway center line extended, ft
α_i	indicated angle of attack, deg
β_i	indicated angle of sideslip, deg
δ_e	elevator deflection, deg

δ_f flap deflection, deg
 δ_r rudder deflection, deg

DISCUSSION

Basic Aerodynamic and Stalling Characteristics

In the landing or take-off maneuver, the imminence of heavy buffeting, stalling, or other deleterious characteristics will require operational limitations to avert possible hazardous regimes or will impose additional requirements for safety of operation. Inasmuch as both landing and take-off speeds have been related to the 1g stall speed and stall characteristics of the unswept-wing piston-engine transports, the stall characteristics of the jet transports should be examined in the same light. Figures 2 and 3 illustrate the stalling and flight-determined aerodynamic characteristics of the test airplane in the take-off or approach configuration with a 30° flap deflection for a normal mid-center-of-gravity position and a wing loading of 68 pounds per square foot. Initial buffet occurred very near the peak value of normal-force coefficient attainable. This was followed by a mild pitch-up, as shown by the appreciable increase in angle of attack with no additional control input and even with a reversal of control force and deflection. Increased buffeting accompanied this phenomenon. It can be seen that the pitching-moment-coefficient curve approaches neutral stability in the pitch-up region; however, the pitching rates experienced during pitch-up were quite mild, and there was no tendency to roll off on one wing. Recovery was easily accomplished by applying power and relaxing the back pressure on the control column. As would be expected for any swept-wing configuration, the drag coefficient increased rapidly with increase in angle of attack; the magnitude of drag at $\alpha_i = 10^\circ$ to 12° was almost double that at $\alpha_i = 0^\circ$ to 2° .

A significant item to be noted from the data presented in figures 2 and 3 is the determination of the stall speed - defined by the occurrence of maximum airplane normal-force coefficient at a 1g condition - which occurred at an indicated speed of 123 knots and at a moderate angle of attack. A lower, but unusable, speed - approximately 114 knots - was attained in this maneuver by increasing the angle of attack beyond that for wing flow separation in the region where drag increased rapidly despite the decrease in wing lift and the airplane was at a condition of less than 1g and losing altitude. To illustrate, the sink rate attained in this maneuver at the minimum speed point was of the order of 2,500 feet per minute. Therefore, it is recommended

that the stall speed for the jet transports be based on maximum normal force or maximum lift as defined by wing stall, inasmuch as lower speeds attainable beyond this point are not usable close to the ground.

It should be noted that the stall speed as defined by this criterion is significantly higher than that specified in the manufacturer's flight handbook ($V_S \approx 103$ knots for the conditions specified in figs. 2 and 3). However, in order to discuss the take-off and landing evaluation on a basis compatible with existing and more familiar criteria, manufacturer's flight handbook values of stall speed are used as a reference in the remainder of this paper.

Factors Affecting Take-Off

In evaluating the factors affecting the take-off problem, items of primary concern are the length of runway required and the ratio of take-off to stall speed for the diverse loadings and operating conditions to be encountered in normal airline operation. Although the present study did not encompass all the conditions encountered in airline operation, several pertinent factors were evaluated. Figure 4 illustrates two take-offs of the test aircraft at essentially the same loading conditions. The solid lines show a normal take-off in which the nose wheel was lifted clear of the ground at about 5 knots below take-off speed. Subsequent to lifting of the nose wheel, the angle of attack increased rapidly and the airplane lifted off the ground. The dashed lines illustrate an early-rotation take-off, wherein the airplane was rotated at about the handbook stall speed V_S and an appreciable angle of attack was attained. After a few seconds the decrease in acceleration resulting from the increase in drag was quite noticeable to the pilot, so he relaxed his pull on the control column and the angle of attack decreased to allow improved acceleration. Several knots below the take-off speed, the aircraft was again rotated and it became airborne at a moderate angle of attack. In both instances, the angles of attack attained were below that for wing-flow separation. It is obvious that the take-off involving early rotation required more time and involved a greater take-off distance than a normal take-off. In contrast to the present piston-engine transports, which almost fly themselves off the ground with little rotation, it was found that swept-wing aircraft required rotation to become airborne.

A summary of the effects of early rotation during several take-off runs is shown in figure 5 as the variation of nose-wheel lift-off speed and airplane take-off speed, expressed as a fraction of V_S , plotted against take-off distance for a wing loading of 86 pounds per square foot. Each rectangular area shown here represents a grouping of several test points. It will be noted that normal nose-wheel lift-off occurred

near $1.2V_S$, with airplane lift-off occurring at a slightly higher speed after a take-off run of about 6,800 feet. By contrast, early nose-wheel lift-off occurred below $1.0V_S$, with airplane lift-off occurring near $1.3V_S$ after a much longer take-off run of about 9,000 feet. One point to note is the magnitude of the take-off distances recorded as compared with the length of existing runways at major airports throughout the United States (shown by the cross-hatched area at the bottom of fig. 5). For the early-rotation take-offs discussed, it is obvious that the airplane would not have become airborne before running off the end of the runway at several of these airports. No attempt was made to determine minimum take-off speed or distance; however, it was ascertained that take-off at a slightly higher speed than normally used facilitated a more rapid rate of climb and an impression of better handling characteristics, but required longer take-off distances.

The effect on take-off ground run of over-rotating the airplane even during a normal-type take-off can also be serious because of the excessive drag accompanying the use of large angles of attack. This effect is illustrated in figure 6 for $W/S = 111$ pounds per square foot and $\delta_f = 40^\circ$. The open circle showed where the airplane lifted off after a normal-type take-off at 9,500 feet. For the solid circle, take-off speed was attained at the same point as for normal rotation, but due to an over-rotation of about 2° to 3° , and after essentially maintaining this attitude, the airplane became airborne at a slightly higher speed and after an additional 3,500 feet of ground run.

Inasmuch as the pilot does not have a sufficiently accurate indication of airplane attitude once the nose wheel is off the ground, an angle-of-attack indicator was installed in the cockpit and used during some of these tests. The pilot found this indicator to be quite beneficial when coordinated with the other instrumentation, and it enabled him to attain proper take-off attitude at reasonable speeds below his intended take-off speed, and to avoid the large angles of attack that produce major increases in drag. He also found the angle-of-attack indicator useful for maintaining proper attitude for climb-out.

In general, if early nose-wheel lift-off is effected and the airplane is rotated to an appreciable attitude, a noticeable decrease in longitudinal acceleration is experienced with an attendant increase in the take-off distance; whereas, if the airplane attitude is maintained at a low angle until just a few knots below take-off speed, the acceleration to the take-off point and the take-off distance are not materially affected. However, without the use of some instrument such as an angle-of-attack indicator, the pilot does not have a sufficiently accurate indication of airplane attitude once the nose wheel is off the ground, and significant increases in take-off distance can result from over-rotation.

Approach and Landing Characteristics

Because of the appreciable dihedral effects exhibited by swept-wing aircraft, particularly at low speeds, and the slow rotational speeds encountered in this speed regime, it was felt that the dynamic lateral-directional characteristics and lateral control available would measurably affect the approach and landing characteristics of the swept-wing transports. To determine the desirable or usable levels of lateral control and yaw damping for the approach and landing regime, preliminary studies were made at low altitude to document the control and damping characteristics, and these characteristics were then evaluated in approach and landing maneuvers.

Dynamic lateral-directional characteristics.- In evaluating the lateral-directional characteristics, the test airplane was initially investigated without damper augmentation and with normal damper gain. In order to investigate the handling characteristics with significantly worse damping than that produced by the basic airframe, tests were also made with reversed damper setting. The dynamic lateral-directional characteristics of the test airplane for three yaw-damper gain settings and two flap configurations are shown in figure 7 as variations with indicated airspeed of the period of the oscillation and the time to damp the oscillation to half amplitude or to double the amplitude. It can be seen that the various damper settings had a slight effect on the period of the oscillation at all speeds and thereby slightly affected the apparent stability. Also, the basic aircraft exhibited essentially undamped (or neutrally damped) characteristics after an initial disturbance, whereas the reversed damper setting caused the lateral-directional oscillations to be highly divergent at all speeds. Although use of a dynamically unstable airplane is highly unlikely, reversed damper settings were used to determine minimum levels of stability which could be tolerated in emergency conditions.

In general, the basic airplane performed well in smooth air and did not present a problem from the viewpoint of lateral-directional dynamics. However, the pilots considered use of a yaw damper necessary, particularly after a course correction or in rough air where the high dihedral effect produced an appreciable amount of rolling when a directional oscillation was experienced. Since the period of the oscillation was reasonably long, it was possible to control the airplane in rough air with damper off and with damper reversed; however, with damper reversed much effort and cross-control coordination by the pilot were necessary and would result in considerable discomfort to passengers. For even the most divergent conditions investigated, the aircraft characteristics would not constitute an emergency condition at these low speeds.

Lateral-control characteristics.- Since the requirement for low-speed maneuvering is far more stringent than for high-speed maneuvering, it is felt that the low-speed regime will generally dictate the lateral-control requirements of the jet transport. Inasmuch as civilian requirements are not as specific as military requirements with regard to desirable control levels, it was thought that a measure should be made of lateral-control levels in terms of some criterion. To determine the suitability of various levels of lateral control, the test airplane was evaluated with several combinations of conventional trailing-edge ailerons and either inboard spoilers, outboard spoilers, or both sets of spoilers. Figure 8 presents a summary of the lateral control available with full control deflection for each of two flap configurations with the test airplane, and these results are presented in terms of several possible control criteria. The solid lines represent the rolling power when full ailerons and spoilers are used, and the dashed lines represent the rolling power when ailerons alone are used. With ailerons and either inboard or outboard spoilers available, the rolling characteristics are about midway between the solid and dashed curves shown. Comparative data for the B-47A airplane, which utilizes ailerons and flap-aileron for control power in the landing configuration, are presented on the right of figure 8. The improved roll performance of the test airplane with the spoiler-aileron combination as compared with that available with ailerons alone is readily apparent, regardless of the roll criteria used. The rolling power available with spoilers and ailerons on the test airplane and with controls on the B-47A, in terms of maximum roll rate and $pb/2V$, appears similar and also exceeds military specifications for such large aircraft, whereas the rolling power of the ailerons alone on the test airplane does not meet military specifications. However, even these high levels of lateral control produced on both airplanes appeared somewhat marginal in rough air during the final phases of landing, where small changes in bank angle are generally required and aircraft response becomes most important. The rolling power of the test airplane was appreciated by the pilot more than that of the B-47A because of its greater roll acceleration, as shown by comparing the plots of time to roll 10° , and also because the control-wheel rotation involved with full control deflection was appreciably less than on the B-47A. For the large transport-type airplane, it is felt that a suitable roll criterion for the landing configuration would be a specification for a given change in bank angle - such as 10° - within a finite time.

Space-positioning studies and evaluation of glide-path controls.- To determine the limits of aircraft controllability for performing the landing approach maneuver, both under VFR and ILS conditions, space-positioning studies were performed with the test airplane, utilizing various control techniques and various aircraft characteristics. Combinations of ailerons and spoilers were used to provide lateral control,

the lateral-directional damping was varied by appropriate damper settings, and various amounts of symmetrical spoiler projection were used as speed brakes to provide added control over the glide slope. Figure 9 shows a perspective of the space-positioning and landing-approach area used, extending from the outer marker to the runway, and the relation of this area to the runway. Beginning at the outer marker, which was 5 miles from the end of the runway, VFR approaches were attempted from various lateral displacements up to 6,000 feet from the runway center line extended, and from various vertical displacements up to 3,500 feet above the runway surface. When ILS approaches were evaluated, the lateral displacement limits were only 3,000 feet because this was the limit of the range. For all approaches, the airplane bank angle was limited to a maximum value of 30° .

For either visual or instrument conditions, the lateral control available with ailerons alone or ailerons and spoilers was adequate to permit normal landing approaches from any laterally displaced position at the outer marker up to the limits tested; however, when the spoilers were not available for use as glide-path controls, vertical displacements up to only about 3,000 feet could be used.

The various magnitudes of lateral-directional damping used had essentially no effect on the space-positioning limitations determined. Essentially similar effects were experienced with the basic and the positively damped airplane; however, pilot effort and control movement - particularly rudder control - exhibited a threefold increase when a reversed damper setting was used. (See figs. 10 and 11.) It is believed that much of this pilot effort and pedal force resulted from rudder-force feedback.

In all cases investigated, the airplane was maneuvered onto the glide slope from various vertical and lateral displacements before it was about 2 to 3 miles from the end of the runway. The use of glide-path controls (spoilers) made this task especially easy, but produced buffet similar to stall buffet at extremely low speeds. From the pilot's viewpoint, the use of glide-path controls in conjunction with higher throttle settings was more desirable for approach control than the technique of lower throttle settings with no glide-path control available. Further study of speed brakes for glide-path control in a penetration-type landing approach revealed that the time required from a 20,000-foot altitude to touchdown could be reduced by approximately $1/3$ through the use of glide-path controls. (See fig. 12.)

When performing the landing approaches under ILS conditions, the pilot felt he was using the controls and working to a greater extent than when operating under VFR conditions from comparable positions at the outer marker; however, the flight records did not support this

contention. Also, the flight speeds in IFR approaches were more nearly constant but of the same order of magnitude as during VFR approaches.

Final approach and touchdown.- In the final phases of the approach, the piloting technique for control of airspeed and altitude was gradually changed so that the throttle was used for altitude control and the elevator was used for control of airspeed. This technique became mandatory as the touchdown was approached and provided adequate control of the aircraft rate of descent. Although the controllability problem was not evaluated up to the present weather minimums of 200 feet at 1/2 mile from touchdown, the altitude at the 1/2-mile point (which was generally about 12 seconds from touchdown) ranged up to 128 feet with accompanying sink rates up to 1,100 feet per minute. Also, despite the fact that the vertical velocity at touchdown ranged as high as $7\frac{1}{2}$ feet per second, most touchdowns were performed at a rate of descent of less than 3 feet per second. These values of time, vertical velocity, and altitude, near touchdown, emphasize the range of controllability required for such large aircraft. As might be anticipated, the rates of descent and the altitude levels in the approach and landing were considerably lower under ILS flight conditions than under visual approaches.

The level of airspeeds utilized during the approach and touchdown under VFR conditions is shown in figure 13 for a flap deflection of 50° . At the 1/2-mile point, represented by the open symbols, the airspeeds generally were in the range of $1.45V_S$ to $1.55V_S$ because of the improved longitudinal and lateral controllability as compared with lower speeds. At touchdown, represented by the solid symbols, the airspeeds were in the range of $1.27V_S$ to $1.37V_S$ and in the "bucket" of the drag curve where the lift-drag ratio was essentially maximum. The imminence of buffet and more difficult control of sink rate at lower speeds influenced the choice of these touchdown speeds. During ILS approaches, a smaller flap deflection was maintained nearer to touchdown than for VFR conditions. At the 1/2-mile point, the level of airspeed was generally about $1.4V_S$ to $1.45V_S$, and the pilot preferred to maintain the smaller flap deflection and this airspeed until he established visual contact to insure a better go-around capability. Thereafter, additional flap deflection was added and the speed was decreased in the flare.

Although it was possible to perform the approach and landing with a constant stabilizer trim setting without encountering elevator control forces greater than about 20 pounds, the pilot found it more comfortable to use the stabilizer to reduce the control forces, maintaining just sufficient force to provide control feel. Lateral-directional damping had essentially no effect on the pilot's ability to perform the landing maneuver; however, greatly increased effort and concentration were required for the dynamically divergent damper configuration, as previously mentioned. In the final stages of landing, the level of

lateral control produced by ailerons alone appeared inadequate because of the requirements for compensating for cross-wind effects. With the lateral control power of the ailerons and spoilers, control was marginal in rough air because of the time required to raise a low wing in the proximity of the runway. With cross winds of the order of 12 to 15 knots, a significant amount of lateral control up to the maximum available was utilized during landing and after touchdown.

In performing landings with appreciable crosswinds, a crabbed heading into the wind could be maintained to touchdown, but the pilot found this uncomfortable. Using the crabbed heading up to the 1/2-mile point and then performing a slight sideslip to maintain the flight path to touchdown proved to be a better technique.

CONCLUSIONS

An investigation of the low-speed operational area of large jet transport airplanes resulted in the following conclusions and recommendations:

1. Stall speed should be based on maximum airplane lift at a 1g condition, inasmuch as minimum speeds attainable only with attendant high sink rates are not realistic.
2. Early nose-wheel lift-off and rotation of the airplane to appreciable values of angle of attack or over-rotation at the proper take-off speed produced increases in take-off distance which could affect the success of the take-off. An angle-of-attack indicator helped the pilot attain proper airplane attitude at take-off speed so that optimum take-off and climb-out could be accomplished and large angles of attack that produce considerable drag could be avoided.
3. Space positioning under VFR conditions from various realistic final-approach positions can be limited by inadequate glide-path control, but was not limited by the minimum levels of lateral-control power and lateral-directional damping of the investigation.
4. Approach speeds at 1/2 mile from touchdown were about $1.45V_S$ to $1.55V_S$ (where V_S is handbook stall speed) because of the improved longitudinal and lateral controllability as compared with lower speeds. Imminence of buffet and more difficult control of sink rate at lower speeds influenced the choice of touchdown speeds; these speeds ranged from $1.27V_S$ to $1.37V_S$, which corresponded to near-maximum lift-drag ratio.

5. Lateral-control power will be dictated by the requirements of the landing maneuver because of the high dihedral effect and low response rates. It is felt that a suitable criterion for adequate lateral control in the landing configuration would be a specification for a given change in bank angle - such as 10° - within a finite time.

6. Although lateral-directional dynamic instability within the limits investigated could be controlled during approach and landing because of the reasonably long period of the oscillation, this condition should be considered for emergency use only, and positive damping is recommended, especially in turbulent air.

REFERENCE

1. Butchart, Stanley P., Fischel, Jack, Tremant, Robert A., and Robinson, Glenn H.: Flight Studies of Problems Pertinent to High-Speed Operation of Jet Transports. (Prospective NASA paper.)

TABLE I

OUTLINE OF LOW-SPEED JET-TRANSPORT STUDIES

1. FACTORS AFFECTING TAKE-OFF SPEED AND ATTITUDE
2. AIRPLANE APPROACH AND LANDING CHARACTERISTICS
 - a. EFFECTS OF YAW DAMPING ON LATERAL-DIRECTIONAL CHARACTERISTICS
 - b. LATERAL CONTROL REQUIREMENTS
 - c. SPACE POSITIONING DURING LANDING APPROACH, INCLUDING IFR OPERATIONS
 - d. EFFECTIVENESS OF GLIDE-PATH AND SPEED CONTROLS
 - e. FACTORS AFFECTING CHOICE OF LANDING SPEEDS

TEST AIRPLANE

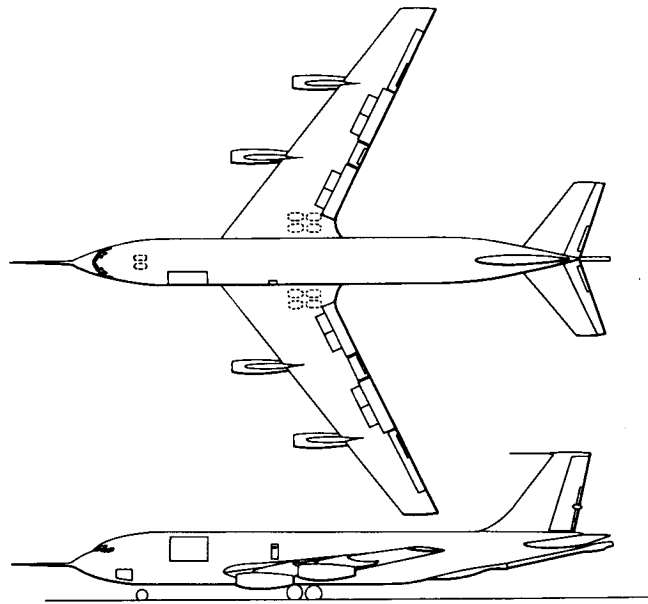


Figure 1

STALL TIME HISTORY

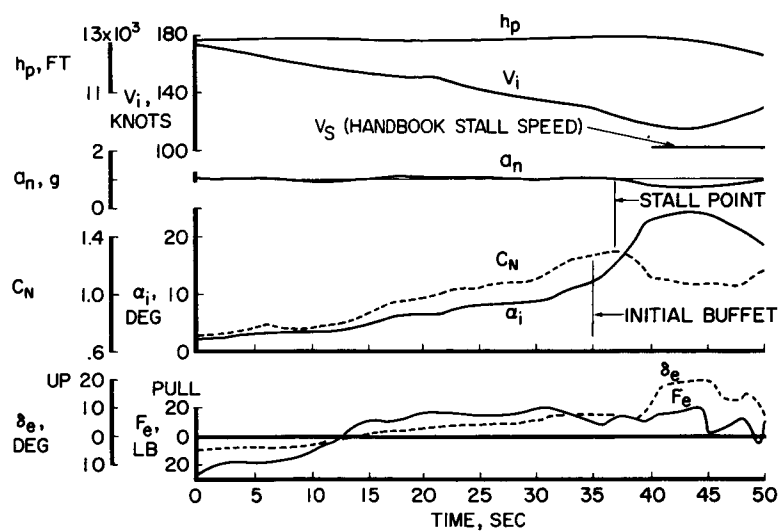
 $\delta_f = 30^\circ$ $CG = 26\% \text{ MAC}$ $W/S = 68 \text{ LB/SQ FT}$


Figure 2

BASIC AERODYNAMIC CHARACTERISTICS

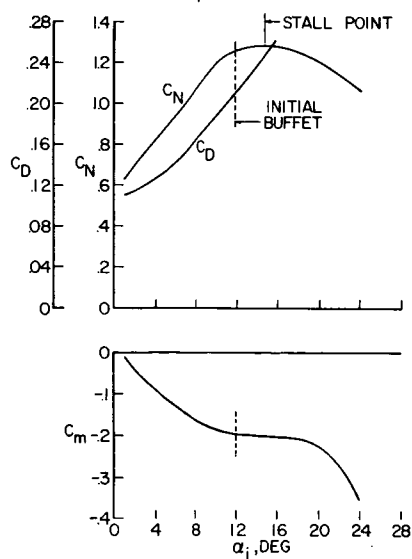
 $\delta_f = 30^\circ$


Figure 3

EFFECT OF EARLY ROTATION ON TAKE-OFF PERFORMANCE

$\delta_f = 30^\circ$

$W/S = 86 \text{ LB/SQ FT}$

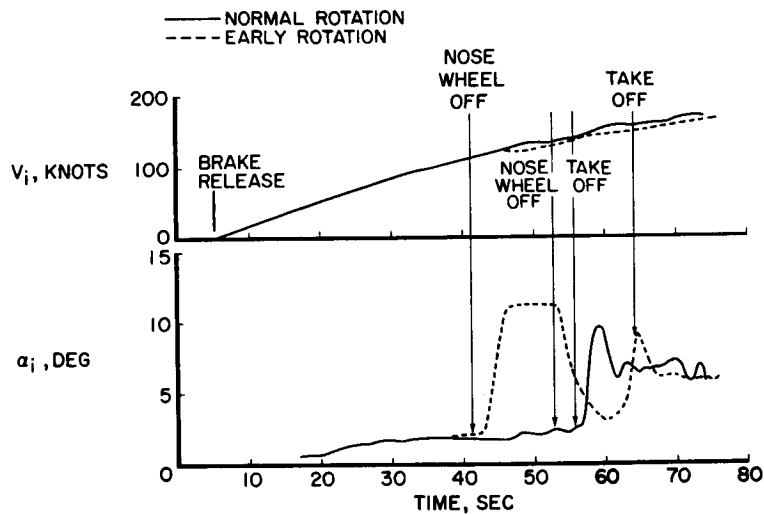


Figure 4

EFFECT OF EARLY ROTATION ON TAKE-OFF PERFORMANCE

$\delta_f = 30^\circ$

$W/S = 86 \text{ LB/SQ FT}$

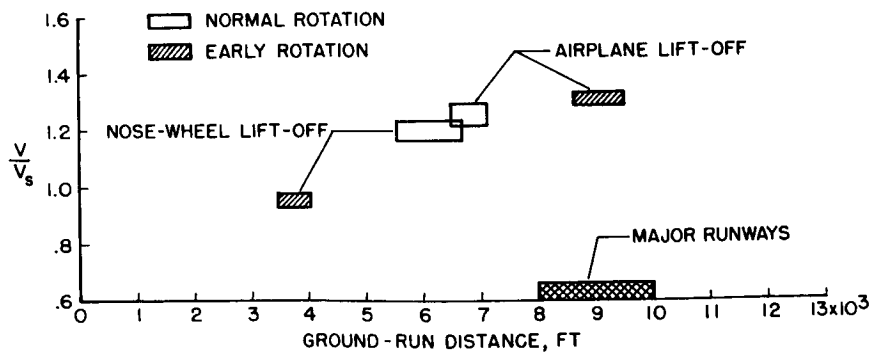


Figure 5

EFFECT OF OVER-ROTATION ON TAKE-OFF PERFORMANCE

 $\delta_f = 40^\circ$ W/S = 111 LB/SQ FT

○ NORMAL ROTATION

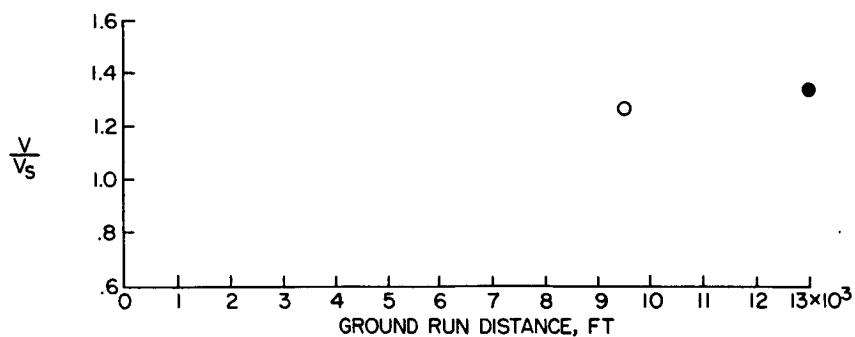
● 2° TO 3° OVER-ROTATION

Figure 6

LATERAL-DIRECTIONAL DYNAMIC CHARACTERISTICS

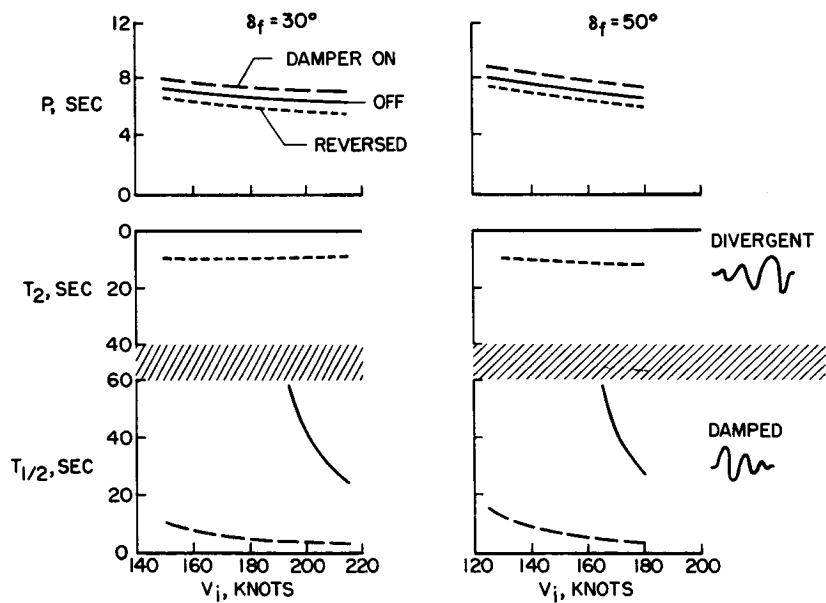


Figure 7

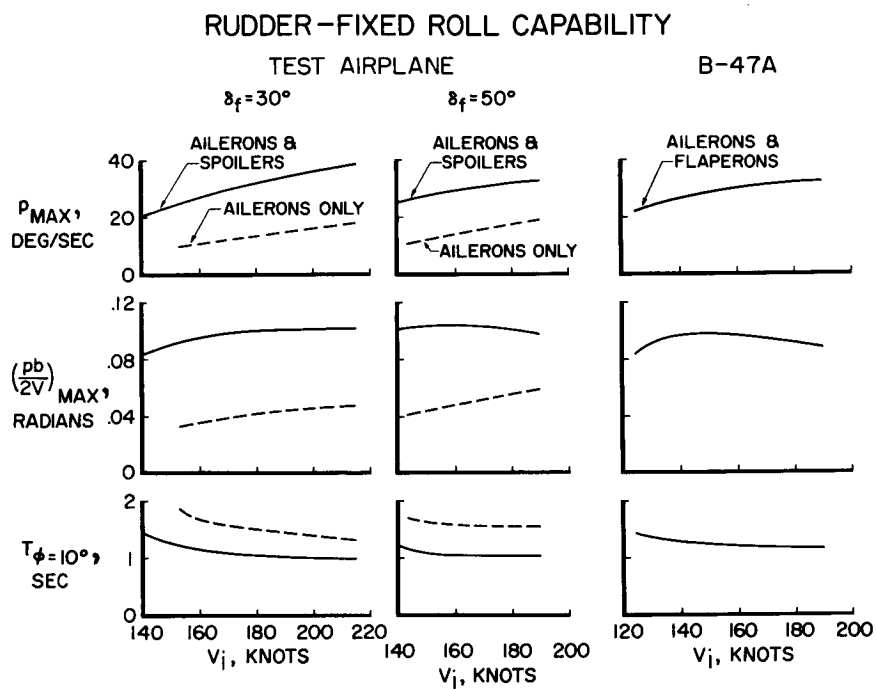


Figure 8

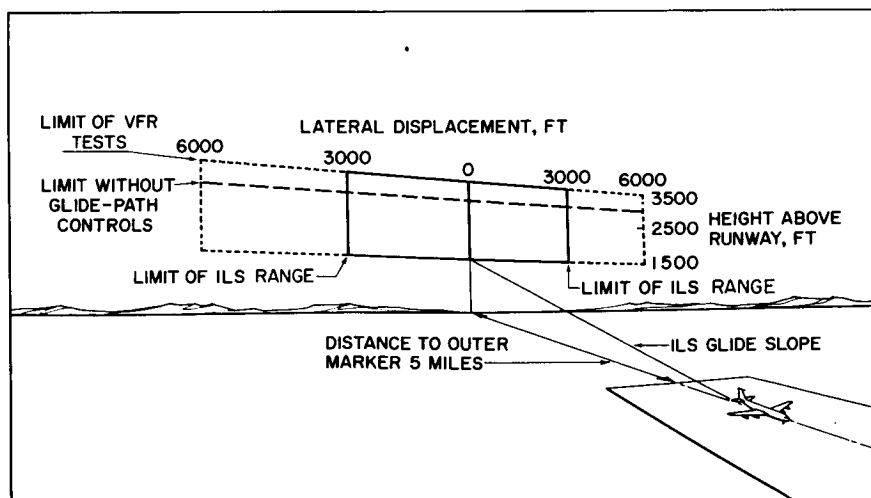
SPACE-POSITIONING EVALUATION

Figure 9

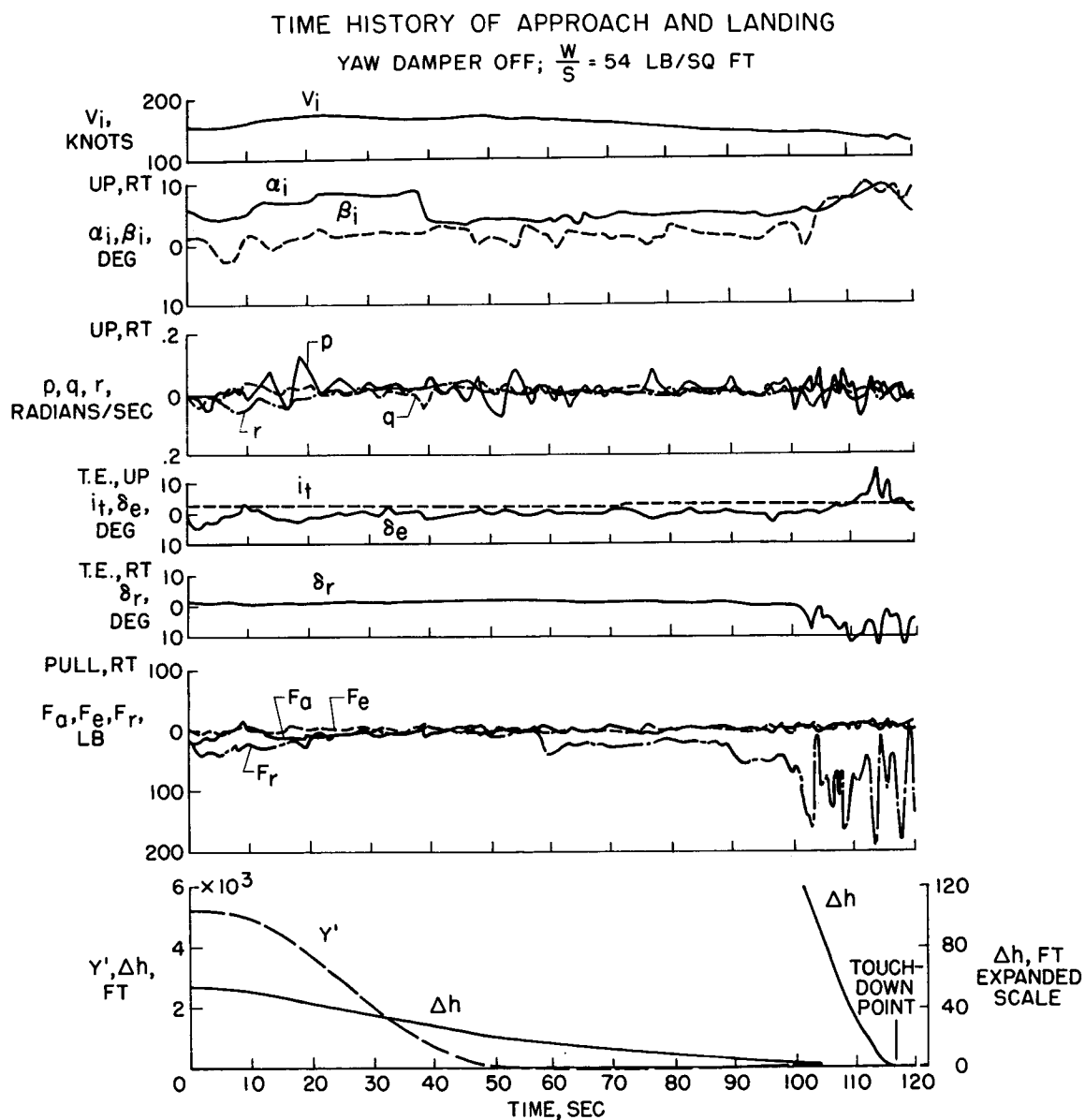


Figure 10

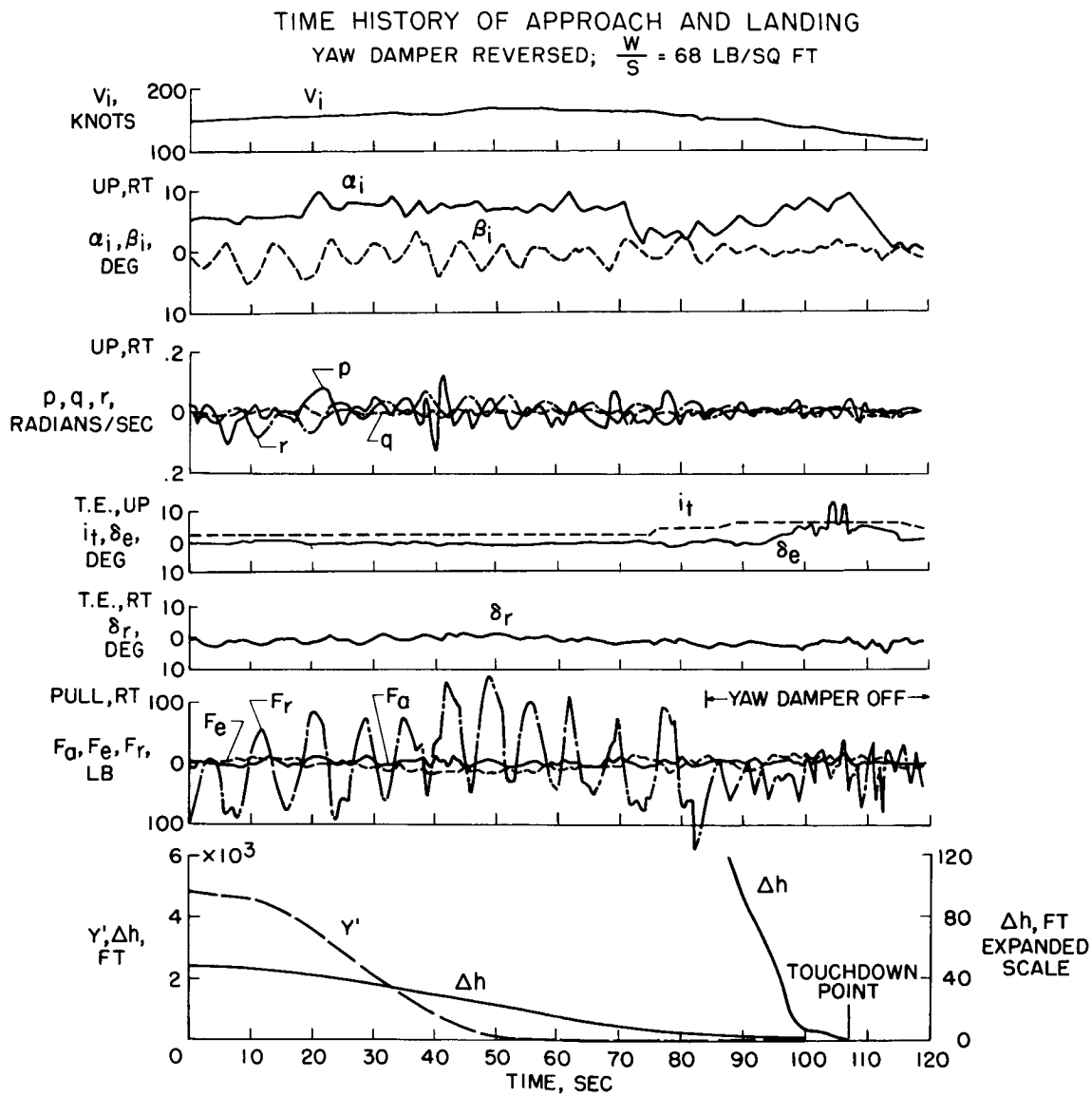


Figure 11

EFFECTIVENESS OF GLIDE-PATH CONTROLS PENETRATION-TYPE LANDING APPROACH

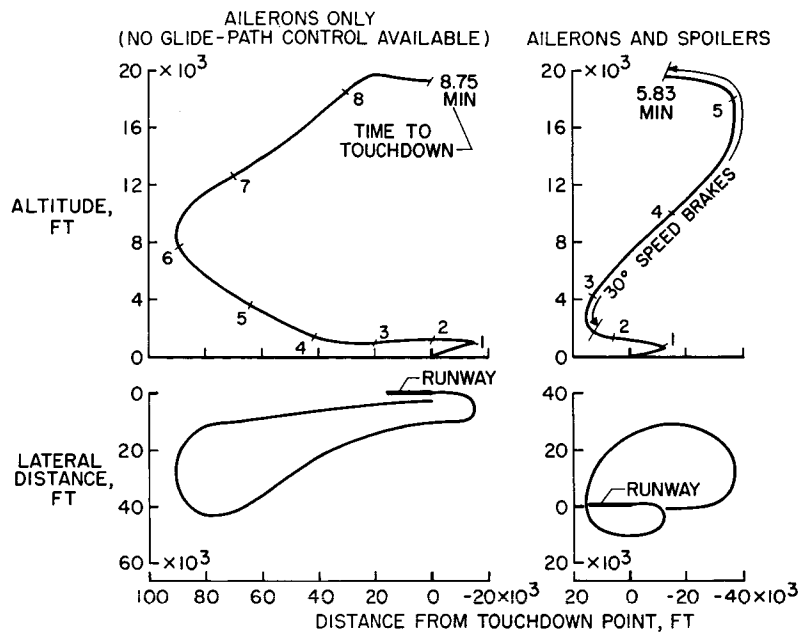


Figure 12

AIRPLANE APPROACH VELOCITY

 $\delta_f = 50^\circ$

VFR CONDITIONS

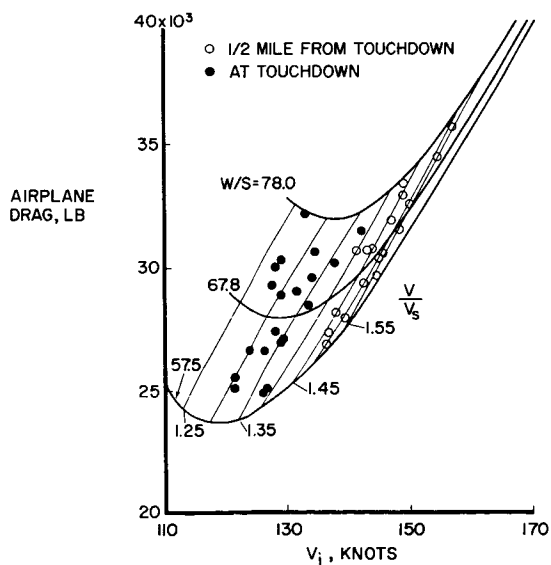


Figure 13

SOME POSSIBLE DEVELOPMENTS IN VTOL TRANSPORT AIRCRAFT

By Marion O. McKinney, Jr.

Langley Research Center

INTRODUCTION

The purpose of this paper is to give the reader some "feel" for the types of vertical-take-off-and-landing (VTOL) transport aircraft that might be developed in the future. A discussion is included of three types of VTOL aircraft that are now undergoing extensive research and development and have already undergone flight tests in the flying-test-bed stage. Some speculations on the extrapolation of these three general types of VTOL aircraft to possible future transport aircraft are presented and some figures on physical characteristics and performance are given to indicate what the VTOL feature might cost. It should be emphasized that this paper is not intended to be an all-inclusive presentation covering every possible type of VTOL aircraft and every field of application but is intended only to give the reader some background for anticipating possible developments in the field.

UNLOADED ROTOR CONVERTIPLANE CONFIGURATION

The unloaded rotor convertiplane has received considerable attention over the past few years and a flight-test vehicle, the McDonnell XV-1, has been flight tested throughout the entire range of operations. A photograph of the XV-1 is shown in figure 1. It has a helicopter-type rotor driven by pressure jets for use in hovering and low speed flight and has a fixed wing and pusher propeller for cruising flight. In hovering flight all the power is applied to the rotor, and the machine is essentially a helicopter. In cruising flight all the power is applied to the propeller, and the rotor autorotates and supplies only about 15 percent of the lift while the wing supports most of the weight. In the transition condition between hovering and cruising flight, power is gradually shifted over from the rotor to the propeller, or vice versa.

The unloaded rotor configuration is already being developed into an operational transport in England as the Fairey Rotodyne which is shown in figure 2. This machine, which Fairey calls the "First VTOL Airliner," can seat up to 48 passengers. It is powered by two Napier Eland engines, of about 3,500 horsepower each, which drive either the tractor propellers or air compressors that provide compressed air to the pressure jets on

the rotor tips. The Rotodyne is evidently intended for a dual mission. One mission is to serve as a feeder-line transport to provide service to small communities which have no airport suitable for the operation of conventional transport airplanes. The other mission is to provide rapid transportation between city centers up to several hundred miles apart by operating from downtown heliports rather than from the more remote airports required for conventional airplanes. For example, the time between downtown air terminals in London and Paris is about four hours by Viscount and would be about two hours by Rotodyne.

One question that always comes up in connection with VTOL aircraft is, how much extra is the VTOL feature going to cost. Some idea of the cost for this type of aircraft might be gained by comparing the Rotodyne with the Fairchild F-27 transport which is shown in figure 3. The F-27 is a very modern feeder-line transport with good short-field performance and is of a size directly comparable with the Rotodyne. It should be possible therefore to get a fairly accurate direct comparison of the VTOL and conventional transport. Some pertinent figures for comparison are given in table I. The data for the F-27 were taken from "Aviation Week" and those for the Rotodyne from the "Aeroplane." These data show that the Rotodyne is slightly heavier, has a lower cruising speed, and has a shorter range with the same payload than the Fairchild airplane. It is evident that the operating cost of the heavier, more powerful, and more complicated VTOL aircraft will be greater than that of the conventional transport. The advantage of the VTOL machine must therefore come entirely from the VTOL feature itself and must offset its poorer performance and higher operating cost. In this case it would seem that, except in the case of routes over water, the Rotodyne type machine is not so much in competition with conventional feeder-line transports as it is in competition with surface transportation over routes for which air transportation is not now competing or is not competing successfully. An example of such use is operation over short distances between large cities such as New York and Philadelphia where the travel time to the airports makes air transportation slower than surface transportation or over routes from big city airports to smaller surrounding communities not now served by air transportation.

PROPELLER-POWERED VTOL

The tilting-wing-and-propeller VTOL configuration is a very attractive configuration that is receiving considerable attention from a number of aircraft manufacturers. A flight-test vehicle of this general type, the Vertol 76 airplane, is shown in figure 4. In this configuration the wing is at approximately 90° incidence for take-off and landing

and is rotated slowly to approximately 0° incidence in making the transition to normal forward flight. With the wing at 0° incidence the aircraft is essentially a conventional airplane. This machine has already been flown in hovering flight, has made vertical take-offs and landings, and has repeatedly made the transition from hovering to normal forward flight and back to hovering.

No actual VTOL transport airplane of this type is either built or under construction. Some idea of how a VTOL transport based on this principle might look, however, may be gained from figure 5 which shows a drawing of a transport design by one of the aircraft manufacturers. This design has four large propellers driven by turboprop engines and has auxiliary jet engines at the rear of the fuselage for pitch control in hovering flight. The artist has indicated the operation of the airplane from a heliport located on a pier over water near the center of a city. This type of facility might offer an interesting solution to a number of the operating problems of such an aircraft.

The cost of the VTOL feature in this class of airplane is indicated in table II. The data in the right-hand column present some calculated characteristics of a hypothetical VTOL transport and those in the left-hand column present the calculated characteristics of a conventional turboprop transport laid out to carry the same payload for the same distance. Since it was necessary to use calculated characteristics for the VTOL transport, it seemed fairer to compare them with calculated figures for a hypothetical conventional transport based on the same estimation procedures than to compare them with the actual characteristics of a real airplane. This comparison shows that the VTOL transport required to carry a payload of 50 passengers and their baggage for a range of 900 nautical miles at a cruising speed of 400 knots is about 25 percent heavier and has twice the horsepower of a conventional transport designed for exactly the same mission. The additional power and larger propellers of the VTOL airplane are reflected in its greater empty weight; and the additional gross weight and the somewhat lower propeller efficiency of the oversize propellers of the VTOL airplane are reflected in the additional fuel required. From these data it is apparent that the operating cost of the VTOL transport would be greater than that of the conventional transport because of the greater initial cost and maintenance cost of the heavier, more complicated, and more powerful machine and because of the greater fuel usage of the VTOL airplane. Since this propeller-powered VTOL transport has performance directly comparable with that of a conventional propeller-powered short-haul transport, it can offer considerably faster service between the downtown areas of cities by operating from close-in heliports. This faster service, together with savings in the cost of transportation to and from the airport, may largely offset the higher operating cost of the VTOL airplane.

JET-POWERED VTOL

For a transport airplane a horizontal fuselage attitude seems to be essential. A horizontal-attitude jet VTOL test vehicle which has already been flown in both hovering and normal forward flight and has successfully performed the transition between these conditions is the Bell X-14 airplane shown in figure 6. This machine is powered by two Armstrong Siddely Viper turbojet engines mounted horizontally in the lower forward part of the fuselage. The exhaust of these engines is turned directly downward beneath the center of gravity by means of thrust-diverter vanes to provide the lift for hovering flight. The thrust-diverter vanes are rotated to divert the exhaust backward at progressively larger angles during the transition until the aircraft is wing-borne and the exhaust is directed straight rearward for normal forward flight as a conventional jet airplane. Control in hovering flight is provided by controllable compressed air jets at the wing tips and tail.

Most of the design studies that have been performed for jet VTOL transports have involved a very long step to the case of a supersonic transport. The results of one such design study which has received considerable publicity is the Rolls Royce design shown in figure 7. With a supersonic transport the static thrust of the engines required to propel the airplane in the cruise condition is far less than the weight of the airplane; thus, it seems desirable to make up the deficiency in thrust with a number of special lightweight lifting engines arranged along the side of the passenger compartment. These lifting engines would probably be relatively small, since the best engine specific weight is obtained with fairly small engines, and would probably be turbofan engines with a bypass ratio of about 5 to keep the noise and exhaust velocity relatively low. Even with such engines, however, the noise and the tremendous energy in the exhaust of this large number of engines would undoubtedly constitute formidable problems.

In order to obtain some indication of the cost of the VTOL feature in this class of airplane the two transports indicated in figure 8 were laid out. They were both laid out for a cruising speed of $M = 3$, a gross weight of 400,000 pounds, and a payload of 120 passengers and their baggage. The sketch at the top shows a supersonic configuration designed for normal take-off and landing. This configuration has a wing loading of 65 pounds per square foot which will permit landings at the same speeds as current subsonic jet transports, and it requires 7 engines of a certain size for propulsion in the cruise condition. The lower sketch shows a VTOL configuration with 44 lifting engines located along the side of the fuselage and 6 propulsion engines located in wing-tip nacelles which can be tilted to a vertical position for take-off and

landing. Since this configuration does not rely on the wing for landing, the size of the wing could be made the optimum size for the supersonic cruise condition which, in this particular case, gave a wing loading of 110 pounds per square foot.

Some of the estimated characteristics of these two configurations are shown in table III. They were laid out for the same gross weight and payload, and they have essentially the same empty weight and fuel load and range. The fact that the VTOL configuration has the same empty weight as the conventional configuration in spite of all the lifting engines is, at first, surprising. The three primary factors that enter into this weight picture are that the VTOL configuration has 2,500 square feet less wing area, it requires one less propulsion engine, and it has a much lighter landing gear. The lower landing-gear weight is in line with estimates made by aircraft manufacturers working in the VTOL field; however, since the landing gear is not designed for high-speed rolling take-offs and landings, it probably will be necessary to devise new ground handling procedures to take advantage of this possibility of weight saving.

The main point brought out by table III is that for this class of airplane (the supersonic jet transport) the VTOL airplane is about the same size as the conventional airplane designed for the same mission. The VTOL airplane, however, will obviously be more expensive in initial cost and maintenance because of the lifting engines.

CONCLUDING REMARKS

In conclusion it might be pointed out that VTOL transports seem to be technically feasible and can have good enough performance to be considered for commercial operation, but there is considerable research and development, particularly full-scale flight research to be done before such aircraft can seriously be considered for commercial operation. It also seems that VTOL transports will have higher operating costs than conventional transports. Whether the increased utility of the VTOL aircraft will offset the increased cost and in what fields of application is an open question at the present time.

TABLE I

FEEDER - LINE TRANSPORTS

	FAIRCHILD F-27	FAIREY ROTODYNE
GROSS WEIGHT, LB	35,700	39,000
CRUISING SPEED, KNOTS	230	160
RANGE,* NAUT. MI.	430	260

* WITH 40 PASSENGERS, BAGGAGE, AND RESERVES.

TABLE II

SHORT-HAUL TURBOPROP TRANSPORTS

	CONVENTIONAL	VTOL
GROSS WEIGHT, LB	47,000	60,000
EMPTY WEIGHT, LB	27,700	38,000
FUEL WEIGHT, LB	8,800	10,700
PAYLOAD,* LB	10,500	10,500
HORSEPOWER	8,000	16,000
CRUISING SPEED, KNOTS	400	400
RANGE (WITH RESERVES), NAUT. MI.	900	900

* WITH 50 PASSENGERS AND BAGGAGE

TABLE III

SUPERSONIC TRANSPORTS

	CONVENTIONAL	VTOL
PAYLOAD, LB	26,000	26,000
EMPTY WEIGHT, LB	160,000	158,000
FUEL WEIGHT, LB	206,000	208,000
RANGE (NO RESERVES), NAUT. MI.	3,700	3,800

McDONNELL XV-1



Figure 1

FAIREY ROTODYNE



Figure 2

ROLLS ROYCE SUPERSONIC VTOL TRANSPORT

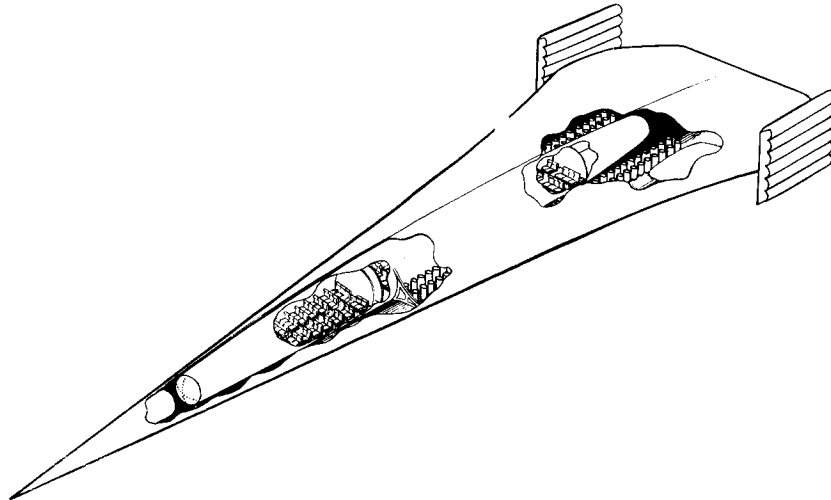
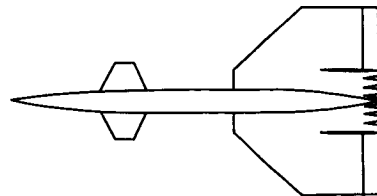


Figure 7

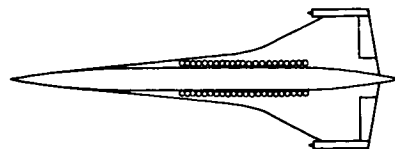
SUPERSONIC TRANSPORTS

CRUISING SPEED, $M = 3.0$
 GROSS WEIGHT = 400,000 LB
 PAYLOAD = 120 PASSENGERS



CONVENTIONAL

W/S = 65 LB/SQ FT
 7 ENGINES



VTOL

W/S = 110 LB/SQ FT
 6 PROPULSION ENGINES
 44 LIFTING ENGINES

Figure 8

TURBOPROP VTOL TRANSPORT

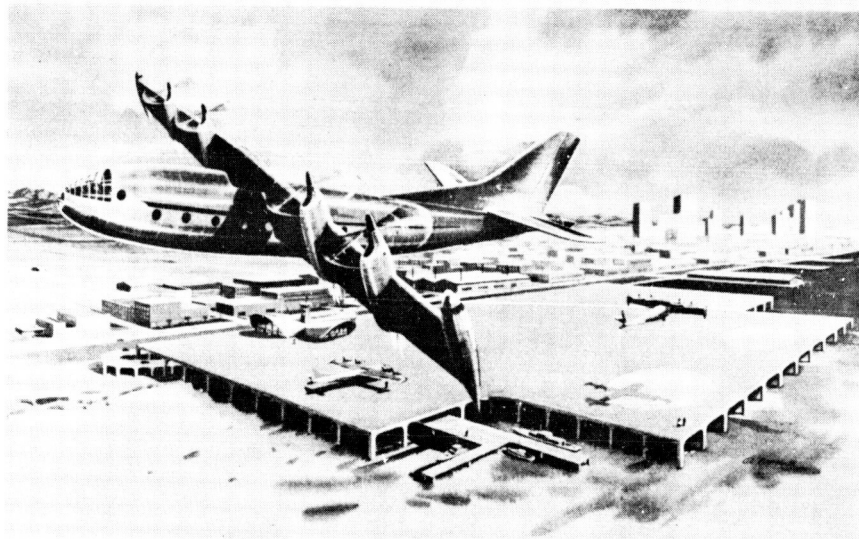


Figure 5

BELL X-14

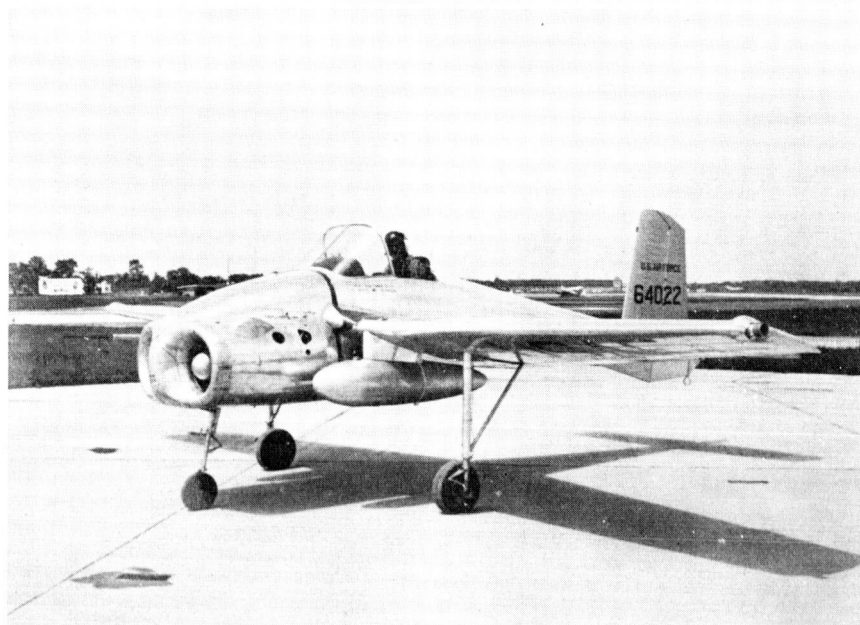


Figure 6

FAIRCHILD F-27

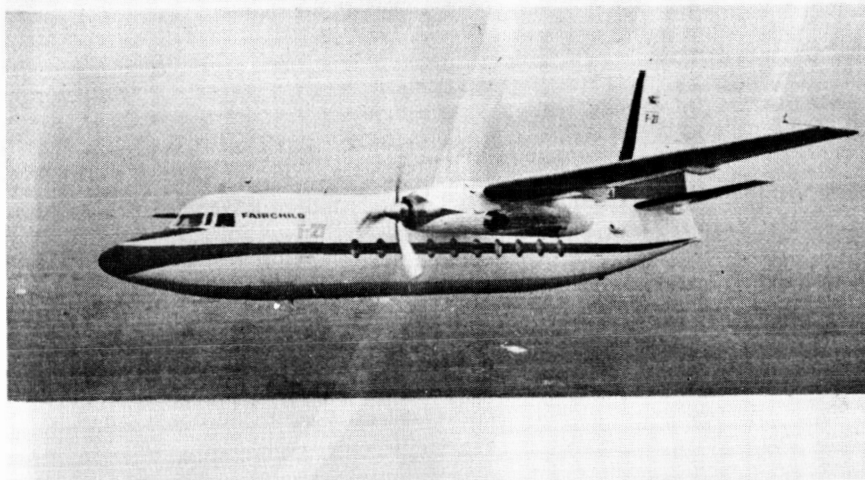


Figure 3

VERTOL 76



Figure 4

USE OF FLIGHT SIMULATORS FOR PILOT-CONTROL PROBLEMS

By George A. Rathert, Jr., Brent Y. Creer,
and Joseph G. Douvillier, Jr.

Ames Research Center

SUMMARY

Comparisons have been made between actual flight results and results obtained with fixed and moving flight simulators in a number of phases of flying airplanes with a wide range of characteristics. These results have been used to study the importance of providing motion stimuli in a simulator in order that the pilot operate the simulator in a realistic manner. Regions of airplane characteristics where motion stimuli are either mandatory or desirable are indicated.

INTRODUCTION

Since real flying is becoming more complicated and expensive, it is necessary to look to flight simulators for an economical means to train pilots and give them realistic practice to maintain their proficiency. Such simulators are finding increasing use in aeromedical research, airplane and systems design, and training; however, they vary widely in type - from a man on a chair in front of an oscilloscope to multimillion-dollar centrifuges. For example, there are two types of training simulators. One, called a procedure trainer, is an exact duplicate of an existing cockpit and is used chiefly to teach instrument layout and specific operating procedures. The other, the type discussed herein, might be called a proficiency trainer because its object is to give the pilot realistic practice in operating the flight controls and in observing the airplane response. Obviously, the value of this equipment to the pilot being trained is greatly enhanced if the right type is chosen, that is, the equipment which makes him use the same inputs and develop the same responses that he would in actual flight. A number of factors which affect this choice have been encountered in various research projects which will be reviewed in order to discuss the extent of simulation required to present certain flying tasks realistically.

DISCUSSION

General Considerations

Figure 1 is a diagram of a typical pilot-operated simulator. The solid-line upper portion shows the basic elements of the fixed simulator and shows the pilot in a cockpit with controls he can move. These control motions are fed into a computer which computes the proper airplane response and the corresponding display information which is then shown to the pilot by the instruments in the cockpit. These visual cues from the instruments are the pilot's only input.

The next stage of refinement is indicated in figure 1 by the dashed-line lower portion. The computer supplies the computed airplane motions to a device which provides motion cues in addition to the visual cues from the instruments. This device can take several forms, with the most common form being a servodriven cockpit or centrifuge which fully reproduces some combination of the correct angular and linear motions. Another less complicated device is a restricted-travel cockpit which supplies a much smaller initial movement but in the correct sense to help the pilot's judgment. Also, there are fixed simulators enclosed in spherical screens on which a moving outside world and horizon are projected. The pilot is given a strong visual illusion of motion like the effect of Cinerama.

In each of these devices the principle is the same; that is, the pilot is shown the instrument display as it would be in actual flight, and he is also placed under motion conditions that may or may not be near those of flight depending on the capability of the simulator. The main problem in choosing a particular training simulator then is the extent of completeness necessary to give the pilot the information he needs to solve his flight problem. Typical questions that might arise concern the extent that the motion stimulus affects the pilot's ability to control bank angle or to damp out a pitching motion and the extent that a given instrument display is influenced by the presence of a motion stimulus as well as by a visual stimulus.

Up to the present time these problems have been examined at the Ames Research Center with the aid of three pieces of motion-simulation equipment. In addition to using numerous production airplanes, variable-stability airplanes have been used in flight to subject the pilot to all six freedoms of motion over a wide level of oscillatory and steady-state conditions. The pilot's capabilities in flight then have been compared with those on various fixed simulators where no motion inputs are present. Also, these tasks have been repeated with, to date, two degrees of rotational motion of the cockpit (pitching and rolling). Although this work is being extended to other more complete motion simulators,

the present results have shown that the importance of motion input is directly a function of the type of task presented to the pilot.

The various piloting tasks where comparisons have been drawn between flight and simulators are landing approach, longitudinal dynamics, longitudinal control, lateral dynamics, instrument presentation, and simulation of particular airplanes. In some of these cases, motion inputs were not necessary. In others, the motion cues were useful and helped the pilot solve his problem more realistically. In still other cases the use of a motion stimulus was mandatory; without it completely wrong or reversed answers were obtained.

Landing-Approach Problem

The landing-approach problem is considered first. Approaches made with the Instrument Landing System were simulated in a wide variety of dynamically stable airplanes in order to study the factors affecting the pilot's choice of approach speed. The scope of this work has been indicated in a previous paper by Fred J. Drinkwater III, Maurice D. White, and George E. Cooper. With regard to the simulator the situation is fairly straightforward. In a landing-approach simulation the critical piece of information that must be given to the pilot is his rate of sink. This can be done by visual instrument alone and no motion inputs are necessary. This does not mean that the pilot would not like motion or use it if given to him. It means that he can get by without it. Here and elsewhere the emphasis is on the distinction between a mandatory stimulus and a merely desirable stimulus.

The degree of correlation between actual flight and the fixed simulator is illustrated in figure 2. The speed chosen when performing the approach on the simulator is shown plotted against the approach speed chosen by the pilots in flight. This correlation was obtained through tests covering 12 airplane configurations and several research and service pilots. There are two qualifications: First, these tests did not cover airplanes with unstable or significantly nonlinear aerodynamics in the landing-approach configuration; and second (a more general qualification), in this and other simulator studies the pilots found it valuable first to simulate an airplane that they had actually flown recently so that they could get the feel of the simulator and then calibrate themselves to build up their confidence. These results and the others discussed were obtained following such a conditioning process, and it appears to be an important step in getting the pilot's cooperation and in using a simulator really successfully.

Longitudinal Dynamics

In the study of longitudinal dynamics numerous studies of flying qualities are made in which test pilots are asked to fly widely different airplane configurations and rate the different combinations according to their desirability. In doing this they fly various standard maneuvers and perform such precision tasks as tracking and formation flying. By comparing their ratings from flight and simulators, some insight is given as to how well the simulator reproduces actual flight in these areas. A typical result is shown in figure 3 which is a cross plot of longitudinal-dynamic-stability parameters with the short-period frequency plotted against the damping ratio. The solid-line curves show the results of an inflight study made by the Cornell Aeronautical Laboratory on a variable-stability airplane. The pilot has designated regions where he regarded the short-period frequency and damping combinations as good, acceptable, poor, and unacceptable. The broken lines show the results of a similar study on a fixed simulator at Ames with different pilots.

The agreement between the two studies is good in the region of moderate frequencies and good damping corresponding to present-day conventional airplanes; therefore, the fixed simulator appears to be very realistic. At short-period frequencies above 0.6 cps, however, the simulator becomes much easier to fly than the airplane and is obviously not realistic. Such a high natural frequency implies a rapid airplane response to the controls, which then feed back to the pilot motions which become increasingly difficult to cope with as the frequency increases and the damping deteriorates. It is interesting to take a data point in this region of high frequency and low damping and quote the full opinion of the Cornell pilot: "Initial response fast and abrupt. Constant short-period oscillation which pilot excites. Must let go of stick to damp out oscillations. Overshoots load factor. Requires constant attention." These comments are typical effects of motion feedback that is too rapid for the pilot to cope with. A moving cockpit with sufficient performance to operate in this region is just now being completed; thus, whether adding the pitching motion alone without vertical or longitudinal accelerations will result in a satisfactory simulation has not yet been determined. However, it is apparent that a fixed simulator is not adequate to train the pilot to cope with airplanes which fly in this region.

Longitudinal-Control System

Considerably intertwined with this subject is the question of the characteristics of the longitudinal-control system. A modified airplane has been flown at the Ames Research Center in which the pilot can vary the static stick gearing or stick force per g, the time constant of the dynamic response, and the breakout force and again select the preferred combinations. A portion of these results is shown in figure 4 where for

two different pilots the maximum-acceptable, the best-available, and the minimum-acceptable time constants have been plotted against stick force per g. This is the equivalent first-order time constant of the control system, the time required for the control surface to reach 63 percent of the steady-state response to a step input of stick force. Broadly speaking, the maximum-acceptable time constant is the value above which the pilot considers the control response too sluggish and the minimum-acceptable time response is the value below which it is too sensitive. It should be pointed out that these results are for constant airframe aerodynamics which appear in the "poor" range in figure 3. The flight results are shown by solid-line curves and, again, the companion fixed-simulator study is shown by dashed-line curves.

In comparing the two pilots, it is interesting to note that the honest difference in opinion between them in flight, shown by the solid-line curves, is accurately reflected in their simulator results, shown by the dashed-line curves. Also, it appears that the fixed simulator is reasonably realistic in the range of interest. One exception must be emphasized in the lower left-hand corner of these figures where the pilot has a rapidly responding control and very high control sensitivity or low stick force per g. In actual flight with pitching motion and acceleration feedback present, the pilot-control-system-airplane combination became unstable and a pilot-induced oscillation was encountered which again could be stopped only by releasing the stick. In the fixed simulator with the motion feedbacks not present, although the pilot correctly derated the combination with a low opinion, he did not encounter any self-induced oscillations. If this problem is of particular concern, then motion or acceleration feedbacks appear to be mandatory. These results were obtained on highly maneuverable fighters; but, even with transports, if it is desired to train pilots to cope with upset maneuvers or damper failures, the regions in figures 3 and 4 where the airplane in question appears should be determined.

Lateral Dynamics

The next pilot task considered is lateral dynamics. A recent study suggested that two important parameters influencing pilot opinion were the roll-damping and roll-control power. Pilot-opinion boundaries based on these two parameters were derived from tests which stressed two very important phases of lateral control: the maximum roll acceleration and rate capabilities desired by the pilot, and the precision of roll control in terms of ability to change bank angle rapidly and stabilize.

The results of the lateral-dynamics study are shown in figure 5. The constant pilot-opinion boundaries are shown as a function of a roll-damping parameter and a roll-control-power parameter. Flight results are shown by a solid-line curve, the moving simulator by a dash-dot

curve, and the fixed simulator by a dashed-line curve. The agreement between all three is satisfactory in the desirable normal operating region where most of the real airplanes that were flight tested appeared. However, the two simulator results diverge very rapidly at higher rolling accelerations, a result indicating that the fixed simulator becomes very unrealistic. It should be noted that a logarithmic scale is used in figure 5. Pilot opinions indicate that, in the region where the fixed simulator is not realistic, the primary difficulty is in obtaining precise control of the bank angle. As this region is entered, the control movement that the pilot has to make to change his bank angle precisely is changing from a simple pulse to a rapid sinusoid. It is easy to conjecture that, at these rolling accelerations, of the order of 500° per second², the actual environment of a rolling cockpit is mandatory in order to reproduce the difficulty of the control problem realistically.

Another point of interest is that, at very low rolling rates encountered in a sluggish airplane, the moving simulator is easier to fly than the fixed simulator because the motion cues, particularly the acceleration, help the pilot considerably. Again, in order to make these results meaningful in connection with the simulation of a transport airplane, it would be necessary to examine possible critical maneuvers such as collision avoidance or emergency corrections to the Instrument Landing System, to determine the rolling performance actually used, and to see where a particular airplane appears in figure 5.

Instrument Presentation

Instrument presentation is as interesting as it is controversial. The simulator work discussed concerns presentation of the attitude of the airplane, especially bank angle, to the pilot. The example shown (see fig. 6) consists of two alternative fire-control-system presentations shown to the pilot on an oscilloscope. The one on the left consists of a reference circle fixed with respect to the instrument case and a moving target dot displaced from the center of the circle according to the position of the target relative to the attacker. The pilot tracks the moving target dot with the fixed circle the same as he would track a visual target with a fixed sight ring. In the presentation on the right the target symbol, indicated by a small dash, is fixed in the center of the scope. The attacker is represented by an inverted T displaced from the fixed target according to their relative positions. The pilot tracks by flying the "drone" on to the fixed bar. The matter of concern is the bank-angle presentation. In the case on the left side of figure 6 the bank angle is presented by an artificial gyro horizon; that is, the bar remains parallel to the true horizon while the instrument case (with its reference marks, the pilot, and the airplane) rolls around it. This is called an inside-out presentation. In the case on the right side of figure 6 the bank angle is indicated by the angle between the wings of

the drone and the fixed line across the instrument case which, of course, rolls with the airplane. This is called an outside-in presentation, the view that the pilot would get from a platform behind his airplane. The essential difference between the two is shown by imagining the relative motions involved in the lower two sketches of the presentations in a right-wing-down bank angle of 45° with the target on the horizon to the right. In the inside-out case the target dot is on the horizon but it is displaced to the right, the view that the pilot would get from his window. In this version of the outside-in presentation the drone is banked 45° with respect to the reference bar but 90° with respect to the true visible horizon and is displaced to the left.

As shown in figure 7 both of these presentations have been compared by using flight tests, a moving simulator cockpit driven in pitch and roll, and a fixed simulator. Each of the curves is a composite time history of the radial aim error averaged over about 15 tests. A vertical line divides the time into two regions of the tracking maneuver, a straight nonmaneuvering tail chase and a breakaway into an accelerated turn. It can be seen that in the fixed-simulator results no differences between the presentations appear. The type of presentation did not affect the pilot's performance. In the flight tests during the nonmaneuvering portion the results were the same. In the maneuvering portion of the flight, however, the pilot's performance deteriorated markedly with the outside-in presentation, and the fixed-simulator results are obviously not realistic. In fact, with the use of two experienced test pilots thoroughly trained in standard instrument-flying techniques, the outside-in presentation in some cases actually produced symptoms of vertigo in the maneuvering portion of the test. The pilots attributed the vertigo to the fact that they were getting a visual cue in conflict with the motion stimulus, which was, of course, not present in the fixed simulator. In the rolling-cockpit simulator the comparison between the two presentations is more like that in flight, but it is still not satisfactory. The specific motion and visual cues which produce this very marked effect have not all been traced as yet. It seems apparent, however, that fixed simulation of certain types of instrument presentations for pilot training in maneuvering flight should be viewed very carefully until more is known about this subject.

Complete Flight Simulation of a Particular Airplane

The final category to be discussed is the complete flight simulation of a particular airplane. This is the stage in which all the piloting tasks discussed previously are combined and the various interaction effects are encountered. Unfortunately, research directly applicable to transport airplanes is very limited since nearly all research projects have involved fairly exotic types such as vertical take-off and landing airplanes, the X-15, the X-18, and various satellite and reentry

configurations. However, one principle that is pertinent has been encountered repeatedly. Either in flight or in a simulator increasing demands are, of course, made on the pilot's concentration as he is asked to control the airplane in three dimensions and perform a number of tasks simultaneously. In flight the pilot meets this challenge by concentrating on the obviously difficult tasks and by taking care of the others by instinctive or set behavior patterns. Some of these instinctive responses can be based on rather subtle inputs; in order to achieve a realistic simulator, the pilot must be given the inputs he actually uses or he may be burdened excessively.

One simple example is a satellite-reentry problem in which the pilot was asked to fly at a specified pitch attitude presented to him by an instrument and at the same time maintain his lateral balance with a rather poor control system. The problem was first studied in a fixed simulator which substituted an artificial-horizon instrument for the actual rolling-motion stimulus. In order to perceive a bank-angle error, the pilot had to wait for it to develop on the instrument, make a corrective control motion, wait to observe its effect on the instrument, and so on. This took so much of his concentration that he found the pitch control unsatisfactory and in some cases impossible to cope with. When just the actual rolling motion was added to the cockpit, the pilot could feel even a small roll acceleration instantly through the seat of his pants and could maintain his lateral balance almost instinctively. This left him free to cope with the identical pitch problem satisfactorily, and his opinion of the longitudinal-control system was quite different.

CONCLUDING REMARKS

Comparisons have been made between actual flights and flight-simulator studies in a number of phases of flying airplanes with a wide range of characteristics. There are regions where some form of motion stimulus is desirable or mandatory in order that the pilot operate the simulator realistically, particularly for pitch- and roll-control systems with a sensitive rapid response to control movements and for instrument presentations in maneuvering flight. In a broad range of airplane characteristics that might be termed conventional, however, the fixed simulator with adequate instrument presentation appears to be a realistic and useful device for pilot-proficiency training.

BLOCK DIAGRAM OF SIMULATOR

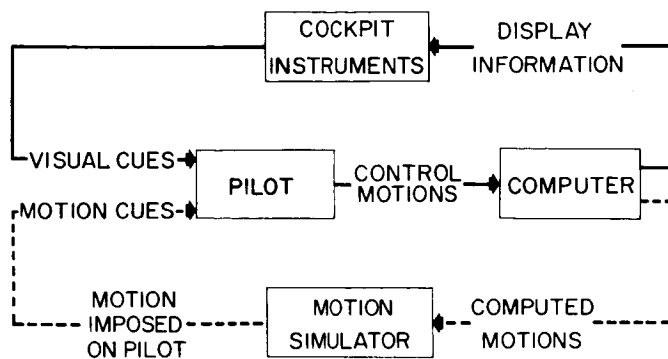


Figure 1

LANDING APPROACH SPEED CHOSEN

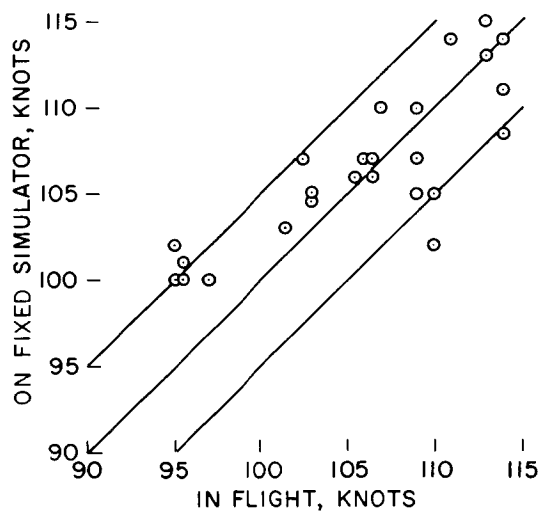


Figure 2

LONGITUDINAL DYNAMICS

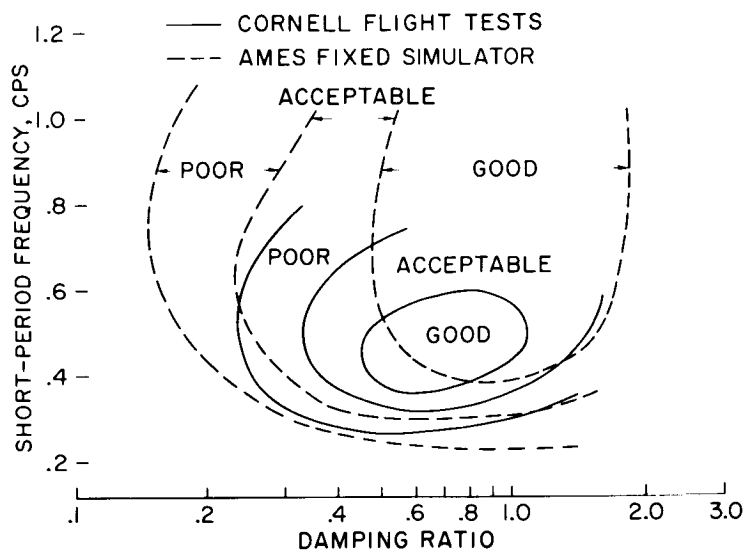


Figure 3

LONGITUDINAL CONTROL

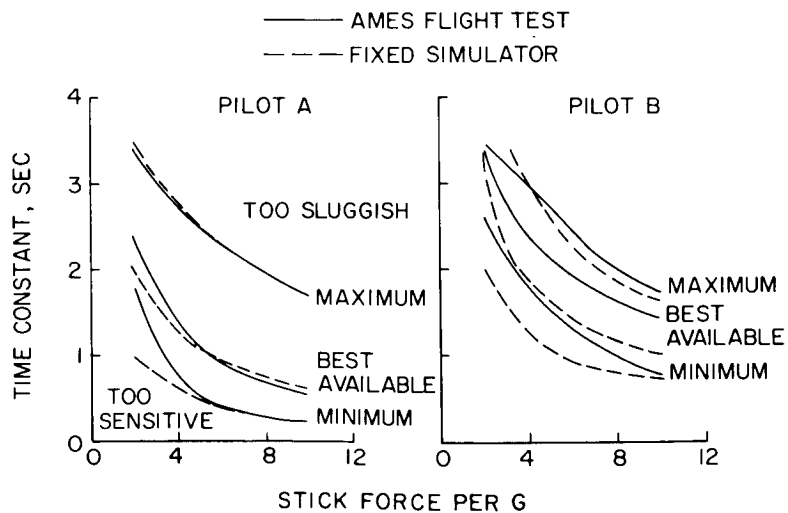


Figure 4

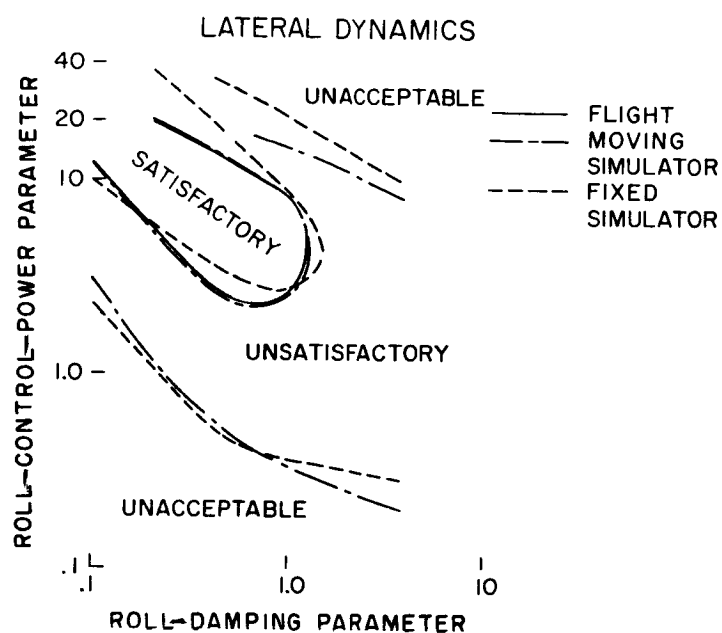


Figure 5

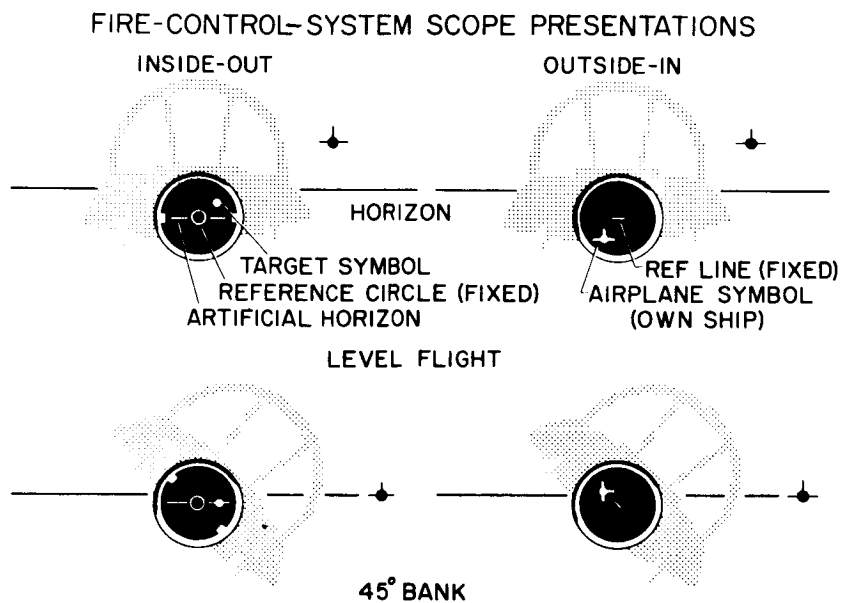


Figure 6

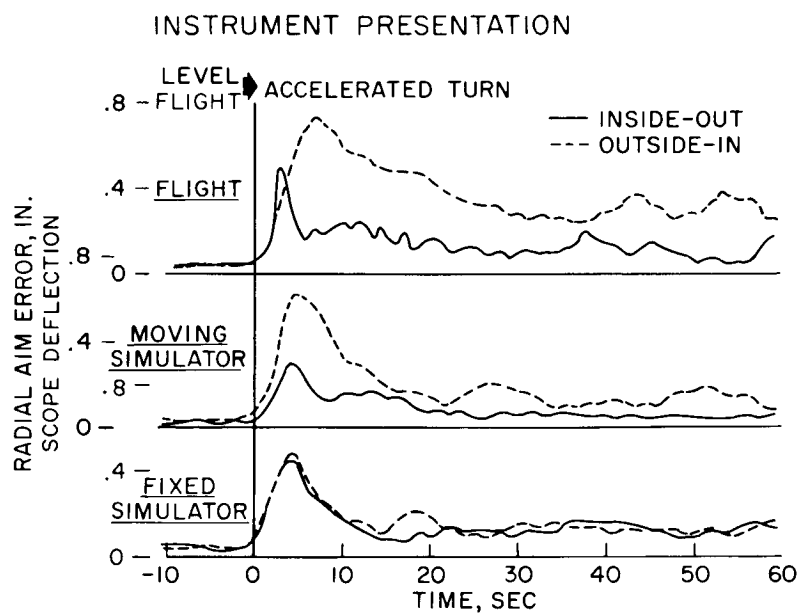


Figure 7

FLYING QUALITIES ASSOCIATED WITH ELECTRONIC FLIGHT CONTROL SYSTEMS

By S. A. Sjöberg

Langley Research Center

INTRODUCTION

The purpose of this paper is to discuss some flight research on the flying qualities associated with electronic flight control systems. With the type of control system to be discussed, there is no fixed relationship between the pilot's stick position and the control surface position as with conventional control systems. Rather a pilot's stick motion commands a proportional change in some airplane response quantity, for example, pitching velocity or normal acceleration. These control systems have certain advantages in overcoming unsatisfactory aerodynamic stability and control characteristics and also they can provide flying qualities features not ordinarily present with conventional controls. With several military airplanes which fly through very large speed and altitude ranges it has been found necessary to use control systems of the type to be discussed in order to provide acceptable flying qualities at all flight conditions.

CONTROL SYSTEMS

Figure 1 shows how control systems of the type used operate. The control system shown in figure 1 is for longitudinal control. Similar systems have been used for lateral and directional control. With this control system a pilot's stick motion simply generates an electrical signal which is proportional to stick deflection. There is no mechanical connection between the stick and the elevator. The electrical signal from the stick causes the actuator to move the elevator. The sensors (which, for example, may be a rate gyro or an accelerometer or both) measure the airplane motion and feed back an electrical signal which opposes the signal from the stick. For this discussion, assume an accelerometer is the primary feedback sensor. Then when the feedback signal from the accelerometer is equal to the stick signal, a steady value of normal acceleration is achieved. Thus, with this control system, a given stick deflection produces a proportional change in airplane normal acceleration and, furthermore, the acceleration for a given stick deflection is the same at any speed, altitude, or center-of-gravity position.

In the absence of any pilot's stick motion the control system acts like a conventional autopilot in that the sensors detect any airplane motion and cause the actuator to move the elevator to stop the motion.

Longitudinal control systems have been tested in which normal acceleration, pitch rate, and pitch attitude were the quantities which were proportional to the pilot's stick deflection. The normal acceleration and pitch rate systems were found to be superior to the pitch attitude system for a maneuvering control. Therefore this paper is concerned only with these two systems. Most of the flight results to be presented are for the normal-acceleration system but much of the discussion is equally applicable to a "pitch-rate" type of control system. Also, it should be mentioned that a pitch damper was used with the normal-acceleration control system to provide increased damping. In conjunction with the longitudinal-control systems, a roll-rate system was used for lateral control and a yaw damper was used in the directional-control system.

The airplane used in the flight investigations was a Grumman F9F-2. This airplane is a subsonic jet-propelled fighter. The range of flight conditions covered was from stalling speeds up to a Mach number of about 0.8 and from low altitude up to about 35,000 feet. Although most of the work done has been directed toward highly maneuverable airplanes such as fighters, many of the results are applicable to any type of airplane.

One of the flight test programs with the F9F-2 was an investigation of the use of the electronic control systems for stabilizing an airplane having static longitudinal instability. This condition has possible application to airplanes designed to cruise at supersonic speeds. With such airplanes, the trim drag at supersonic speeds can be minimized by keeping the longitudinal stability margin small. If the longitudinal stability is small at supersonic speeds, the airplane is likely to be unstable at subsonic speeds. In the F9F-2 program the airplane was made unstable by burning fuel from a forward located fuel tank until the center of gravity was abnormally far rearward.

Figure 2(a) shows the characteristics of the aerodynamically unstable airplane. Shown are traces of flight records of normal acceleration, stick position, and elevator position. The pilot disturbed the airplane with a small stick motion and the airplane diverged rapidly. Although it is not shown in figure 2(a), at about the time the record ended the pilot initiated the recovery from this divergence. As noted at the top of the figure by the symbol x, the center of gravity was about 4 percent of the mean aerodynamic chord back of the stick-fixed maneuver point. The force per unit of acceleration was about -6 pounds per g and the time for a divergence to double in amplitude was about 1 second. With this amount of instability, the pilot, when flying in smooth air, was able to control with reasonable precision by giving his complete attention to control of the airplane. However the workload was extremely high and the pilots did not consider the instability tolerable for even an emergency condition.

Figure 2(b) is for the airplane with the normal-acceleration control system. In the maneuver shown on the left-hand side of the figure, the aerodynamic instability of the basic airplane is the same as in the maneuver shown in figure 2(a). In this case the pilot applied a step input with his stick, and the normal acceleration response of the airplane is typical of that expected for an aerodynamically stable airplane. Also insofar as the pilot is concerned, the airplane appears to be stable. This normal-acceleration control system then was able to provide good flying qualities in spite of the aerodynamic instability. It is of interest to note that the elevator motion bears very little relation to the pilot's stick motion.

The right-hand side of figure 2(b) is also for the airplane with the normal-acceleration system and in this case the basic airplane is aerodynamically stable, the center of gravity being about 4 percent of the mean aerodynamic chord forward of the stick-fixed maneuver point. Again the pilot applied a step input with his stick and the normal-acceleration response of the airplane is very nearly the same as when the basic airplane is unstable. The ratio of steady normal acceleration to stick deflection is the same for both center-of-gravity positions. Thus, if a simple spring feel system is used, the force per g is the same. Also, as previously mentioned, the stick deflection per g and the stick force per g do not vary with speed or altitude. The important point is that, even though large changes in aerodynamic stability occur, many of the changes are not apparent to the pilot in the flying qualities of the airplane and his control task is then simplified.

Another item that past studies have indicated it might be desirable to provide in an airplane is acceleration limiting or "g-restriction"; that is, to restrict the g that a pilot can apply to an airplane.

It may be recalled that, with conventional control systems, the normal acceleration resulting from a given stick deflection is directly proportional to the dynamic pressure and thus at high speeds large accelerations can result from small stick motions. With the acceleration control system the steady normal acceleration for a given stick deflection is the same at all speeds and thus it appears that "g-restriction" might be obtained simply by limiting the stick deflection to the desired value. There is an additional consideration, however. It is that for rapid stick motions the peak value, or overshoot, of normal acceleration should not appreciably exceed the steady-state acceleration.

Figure 3(a) shows some maneuvers made with the acceleration control system to investigate the "acceleration-limiting" characteristics. The flight conditions are noted on the figure and the static margin of the basic airplane was about 5 percent of the mean aerodynamic chord. At zero time this maneuver has already started and the airplane is flying

in a turn at almost $4g$. The maximum rearward stick motion is restricted to about 20° and this value corresponds to a steady acceleration of slightly less than $4g$. While flying in the turn the pilot moved the stick toward neutral to reduce the acceleration and then he moved the stick back against the stop very rapidly. The pilot repeated this maneuver several times, the amplitude of the stick motion being larger each time. Even for these extremely abrupt stick motions there is practically no overshoot of the normal acceleration above the steady value. The control system used does provide excellent acceleration limiting.

Figure 3(b) demonstrates the acceleration limiting characteristics of the control system when the speed is changing. At the start of this maneuver the airplane is in a turn at slightly less than $2g$ at a Mach number of about 0.65. The pilot then reduced the power and the Mach number fell off to about 0.5. The pilot held the stick fixed throughout the run and the acceleration-control system was able to maintain the airplane at a nearly constant acceleration.

Figure 3(b) also illustrates another characteristic, that of "automatic trimming." The constant stick position that is required to maintain a constant acceleration as the speed changes is indicative of the automatic trimming. In $1g$ flight the stick would be neutral and the stick force zero throughout the speed range. In maneuvers involving rapid speed changes, the pilots have found that automatic trimming is very desirable because they are not required to retrim. The automatic trimming does cause the "speed stability" of the airplane to be zero. Most pilots have found the lack of speed stability not to be objectionable even for cross-country flying probably because any speed changes occurred very slowly. However, the addition of an altitude or Mach number hold mode would be very desirable for long period stabilization as, for example, in cruising flight.

One other highly desirable feature provided by the electronic control systems used is that the trim changes associated with transonic speeds and also the trim changes resulting from use of flaps, landing gear, or speed brakes are automatically compensated for and the pilot is not required to retrim.

CONTROLLERS

Another item that has been investigated in conjunction with the automatic control systems is the type of controller which the pilot uses for introducing electrical signals into the control system. Several types of controllers have been used and among these are: conventionally located center sticks, both movable and fixed, and small side-located control sticks. In the pilot's opinion, by far the most satisfactory

of the controllers used is the small side-located stick. Figure 4 is a photograph of one of the side-located controllers used. The stick is located at the end of an armrest at the pilot's side and is operated with the fingers. The forces found desirable with this controller are very light by present standards. For example, a pull force of 5 pounds results in an acceleration of about 5g and a lateral force of 5 pounds produces a rolling velocity of about 150° per second. About 25 pilots have flown with this controller and it has been used for take-offs and landings, and throughout almost the entire speed and acceleration ranges of the airplane. All the pilots have become accustomed to the controller quickly and have found it to be very satisfactory. Also because of the light forces associated with this controller, pilots have commented favorably on the reduced workload required in flying with it.

AIRPLANE RESPONSES IN ROUGH AIR

In addition to the flying qualities tests already discussed, measurements were made of the airplane pitching motions and the normal accelerations that occurred when flying in rough air with the automatic control systems. The test runs were made in clear air turbulence at low altitude and the pilot did a minimum of controlling during the runs. Table I summarizes the results obtained.

The flight conditions are noted on the table and the static margin was about 6 percent of the mean aerodynamic chord. The table lists the normal-acceleration response and the pitching-velocity response for the basic airplane, the airplane with the pitch-rate control system, and the airplane with the normal-acceleration control system. The quantity $(a_n/\alpha_g)_{\text{RMS}}$ is the root mean square of the normal accelerations divided by the root mean square of gust angle of attack and similarly the pitching response $(\dot{\theta}/\alpha_g)_{\text{RMS}}$ is also in terms of the root mean squares.

Comparing the airplane response for the pitch-rate system with that for the basic airplane, there is little difference in either the normal-acceleration or pitching-velocity response. It might be expected that the pitch-rate system would reduce the airplane pitching and for an airplane having low aerodynamic damping this would most certainly be the case. At the low altitude of these tests (about 1,000 feet), the aerodynamic damping of the basic airplane was high and the pitch-rate control system had little effect on the pitching motion of the airplane.

When the results for the normal-acceleration system were compared with those for the other two systems, the accelerations were about 15 percent smaller with the acceleration system but the pitching response was considerably larger. Therefore even though the acceleration system did provide some reduction in normal acceleration near the

center of gravity, the accompanying increase in airplane pitching may make for a rougher ride at some distance from the center of gravity. The increase in pitching that occurred is inherent in the type of acceleration system used, because this system pitches the airplane in attempting to maintain a constant acceleration.

SUMMARY OF RESULTS

Experience with these control systems may be summarized as follows: The flying qualities associated with both the normal acceleration and pitch rate control systems are very good. These systems can overcome unsatisfactory aerodynamic stability and control characteristics and can provide features such as acceleration limiting, automatic trimming, and a constant stick force per g and stick deflection per g. Small side-located control sticks are very satisfactory for use with these systems.

Although the F9F-2 program was primarily concerned with highly maneuverable airplanes such as fighters, many of the results obtained are applicable to any type of airplane.

The biggest drawback to use of these control systems is of course reliability considerations. Several recent military airplanes have used systems similar to those described and also they are contemplated for use in some proposed military airplanes. The indications are therefore that reasonable reliability can be achieved or that satisfactory auxiliary systems can be incorporated.

TABLE I

AIRPLANE RESPONSE IN ROUGH AIR
M=0.56 TO 0.62 h=700 TO 1,200 FT
x=6% MAC

CONTROL SYSTEM	NORMAL-ACCELERATION RESPONSE, $\left(\frac{a_n}{a_g}\right)_{\text{RMS}}$, g/DEG	PITCHING-VELOCITY RESPONSE, $\left(\frac{\dot{\theta}}{a_g}\right)_{\text{RMS}}$, DEG/SEC/DEG
BASIC AIRPLANE	0.67	1.1
PITCH-RATE CONTROL SYSTEM	.66	1.2
NORMAL-ACCELERATION CONTROL SYSTEM	.57	2.6

SCHEMATIC OF AUTOMATIC CONTROL SYSTEM

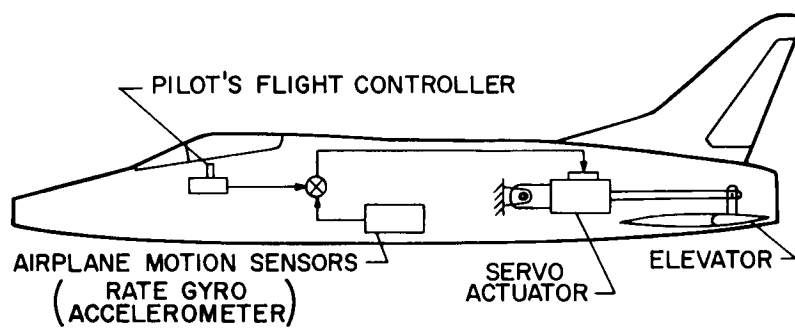


Figure 1

RESPONSE OF UNSTABLE AIRPLANE

$M=0.6$ $h=30,000$ FT
 $x = -4\%$ MAC

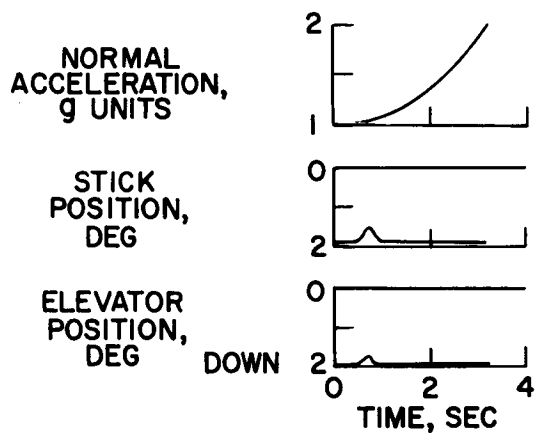


Figure 2(a)

RESPONSE OF AIRPLANE WITH NORMAL-ACCELERATION CONTROL SYSTEM

$M=0.6$ $h=30,000$ FT

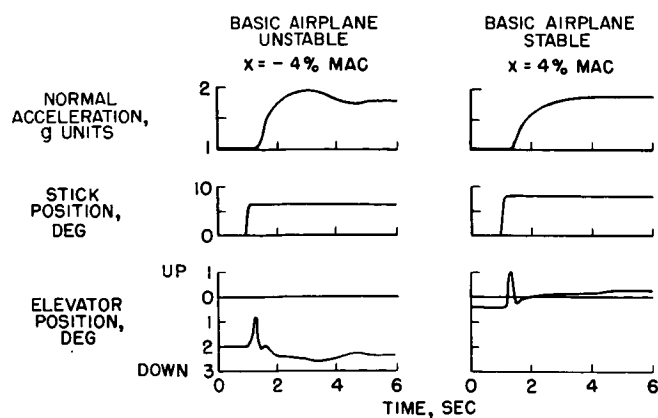


Figure 2(b)

ACCELERATION LIMITING
 NORMAL-ACCELERATION CONTROL SYSTEM
 $M=0.67$ $h=15,000$ FT
 $X=5\%$ MAC

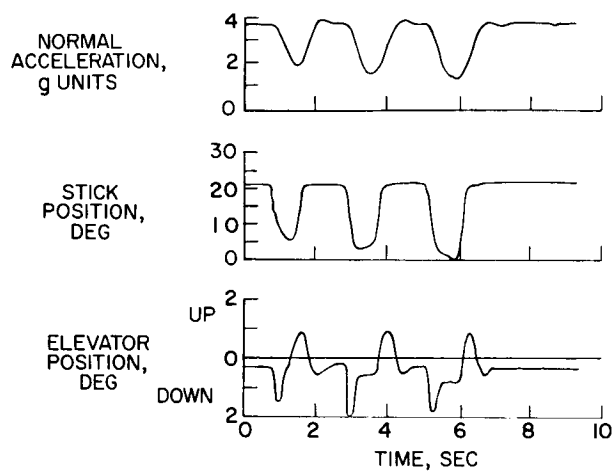


Figure 3(a)

ACCELERATION LIMITING
 NORMAL-ACCELERATION CONTROL SYSTEM
 $h=30,000$ FT
 $X=4\%$ MAC

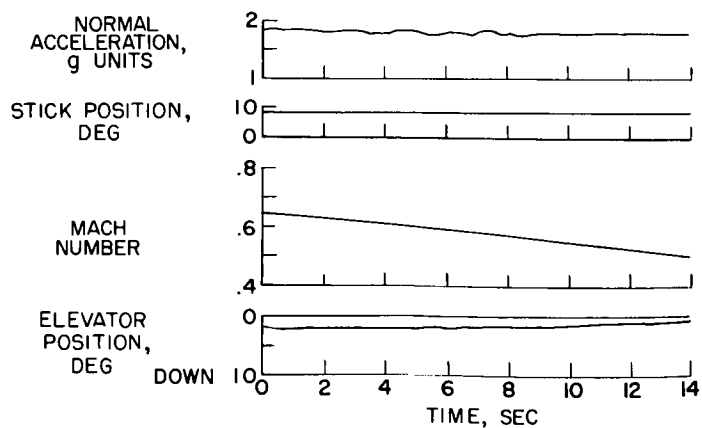


Figure 3(b)



Figure 4

A REVIEW OF ATMOSPHERIC TURBULENCE AND ITS SIGNIFICANCE TO JET-TRANSPORT OPERATIONS

By Roy Steiner and Martin R. Copp

Langley Research Center

INTRODUCTION

Gust and operating data have been collected from airline operations for a number of years. The results obtained from these data-collection programs, together with data from other sources, have served to develop a description of the turbulence in the atmosphere. (See ref. 1.) The purpose of this paper is, first, to review this basic information on the turbulence, especially in regard to its intensity and frequency of occurrence at different altitudes, and second, to examine the significance of the turbulence to jet-transport operations.

OPERATING ENVIRONMENT

Before proceeding with an examination of the turbulence data, the turbulence environment for transport operations is reviewed briefly. Figure 1 illustrates the operating altitudes for both piston and jet transports and the various types of clear-air and cloud turbulence which might be encountered. Current transports in both long and short-haul operations climb and descend rather frequently through both clear-air and cloud turbulence at the lower altitudes. Most storms also extend up to and beyond their cruising altitude. (See ref. 2.) It is expected that jet transports, at their higher cruising altitudes, will fly above or around most of the severe cloud turbulence and, because of their longer flight lengths, will climb and descent less frequently through these lower altitude regions. It appears, therefore, that jet transports will experience less storm turbulence than current transports, but the relative amount of clear-air turbulence is not apparent because of jet-stream turbulence which may be encountered at the high cruising altitudes.

EXPERIMENTAL RESULTS

In order to provide a more quantitative description of turbulence in the atmosphere, the large number of measurements available from the

VG and VGH programs have been used to obtain estimates of the amount and intensity of the turbulence at the various altitudes. In such use of these data, it is usually convenient to separate the lighter intensities or nonstorm types of turbulence from the more severe or storm types of turbulence. (See refs. 1 and 3.) Some of the results relating to nonstorm turbulence are summarized in figure 2.

In figure 2, the percent of flight distance in nonstorm turbulence at the different altitudes is shown by the curves on the left. The relative intensity of the turbulence at the different altitudes is shown on the right. The solid curve in this figure represents estimates based on current data, and the dashed curve represents the estimate made several years ago. (See ref. 3.) When the records were evaluated for these curves, the atmosphere was considered to be turbulent if gust velocities of at least 2 feet per second were measured.

It is seen that the amount of turbulence decreases rapidly with altitude for the lower levels and then increases somewhat between 20,000 and 40,000 feet. This increase reflects the relatively frequent occurrences of clear-air turbulence in jet-stream areas at tropopause levels. For the estimates made several years ago, insufficient data were available to establish these jet-stream effects. The collection of additional data also resulted in the changes noted for the lower altitudes.

The intensity of the nonstorm turbulence as shown on the right is given as a ratio of the turbulence intensity at a given altitude to the intensity at the 5,000-foot-altitude level. The curve indicates that the relative intensity of the turbulence decreases uniformly with increasing altitude. The somewhat more severe turbulence near the earth's surface results from the combined effects of surface roughness and convective activity.

In comparison with this nonstorm turbulence, storms occur only a very small percentage of the time. As shown in figure 3, the percentage of flight distance in storm turbulence amounts to much less than 1 percent at all altitudes. The intensity ratio for storm turbulence is also somewhat different and has been found to remain constant to about 25,000 feet and then to decrease at the higher altitudes.

By combining the information on the intensity ratios for both the storm and nonstorm turbulence given in figures 2 and 3 with the distributions of gust velocities for the lower altitudes (10,000-foot level for storm turbulence and 5,000-foot level for nonstorm turbulence), distributions of gust velocity per mile of turbulence can be estimated for the different altitudes. (See fig. 4.) These curves may then be used with the percentage of flight distance in storm and nonstorm turbulence to obtain estimates of the frequency of occurrence of the gust velocities which would be encountered during transport operations. (See

ref. 1 for a more complete discussion.) These results are shown in figure 5.

The curves shown in figure 5 indicate the average number of gusts which equal or exceed given velocities in 10 million miles of flight at different altitude levels. The curve for 10,000-foot altitude indicates that a gust velocity of 20 feet per second would be exceeded about 10,000 times in 10 million miles of flight at this altitude. With the exception of the curve for the very low altitude range, the distributions indicate a fairly orderly decrease in gust frequency and intensity as the altitude is increased.

COMPARISON OF JET AND CURRENT OPERATIONS

With this information on the gust frequencies and intensities, together with knowledge of the flight plan, it is now possible to estimate the gust histories for given operations. (See refs. 1 and 3.) These estimates have been made for assumed jet-transport operations and will be compared with the measured results for two current transports. The operations considered are summarized in table I.

In table I, the average flight length, cruising altitude and speed, and gross-weight wing loading are shown for piston-engine, turboprop, and jet-transport operations. The values for the piston-engine and turboprop transports were based on VGH measurements from actual operations. The values assumed for the jet operation were based on manufacturer's design studies and flight-test data.

The significant differences in these operations which would affect the gust histories are the longer flight lengths and the higher cruising altitudes for the jet transports.

The effect of these differences on the gust experience is shown in figure 6. The two upper curves represent the measured gust velocities for the piston-engine and turboprop transports. The estimates for the jet transport are shown by the shaded area.

The curves indicate that the gust histories were almost identical for the turboprop and piston-engine operations. Considerably lower values were estimated for the jet transport. The width of the band for the jet-transport estimates depends primarily upon the flight length, and, for the cases selected, the 1,000-mile flights define the upper boundary, whereas the 3,000-mile flights define the lower boundary. It should be noted that the turboprop for this example was utilized on operations very similar to those of the piston-engine transport; thus,

the close agreement in their gust distributions is explained. Other turboprop operations, however, may more closely approach the jet operations.

The gust accelerations were also measured during the piston-engine and turboprop operations and are compared in figure 7 with the estimates for the jet-transport flights. Gust accelerations, as indicated in the figure, are proportional to the slope of the lift curve, gust velocity, and airspeed, and inversely proportional to wing loading. Referring again to the operating characteristics given in table I, the high wing loading for the jet transport and the less severe gust velocities given in figure 6 would tend to reduce the gust accelerations. The higher speeds, on the other hand, would tend to increase the accelerations. These combined effects on the acceleration histories are shown by the results in figure 7.

The curves indicate that the measured accelerations for the piston-engine and turboprop transports are again in close agreement. The jet transport has a slightly less severe acceleration history. For these jet-transport calculations, the long and short flight lengths again define the lower and upper boundaries of the band.

TURBULENCE AVOIDANCE

These acceleration estimates for the jet transport would be modified if the operating airspeeds differed from the assumed speeds. Storm-avoidance procedures, either visually or by use of radar, may also materially affect the accelerations. There are, of course, no operational data available from radar-equipped jet transports, but some indication might be obtained from a review of past radar results. The results from one investigation on the use of airborne radar for storm avoidance on a low-altitude transport operation (ref. 4) are shown in figure 8.

Figure 8 shows the gust accelerations for piston-engine transports flown by the same operator. These two curves represent the data before and after radar was installed in the airplanes. The average cruising altitude and flight length were similar for the two operations, as indicated in the figure. The curves indicate that, for the larger gust accelerations, the values were about 25 percent lower when radar was used for storm avoidance. No reduction was obtained for the small accelerations. These same reductions may not necessarily apply to jet transports, but there is some indication that the large loads may be reduced somewhat for jet operations by radar storm-avoidance procedures.

SUMMARY OF RESULTS

In summary, past VG and VGH measurements provide a description of the turbulence environment in a form suitable for estimating gust and gust-load histories. An application of these data to prospective jet operations indicates that: (1) the gust experience may be reduced significantly relative to current operations, and (2) a somewhat smaller reduction might be expected in the acceleration experience. These reductions become more significant as the flight length is increased.

REFERENCES

1. Press, Harry, and Steiner, Roy: An Approach to the Problem of Estimating Severe and Repeated Loads for Missile Operations. NACA TN 4332, 1958.
2. Anon.: The Thunderstorm. U. S. Dept. of Commerce, June 1949.
3. McDougal, Robert L., Coleman, Thomas L., and Smith, Philip L.: The Variation of Atmospheric Turbulence With Altitude and Its Effect on Airplane Gust Loads. NACA RM L53G15a, 1953.
4. Copp, Martin R., and Walker, Walter G.: Analysis of Operational Airline Data To Show the Effects of Airborne Weather Radar on the Gust Loads and Operating Practices of Twin-Engine Short-Haul Transport Airplanes. NACA TN 4129, 1957.

TABLE I
OPERATIONAL CHARACTERISTICS

AIRPLANE	FLIGHT LENGTH, MILES	CRUISE ALT., FT	CRUISE IAS, KNOTS	WING LOADING, LB/SQ FT
PISTON	800	18,000	220	83
TURBO- PROP	400	14,000	210	65
JET	1,000 TO 3,000	30,000 TO 40,000	275	90 TO 100

OPERATING ENVIRONMENT

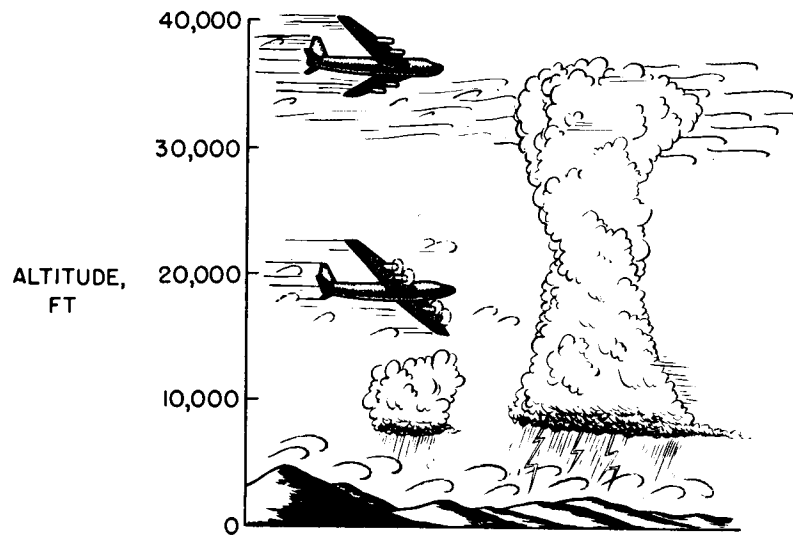


Figure 1

PERCENT AND INTENSITY OF NONSTORM TURBULENCE

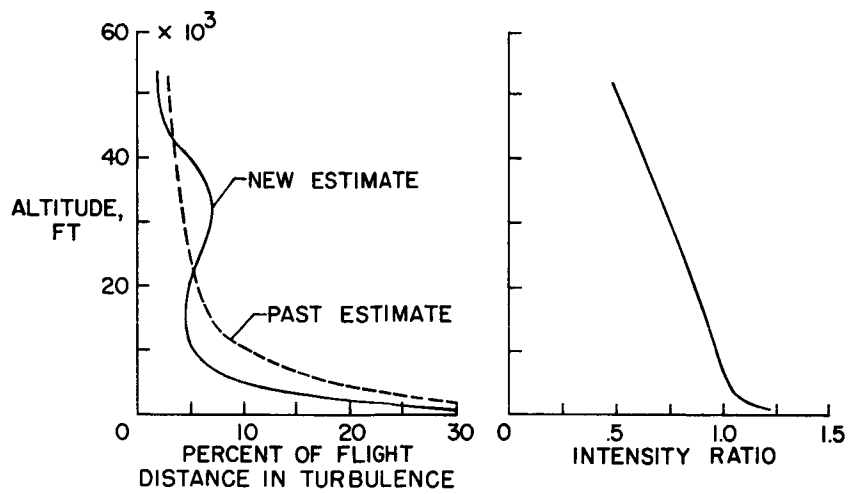


Figure 2

PERCENT AND INTENSITY OF STORM TURBULENCE

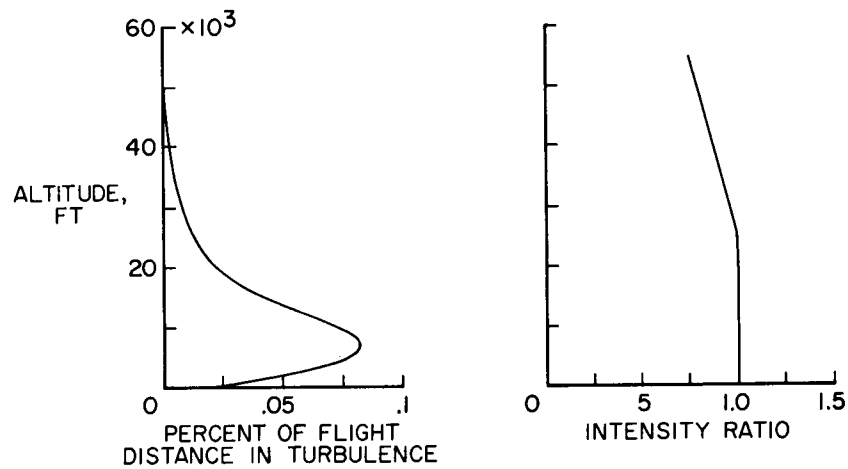


Figure 3

GUST DISTRIBUTIONS BY ALTITUDE FOR STORM AND NONSTORM TURBULENCE

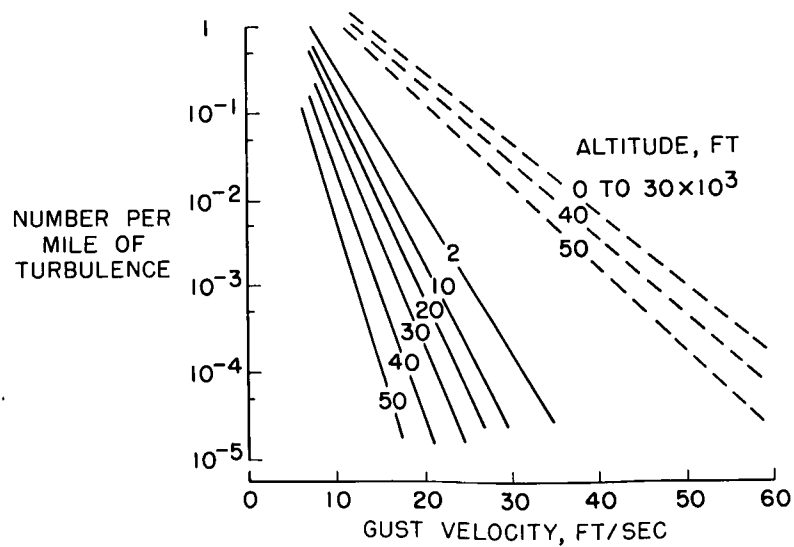


Figure 4

GUST DISTRIBUTIONS BY ALTITUDE FOR AIRLINE OPERATIONS

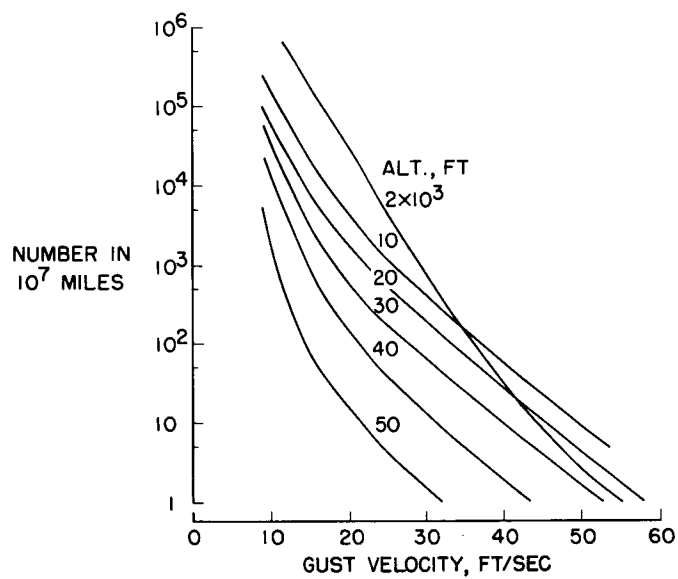


Figure 5

GUST EXPERIENCE

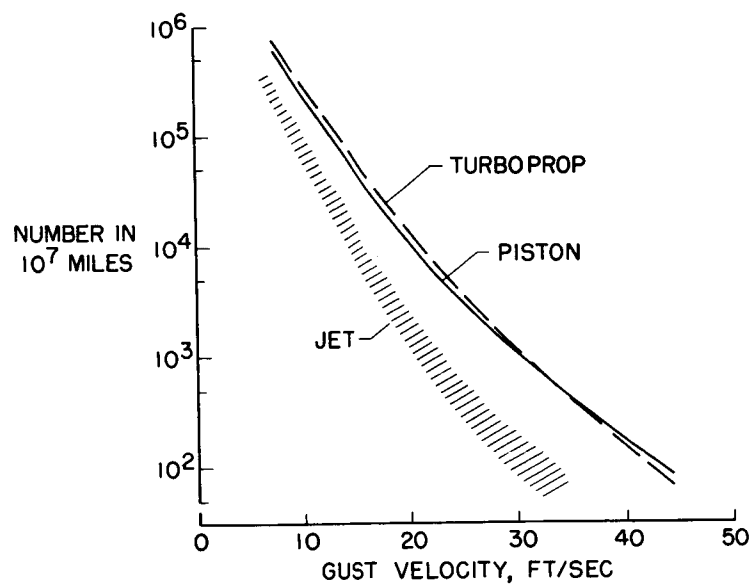


Figure 6

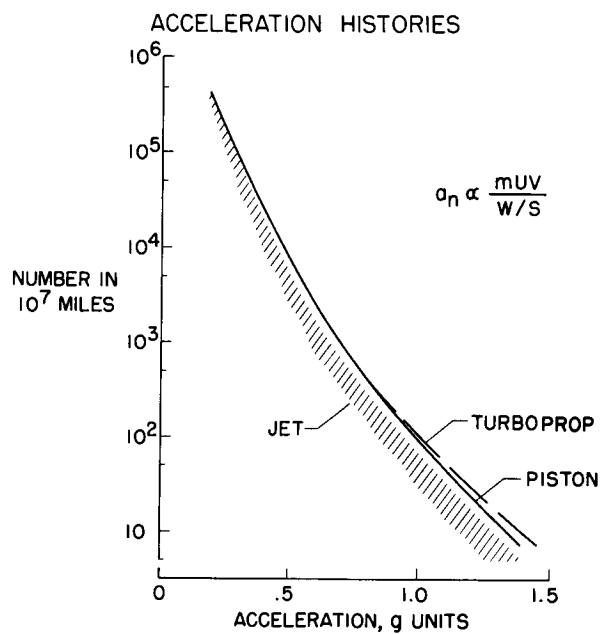


Figure 7

EFFECT OF RADAR ON ACCELERATION HISTORY

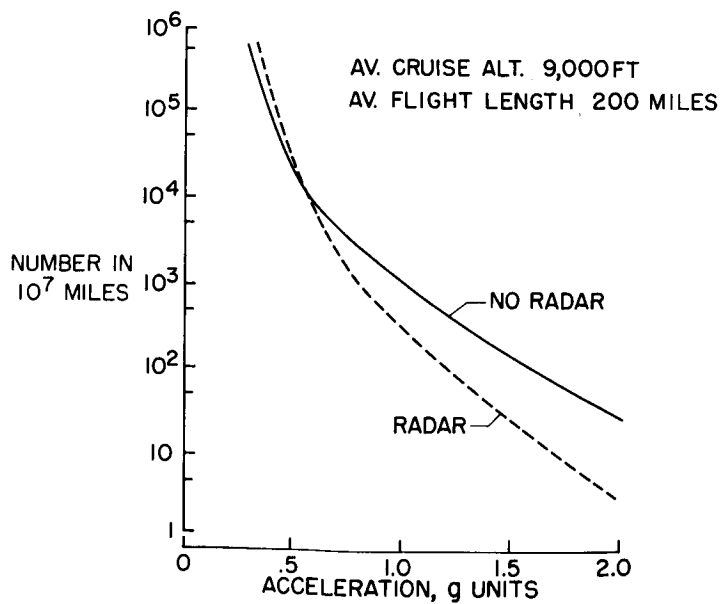


Figure 8

PITCH-UP PROBLEM - A CRITERION AND METHOD OF EVALUATION

By Melvin Sadoff

Ames Research Center

SUMMARY

A method has been described for predicting the probable relative severity of pitch-up of a new airplane design prior to initial flight tests. An illustrative example has been presented which demonstrated the use of this procedure for evaluating the pitch-up behavior of a large, relatively flexible airplane. It has also been shown that for airplanes for which a mild pitch-up tendency is predicted, the wing and tail loads likely to be encountered in pitch-up maneuvers would not assume critical values, even for pilots unfamiliar with pitch-up.

INTRODUCTION

One of the stability problems of concern to airplane design and operational groups in recent years is pitch-up or an inadvertent stalling tendency that usually occurs well below the maximum lift capabilities of an airplane. This pitch-up behavior, insofar as the pilot is concerned, restricts the useful maneuvering range of an airplane since accelerated flight near the pitch-up region may result in unintentional stalls and spins at low dynamic pressures and in excessive airframe loads at high dynamic pressures. One of the important factors contributing to pitch-up is the destabilizing trend in the variation of pitching moment with lift, which is characteristic of airplane configurations with swept wings or horizontal tails placed well above the extended wing-chord plane. Since high-speed performance considerations have generally resulted in the use of these configurations, most current high-performance airplanes exhibit a pitch-up tendency in varying degree. This paper is concerned with two aspects of the pitch-up problem of interest to airplane design and operational groups. First, a method is briefly outlined for assessing the probable relative severity of pitch-up prior to actual flight tests. Even though this method was designed primarily for evaluation of fighter airplanes, its extension to larger, relatively flexible airplanes is demonstrated by means of an illustrative example. Second, the loads aspects of the pitch-up problem are discussed with particular reference to the possibility of exceeding the design wing and horizontal-tail loads in pitch-up maneuvers.

SYMBOLS

C_L	airplane lift coefficient
$C_{L,max}$	maximum lift coefficient
C_m	airplane pitching-moment coefficient
$C_{m\alpha}$	pitching-moment-curve slope
F_S	pilot control force, lb
g	acceleration due to gravity, 32.2 ft/sec ²
I_Y	airplane pitching moment of inertia, lb-ft-sec ²
L_t	maneuvering horizontal-tail load, $I_Y\ddot{\theta}/l_t$, lb
l_t	horizontal-tail length, ft
m	airplane mass, lb-sec ² /ft
n	airplane load factor, g units
q	dynamic pressure, lb/sq ft
V	airplane velocity, ft/sec
W	airplane weight, lb
M	Mach number
$M(\alpha)$	curve defining variation of airplane pitching moment with α , ft-lb
$M_{\dot{\alpha}}$	damping due to $\dot{\alpha}$, ft-lb/radian/sec
M_{δ}	control-surface moment effectiveness, ft-lb/radian
$M_{\dot{\theta}}$	damping due to $\dot{\theta}$, ft-lb/radian/sec
$Z(\alpha)$	curve defining variation of airplane normal force with α , lb
Z_{δ}	control surface lift effectiveness at constant α , lb/radian

α	airplane angle of attack, deg or radians
θ	airplane pitch angle, radians
γ	airplane flight-path angle, radians
δ	control surface deflection, deg or radians
δ_e	elevator deflection, deg
$\dot{\delta}_{rec}$	recovery control rate, deg/sec
$\ddot{\theta}$	airplane pitching acceleration, radians/sec ²

A dot over a symbol denotes the derivative with respect to time.

DISCUSSION

Before outlining methods for assessing the pitch-up behavior of a new airplane design, the pitch-up characteristics of two existing airplanes will first be examined in order to illustrate the basic problem. In figure 1, an experimental time history, representative of a swept-wing medium bomber with a mild pitch-up tendency, is shown. Figure 2 presents a typical time history of a severe pitch-up experienced with a swept-wing fighter airplane. The Mach numbers for these maneuvers were 0.8 at 35,000 feet for the bomber and 0.9 at 35,000 feet for the fighter. The various quantities plotted in these two figures serve to define completely the pitch-up characteristics of these two airplanes and include the pilot control force and position inputs and the airplane angle-of-attack, load-factor, and pitching-acceleration responses. An inspection of these time histories indicates that a severe pitch-up is characterized by large inadvertent increases in angle of attack of 10° or more, by a corresponding increase in load factor of about 25 percent of the design load, and by the extremely large recovery transient (shown by the peak negative pitching acceleration) which resulted from the pilot's applying large and rapid corrective-control inputs in an attempt to minimize the overshoots. For the medium bomber, an attitude overshoot of less than 2° and a load-factor overshoot of about 10 percent of the design load are shown. Also, corrective control was applied at a rather leisurely rate of 3°/sec, and the resulting recovery transient was fairly mild. For the fighter airplane (fig. 2), the pilot's comments indicated that the pitch-up was abrupt and relatively uncontrollable and that maneuvers above the pitch-up boundary would generally result in inadvertent stalling, in possible spin entry, and in exceeding the desired load factor considerably. For the medium bomber (fig. 1), the pitch-up was

described as mild, but with some tendency to exceed the desired load factor. The reversal in the stick-force gradient above the pitch-up boundary was considered objectionable by the pilots, but they still felt that they had considerable control over the peak attitudes and load factors developed during pitch-up.

METHOD OF EVALUATION

In order to determine analytically from available wind-tunnel data the relative severity of pitch-up of a new airplane design prior to actual flight experience, both a rational method for predicting the airplane response during pitch-up and a criterion relating this response to pilot opinion must be established. The former requirement may be satisfied by defining a standard evaluation maneuver based on control inputs that are likely to be used by pilots in pitch-up maneuvers. Figure 3 illustrates the three stages in which this synthesized maneuver is assumed to occur. The first stage is an initial control ramp corresponding to a certain entry load-factor rate into the pitch-up region. (For the present study, this rate was fixed at about 0.5g per second.) The second stage is essentially a time interval equal to the pilot's response time between his initial perception of pitch-up and his application of corrective control. In the third stage, the pilot is assumed to apply corrective control to the forward stop at various rates to check the pitch-up. Before this standardized maneuver can be constructed, it is first necessary to determine an airplane response quantity which the pilot associates with the onset of pitch-up and a reasonable response time. From inspection of time histories of pitch-up maneuvers obtained in flight and from ground tests in a pitch simulator, it was found that the pilot associated onset of pitch-up with a threshold level of pitching acceleration of about 0.15 radian/sec². An average response time of about 0.4 second was also determined. This information, together with basic wind-tunnel data, may then be used to synthesize the model evaluation maneuver and to compute the desired response quantities, which include pitch acceleration and the angle-of-attack and load-factor overshoots.

In order to establish a criterion relating pertinent computed response quantities in pitch-up maneuvers to pilot opinion, this synthesized pitch-up maneuver was applied to six airplanes which exhibited pitch-up tendencies ranging from mild to severe, according to NASA pilots who flew these airplanes. The basic aerodynamic data for these airplanes and the equations of motions used in the computations are shown in figure 4. Airplanes A and B are swept-wing fighter airplanes with elevator control. Airplanes C, D, and E are swept-wing fighter airplanes with all-movable stabilizers. Airplane F is a swept-wing medium bomber with elevator control. Computations were made for these six reference

airplanes at a Mach number of about 0.9, since flight tests indicated that the pitch-up was most severe at this speed. Also, computations were performed for each airplane at two altitudes: 35,000 feet, which was the altitude at which most of the research flight experience was obtained with these airplanes, and at lower altitudes where the pitch-up region was assumed entered in a 6g maneuver for the fighters and in a 3g maneuver for the bomber. Before the results of the computations are presented, the objectives of a criterion based on these computed results should be noted. They are as follows:

(1) The criterion should validate the computational procedure based on the synthesized pitch-up evaluation maneuver.

(2) The criterion should then enable design or operational groups to assess the severity of pitch-up of a given design relative to that of six existing reference airplanes already evaluated by NASA pilots.

(3) The criterion should provide some information relating the magnitude of the overshoots to the pilots' control response initiating the recovery phase of the pitch-up maneuver. (As will be noted subsequently, this is of importance in assessing the probability of critical tail loads being encountered in pitch-ups.)

The primary results of the computations are presented in figure 5 where the computed overshoots at an altitude of 35,000 feet and a Mach number of about 0.9 are related to numerical pilot-opinion ratings obtained during flight evaluations of the six reference airplanes. These results are given for a relatively low recovery control rate of $10^\circ/\text{sec}$ because it was found that the pilots based their opinions on the overshoots associated with these low rates rather than the maximum that they were capable of applying. The pitch-up rating schedule used during the flight evaluation is explained in table I. It is shown in figure 5 that a good correlation exists between the magnitudes of the overshoots and the results of flight evaluations, and this agreement lends some confidence to the computational procedure used. For example, airplanes A and B with α overshoots in excess of about 11° were assigned unsatisfactory ratings of 8 and 7, respectively. As noted in table I, these ratings are reserved for airplanes with a relatively severe pitch-up for which there is an increased tendency for the pilot to apply large, abrupt corrective control. On the other hand, airplanes E and F with an α overshoot generally under 4° were assigned a marginally satisfactory rating of 2 which implies a mild, barely perceptible pitch-up with little tendency for the pilot to apply extreme corrective control to check the pitch-up. By comparing the critical computed overshoots with the corresponding values for these six reference airplanes, design and operational groups are also provided with a method for assessing the probable relative severity of pitch-up of a new design. Applied in this manner, the method is also useful for determining the modulating effects of

aerodynamic modifications or automatic control devices on a given design. Also, if the pilot rating schedule in table I or the results presented in time-history form in figures 1 and 2 are referred to, it is noted that as the magnitude of the computed overshoots increases and pilot opinion deteriorates, the pilot corrective-control response tends to become more extreme and results in violent recovery transients and increased maneuvering tail loads.

ILLUSTRATIVE EXAMPLE

To illustrate the use of this method in evaluating the pitch-up behavior of a large airplane, the procedure used for the medium swept-wing bomber will be examined. For large flexible airplanes of this type, the computational procedure was different in two important respects from that used for the fighters. First, since the computed pitching acceleration did not build up to the threshold value established from simulator and flight tests of fighters, it was found necessary to alter the standard evaluation maneuver. This was accomplished by assuming that the pilot initially perceives pitch-up at an angle of attack corresponding to the initial sharp destabilizing break in the pitching-moment curve - in this case, where the airplane stability first reduces to zero. Second, it was found that the effects of flexibility had an important bearing on the computed pitch-up behavior of this airplane. For example, as shown in figure 6, neglecting these effects by using rigid-model pitching-moment data resulted in a computed α overshoot of about 8° . This value compares rather poorly with the actual value of about 2° computed for the flexible airplane. The point to be made here is that for large flexible airplanes, the effects of flexibility, particularly those on the airplane pitching-moment curve, must be properly accounted for before a reasonable prediction of pitch-up behavior can be attempted.

A word of caution should be injected here. Since the rating schedule shown in table I was used primarily for fighters, there may be some question of its applicability to transport types. NASA pilots who have flown both fighters and transports feel that transport requirements should be somewhat more severe than those for fighters because of additional considerations for passenger comfort and lower design load factors. They have indicated, tentatively, that acceptable transport ratings would fall in the range of 0 to 2, rather than the 0 to 5 range noted for the fighters in the table. This implies that only a mild pitch-up, comparable to that observed for the swept-wing medium bomber, would be considered acceptable for jet-transport airplanes. However, the actual range of acceptable behavior for transports would have to be defined by the appropriate certifying agency.

LOADS ASPECTS OF THE PITCH-UP PROBLEM

It was noted previously that one facet of the pitch-up problem of concern to operational groups was the possibility of inadvertently exceeding the design wing and tail loads in pitch-up maneuvers. This possibility is examined first at the relatively high altitude of 35,000 feet where the pitch-up region is entered at load factors well under design values for the six airplanes considered in this study. In figure 7, bar graphs of the computed peak load factors and maneuvering tail loads are shown for the two airplanes rated unsatisfactory by the pilots - airplanes A and B - and for the two airplanes rated marginally satisfactory - airplanes E and F. Results are presented for two recovery control rates in each case, a relatively low rate of $10^\circ/\text{sec}$ and the maximum rates possible. The load-factor overshoots and maneuvering tail loads for these four example airplanes are shown by the shaded areas in this graph. Note that the tail loads have been nondimensionalized by dividing by the airplane weight. It is evident from these results that the loads problem is not likely to be critical in pitch-up maneuvers encountered at these flight conditions. The maximum load factors, even for airplanes with relatively severe pitch-up tendencies, remain well under design values, due either to $C_{L,\text{max}}$ limitations or to the reduced lift-curve slope characteristic of these airplanes in the pitch-up region. Similarly, the maneuvering tail loads do not attain critical values due either to typical limitations imposed by the forward control stop or to the maximum recovery control rates available on these airplanes.

The more critical flight conditions at lower altitudes and higher dynamic pressures where the pitch-up region is entered at load factors close to design levels are examined next. In this case, it might be expected that both the wing and tail loads may assume critical values. To illustrate this, the results of computations where the pitch-up region is entered at about 80 percent of the design load factor, that is, about 6g for the fighter types and 3g for the bomber airplane, are presented in figure 8 for the four example airplanes. It may be seen from these results that the pilot is faced with a difficult problem, particularly if he penetrates the pitch-up region at this flight condition with an airplane with a moderately severe pitch-up tendency. If he attempts to check the pitch-up with high recovery control rates, the wing loads in excess of design values are minimized, but at the expense of the maneuvering tail loads exceeding design levels. On the other hand, if relatively low recovery control rates are used, the wing loads tend to exceed the design load considerably. For the two airplanes whose pitch-up behavior was considered fairly mild by the pilots at 35,000 feet, the overshoots, even for these critical flight conditions, are relatively small and unaffected by recovery control rate. For this reason, in addition to the reduced probability of extreme recovery control rates

being applied to check mild pitch-up tendencies, the possibility of exceeding the design tail loads in pitch-up maneuvers, even for pilots relatively inexperienced with pitch-up, is considered fairly remote.

CONCLUDING REMARKS

A method has been described for predicting the probable relative severity of pitch-up of a new airplane design prior to initial flight tests. An illustrative example has been presented which demonstrated the use of this procedure for evaluating the pitch-up behavior of a large, relatively flexible airplane. It has also been shown that for airplanes for which a mild pitch-up tendency is predicted, the wing and tail loads likely to be encountered in pitch-up maneuvers would not assume critical values, even for pilots unfamiliar with pitch-up.

TABLE I

PILOT RATING OF PITCH-UP

ADJECTIVE RATING	NUMERICAL RATING	DESCRIPTION
SATISFACTORY	0	SATISFIES STABILITY AND CONTROL REQUIREMENTS
MARGINALLY SATISFACTORY	1 2	PITCH-UP BARELY PERCEPTIBLE ---- LITTLE TENDENCY FOR PILOT TO APPLY RAPID AND EXCESSIVE CORRECTIVE CONTROL
UNSATISFACTORY BUT ACCEPTABLE	3 4 5	PITCH-UP IS MORE APPARENT ---- THERE MAY BE SOME TENDENCY FOR THE PILOT TO APPLY RAPID AND PERHAPS EXCESSIVE CORRECTIVE CONTROL
UNSATISFACTORY	6 7 8	PITCH-UP SEVERE RANGING FROM CONTROLLABLE ONLY WITH GREATEST DIFFICULTY TO PRACTICALLY UNCONTROLLABLE ---- INCREASED TENDENCY FOR THE PILOT TO APPLY RAPID AND EXCESSIVE CORRECTIVE CONTROL
UNACCEPTABLE	9 10	PITCH-UP SO SEVERE THAT AIRPLANE IS UNCONTROLLABLE ---- SOME POSSIBILITY OF ENTERING A SPIN OR OTHER UNUSUAL MANEUVER FROM WHICH RECOVERY MAY BE DIFFICULT OR IMPOSSIBLE

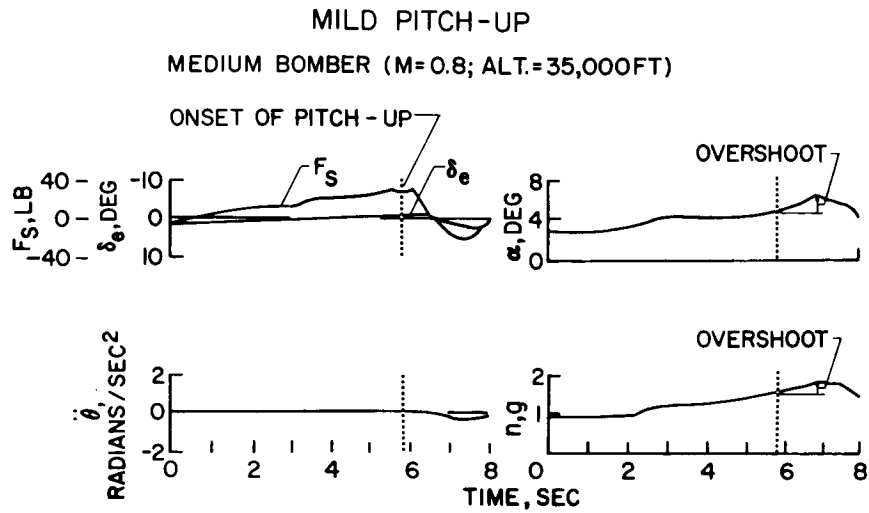


Figure 1

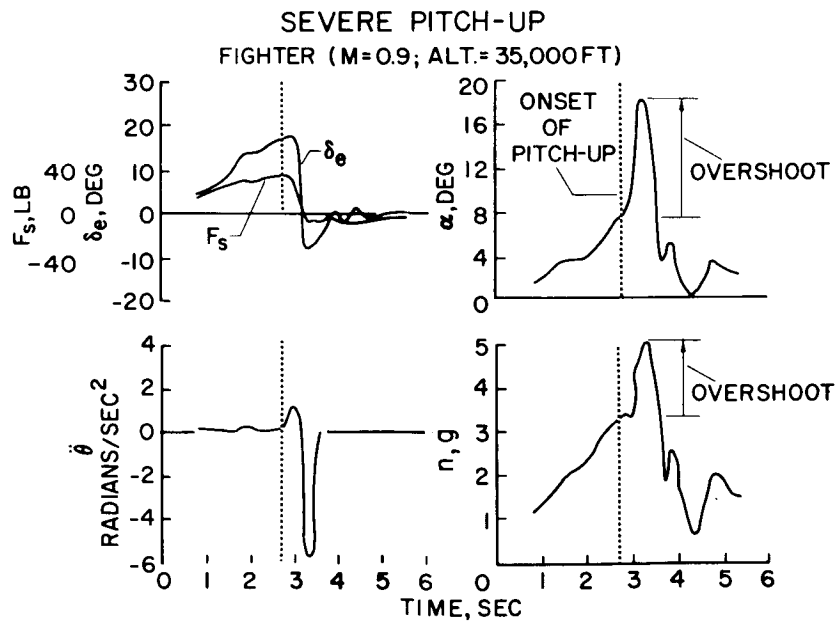


Figure 2

SYNTHESIZED PITCH-UP MANEUVER

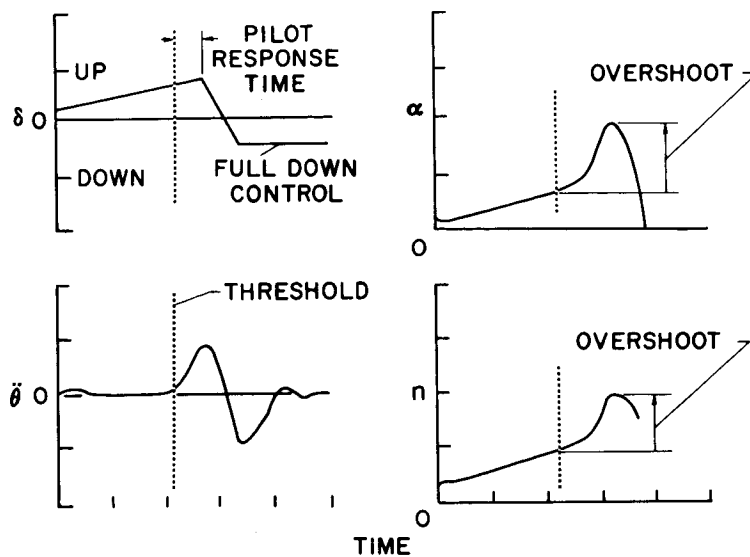


Figure 3

BASIC AERODYNAMIC DATA
FOR SIX REFERENCE AIRPLANESEQUATIONS OF MOTION: $-mV\dot{\gamma} = Z(\alpha) + Z_\delta\delta$

$$I_Y \ddot{\theta} = M(\alpha) + M_\alpha \dot{\alpha} + M_{\dot{\theta}} \dot{\theta} + M_\delta \delta$$

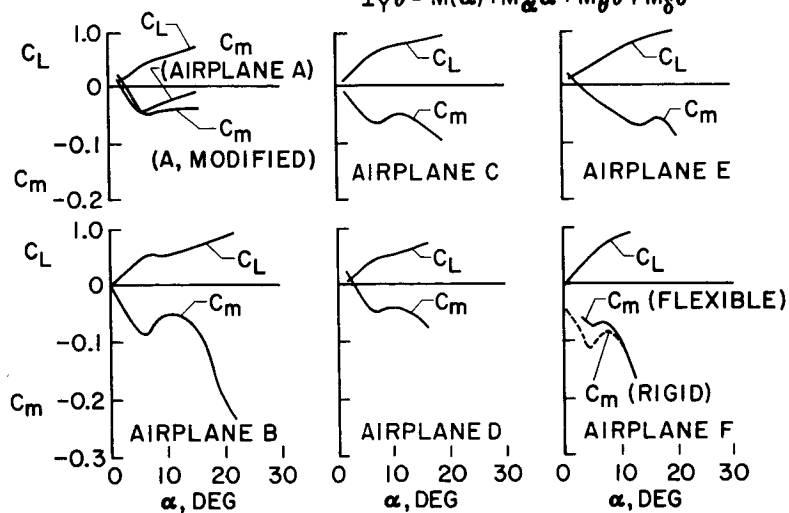


Figure 4

CALCULATED OVERSHOOTS VERSUS FLIGHT RATINGS

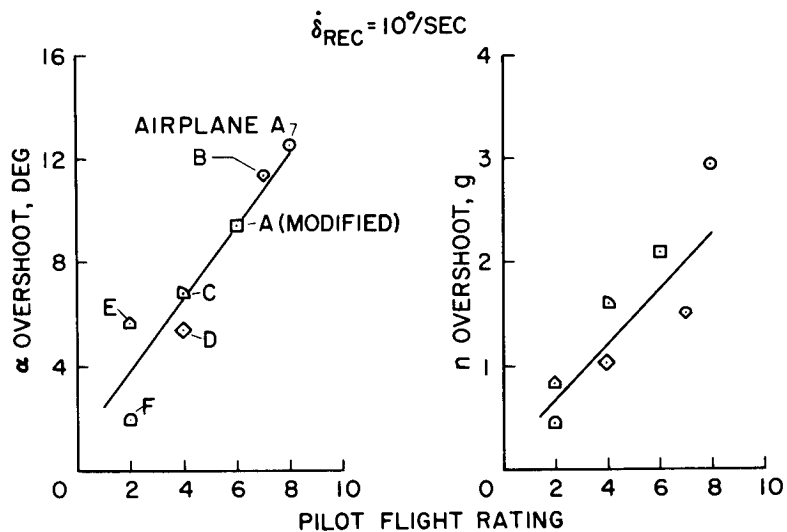


Figure 5

EFFECTS OF FLEXIBILITY

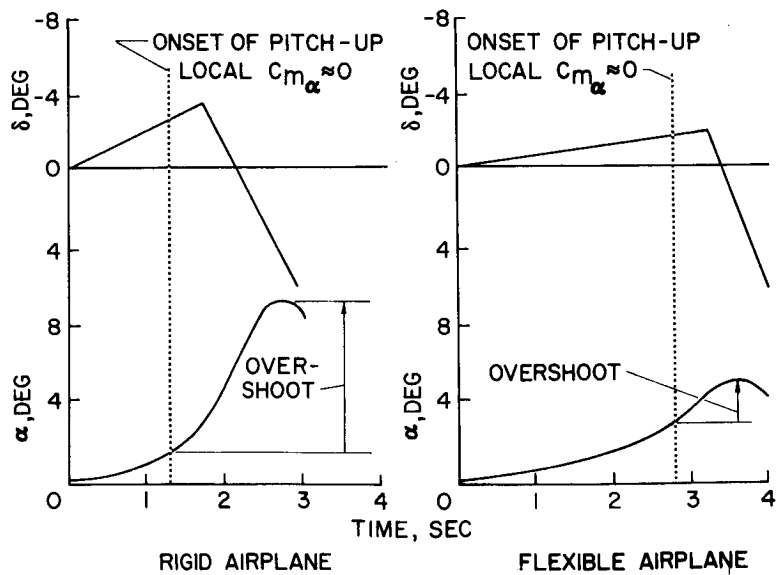


Figure 6

PEAK LOAD FACTOR AND TAIL LOADS
AT 35,000 FEET

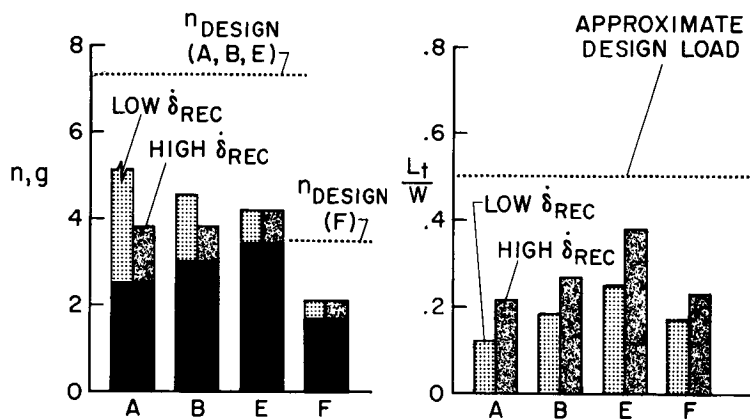


Figure 7

PEAK LOAD FACTOR AND TAIL LOADS
AT LOWER ALTITUDES

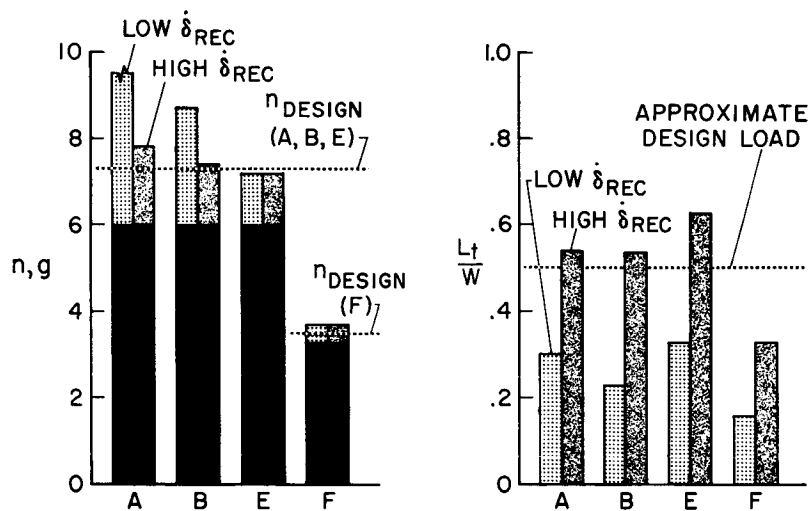


Figure 8

SOME EFFECTS OF YAW DAMPING ON AIRPLANE MOTIONS AND
VERTICAL-TAIL LOADS IN TURBULENT AIR

By Jack Funk
Langley Research Center

and T. V. Cooney
NASA High-Speed Flight Station

SUMMARY

Results of analytical and flight studies are presented to indicate the effect of yaw damping on the airplane motions and the vertical-tail loads in rough air. The analytical studies indicate a rapid reduction in loads on the vertical tail as the damping is increased up to the point of damping the lateral motions to $1/2$ amplitude in one cycle. Little reduction in load is obtained by increasing the lateral damping beyond that point. Flight measurements made in rough air at 5,000 and 35,000 feet on a large swept-wing bomber equipped with a yaw damper show that the yaw damper decreased the loads on the vertical tail by about 50 percent at 35,000 feet. The reduction in load at 5,000 feet was not nearly as great. Measurements of the pilot's ability to damp the lateral motions showed that the pilot could provide a significant amount of damping but that manual control was not as effective as a yaw damper in reducing the loads.

INTRODUCTION

The trend toward increased operating altitudes and the use of swept wings on newer transports contribute to a deterioration of lateral-directional damping. Because of the low damping, disturbances caused by turbulence result in large-amplitude oscillatory motions. Such oscillations are objectionable to the pilot and passengers and, in addition, produce sizable loads in the vertical-tail structure. The NASA has been conducting analytical and experimental studies to determine the effect of damping on the lateral motions of the airplane and on the vertical-tail loads in rough air. This paper presents some results of these studies to show the effect of damping on the motions and loads in rough air, and to indicate the reductions obtained by increasing the damping.

CALCULATIONS

Effect of Period and Damping

Calculations for the effect of period and damping on the loads on the vertical tail due to turbulence were made on the assumption that the only parameters of importance are the period and the damping of the lateral motions. A brief analysis indicated that, for most airplanes, other parameters can be neglected without too much loss in accuracy. On this basis, calculations were made for the ratio of the sideslip angle at the vertical tail to the gust angle, which is a measure of the load on the vertical tail.

The results of the calculations are shown by the three curves in figure 1. The ordinate values are the ratio of the root-mean-square sideslip angle at the vertical tail to the root-mean-square gust input angle. These values for three lateral frequencies are plotted against the damping parameter, which is the reciprocal of the number of cycles to damp the lateral motion to $1/2$ amplitude. The lateral frequency is expressed in terms of the wavelength of the lateral oscillation in feet and is the product of the lateral period in seconds and the true airspeed in feet per second. The three frequencies shown cover the range for most transport airplanes.

The curves in figure 1 show that as the lateral damping of an airplane is increased, the loads on the vertical tail in rough air decrease rapidly until the damping parameter reaches a value of about 1 (that is, a damping of the lateral motion to $1/2$ amplitude in one cycle). Little is gained by increasing the damping beyond this point. Figure 1 also indicates that a 2-to-1 change in the wavelength of the lateral motion has only a small effect on the vertical-tail loads.

Trend in Vertical-Tail Loadings of New Transports

The calculations presented in figure 1 can be used to indicate the trend in loads on the vertical tail surface in rough air for some of the newer transports. The symbols locate some representative transport airplanes on the curves according to the damping of the lateral motions under given operating conditions. The open circles represent three swept-wing jet airplanes without yaw dampers flying at about 35,000 feet. The solid circles are for the same airplanes and altitudes but with yaw dampers in operation. The diamonds show the damping at 10,000 to 15,000 feet for several unswept-wing piston-engine airplanes which have proved to be satisfactory in service.

A comparison of the ratios of sideslip angle to gust angle for the airplanes denoted by the symbols in figure 1 indicates the following results for flight in the same intensity of turbulence: Swept-wing airplanes operating at 35,000 feet without yaw dampers can be expected to experience much higher vertical-tail loads than current transports operating at 10,000 to 15,000 feet. With yaw dampers in operation, however, the high-altitude airplanes can be expected to experience almost the same vertical-tail load as current transports.

FLIGHT TESTS

Effect of Yaw Dampers

Some time histories of measurements of the motions and vertical-tail loads experienced in rough air by a jet airplane which has a configuration generally similar to the new transports are shown in figures 2 and 3. Figure 2 shows time histories of the lateral gust velocity (expressed as the gust angle-of-attack changes at the vertical tail), the sideslip angle, the vertical-tail bending strains, and the rolling and yawing velocities of the airplane. These measurements were made at a Mach number of 0.6 at 35,000 feet. The yaw damper was not in operation during the run shown in figure 2 and the pilot was flying "hands-off" as much as possible. The time histories indicate that under these conditions the airplane experienced large rolling and yawing motions at the Dutch roll frequency of about 1 cycle in 5 or 6 seconds. An important point to note is that the amplitude of the sideslip angle is 3 or 4 times the amplitude of the gust input angle. Another point is that the measured tail strains closely follow the sideslip motions of the airplane, thereby indicating that most of the tail strains result from the motions of the airplane and very little from what might be considered the direct gust effect.

Figure 3 shows time histories of the same quantities measured in turbulence of about the same intensity and under similar flight conditions but with the yaw damper in operation. It is apparent from a comparison of figures 2 and 3 that the yaw damper reduces the amplitudes of both the lateral motions and the tail strains by a considerable amount.

The magnitude of this reduction in tail strain is shown in figure 4. Figure 4 shows the percentage of time the root bending strains of the vertical tail were above a given level in the tests of the swept-wing jet airplane at an altitude of 35,000 feet and a Mach number of 0.6 and at an altitude of 5,000 feet and a Mach number of 0.3. The two flight Mach numbers correspond to about the same dynamic pressure at both altitudes. The solid lines show the results for the runs with yaw damper off, and the dashed lines for yaw damper on.

It is obvious from a comparison of the curves in the left-hand plot of figure 4 that yaw damping reduces the magnitude of the loads considerably at high altitudes. This reduction is about 50 percent at 35,000 feet. At 5,000 feet, where the damping in yaw for the basic airplane is better, the benefit of yaw damping is much less, as shown in the right-hand plot of figure 4.

Yaw-Damping Effectiveness of a Pilot

So far the discussion has been concerned with the effect of yaw dampers in alleviating airplane motions and vertical-tail loads in rough air. One additional question of interest concerns the ability of a pilot to control the airplane in the event of damper failure.

In order to assess the effectiveness of the pilot in damping the Dutch roll motions of an airplane, flight tests have been made in turbulent air, first with the pilot flying essentially hands-off and then with the pilot controlling the lateral motions. Figure 5 summarizes the results of these tests.

The results in figure 5 indicate the percentage of time the side-slip angle and vertical-tail strains were above a given level. Tests without the yaw damper are indicated by solid lines; those with pilot control of the yawing motion, by long-dash lines; and those with yaw damper on, by short-dash lines. These tests were made at 21,000 feet at a Mach number of 0.6.

The results indicate that the damping provided by the pilot resulted in a significant reduction in the lateral motions of the airplane and the vertical-tail loads. This damping provided by the pilot, however, was not as great as that provided by the yaw damper. The pilot commented that the long-period oscillation can be readily damped out but that over a long time interval such constant control effort would become tiresome.

CONCLUSIONS

Analytical and flight studies of the effect of yaw damping on airplane motions and vertical-tail loads have resulted in the following conclusions:

1. Theoretical considerations indicate that little reduction in vertical-tail loads is obtained by increasing the damping beyond the point where the oscillations damp to $1/2$ amplitude in one cycle.

2. Measurements on a large jet airplane in rough air at 35,000 feet have indicated that yaw-damper operation resulted in a 50-percent reduction in both aircraft motions and vertical-tail loads. At 5,000 feet, where lateral damping is better, benefits of the yaw damping are much less.

3. It would appear that a pilot may be able to provide sufficient damping in the event of failure of the yaw damper.

CALCULATED EFFECT OF DAMPING ON VERTICAL-TAIL LOADS

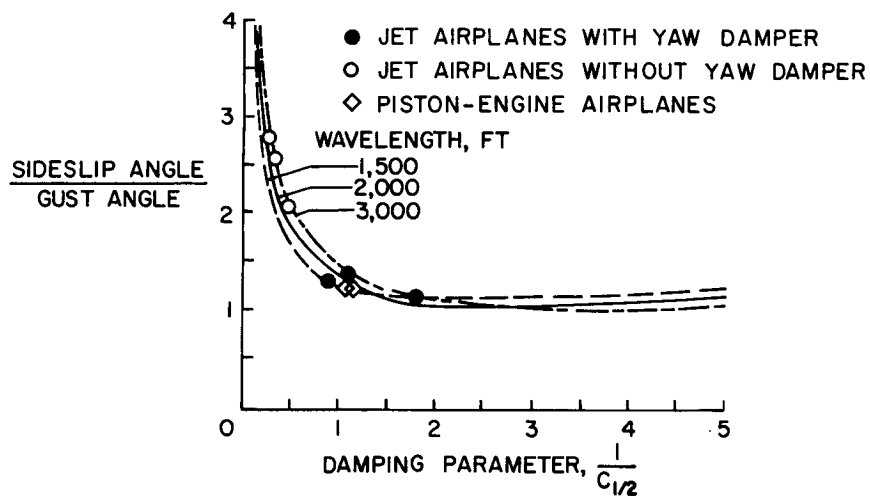


Figure 1

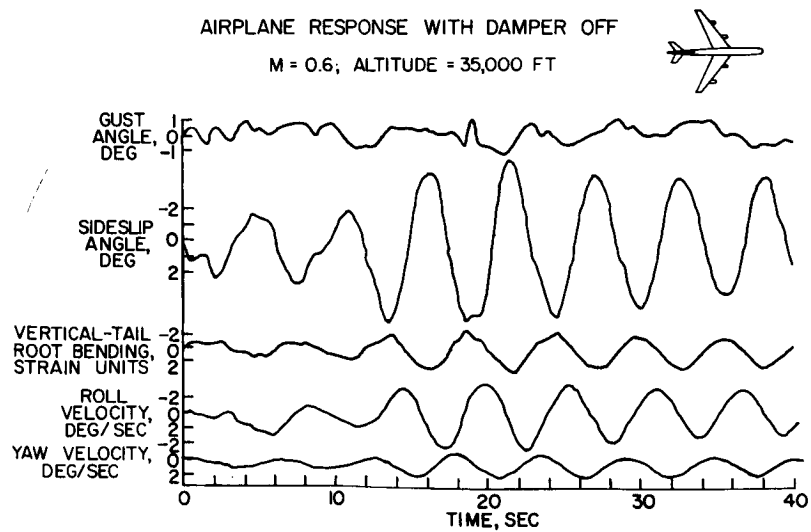


Figure 2

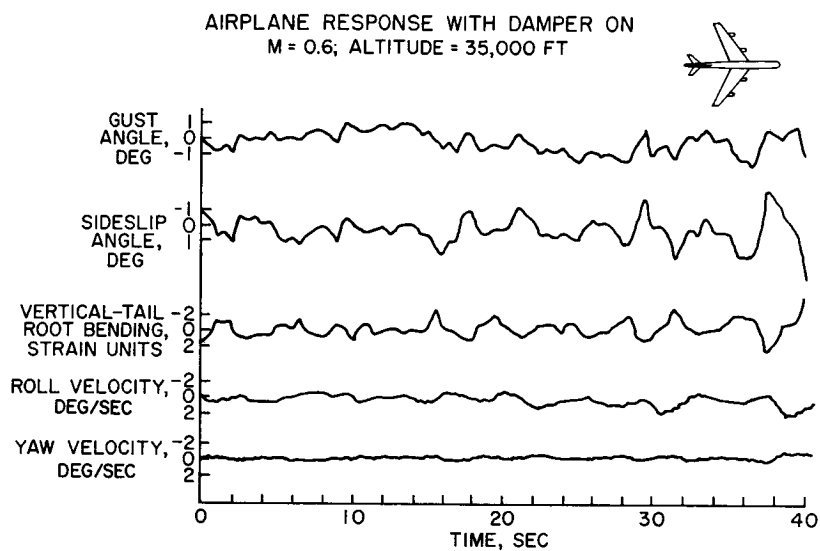


Figure 3

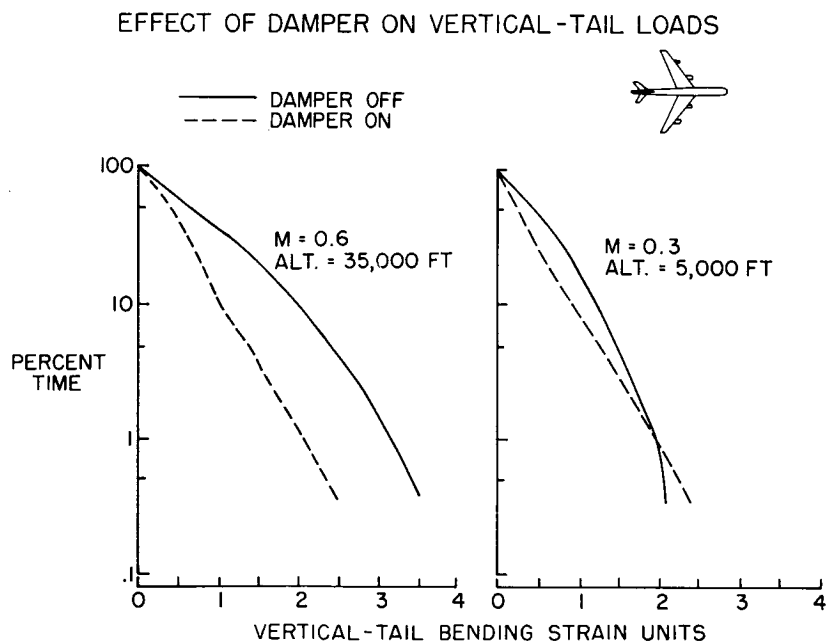


Figure 4

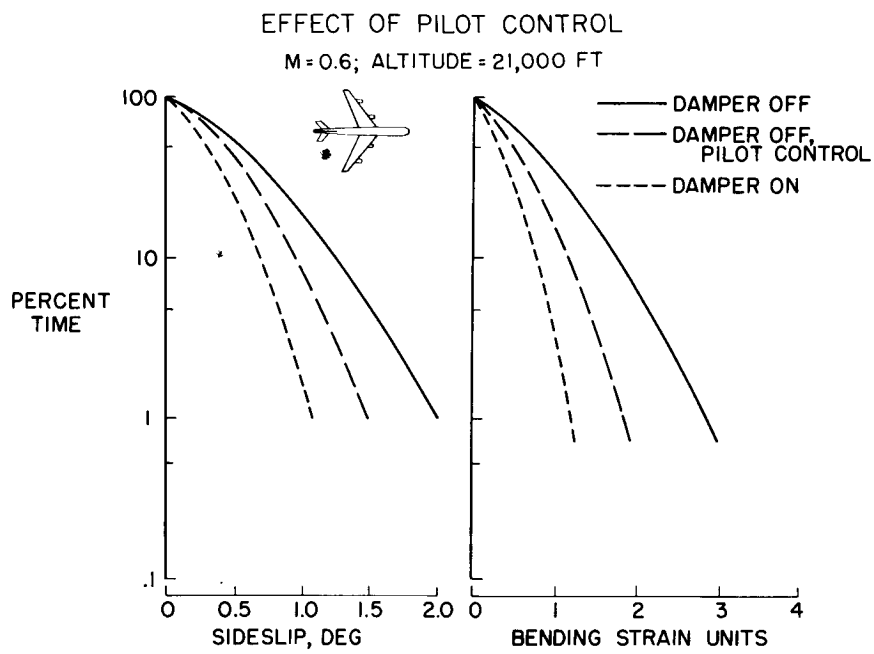


Figure 5

FLIGHT STUDIES OF PROBLEMS PERTINENT TO HIGH-SPEED

OPERATION OF JET TRANSPORTS

By Stanley P. Butchart, Jack Fischel,
Robert A. Tremant, and Glenn H. Robinson

NASA High-Speed Flight Station

SUMMARY

A flight investigation was made to assess the potential operational problems of jet transports in the transonic cruise range. In this study a large multiengine jet airplane having geometric characteristics fairly representative of the jet transport was used; however, in order to ensure general applicability of the results, the aerodynamic characteristics of the test airplane were varied to simulate a variety of jet-transport airplanes.

Some of the specific areas investigated include: (1) an overall evaluation of longitudinal stability and control characteristics at transonic speeds, with an assessment of pitch-up characteristics, (2) the effect of buffeting on airplane operational speeds and maneuvering, (3) the desirable lateral-directional damping characteristics, (4) the desirable lateral-control characteristics, (5) an assessment of over-speed and speed-spread requirements, including the upset maneuver, and (6) an assessment of techniques and airplane characteristics for rapid descent and slow-down.

The results presented include pilots' evaluation of the various problem areas and specific recommendations for possible improvement of jet-transport operations in the cruising speed range.

INTRODUCTION

In an assessment of problems other than those encountered in the take-off and landing area which could possibly affect operations of jet transports, the region determined as most likely to be critical was the transonic region because of the changes in aerodynamic phenomena which could affect the safety or comfort of flight. Although the effects occurring in this speed range have been extensively explored by research

and military aircraft and are well known, some question exists regarding the importance of these effects on civilian passenger-carrying airplanes.

For the purpose of investigating the overall significance of these effects as they might affect airline operations, a large multijet airplane, basically similar to the jet transports currently being produced, was utilized to evaluate the specific problem areas.

SYMBOLS

a_n	normal acceleration, g units
b	wing span, ft
C_m	airplane pitching-moment coefficient
C_N	airplane normal-force coefficient
F_e	longitudinal control force, lb
M	Mach number
M_1	Mach number at initiation of maneuver
p	rate of roll, radians/sec
$p b / 2 V$	wing-tip helix angle or lateral control effectiveness parameter, radians
S	wing area, sq ft
T	engine thrust, lb
$T_{1/2}$	time for lateral-directional oscillation to damp to half amplitude, sec
T_2	time for lateral-directional oscillation to double amplitude, sec
$T_{\phi=30^\circ}$	time to change bank angle 30° , sec
V	true velocity, ft/sec
V_i	calibrated indicated airspeed, knots

W	airplane weight, lb
α_1	indicated angle of attack, deg
δ_e	elevator deflection, deg

PROBLEM AREAS IN JET-TRANSPORT OPERATION

The problem areas to be considered in the present investigation of jet transports are as follows:

- (1) Overall longitudinal stability and control characteristics at transonic speeds
- (2) Buffeting
- (3) Desirable lateral-directional damping characteristics
- (4) Desirable lateral-control characteristics
- (5) Overspeed and speed-spread requirements
- (6) Techniques and airplane characteristics for emergency descent and slow-down.

For the purpose of this study, a large multijet airplane basically similar to jet transports now in production was tested in flight. This airplane configuration had a 35° sweptback wing of aspect ratio 7.1. A two-view drawing of the airplane is shown in figure 1.

RESULTS AND DISCUSSION

Trim Characteristics

Inasmuch as the economics of jet-transport operation will dictate that airplanes of this type cruise in the transonic speed range, they will be flying in a region where the usual unstable longitudinal trim variations will be encountered. A question exists as to whether this is a potentially dangerous area in which to operate. Figure 2 shows typical trim variations of elevator force and position with Mach number for two altitudes; stabilizer setting was held constant. The solid lines represent operation in level flight (normal acceleration of 1 g) and the dashed lines represent trim level for a normal acceleration

of 1.5g. When the airplane accelerated longitudinally in level flight through the speed range to the unstable region of the trim curve, the force reversal was mild and occurred at such a rate that the airplane could be trimmed at all times. For example, at an altitude of 25,000 feet, approximately 75 seconds was required for a Mach number increase from 0.75 to 0.85, and at 35,000 feet the time required for a similar increment in speed was approximately doubled. In decelerating through this "tuck" or transonic region, the force change from an unstable trend to a stable trend occurred at a more rapid rate, depending on the technique used for slow-down, but was still considered slow enough to enable the pilot to maintain a 1g trim condition at all times. For example, when the airplane decelerated with throttles in the idle position and speed brakes extended, approximately 35 seconds was required for a Mach number decrease of 0.1 at 25,000 feet. Should a pilot decelerate while holding the stick force constant or while increasing the stick force to obtain a higher normal acceleration, it is possible to obtain higher levels of normal acceleration, perhaps approaching structural limits, as a result of control reversal in the transonic region. This possibility is apparent from the trends and levels of control force and position for trimmed flight at 1g and 1.5g shown in figure 2. The trend of the power-off trim variations through the speed range was similar to that shown for the power-on condition; however, the levels of force and elevator position required were somewhat higher for the power-off condition. When the airplane decelerated (decreasing M) with engines idle and speed brakes open, the trim variations were similar in trend and magnitude to those shown for the power-on acceleration (M increasing), so that the individual effects on trim associated with these variables were indicated to be compensating. It is believed that if this transonic region were traversed appreciably faster with the force variations shown, or if the changes in control force were approximately doubled with the existing rate of Mach number change specified, the trim variations would be very objectionable. From consideration of these factors, it appears that a force variation with speed of 40 or 50 pounds should be the maximum allowable.

Although the trim variations recorded over the transonic speed range appear more acute for the higher altitude, this difference was not readily apparent to the pilot. The variation with Mach number of elevator position and force required for trimmed flight at a normal acceleration of 1g in the transonic region was essentially unaffected by changes in center-of-gravity position. Operation under instrument flight conditions in the transonic region provided no additional handling difficulties, inasmuch as operation under visual flight conditions required the use of instruments to control the flight path at high altitude.

Cruising in the unstable portion of the transonic region with auto-pilot off requires constant pilot attention, since small disturbances of equilibrium conditions have a divergent effect on speed and altitude. Performing a change in heading in the unstable trim region provides added difficulty for the pilot in maintaining altitude control because of the forward stick displacement required as the speed tends to decrease.

From the pilot's viewpoint, it would be desirable to have the unstable force variations masked in order to provide stable trim force variations throughout the speed range.

Pitch-Up Characteristics

In maneuvers to normal acceleration in excess of $1g$ with swept-wing airplanes, pitch-up has been encountered which was quite severe for the smaller aircraft and often bordered on being dangerous. Data obtained on the test airplane during an accelerated maneuver are presented in figure 3, together with comparable data obtained with the B-47 airplane. Time histories of similar slow-rate wind-up turns are shown as variations of stick force, elevator angle, normal acceleration, and angle of attack for each aircraft. Also shown are corresponding variations of airplane pitching moment with angle of attack. Despite the decrease in stability with increase in angle of attack for the test airplane, as exhibited by the decrease in slope of the pitching-moment curve, the rates of rotation were so low that the pilot generally was not cognizant of this pitch-up effect. This mild effect can be attributed to the gradual change in slope of the pitching-moment curve and the large aircraft inertia. The airplane was controllable at all times. However, if the change in slope of the pitching-moment curve is more radical and exhibits an unstable trend, as shown for the B-47, the pitch-up is very apparent and can be potentially dangerous at altitudes where design limits can be exceeded in the overshoot of normal acceleration. For this degree of instability with the large aircraft, recovery from pitch-up is slow and generally requires appreciable pilot effort. For both airplanes, buffet barely preceded the pitch-up and could serve as a warning for slow rates of entry. If the control system is such that the stick-force gradient has an abrupt decrease with increased normal acceleration, an apparent pitch-up, which can be potentially dangerous, is evident to the pilot.

Buffeting Characteristics

When Mach number increased in level flight at altitudes above approximately 25,000 feet, or when maneuvers were performed to levels

of normal acceleration in excess of $1g$, buffeting was encountered. Figure 4 shows the variation of normal-force coefficient with Mach number for the onset of buffeting for the test airplane. The buffeting is first perceptible to the pilot through the control column and is similar to rough-air turbulence; the intensity rise is quite gradual with increase in speed or normal acceleration. On this airplane the severity of buffeting did not appreciably limit aircraft maneuvering up to the maximum of $2g$ tested. However, consideration of passenger comfort may dictate that the aircraft be operated sufficiently below this boundary to permit normal maneuvering without encountering buffeting. For example, for an airplane with a wing loading of 75 lb/sq ft operating at an altitude of $35,000$ feet, for which the lower dashed line in this figure shows the variation of level flight ($1g$) normal-force coefficient with Mach number, a normal operating Mach number 0.03 below that for level-flight buffeting would provide a normal-acceleration maneuvering range of $0.5g$ prior to encounter of buffeting at essentially constant speed.

Although little difference could be detected between the buffeting encountered at high speed and that produced by high-altitude turbulence, it is believed that buffeting would serve as a warning, in any case, for the pilot to slow down.

For an airplane that was performance-limited in level flight to operation slightly above or in the buffet boundary, an accelerated longitudinal maneuver would cause a decrease in speed so that the variation of C_N with M would parallel the buffet boundary with little or no increase in buffet severity. For an airplane that was not performance-limited and which could operate at speeds well into the buffet boundary, an accelerated maneuver could produce sizable increases in severity of buffeting.

Lateral-Directional Damping Characteristics

In order to evaluate the degree of lateral-directional damping desired for high-altitude cruise, various lateral-directional dynamic characteristics were obtained on the test airplane by using a yaw damper. The dynamic characteristics shown in figure 5 were obtained by varying the yaw-damper gain setting. This figure shows the variation of time to damp to half amplitude or the time to double amplitude of the lateral-directional oscillation with Mach number. Data are presented for three damper conditions: damper on, off, and reversed. Reversed damping was evaluated to investigate handling characteristics with materially less damping than that produced by the basic airframe. At Mach numbers below about 0.84 the damping of the basic airplane with damper off was satisfactory in smooth air in straight and level flight

but was considered marginal for smooth-air maneuvering, because of the residual induced oscillations. During high-altitude flight in turbulence, the damping became unsatisfactory. In this speed range the damping provided with damper on was particularly beneficial at high altitude and in rough air and would provide a margin of comfort for passenger-carrying aircraft. At near maximum speeds it was sometimes difficult to appreciate any additional damping provided by the yaw damper because of the improved aerodynamic damping. The level of damping provided by the reversed damper was entirely unsatisfactory and would constitute an emergency condition from structural considerations, even though the pilot could control the aircraft. From the viewpoint of airplane controllability and passenger comfort, it is felt that lateral-directional damping should be sufficient to damp any oscillation to half amplitude within 3 or 4 seconds.

Evaluation of Desirable Lateral-Control Characteristics

Lateral-control requirements for the high-altitude cruise condition appear to be much less stringent than for the low-speed landing and take-off condition that is discussed in reference 1. Figure 6 shows the results of rudder-fixed aileron rolls where time to bank 30° , maximum helix angle, and maximum roll rate are plotted against Mach number. The data are presented in these three forms for comparison and discussion purposes. The solid lines show the lateral-control power produced by full deflection of inboard ailerons alone, and the dashed lines represent the lateral-control power produced by inboard ailerons and all spoiler controls. The control levels produced by ailerons and either inboard or outboard spoilers were evaluated and provided intermediate control levels, as anticipated. The apparent decay in performance above a Mach number of approximately 0.8 is a result of spoiler blow-down with increasing dynamic pressure.

The helix angle of 0.02 shown for ailerons alone appears to be low when compared with the Air Force requirement of 0.07 for transport aircraft. Testing has shown that for small course corrections or heading changes requiring up to 30° bank angle, ailerons alone gave a comfortable rate of roll. It is believed that a roll rate of not more than 0.2 or 0.3 radian per second should be adequate for normal operations.

For this particular airplane configuration the absence of spoiler buffeting, when ailerons alone are used for lateral maneuvering, is an added attraction for pilots and passengers alike. With an aim at keeping as much lateral control as possible for collision avoidance, some thought might be given to the use of a differential control where the spoilers would be employed after approximately 60 to 70 percent of the control-wheel "throw."

Assessment of Overspeed Capabilities

As the aircraft designer labors to make his airplane go ever faster, the existing problems of overspeed and speed control become still greater because of the possibility of exceeding design limits, even in level flight. Figure 7 shows the potential of the airplane in exceeding the dynamic-pressure design limits in case climb power is retained after level off at altitude. The solid lines represent the data from tests at two altitudes for a thrust-weight ratio of 0.23. At 12,000 feet and a climb speed of 280 knots, approximately 75 seconds was required before an arbitrary placard speed of 350 knots was reached. At 25,000 feet a full 2 minutes elapsed for essentially the same increase in speed. The dashed lines represent data for the same airplane using engines having thrust-weight ratios of 0.29, and even greater thrust potentials can be imagined. The seriousness of the problem is somewhat reduced at higher altitudes, where the airplane has Mach number limitations and the pilot has a certain amount of buffet warning. At lower altitudes where the transport has dynamic pressure limitations, the pilot has only his airspeed instrument to warn him of approaching limits. This instrument could be neglected during instrument-flight conditions involving increased cockpit activity and attention to other details. The addition of a horn, bell, or warning light, or a combination, appears to be the best solution to the problem.

Upset-Maneuver Evaluation

Closely associated with the level-flight overspeed problem is the possibility of the airplane exceeding design limits during a so-called "upset" maneuver resulting in a dive. In order to provide information leading to speed-spread requirements, an evaluation of various upset maneuvers was made. In general, the upsets were initiated from cruise in level flight by pilot-induced control movement. Figure 8 shows the results of some of these tests performed at two altitudes for various dive angles. At 25,000 feet, a placard speed of 365 knots was used, and the upset maneuvers were started 25 to 45 knots below this placard speed. The time required to reach maximum speed is shown as the end point of each maneuver; however, the recovery technique was started earlier as shown by the marks indicating throttle to idle or speed brakes open. For the 35,000-foot condition a Mach number of 0.9 was used for the placard speed and starting Mach numbers as high as 0.875 were used. Dive angles varied from 4° to 16° .

It was felt that placing the airplane in a dive by elevator control was rather unrealistic and a more severe requirement might result when the upset maneuver was executed by a runaway stabilizer trim motor. In these tests the copilot initiated the upset by use of the stabilizer trim switch, and the pilot's task after recognizing the

upset was first to halt the runaway condition and then to recover. An example of this type of maneuver is shown for an altitude of 35,000 feet (fig. 8) at a dive angle of 4° which resulted in a speed increase of approximately 10 knots. This method of testing pointed up the desirability of having a positive nose-up trim change with application of speed brakes, which materially helped in recovery where elevator stick force was high as a result of runaway trim. The pilot was usually aware of the upset in 2 to 3 seconds, and recovery action was taken immediately, using not over 1.5g. The speed brakes were most effective in controlling speed, as can be seen by the short time interval between their application and the maximum speed attained.

A few more comments pertinent to the upset condition and speed-spread requirements are considered necessary. It is difficult to specify exact speed-spread requirements because of the important effect of the drag rise in limiting aircraft maximum speeds. An example of this can be seen in figure 8 for an altitude of 35,000 feet, where an upset initiated at $M \approx 0.875$ with an 11° dive angle produced a smaller speed increment than an upset initiated from $M \approx 0.805$ with a 12° dive angle. Thus, an airplane having its limiting or design speed barely in the drag-rise region might be unduly penalized by a speed-spread requirement based on a given upset maneuver compared with another airplane having its limiting or design speed well into the drag-rise region.

Slow-Down and Descent Evaluation

The inability to slow down a fast-moving transport becomes greater as speed and weight are increased. The need for a slow-down capability may arise when encountering heavy turbulence or in an aircraft emergency. Figure 9 shows the time required to slow down to the landing-gear placard speed from cruise conditions at two altitudes. Various techniques were used such as throttle "chop" to idle; throttle chop T plus opening of speed brakes B; and finally throttle chop T, speed brakes B, and a 1.5g turn or pull-up W. For the 35,000-foot altitude the time required was cut in half when speed brakes were added to the throttle chop. This time was again cut in half when a 1.5g pull-up was used with the throttle chop and speed brakes. Obviously, this last method cannot be used where strict altitude limits are needed but does illustrate the potential available if a slight pull-up could be used. In the test cases approximately 1,200 feet altitude was gained during the maneuver.

The penalties associated with providing adequate drag by means of speed brakes have caused a general use of the landing gear as a drag device. Probably the greatest single improvement for slow-down capabilities, therefore, would be in the designing of the landing gear for

operation at speeds at or near cruise conditions. A landing gear that could be lowered at all operational speeds should be available at all times when operating above 30,000 feet. This requirement becomes of prime importance when emergency descent from altitude is considered. Figure 10 illustrates this point by showing the descent capabilities of the test airplane utilizing two different techniques. Descent performed with the normal technique, represented by the solid line, utilized a throttle chop T (at time zero) and extension of landing gear G. The emergency technique, represented by the dashed line, was performed with a throttle chop, extension of landing gear G, and opening of speed brakes B. Also shown is a curve representing the time for personnel unconsciousness at a given altitude upon complete loss of cabin pressurization. It can be seen that when the airplane cruises at an initial Mach number $M_1 = 0.88$ at an altitude of 35,000 feet, more than 30 seconds of throttle at idle were necessary before gear-down speed was reached. When this time is compared with the 30 seconds shown for loss of consciousness at this altitude, any time saved in using all drag devices is of great importance. Had it been possible to lower the landing gear at cruise speed, the descent curve could possibly remain within consciousness levels. For the emergency descent initiated from an altitude of 40,000 feet, maximum speed attainable was below gear placard speed and consequently the gear could be lowered immediately.

The emergency descent technique provided rates of descent up to about 9,000 feet per minute, which is a marked improvement over the normal technique; however, the buffeting, noise, and objectionable airplane attitude associated with this technique would obviously limit its use to emergencies only.

Supersonic Pass Evaluation

Some question has existed regarding the effects on a large jet transport resulting from the passing of another aircraft in close proximity at supersonic speeds. An evaluation of this potential problem area was performed with the test airplane, which was flown at an altitude of 35,000 feet and a Mach number of 0.8. An overtaking fighter airplane was used to generate the supersonic flow field. Data were obtained from a pass of the supersonic airplane flying 500 feet directly below the test airplane at $M = 1.2$ and then from a lateral pass with 500 feet of separation at $M = 1.8$. In neither instance did the test airplane experience any measurable changes in angle of attack or sideslip. For the underneath pass, the normal-acceleration excursion was $\pm 0.05g$. For the lateral pass, the vertical-tail load was less than 1 percent of the design limit load. In both cases the pilot could barely detect the passing shock wave.

CONCLUDING REMARKS

The following conclusions are based on a flight evaluation of the problems that could affect operation of jet transports in the transonic region:

1. Unstable control characteristics encountered in the transonic speed range are controllable if the magnitude of force reversal and rate of speed change are moderate. From the pilot's viewpoint, it would be highly desirable to provide some automatic device to give stable trim control-force variations in the transonic region; however, with such automatic device inoperative, the basic airplane force variation with speed should be no greater than about 40 or 50 pounds.
2. A normal operating Mach number approximately 0.03 below that for level-flight buffeting is recommended to provide an adequate maneuvering range.
3. A slight reduction in longitudinal stability can be tolerated because of the slow pitch rates involved.
4. From the viewpoint of airplane controllability and passenger comfort, it is believed that lateral-directional damping should be sufficient to damp any oscillation to half amplitude within 3 or 4 seconds.
5. A roll rate of 0.2 to 0.3 radian per second was found to be adequate for normal high-speed maneuvering.
6. Inasmuch as a potential exists for exceeding maximum-speed design limits, especially at lower altitudes where warning provided by such phenomena as buffeting is not present, it is recommended that a horn or other device be provided as a warning to the pilot.
7. An upset maneuver induced by stabilizer input, which was judged to be a realistic evaluation maneuver, provided a speed increment of the order of 10 to 15 knots, and recovery from this maneuver was readily effected.
8. In order to perform optimum slow down or descent such as might be required for emergency conditions, extension of the landing gear to provide drag at all operational speeds above 30,000 feet is recommended.

REFERENCE

1. Fischel, Jack, Butchart, Stanley P., Robinson, Glenn H., and Tremant, Robert A.: Flight Studies of Problems Pertinent to Low-Speed Operation of Jet Transports. (Prospective NASA paper.)

TEST AIRPLANE

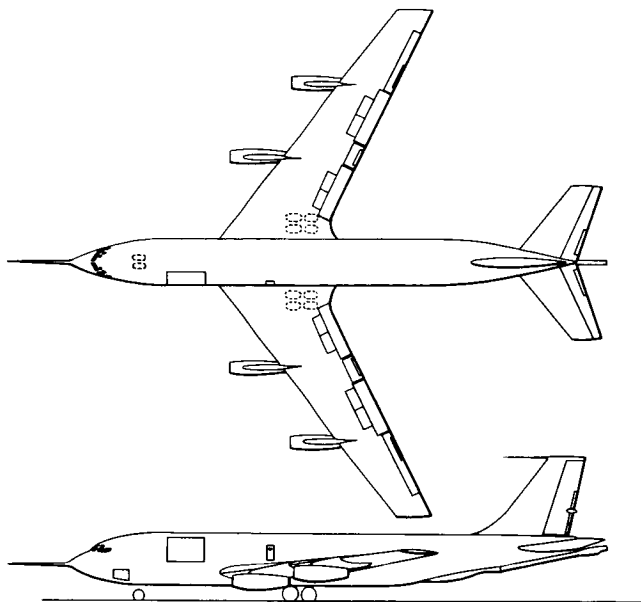


Figure 1

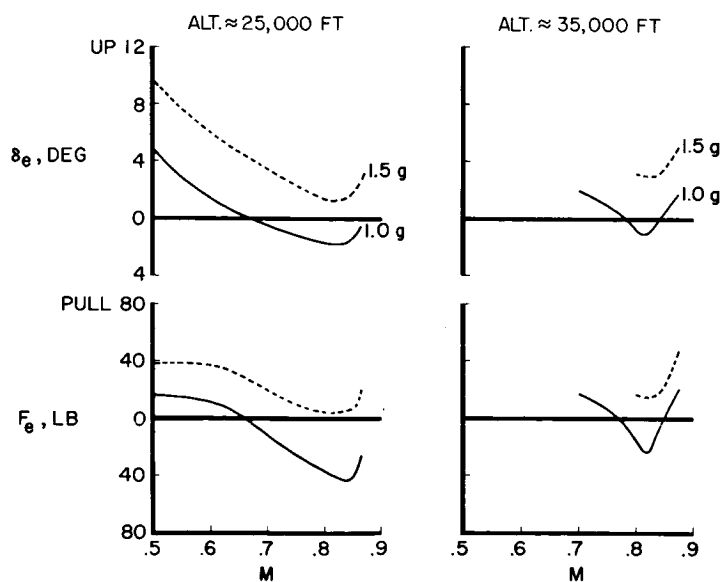
LONGITUDINAL TRIM CHARACTERISTICS
POWER ON

Figure 2

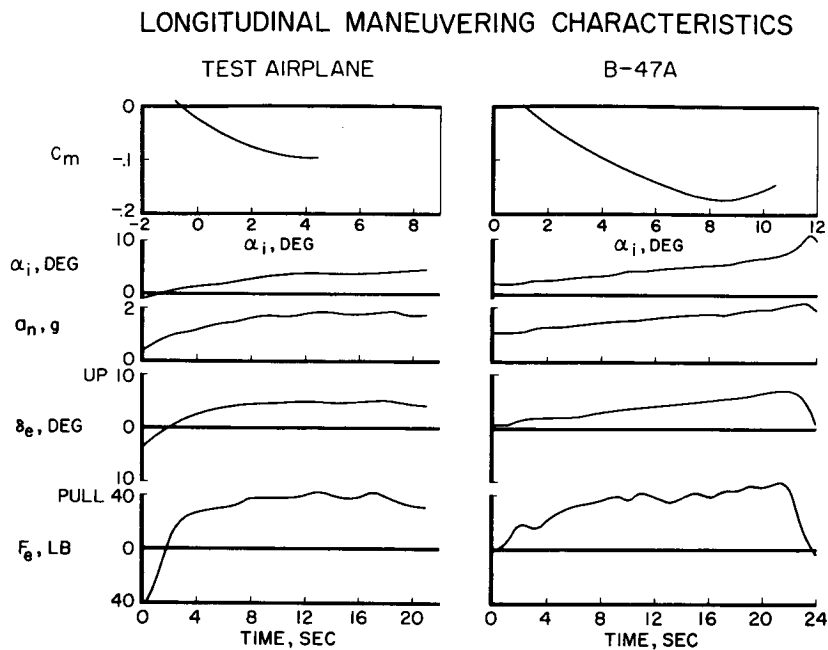


Figure 3

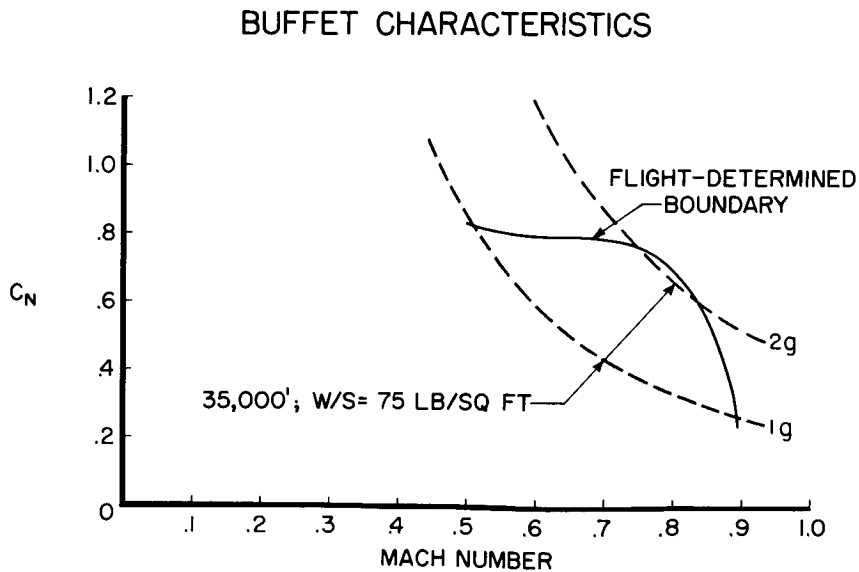


Figure 4

DYNAMIC LATERAL-DIRECTIONAL CHARACTERISTICS

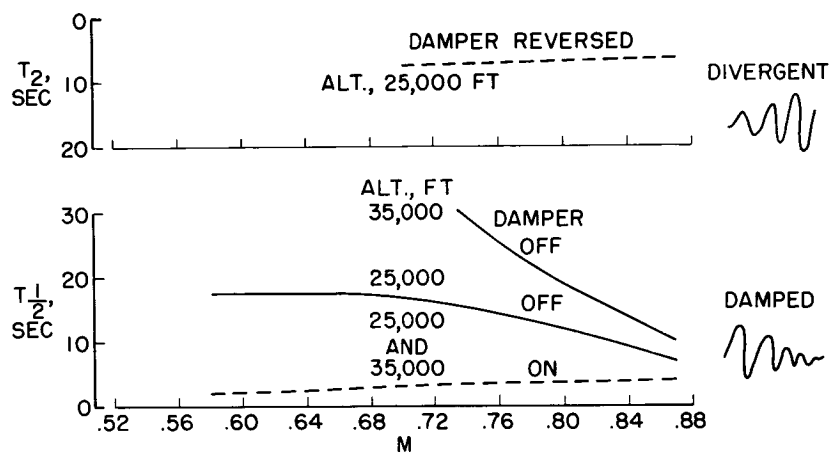


Figure 5

RUDDER-FIXED ROLL CAPABILITY

ALT. = 35,000 FT

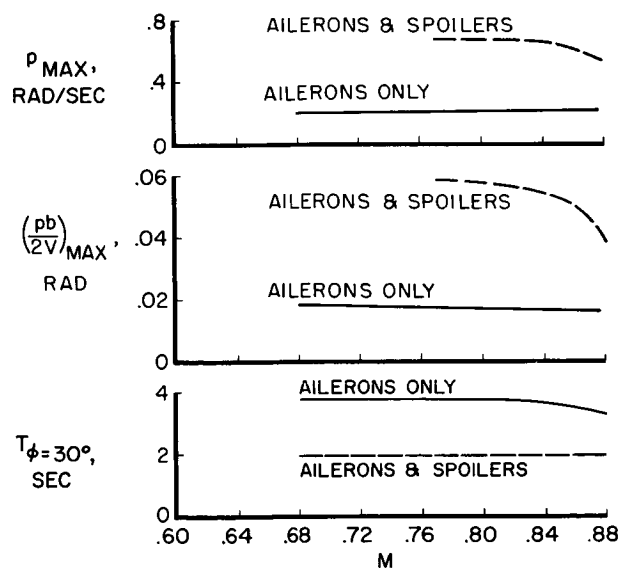


Figure 6

CLIMB-POWER ACCELERATION

W/S = 84 LB/SQ FT

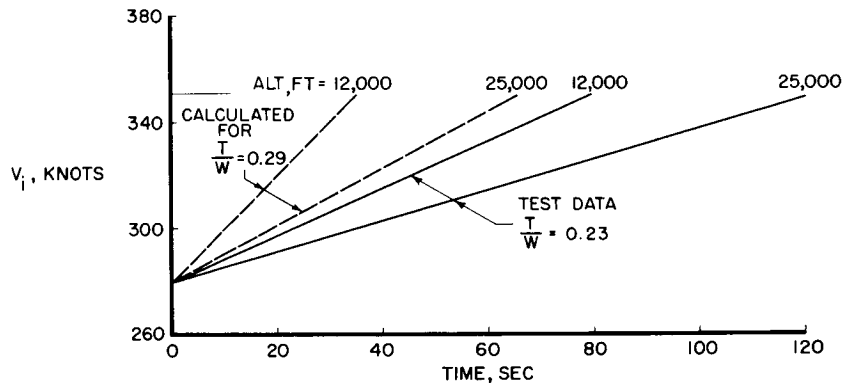


Figure 7

SUMMARY OF UPSET EVALUATION

ALT. = 25,000 FT

ALT. = 35,000 FT

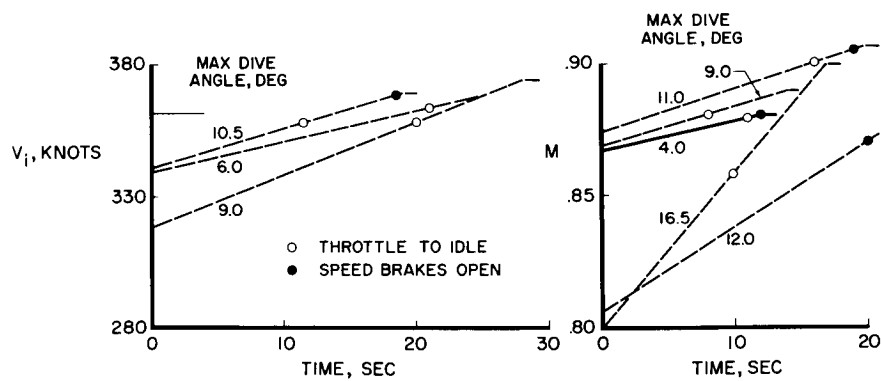


Figure 8

SLOW-DOWN CHARACTERISTICS

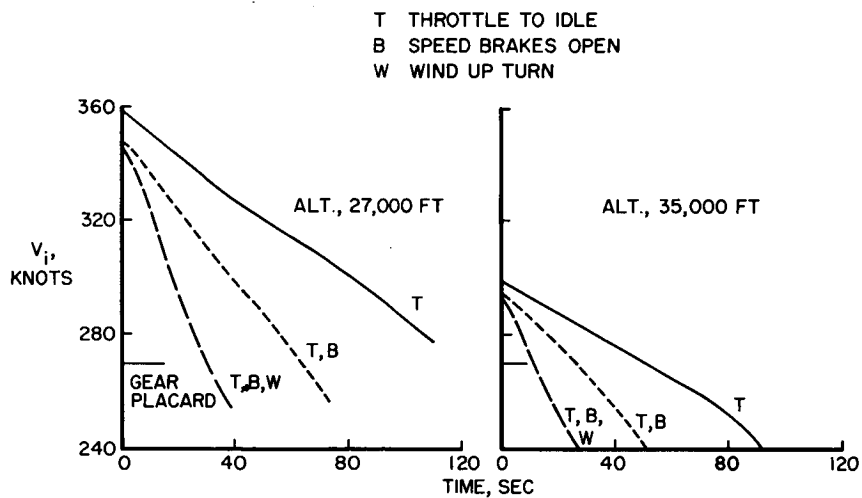


Figure 9

DESCENT CHARACTERISTICS

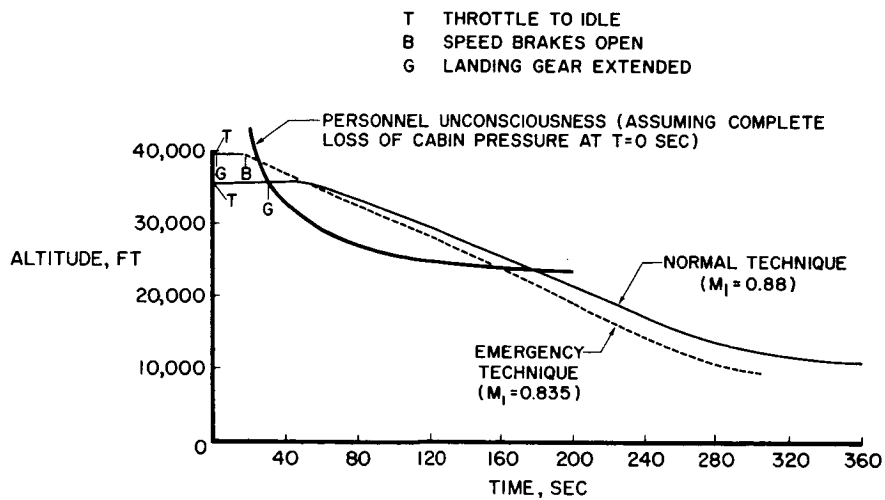


Figure 10

A COMPENSATED STATIC-PRESSURE TUBE FOR FUSELAGE-NOSE INSTALLATIONS

By William Gracey and Virgil S. Ritchie

Langley Research Center

SUMMARY

A static-pressure tube designed to compensate for the position errors of fuselage-nose installations in the subsonic speed range is described. This type of tube has an ogival nose shape with the static-pressure orifices located in the low-pressure region near the tip. The results of wind-tunnel tests of these compensated tubes at two distances ahead of a model of an aircraft showed the position errors to be compensated to within 1/2 percent of the static pressure through a Mach number range up to about 1.0. By a refinement in the location of the orifices, the compensation was extended into the supersonic speed range up to a Mach number of 1.18. The effect of angle of attack on the errors of the compensated tubes is also presented.

INTRODUCTION

As the cruise speeds of transport aircraft are extended into the transonic and supersonic speed ranges, the altitude errors due to the static-pressure source will, in general, become very much larger than those for subsonic speeds. This will be particularly true for fuselage-nose installations, the errors of which can reach enormous proportions just prior to the passage of the fuselage bow wave. The fuselage-nose installation, on the other hand, is most desirable for supersonic operation because, once the fuselage bow wave has moved to the rear of the static-pressure tube, the tube becomes isolated from the flow field of the aircraft. In order to realize the advantages of the fuselage-nose installation in the supersonic speed range, the Langley Research Center has been investigating the possibility of developing a static-pressure tube which would compensate for the position errors of nose installations in the subsonic speed range. The results of this investigation will be discussed following a review of some aspects of the altitude-measuring problem.

SYMBOLS

$\Delta h_{30,000}$	altitude error at 30,000 ft
p	static pressure
M	Mach number
x	distance from nose of tube to orifice
d	maximum diameter of tube
D	maximum diameter of body

DISCUSSION

Figure 1 shows the allowable tolerances for the altitude errors due to the static-pressure source as specified for civil and military aircraft. In this figure the altitude error Δh at an altitude of 30,000 feet is plotted as a function of Mach number M . At a Mach number of 0.9, the Mach number range where the new jet transports will be operating, the tolerance for civil aircraft is ± 900 feet and that for military aircraft is ± 230 feet. When these errors are compared with the vertical separation minimums which, for reciprocal headings, are 1,000 feet for altitudes up to 29,000 feet and 2,000 feet for the altitude range above 29,000 feet, it will be apparent that the civilian aircraft allowance is too large for both 1,000-foot and 2,000-foot minimums and that the military aircraft allowance is probably too large for 1,000-foot minimums, especially when it is considered that this is only one of the errors that determine the accuracy of the altitude measurement. In view of this situation, the International Civil Aviation Organization (ICAO) has recommended a tolerance of ± 50 feet for all speeds and altitudes. This tolerance represents a degree of accuracy which would be difficult to achieve with present-day instrumentation and techniques. A more realistic value, for the present time, would be a tolerance of $\pm 1/2$ percent of the static pressure. This value corresponds to an altitude error of 140 feet at sea level, 110 feet at 30,000 feet, and about 100 feet at 60,000 feet.

Figure 2 shows the calibrations of representative static-pressure-tube installations on the fuselage nose, the wing tip, and the vertical fin. Again, the altitude errors at 30,000 feet are plotted as a function of Mach number. For each of the three installations, the errors increase rapidly in the high subsonic speed range and reach peak values

just prior to the passage of the bow waves. At this point the error of the fuselage-nose installation becomes that of the isolated tube, which for this case is assumed to be zero. The errors of the wing and fin installations, on the other hand, continue to vary by large amounts in the supersonic speed range. The large increase for the wing installation is due to the rearward bending of the fuselage bow wave; once this bow wave has moved to the rear of the static-pressure tube, the error of the wing installation becomes that of the isolated tube, which is again assumed to be zero.

As an aircraft would not be expected to cruise for any length of time in the Mach number range around 1.0, it is believed that, from the standpoint of vertical separation, the aircraft operator will be mainly concerned with the altitude errors in the Mach number range up to 0.9 and in the Mach number range above 1.1. On this basis, the errors of these installations at a Mach number of 0.9 are 100 feet for the fin installation, 400 feet for the wing installation, and 1,000 feet for the fuselage-nose installation. In the Mach number range beyond 1.1, the error of the nose installation is, of course, zero. The errors for this particular fin installation reach values of about 600 feet and the errors for the wing installation reach values of about 2,800 feet.

Figure 3 shows the calibrations of a number of fuselage-vent installations. These calibrations were chosen to show that the errors of vent installations at subsonic speeds may be either positive or negative, this result being in contrast to the errors of the static-pressure-tube installations (fig. 2) which, at subsonic speeds above the stall region, are in all cases negative. At a Mach number of 0.9, the errors range from -300 feet to 700 feet, and in the Mach number range beyond 1.1 the errors are about 1,300 feet and 1,700 feet.

It will be apparent from the magnitudes of the errors of these installations that some means must be found to reduce the static-pressure errors if altitude errors on the order of 100 feet are to be achieved. The static-pressure errors may be minimized in any one of a number of ways: (1) by the use of an electro-mechanical compensator which computes the error and applies a correction before the altitude indication is displayed, (2) by the use of two static-pressure installations (for example, it would be possible to use a fin installation up to a Mach number of 0.9 and then, at supersonic speeds, to switch to a fuselage-nose boom which, in this case, could be relatively short), and (3) by changing the local pressure at the static-pressure source to values corresponding more closely to free-stream values.

As shown on figure 4, the last method can be applied to fuselage-nose installations by the use of a novel form of a static-pressure tube. This tube has an ogival nose shape with the static-pressure orifices located in the low-pressure region near the tip. The two curves on this

figure represent the position-error variations, as determined by wind-tunnel tests, at two positions ahead of a model of an aircraft configuration. The position error Δp is presented as a fraction of the static pressure and is plotted as a function of Mach number. By the proper combination of nose shape and orifice location, it is possible to produce a static-pressure-error variation with Mach number which will be a mirror image of the position-error variation at a given position ahead of the fuselage. The results of the tests of the two tubes at distances of 0.27 and 0.95 fuselage diameters ahead of the fuselage nose are shown by the symbols along the zero-error line. These results show that, even for positions as short as 0.27 fuselage diameter, the position errors of the fuselage can be compensated to within 1/2 percent of the static pressure throughout the subsonic speed range. It should be noted that, after the passage of the fuselage-bow shock, the error for the long-nose tube falls to a negative value. The reason for this is shown on figure 5.

Figure 5 presents typical pressure distributions along the nose of the tube at subsonic and supersonic speeds. On this figure the static-pressure-error coefficient $\Delta p/p$ is plotted as a function of the distance x/d along the tube. For the position of the orifices on the tube shown in figure 3, the error at subsonic speeds is negative (as is required for compensation) and the error at supersonic speeds (which would be that of the isolated tube) is also negative. If the orifices had been located at a position of about $2.7d$, the error at subsonic speeds would have about the same negative value as at $x/d = 5$ and the error at supersonic speeds would be zero. Although a tube with the orifices at $2.7d$ was not tested on a fuselage-nose installation during this investigation, the long-nose tube shown in figure 4 was altered by locating three sets of orifices in the region near $x/d = 2.4$; thus, the positive pressure at these orifices would balance the negative pressure of the rear set of orifices ($x/d = 5$) and would produce a zero error at supersonic speeds.

The results of tests of this tube are shown in figure 6. The curve in this figure represents the position-error variation at a distance of about 1 fuselage diameter ahead of the model aircraft. The results of the tests of this tube, as shown by the symbols along the zero-error line, show the position errors to be compensated for throughout the subsonic speed range and, at supersonic speeds, the error of the isolated tube to be within 1/2 percent of the static pressure for Mach numbers up to 1.18, the limiting Mach number for these tests.

The effect of angle of attack on the errors of these static-pressure tubes is shown in figure 7. For this case the static-pressure-error coefficient is plotted as a function of the angle of attack of the tube. The lower curve shows the effect of angle of attack for a

tube with the orifices encircling the tube. For an angle-of-attack change of 4° (the variation which would be expected for a level-flight cruise of about 3,000 miles), the additional error due to angle of attack is about $1/4$ percent of the static pressure. For a wider range of angle of attack, the location of two orifices 37.5° on either side of the bottom will extend the range of insensitivity to at least $15\frac{1}{2}^{\circ}$, the limiting angle of attack of these tests.

During the course of the investigation in the Langley Full-Scale Division several additional variables and design features were tested. (Results of these tests are unpublished.)

CONCLUDING REMARKS

In conclusion, the results of this investigation have shown that it is possible, by the use of a comparatively simple form of static-pressure tube installed on a relatively short boom, to compensate for the position errors of fuselage-nose installations in the subsonic speed range and thus to realize the advantages of nose installations in the supersonic speed range.

ALLOWABLE ALTITUDE ERRORS

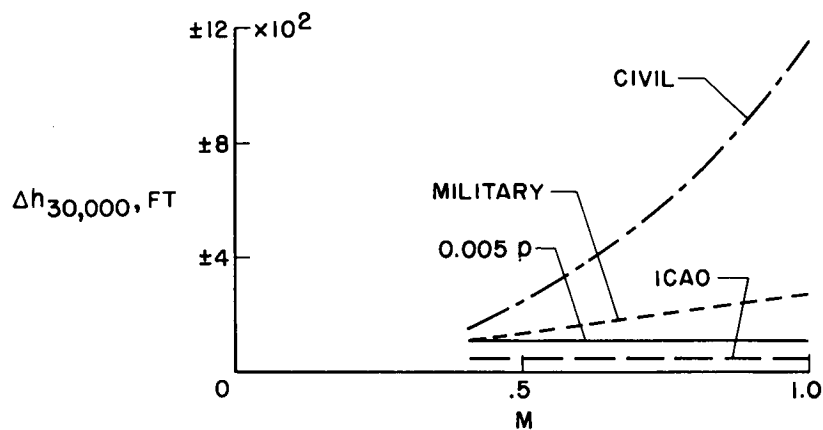


Figure 1

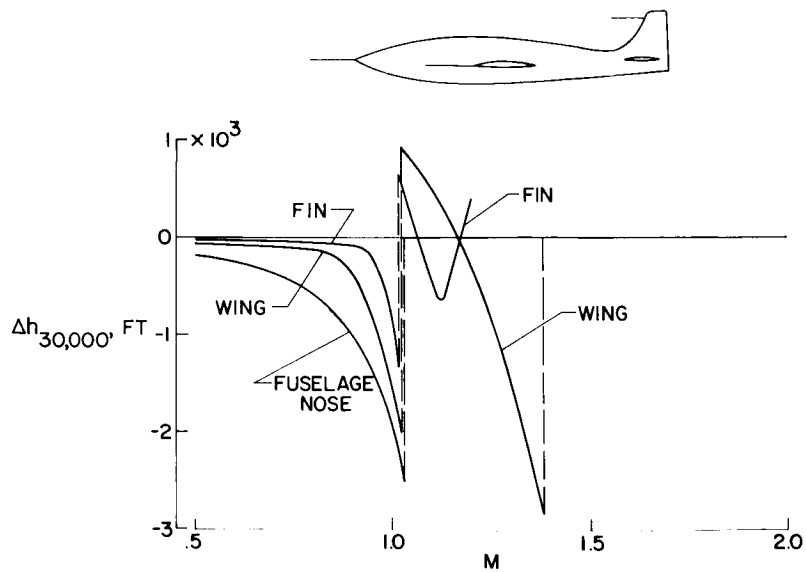
ALTITUDE ERRORS
STATIC-PRESSURE-TUBE INSTALLATIONS

Figure 2

ALTITUDE ERRORS FUSELAGE VENT INSTALLATIONS

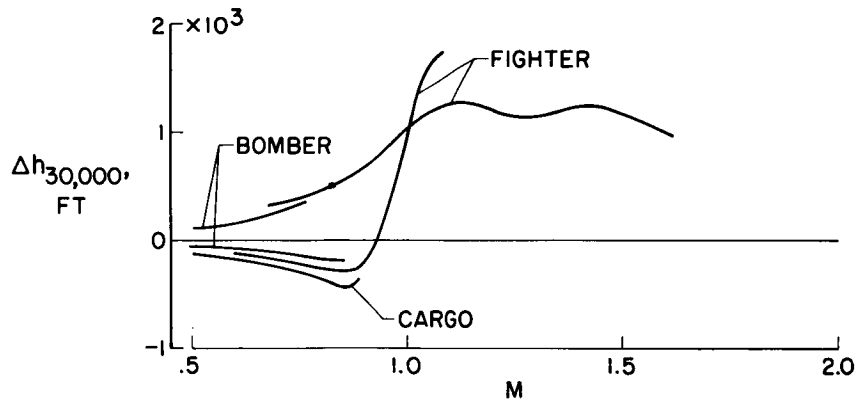


Figure 3

AERODYNAMIC COMPENSATION OF POSITION ERROR

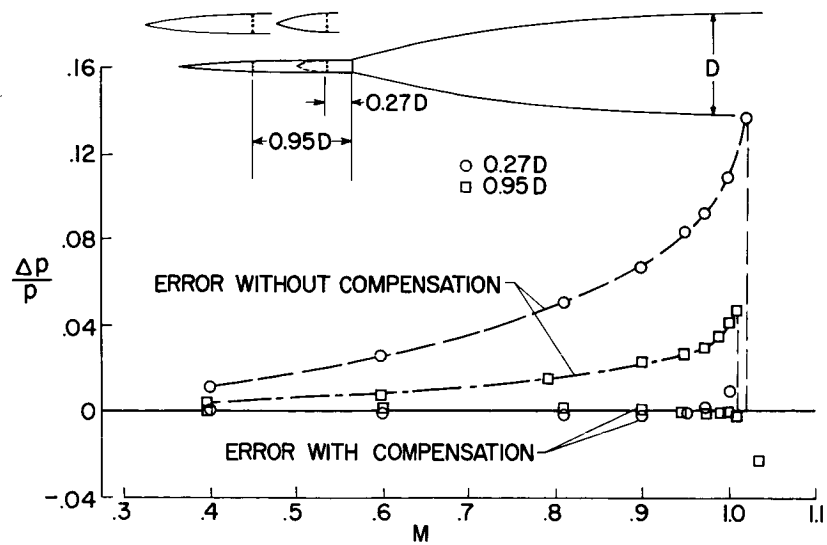


Figure 4

PRINCIPLE OF DESIGN FOR SUPERSONIC SPEED

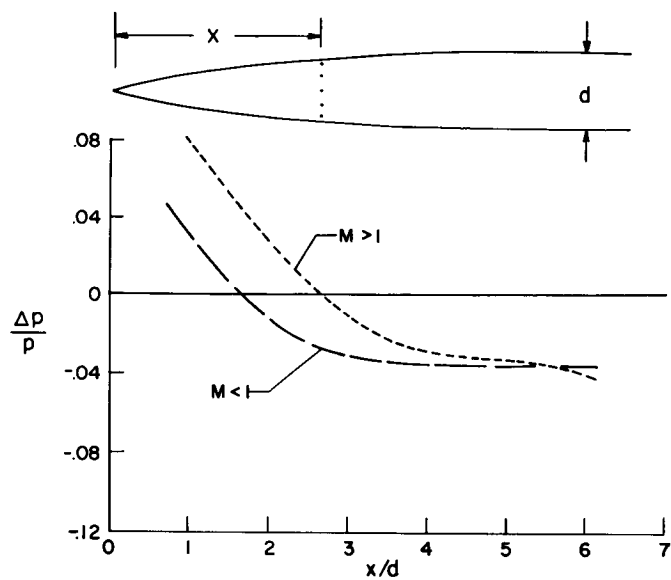


Figure 5

APPLICATION TO SUPERSONIC AIRCRAFT

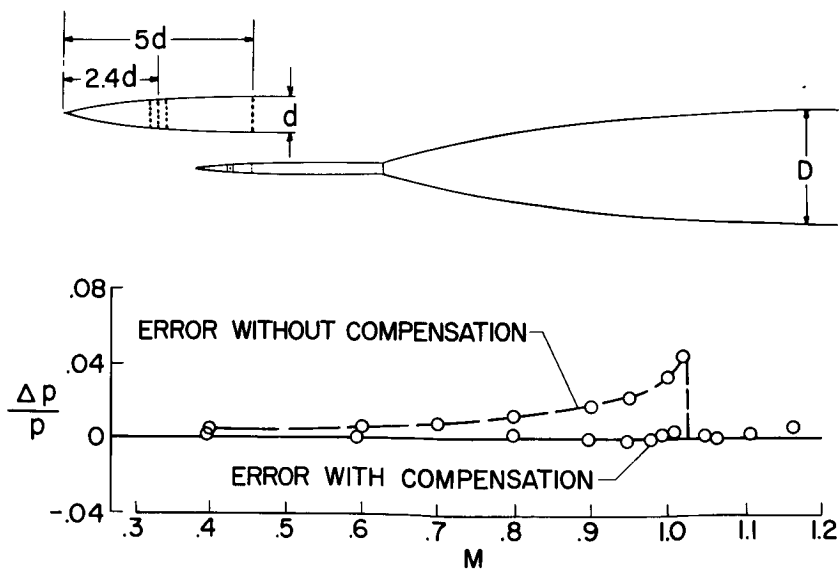


Figure 6

COMPENSATED TUBES AT ANGLES OF ATTACK
 $M = 0.6$

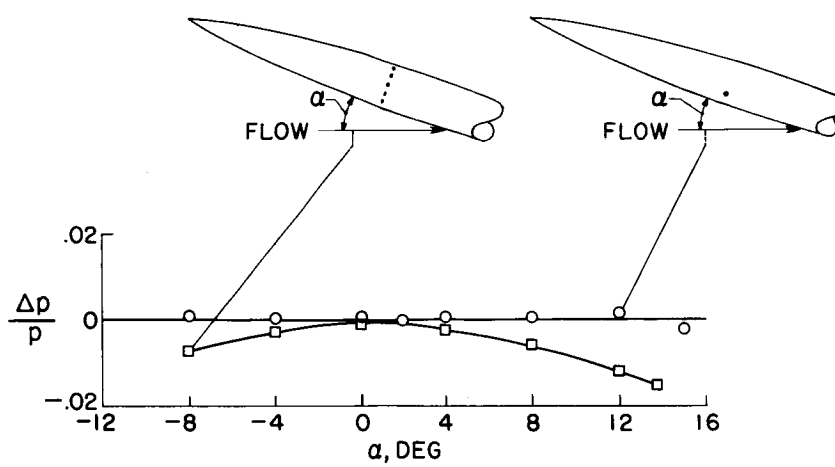


Figure 7

ELECTROSTATIC HAZARDS DURING HIGH-SPEED FUELING

By I. Irving Pinkel

Lewis Research Center

INTRODUCTION

The design of high-speed fueling systems for jet aircraft has raised concern for fire in the airplane fuel tank ignited by electrostatic sparks. The electrostatic charge that produces these sparks is generated and transported by the fuel as it flows through the components of the fueling system to the fuel tank where jet fuels often establish combustible atmospheres. Petroleum industry experience indicates that the high-speed fueling rates being considered for jet aircraft approach the values that have caused tank explosions in refineries.

In order to assess this hazard for aircraft, the petroleum and aircraft industries are cooperating in a study under the Coordinating Research Council. Their work, so far, has shown that sparks can appear in tanks being fueled at moderate flow rates with unaltered batches of JP-4 fuel which have a greater than average electrostatic activity. Since the results of this latest work increases our concern, it was considered desirable to review the basic nature of this problem at this conference, as it may prove to be an operating problem that the jet transport manufacturer and operator must consider. An excellent reference (ref. 1) is now available which presents a complete treatment of the material of this paper.

DISCUSSION

The problem is discussed conveniently with reference to figure 1, which shows a schematic arrangement of an aircraft ground fueling system. This ground fueling system consists of a fuel storage tank, a pump, a line to the fuel filter, and a line to the aircraft tank.

Fuel is charged as it flows by any surface in the fueling system. The rate of fuel charging increases with the surface area wetted by the fuel and approximately with the square of the fuel flow speed. This **strong** dependence of fuel charging rate on fuel flow speed is one of the principal reasons for concern in high-speed fueling systems. The filter is the site of the highest fuel charging rate because of the large surface area it presents to the fuel and the high velocities attained by the fuel in its narrow flow passages.

Appreciable fuel charging also occurs in the fuel lines. The fuel acquires one charge, either positive or negative, and the inner wall of the line acquires the opposite charge. Once this charge separation occurs an electric field is established between the charged fuel and the line wall. This electric field produces an electric current through the fuel to the line wall that tends to reduce the charge carried by the fuel. The magnitude of the current varies with the electric field strength between the fuel and the wall and the electrical conductivity of the fuel. For fuels having the same charging tendency, those with the highest electrical conductivity are to be preferred because they discharge most readily by electrical conduction to the line wall.

A plot of the variation of the charge carried by the fuel as a function of location in the fueling system would then have the general character shown in figure 2. Starting from the pump, there is a continuous increase in fuel charge as the fuel flows along the line. If the fuel line is long enough, the maximum charge would occur at some location where the charging rate and discharge rate by electrical conduction through the fuel to wall layer would be equal. No further increases in fuel charge occurs until the fuel filter is reached. In passage of the fuel through the filter the fuel charge reaches peak values. The strong electric field that now exists between the fuel and the line provides a charge relaxation rate by electrical conduction through the fuel which is greater than the charge separation rate in the fuel line after the filter. The fuel charge declines with displacement along the line.

If the line between the filter and tank is long enough, the charge carried by the fuel will decline to the maximum that the line alone would have developed without the filter. If this line is short, then the fuel carries the high filter-outlet charge into the tank.

As the tank fills with charged fuel, an electrostatic field develops between the fuel and the metal tank. This field increases with the height of the fuel level in the tank. If the tank fills slowly, appreciable fuel charge can leak to the tank wall by conduction. If the filling is rapid, less relief is obtained by charge conduction.

The electrostatic field between the fuel and the tank exists whether or not the tank is grounded. In the ungrounded tank, the charge appears on the tank wall by induction according to the schematic arrangement of figure 3. Assume that the fuel carries a negative charge. Then positive charges are attracted to the inside tank surface and negative charges are repelled to the outer surface. The field between the fuel surface and the inner tank wall may exceed the breakdown value and a spark may jump through the gas space. If there is enough energy in the spark, it will ignite a combustible atmosphere in this gas space above the fuel.

measures can be taken. Some of these are illustrated in figure 4 which shows a schematic representation of a fuel system. In the system shown, the fuel filter is separated by a long length of line from the tank to allow time for charge relaxation by electrical conduction through the fuel before the fuel enters the tank. Also shown is a grid of wires floating on the fuel surface. This grid is electrically connected to the tank wall. In this way the potential of the fuel surface is brought close to that of the tank wall and strong electrical fields in the vapor space are avoided. The practicality of the floating grid for aircraft use is questionable. Also, a radioactive source can be placed in the tank to ionize the gas space and increase its electrical conductivity. This would have the effect of electrically connecting the fuel surface and the tank wall so that strong electric fields between them will not develop. This approach is being evaluated by one of the oil companies. In all probability all measures would not be required in any one fueling system.

From the standpoint of the airplane industry, the most desirable solution would be to remove the constituents in the fuel responsible for its charging tendency. Unfortunately these constituents are contaminants that are present in trace amounts and their removal would be costly. Also, many of the contaminants are introduced into the fuel during storage and transfer after refining. The alternative solution would be to find acceptable fuel additives that raise the electrical conductivity of the fuel by a factor of a thousand or more without increasing the charging tendency significantly. Recently, one of the oil companies has announced an effective antistatic additive that is effective in concentrations of several parts per million in the fuel. The additive is a mixture of two salts. Past experience has shown that the addition of a single salt to the fuel increases its electrical conductivity and its charging rate to about the same degree. No real advantage results from such addition. By using two salts, the electrical conductivity of the fuel is increased many times more than the charging tendency to produce a net safety advantage.

Before fuel additives can be accepted for aviation, it must be demonstrated that the additive is not lost by deposition on the walls of storage tanks or in the filter or by reaction with other additives, such as corrosion inhibitors. Its suitability in the engine must also be demonstrated.

CONCLUDING REMARKS

Work conducted on this problem to date suggests that fuels with dangerous electrostatic activity occur infrequently. As an interim solution to the problem it has been recommended that an instrument be

When the tank is ungrounded, the charge on the outside surface of the tank produces an electrostatic field exterior to the tank. A grounded conductor accidentally placed close to the outside wall may draw a spark if this external field is strong enough. If this grounded conductor strikes the spark near the tank vent where a combustible atmosphere may exist, the resulting flame may enter the tank.

This hazard may be avoided by electrically connecting the tank to the ground and drawing off the external charge. The charge on the inside wall of the tank is held in place by the attraction of charges of opposite sign in the fuel. The electric field within the tank remains. Grounding does not eliminate the ignition hazard within the tank.

In the recent cooperative study of the petroleum and airframe industry, sparks have been detected in a 5,000-gallon laboratory tank made available by Wright Air Development Center of the U. S. Air Force. Sparks were obtained when a metal probe extended from the tank wall to the fuel surface. (See fig. 3(b).) The end of the probe provides a point of concentration of the electric field which promotes spark formation. A metal can floating on the fuel near the tank wall provided a spark as well. The can may represent a detached piece of tank instrumentation or an object accidentally introduced in the tank. The probe may represent part of the liquid-level-indicating instrumentation or a nozzle from an overhead fueling line. Other work suggests that the crests of ripples on the fuel surface produced by the high-speed fuel stream entering the tank may constitute a point of field concentration similar to that provided by the probe. A spark may then strike from the ripple crest directly to the ceiling of a nearly full tank. (See fig. 3(a).)

The sparks obtained in this study were found to have sufficient energy for fuel ignition by measuring the strength of the radio signal emitted by the spark. An aerial within the tank picked up the signal. The spark itself was observed by a photomultiplier whose light-sensitive tube was also contained within the tank (not shown in the figure). An atmosphere of CO_2 in the vapor space prevented ignition when sparking occurred.

In view of these results, a second phase of the cooperative industry program has been proposed which involves a study of the electrostatic hazard in actual fuel systems of current airplanes. This work is to be supplemented by studies in small-scale fueling systems to establish a method for extrapolating results obtained on convenient small-scale fuel systems to full scale.

In the event that future work with actual aircraft fuel systems shows the need for protection from electrostatic sparks, several

devised to be part of the fueling system which indicates when a fuel with high charging tendency is being handled. On these infrequent occasions the operator simply reduces the fueling rate to avoid dangerous electrification. The possibility of such a service instrument will also be explored in the future cooperative program.

REFERENCE

1. Klinkenberg, A., and Van der Minne, J. L., eds.: Electrostatics in the Petroleum Industry. Royal Dutch/Shell Res. and Dev. Rep., Elsevier Press Inc. (Houston, Texas), 1958.

GROUND FUELING SYSTEM

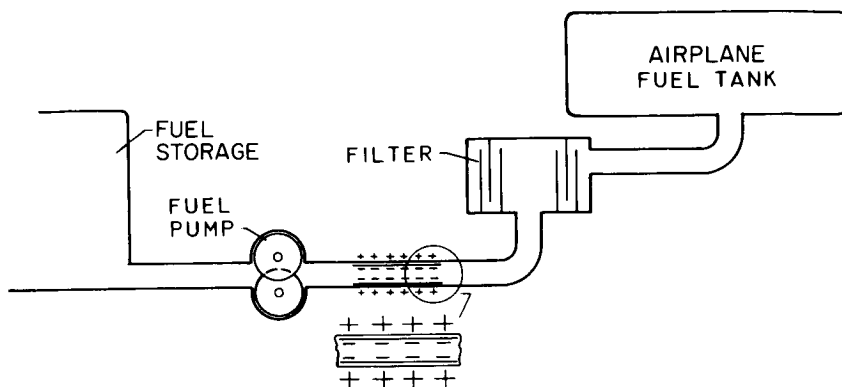


Figure 1

CHARGE CARRIED IN FUELING SYSTEM

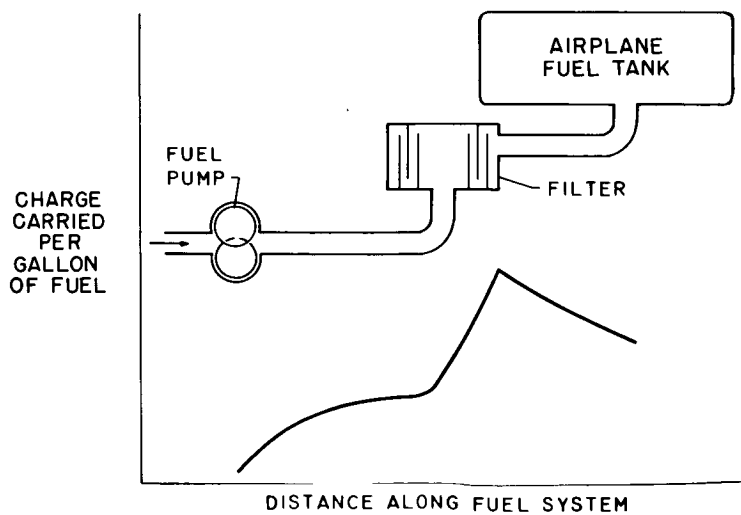


Figure 2

SCHEMATIC REPRESENTATION OF FUEL TANK CHARGE

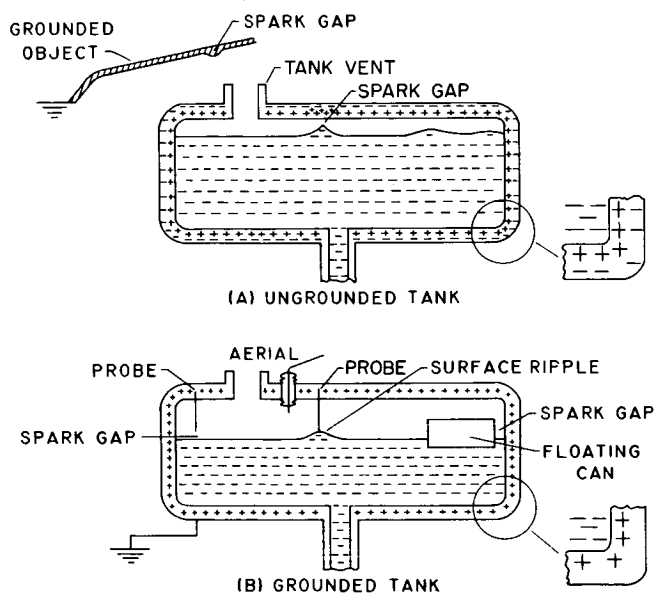


Figure 3

METHODS FOR PREVENTING ELECTROSTATIC SPARKS

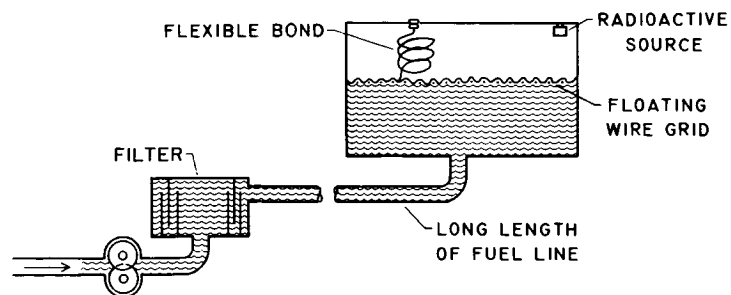


Figure 4

JET-FUEL JETTISONING

By Herman H. Lowell

Lewis Research Center

This investigation has had as a principal aim the determination of minimal allowable altitudes for jettisoning with different jet fuels under varying conditions. The criterion to be applied is the avoidance of flammable concentrations of fuel in the air at ground level. As a practical matter, this means keeping the fuel-air ratio below the lean flammability limit.

The special concern with jettisoning of jet fuels, as distinguished from gasolines, arose because evaporation rates for jet fuels were known to be much less than for gasolines. Therefore, as compared with jettisoned gasoline, a greater fraction of jettisoned jet fuel will reach the ground.

When, however, all the significant factors, including evaporation, were considered, the conclusion was reached that despite the lower evaporation rates of jet fuels little modification of existing jettisoning practices was actually indicated. The substance of this paper is a description of the principal elements in the analysis which lead to this conclusion.

The typical jettisoning situation is shown in figure 1. An aircraft ejects fuel at low or moderate pressure either through two tubes or along two chutes at a rate sufficient to dump a major fraction of the fuel load in some 20 or 25 minutes.

Locations of the exit points range from just outboard of each main wheel well to positions several feet inboard of each wing tip.

Upon contact with the airstream, the fuel stream is broken up into droplets of varying diameters which are then decelerated to zero air-speed within a few feet and form a plume, or horizontally extended and initially narrow cloud, which gradually sinks toward the ground and spreads both vertically and horizontally. Settling and spreading of the fuel plume is critically dependent on droplet size distribution. The relative contributions to the total liquid volume of droplets of varying diameters are indicated approximately in figure 2. The curve corresponds to a jettisoning airspeed of about 250 knots. Because of the increasingly violent impact of fuel and air, the average droplet size will decrease with increasing flight speed during jettisoning. It will be noted that droplets of about 200 microns diameter (or about

0.02 centimeter) make the chief contribution to the total volume for the 250-knot case. A maximum size of about 2,000 microns is indicated. This distribution estimate is based in part on actual British tests made a few years ago in which an airplane spilled various liquids through a nozzle from a very low altitude.

As a fuel plume sinks toward the ground and spreads, the droplets evaporate as they fall. The most volatile constituents of the fuel are vaporized most rapidly. The droplet diameters and individual masses decrease, and droplet composition changes. The fuel vapors are left aloft as the liquid droplets descend toward the ground, and the total liquid mass decreases.

It should be noted that in the analytical studies made in connection with this investigation, one assumption made was that the two plumes coalesce a short distance behind the aircraft into a single plume. This simplification was known to be invalid in many situations. However, this assumption, along with others that were made, was of such a nature that predicted allowable jettisoning rates should be on the low, or safe, side.

The matter of flammability is now considered in somewhat greater detail. No experimental data concerning lean flammability limits are available for fuel clouds similar to these fuel plumes. For sprays consisting of droplets smaller than those typical of such fuel plumes, a few experimental data are available. Such data indicate that a lean flammability limit for a mixture of fuel and air will remain essentially fixed whether the fuel is in vapor form or liquid droplet form or some combination for a fixed overall fuel-air ratio.

Therefore, the generally accepted fuel-air ratio of 0.035 was adopted as the lean flammability limit for all jet fuels. Moreover, this limit has the same value over a wide range of altitudes. If anything, the lean limit expressed as a fuel-air ratio will actually be larger when a portion of the fuel is in liquid form.

The problem, then, reduces to the determination of conditions under which a fuel-air ratio of 0.035 will not be exceeded at ground level for ground altitudes between sea level and, say, 10,000 feet. There are three principal factors which determine the actual fuel concentration at any given altitude.

The first is the quantity of fuel jettisoned per unit distance of aircraft travel. For example, at an airspeed of 250 knots and a jettisoning rate of 100 pounds per second, there would be nearly 240 pounds of fuel released per 1,000 feet of aircraft travel. The jettisoning rate cited is slightly lower than the maximum expected for current jet transports.

The second factor is the horizontal and vertical spreading of the droplet plume or cloud as caused both by atmospheric turbulence and by varying rates of fall of droplets of differing diameters. The turbulence-spreading calculations involved concepts, equations, and numbers which are discussed in some detail in reference 1. The effect of atmospheric turbulence on the spreading of the fuel plume cannot in practice be isolated from other influences. However, the qualitative nature of spreading caused by turbulence alone is indicated in figure 3. Several successive stages in the spreading of a fuel-droplet plume during a short period after formation are shown. In particular, the variation of concentration of fuel with distance from the plume center line is indicated. In general, the curve of fuel concentration tends to flatten and spread rather uniformly with time under ideal conditions. The spreading rate increases with increasing severity of atmospheric turbulence. On a comparatively quiet day, fuel droplets tend to separate at speeds below about 3 feet per second, whereas on gusty days the separation speed may be several or even many times this value. Under the highly irregular conditions existing near thunderheads or strong cold fronts, no predictions are possible except that spreading will then be extremely rapid. It should be explicitly noted that only existing atmospheric turbulence was considered; aircraft-generated turbulence (e.g., vortices shed by wing tips) was ignored.

The third principal factor affecting fuel concentration is the vertical spreading caused by variation of falling speeds among droplets of differing diameters. Falling speed as a function of droplet diameter is presented in figure 4. The assumption is made here that no evaporation is occurring; in general, droplets of jet fuels will not evaporate at significant rates at air temperatures below -30°C . It is seen that falling speeds approach 20 feet per second for the largest droplets (of about 2,000 microns diameter) but decrease to 2 feet per second at 200 microns and, of course, are much lower for still smaller droplets.

Using these calculated speeds, which do not vary significantly with altitude below 7,000 feet, the vertical distribution of droplets falling from 5,000 feet was calculated and is shown in figure 5. It is seen that 30 minutes after release a 100-micron droplet will fall less than 1,500 feet, whereas a 1,500-micron droplet will fall 5,000 feet in $5\frac{1}{2}$ minutes. A 500-micron droplet, of perhaps the greatest interest, will fall 1,600 feet in 5 minutes and will reach the ground in about 13 minutes.

It is again noted that these results apply to the "no evaporation" or low-temperature situation. When significant evaporation occurs, these results may be markedly altered.

With evaporation, the droplet diameter decreases as the droplet falls. Accordingly, the falling speed decreases. This effect is

illustrated by figure 6. In this figure the effect of evaporation on distance of fall for droplets of three different diameters is considered. At each diameter, the vertical position is indicated as a function of time both for a droplet that is evaporating comparatively rapidly and one that is evaporating very slowly.

After 5 minutes (300 seconds) the 500-micron droplet has fallen, at -30°C , 1,600 feet; whereas, at 30°C , it has fallen only 1,100 feet. For the larger droplets, the effect of evaporation on distance of fall is less pronounced.

The effect of air temperature changes on droplet fall is presented more directly in figure 7. The distance of fall for two periods of fall is given for droplet diameters of 500, 1,000, and 1,500 microns. At the end of a 100-second interval, under the conditions stated in the figure, relatively little change of distance of fall occurs over the large temperature range of 30°C to -30°C . However, at 300 seconds the distance of fall of a 500-micron droplet varies 50 percent, and the distances of fall of droplets of 1,000- and 1,500-micron diameters vary by smaller, but significant, percentages over this temperature range.

Accordingly, one principal effect of evaporation is to alter differences in fall rate among droplets of varying diameters. As a result, vertical spreading caused by differences of fall rates is changed. Further, the droplets require longer periods to reach the ground, subjecting the fuel plume to turbulent spreading for longer periods.

While the droplet diameter is decreasing with evaporation, the mass of each droplet is decreasing correspondingly. Since the vapor, as has been noted, remains aloft, the amount of fuel reaching the ground is principally that present in liquid droplet form. Therefore, the loss of mass of a droplet is an important consideration. In figure 8, the ratio of the remaining mass of a droplet to the original mass is shown as a function of distance of fall. Such ratios are indicated for droplets having initial diameters of 500 and 1,500 microns and at air temperatures of plus and minus 30°C . Clearly, at high temperatures a considerable loss of mass occurs in the case of JP-4 fuel. For example, less than 10 percent of the original 500-micron droplet is left after a fall of 1,000 feet at 30°C . Some loss, about 15 percent, occurs at -30°C . In general, such small losses may be ignored.

The very large effect of air temperature change on evaporation rates and, therefore, on the total liquid fuel present at a given altitude, is indicated more directly by figure 9. The ratio of the residual droplet mass to the original mass is given in the figure as a function of air temperature for two distances of fall and for the three droplet diameters of 500, 1,000, and 1,500 microns. The very great rate of

increase with temperature of mass-loss rate of 500-micron droplets is obvious even in the case of a 500-foot fall. The effect is less pronounced at the larger diameters, but even a 1,000-micron droplet loses a significant part (more than 20 percent) of its mass during a 1,000-foot fall at air temperatures at altitude (above -20°C), corresponding to sea-level temperatures higher than -10°C .

A few results have been given from among an extensive set covering ranges of starting altitude, droplet diameter, air temperature, and fuel. It is now remarked that at altitudes below 10,000 feet changes of jettisoning altitude have comparatively little effect on droplet histories except through changes in air temperature at altitude. The result is that changes of air pressure and density with altitude may be ignored for engineering purposes when droplet calculations are being made. However, the air temperature at jettisoning altitude must be carefully taken into account because of the effect on evaporation.

Calculations yielding safe jettisoning rate as a function of ground clearance were made for four different weather situations taking into account vertical and horizontal spreading. Figure 10 shows the variations in allowable jettisoning rates with ground clearance for a cold quiet day, a cold gusty day, a hot quiet day, and a hot gusty day. For the quiet day, a wind of about 4 miles an hour was assumed. For the gusty day, a wind speed varying with altitude but having a value of about 22 miles per hour at 1,000 feet was assumed. Many weather situations of winter and summer are typified by one or the other of these selected atmospheres. Weather situations of spring and fall are, of course, of an intermediate nature. The figure indicates that at an expected current maximum jettisoning rate of 100 pounds per second (or 240 pounds per 1,000 feet at 250 knots) ground clearances of less than 100 feet are allowable under the most favorable conditions, that is, in hot windy weather. However, even under the least favorable conditions, that is, on a quiet cold day, the ground clearances indicated in figure 10 are very modest. For example, if the aircraft is merely 100 feet or so above the ground, no flammable condition should result at ground level. At jettisoning rates of about 420 pounds per second, or 1,000 pounds per 1,000 feet at 250 knots, a ground clearance of 300 feet would be required under these unfavorable conditions. Predictions of this kind are subject to nature's whims. Random air motions near the ground decrease the dependability of calculations to such an extent that these results are not really reliable at ground clearances below, say, 200 feet, particularly in view of the neglect of downwash effects.

Nevertheless, most of the jettisoning rates appearing in the figure are much higher than any now contemplated, and it appears to be safe to say that jettisoning at rates expected for current jet transports will be permissible at ground clearances above 500 feet under virtually all

atmospheric conditions. It is emphasized that the sole criterion applied in this investigation was flammability of a fuel-air mixture; ground contamination was not considered.

In that connection it should be noted that should there be any substantial accumulation of liquid droplets on any surface at or near ground level, a hazard may conceivably exist which was not investigated. Such a condition is considered improbable, but the calculation techniques developed in this study could be applied to that question should the need arise.

REFERENCE

1. Anon.: Meteorology and Atomic Energy. U. S. Atomic Energy Comm., July 1955, pp. 38-58. (Available from Supt. Doc., U. S. Govt. Printing Office.)

TYPICAL PATTERN OF JETTISONED JET FUEL DROPLET PLUMES

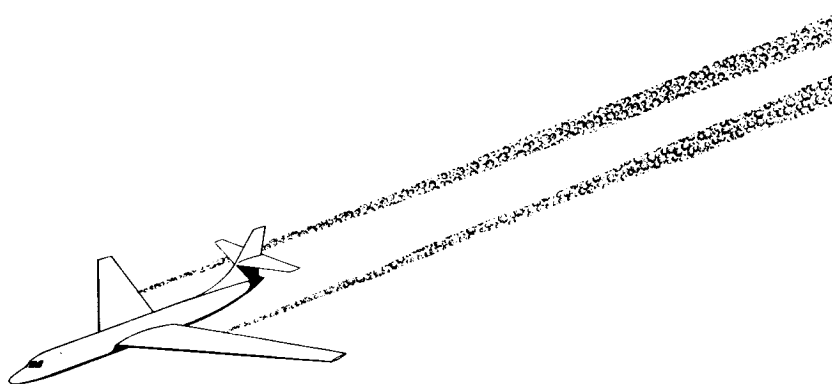


Figure 1

VOLUME DISTRIBUTION OF FUEL DROPLETS

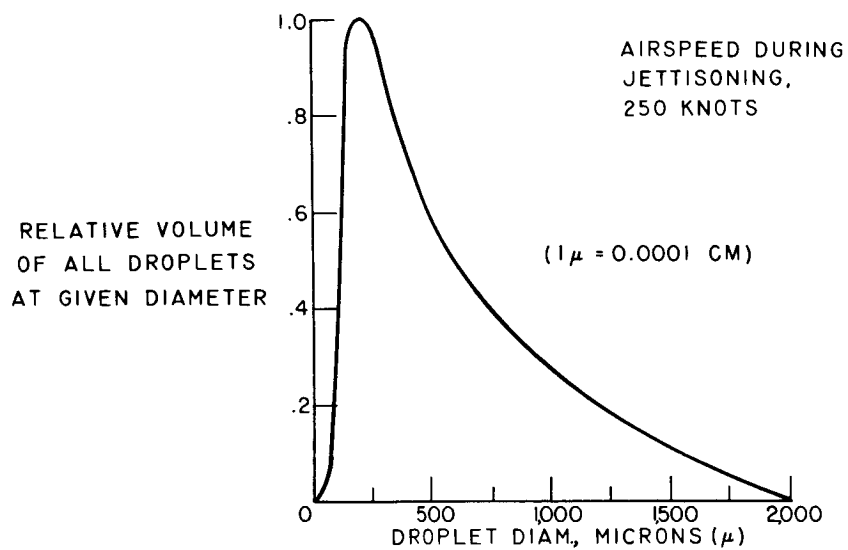


Figure 2

SPREADING OF FUEL PLUME NEAR AIRCRAFT

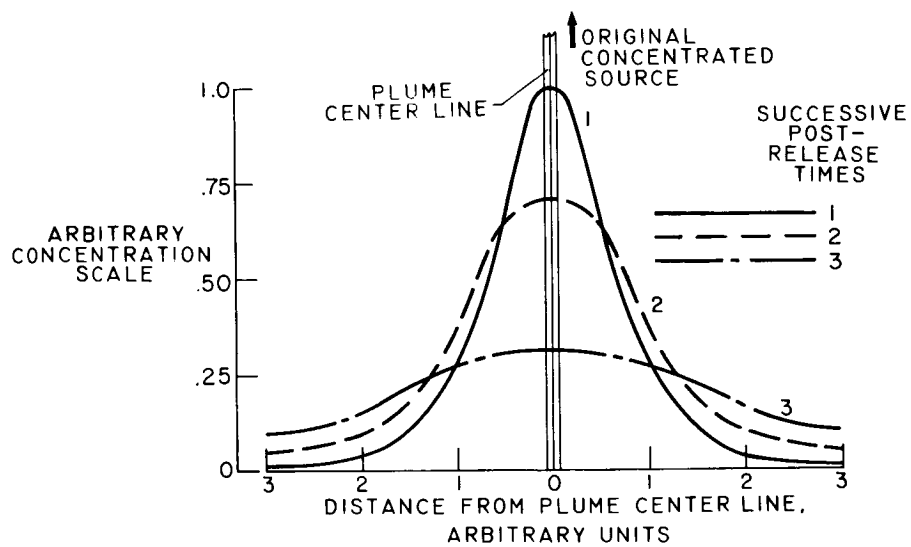


Figure 3

SPEEDS OF FREE FALL OF FUEL DROPLETS

FUEL, JP-4; ALTITUDE, 1000 FT (STANDARD ATMOSPHERE)

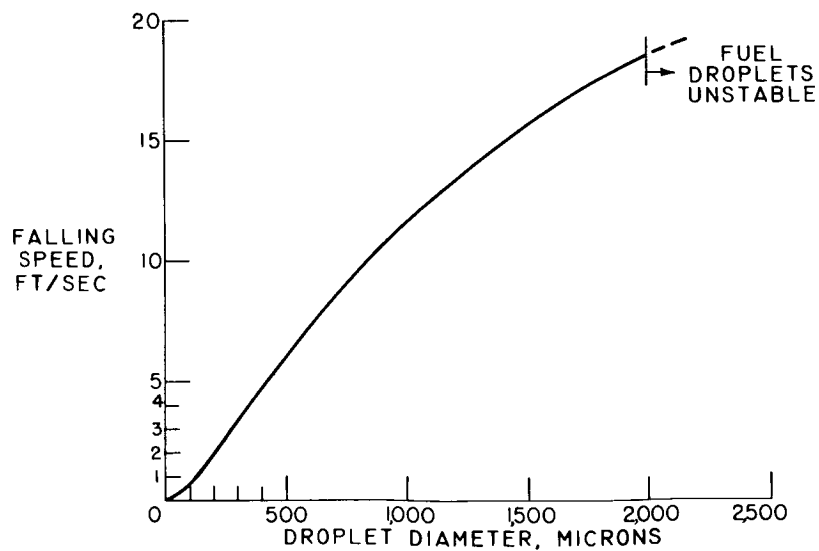


Figure 4

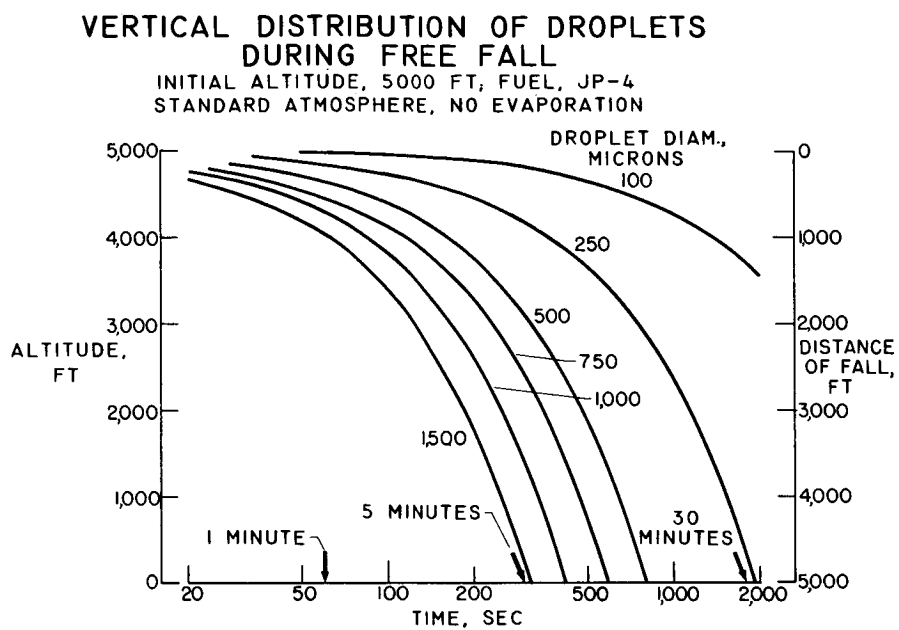


Figure 5

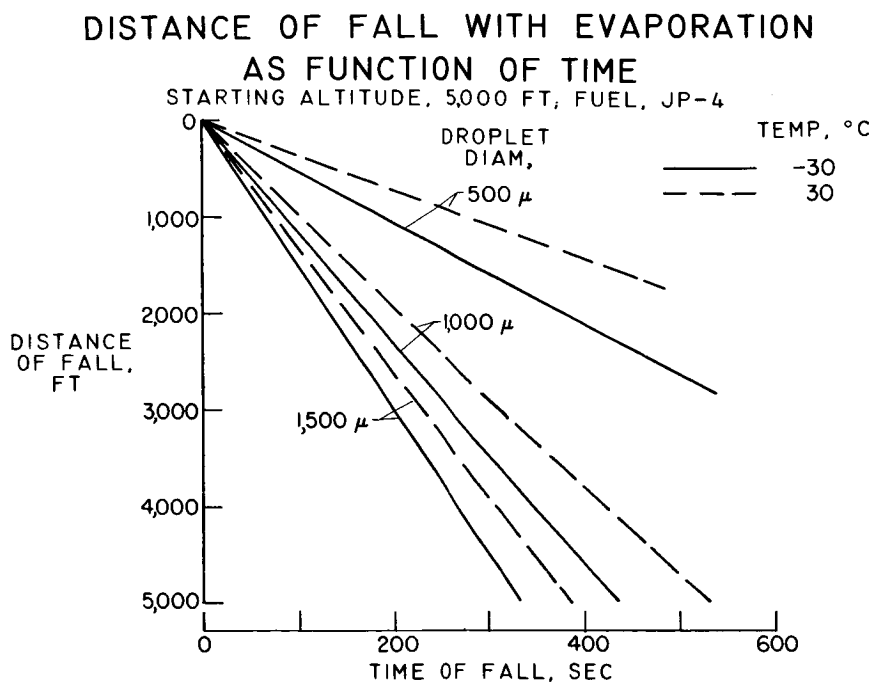


Figure 6

EFFECT OF AIR TEMPERATURE ON DROPLET FALL

STARTING ALTITUDE, 5,000 FT, FUEL, JP-4

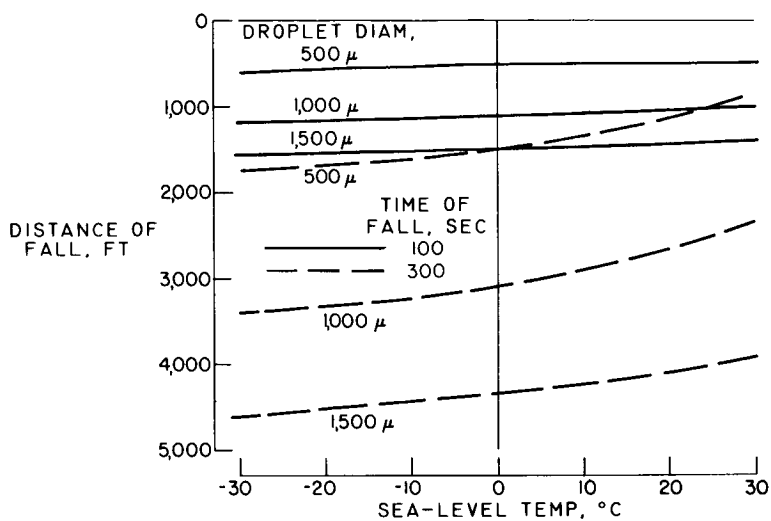


Figure 7

LOSS OF DROPLET MASS DURING FALL WITH EVAPORATION

STARTING ALTITUDE, 5,000 FT, FUEL, JP-4

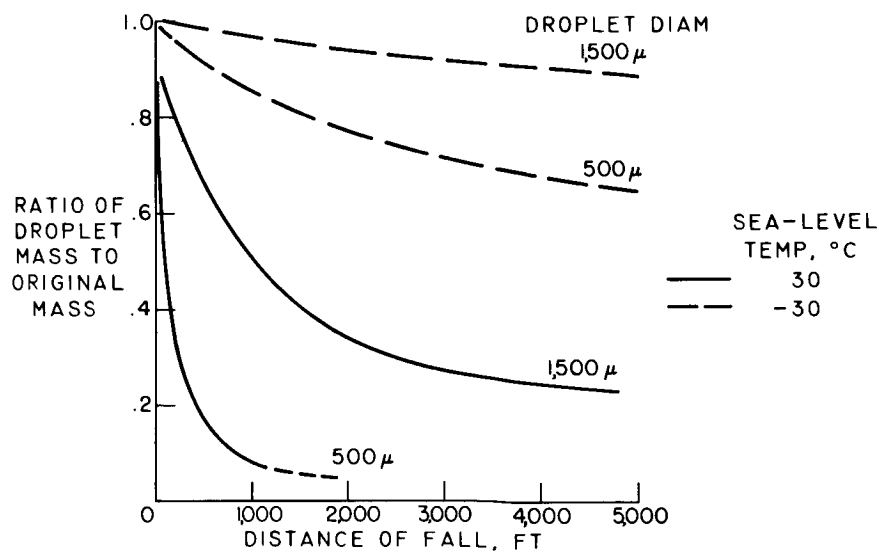


Figure 8

EFFECT OF AIR TEMPERATURE ON LOSS OF DROPLET MASS DURING FALL

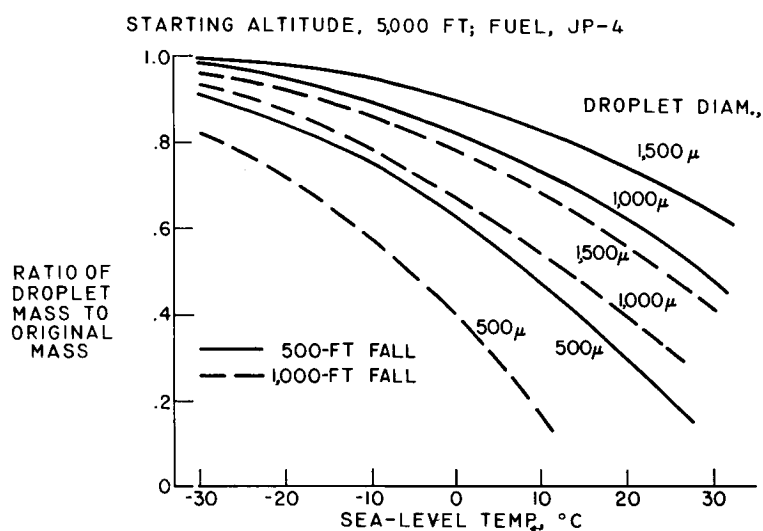


Figure 9

SAFE FUEL JETTISONING RATES

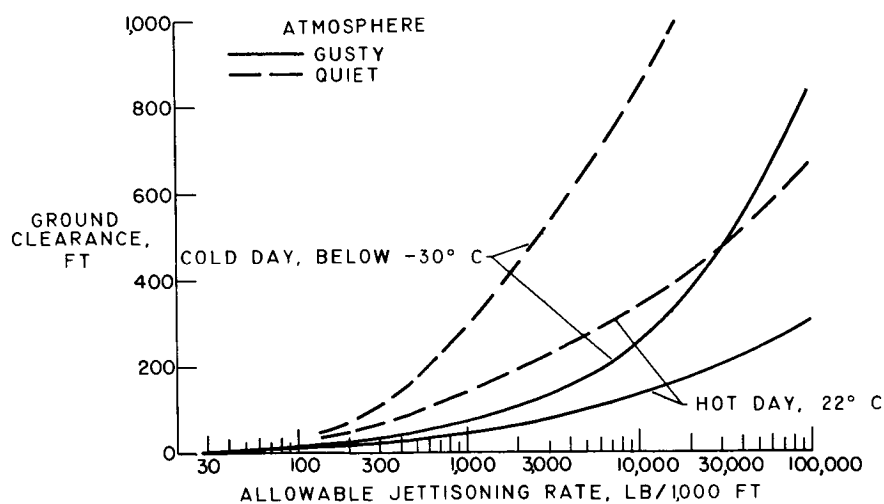


Figure 10

CRASH-FIRE-PREVENTION SYSTEM FOR THE

T-56 TURBOPROPELLER ENGINE

By Arthur M. Busch

Lewis Research Center

BACKGROUND

As part of a continuing study of crash-fire safety for turbine-powered aircraft, the Lewis Research Center has recently completed an evaluation of the crash-fire-protection requirements for the T-56 turbopropeller in a cooperative program with Allison Engine Division, sponsored by the Air Force. This work followed an extensive laboratory and full-scale-airplane investigation of crashes with turbojet airplanes, in which it was learned that fuel spilled when the crash occurs is often ingested into the engine with intake air. This ingested fuel may be ignited by combustor flames and by some of the hot metal of the engine interior. The resulting flames issue from the engine tailpipe and ignite other fuel spilled around the crashed airplane to set the main fire. As an illustration of this fire-setting process, a motion picture in color was taken of a crash test of an F-84 airplane conducted during this study. In these crash tests, the airplane accelerated under its own power along a runway, where it attained a speed of about 100 miles per hour. Barriers at the end of the runway tore open the airplane fuel tanks and inflicted other structural damage. Wing and fuselage fuel tanks tore open and spilled fuel that had been dyed red. The fuel ignited as it was drawn through the engine; and the tailpipe torching spread fire to the cloud of fuel engulfing the airplane.

Fire-setting by the turbojet was prevented in this study when means were employed to extinguish combustor flames and to cool and "inert" dangerous hot metal parts of the turbojet immediately upon crash. (Water was the cooling and inerting agent.) The effectiveness of these means of fire prevention is illustrated in the motion pictures of another F-84 equipped with a crash-fire-prevention system. Again, the plane accelerated toward the barrier under the same conditions as the previous crash. In this crash, however, the fire-prevention system was actuated at the barrier. Also, instead of fire, steam issued from the tailpipe. This steam was produced by the water that cools and inerts the engine interior. No fires resulted and it appeared that similar protection would work in a turbopropeller engine, because the combustor flame and hot-metal ignition sources that were found in the turbojet engine are also present in the turbopropeller engine. However, the turboprop differed in a few ways from the older turbojets that had been

studied. The differences are indicated in figure 1. A diagram of the T-56 turbopropeller engine is shown for comparison with the older J-30 turbojet engine. Both engines have the same power-section diameter and about the same mass air flow. The additional stages of the turboprop compressor produce higher metal temperatures associated with the higher compression ratio. Notice that the maximum diffuser temperature was 600°F for the turboprop as compared with 350°F for the turbojet. Because of the high temperatures in the rearward stages of the compressor of the T-56 engine, the fuel taken into the engine is preheated and therefore ignites more rapidly. The combustor sections and the fronts of the turbines of both engines, however, have similar temperatures. The four-stage turbine rotor of the turboprop has greater mass and heat capacity than the single rotor of the J-30 turbojet. The turboprop turbine also has many hidden surfaces which can not be sprayed directly with cooling and inerting agent. However, the exhaust nozzle of the turboprop runs cooler (at 900°F) than that of the turbojet (at $1,100^{\circ}\text{F}$).

If means are provided to shut off fuel flow to the combustors in a crash in an effort to avoid fire, the propeller stops the coasting rotor in the turboprop quickly, whereas the unhindered rotor of the turbojet takes longer to stop. This difference in rates of coastdown affects the amount of air that is pumped through the engine during coastdown in a crash. The rapid coastdown of the turboprop is caused by the air drag of the propeller and an antiwindmill brake in the turboprop.

Figure 2 shows a comparison of mass air flows of the two engines as a function of the time after fuel shut-off. Mass air flow in pounds per second is plotted against the elapsed time after fuel shut-off in seconds. Notice that the turbojet would still be turning and pumping a few pounds per second when the turboprop had stopped at 45 seconds in a normal coastdown. A feathered propeller stops rotation and air flow even more quickly, in 13 seconds. If, in a crash, the propeller were to drag the ground to a maximum within the stress limits of the gearing, it is conceivable that air pumping could stop in about 1 second.

The significance of these air flows in the design of a crash-fire inerting system lies in the fact that the air not only carries crash-spilled fuel into the engine, but also helps distribute the water for inerting within the engine. The continued air flow of the turbojet makes possible a simpler water-spray inerting system, in which less water is used, than a comparable turboprop engine.

EXPERIMENTAL PROCEDURES

With all of the differences between the turboprop and turbojet taken into account and with a temperature survey of the engine used as a basis, a crash-fire-prevention system that would quickly stop the flow of fuel to the combustors and distribute coolant to the hot metal parts was built for the T-56 engine.

For the purpose of evaluating the effectiveness of the system, trial runs were made that simulated severe crash fuel spillage. For these trials, the engine was mounted on a portable test stand consisting of a stripped C-82 airframe. The mounted test engine is shown in figure 3. The cargo compartment was used to house the control room. This three-wheeled test stand allowed the engine to be oriented to various wind directions, and to be hangared for experimental modifications.

A trial run of the experimental prevention system was conducted in the following manner: With the test stand and engine tied down to the run-up apron, the engine temperatures expected in a take-off or landing crash were duplicated by running the engine at take-off power long enough to heat it to equilibrium temperatures. Then, at a moment that corresponds to airplane crash, the crash-fire-protection system was actuated. The protection system shut off the fuel flow to the combustors and stopped the engine. As the engine coasted down, the protection system sprayed water on the hot metal inside the engine. During coastdown, JP-5 fuel was sprayed into the inlet to simulate crash fuel spillage. In addition, because fuel can enter the inlet and exhaust after coastdown in a crash, fuel was also sprayed into both the inlet and exhaust for 15 minutes after the engine stopped. Because the preliminary system used in the trial runs was inadequate, the test sprays caught fire when the turbine rotor surfaces reheated after the system was actuated. Film sequences of this test showed the engine running at take-off power until the metal temperatures reached equilibrium. Shortly afterward, the protection system was actuated; then a cloud of inerting water and test fuel could be seen to come out of the exhaust as the engine coasted down. Excess test fuel was seen to pour back out of the inlet. Motion pictures were also taken of the tailpipe. As the cloud of water and fuel vapor cleared fire was seen to issue from the exhaust nozzle. On the basis of information from trials such as these, the system was modified to a completely effective form so that no fires occurred in such trials.

DESCRIPTION OF CRASH-FIRE-PREVENTION SYSTEM

Figure 4 shows a diagram of the final system that had a consistent ability to prevent all fires in trials of this kind. In the design of this system, the aim was to provide economy of water and simplicity of installation. This protection system for the inside of the engine must both extinguish the combustor flame and inert the hot metal until it is cooled. For this purpose, a combustor fuel shut-off and two types of water-spray systems were used.

Fuel flow to the combustors is stopped at the fuel shut-off and drain valve. This valve also opens the engine fuel manifold to an over-board drain and allows the gas pressure in the combustors to blow the fuel back out of the manifold. The flame is extinguished in less than 0.1 second, by preventing the fuel nozzles from dripping.

The type of water system needed to inert and cool the hot metal in the initial part of the coastdown, while the air flow is great, consists of high-rate sprays which cool the thin, hot metal of the combustion section. Thirty-five pounds of water is discharged in 10 seconds. Two simple orifices discharge water on the last stage compressor rotor blades ahead of each of the six combustors. Another simple orifice, housed in the strut-fairing between each combustor, discharges water against the diffuser-inner-fairing. The air flow picks up the water from these two sets of sprays and carries it to most of the combustor outside surfaces. A small nozzle sprays water on the outside of each combustor in this zone of slow air flow. These three groups of water sprays, supplied from a single, pressurized tank, completely wet the outside of the combustors.

A low-rate, long-duration type of water spray was needed on the massive turbine rotor and rear bearing support structure. The large heat capacity of the rotor and support structure will reheat the surfaces to ignition temperatures if the sprays are stopped too soon. Nozzles at the front and rear of the rotor and at the inner and outer surfaces of the support structure spray 9 pounds of water on these surfaces over a 90-second period. In addition, 8 pounds of water is sprayed for 10 minutes through three nozzles in one location in the top of the turbine casing and onto the turbine rotor to provide cooling and inerting steam. The water required in the turbine-section systems is modest because some protection is provided by water from upstream systems entrained in the coastdown air flow. With such a crash-fire-protection system installed, 20 consecutive successful trials of this system, using this total of 52 pounds of water, were made.

DESCRIPTION OF ALTERNATE SYSTEM

The installed weight and complexity of the crash-fire-prevention system just described (fig. 4) could be reduced by substituting the flight-fire extinguishing agent, already carried in the nacelle, for a portion of the cooling and inerting water. Such a modification of the water system was studied. (See fig. 5.) The flight-fire extinguishing agent used was bromotrifluoromethane (CBrF_3). The 8 pounds of water and the three nozzles which spray through the turbine casing and onto the rotor, plus the 2 pounds of water from the 9-pound tank, are replaced at no weight penalty to the airplane by 10 pounds of CBrF_3 , applied over a 10-minute period at the front and rear of the rotor. This combined system of water and CBrF_3 , which used only 42 pounds of water instead of 52 pounds, also gave consistent protection up to 15 minutes after the system was actuated. This use of the flight-fire agent for the crash-fire system does not prevent its use for flight fires.

CONCLUDING REMARKS

The systems that have been described provide protection only from ignition sources inside the engine. Although a few exploratory severe fuel-spray tests on the outside surfaces of this engine indicated that these surfaces are not likely to start fires when there is air circulation, both the exterior of the engine and any exhaust duct should be subjected to fuel-spray trials in the air flow and temperature environment provided by the airframe in which they are installed.

As regards the crash-fire protection for the rest of the airplane, previous crash experience showed that the electrical systems must be shut off at the moment of crash, and auxiliary equipment that may have hot surfaces during a crash must also be inerted and cooled. Finally, some means must be provided for actuating these crash-fire prevention systems. Because of reliability considerations, manual actuation is favored at present.

In conclusion, the technique of shutting off the fuel flow to the combustors and of cooling and inerting the hot metal surfaces may be applied to other high-compression multistage turbine engines to prevent them from setting crash fires.

TURBOPROP VS OLDER TURBOJET

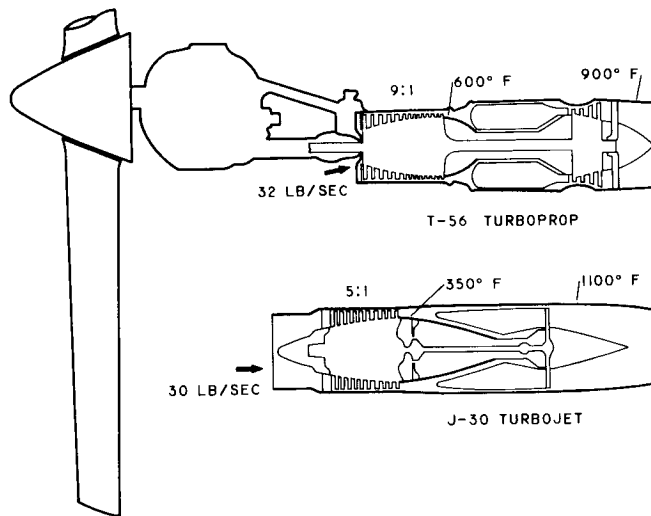


Figure 1

COASTDOWN AIR FLOWS, TURBOPROP VS TURBOJET

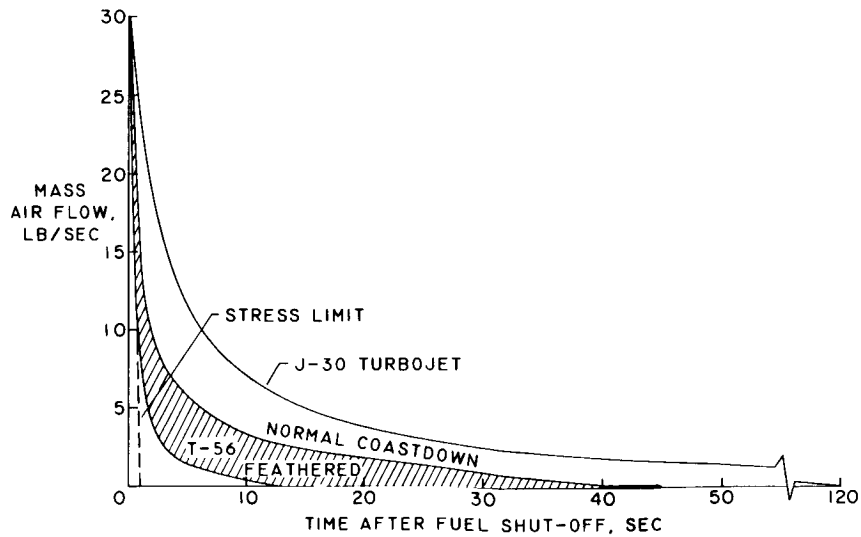


Figure 2

MOVEABLE TURBOPROP TEST STAND

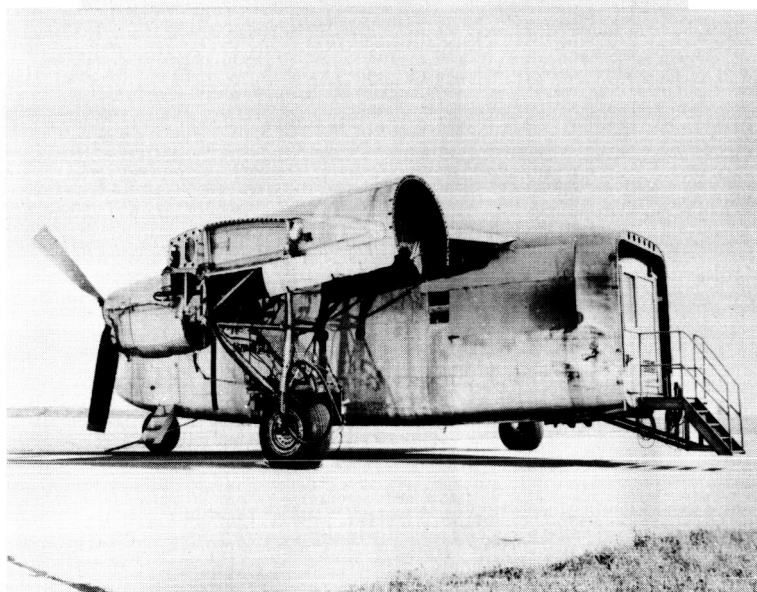


Figure 3

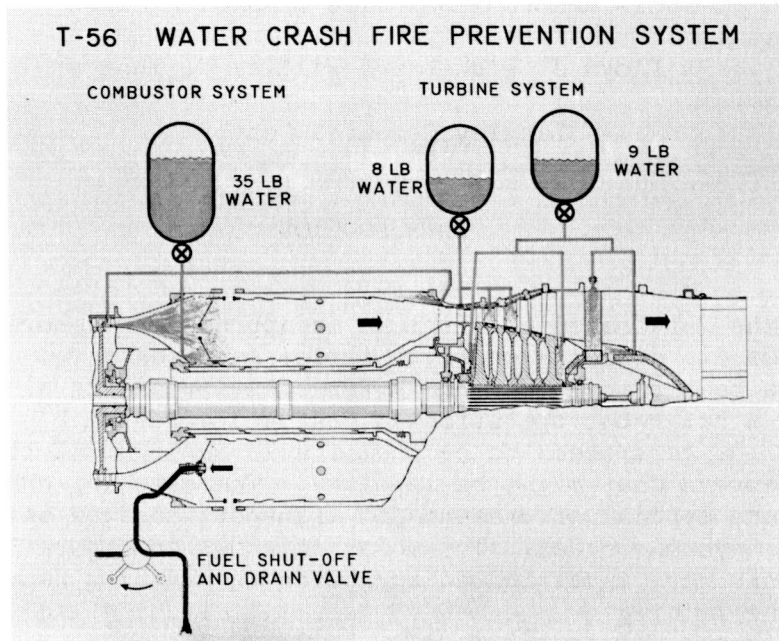


Figure 4

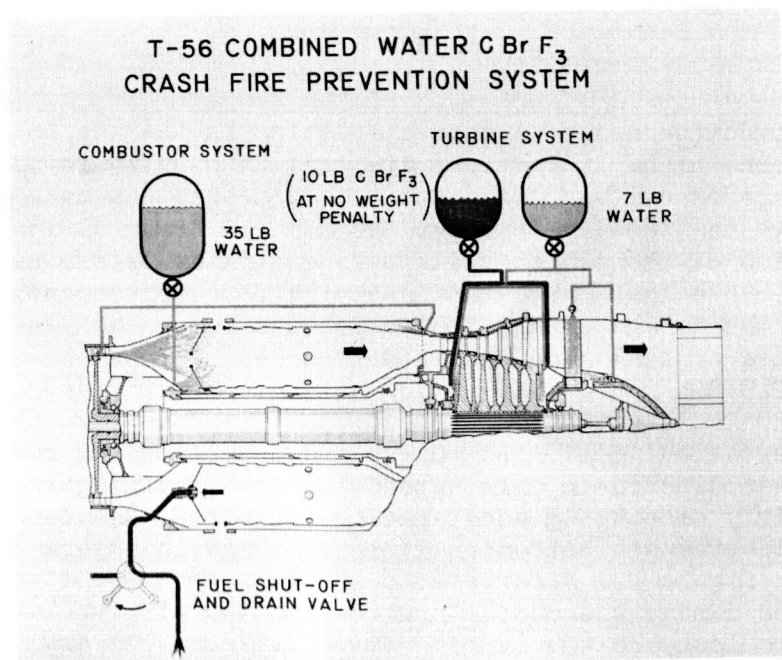


Figure 5

JET-TRANSPORT DITCHING CHARACTERISTICS

By Lloyd J. Fisher and William C. Thompson

Langley Research Center

INTRODUCTION

Since the jet-transport airplane is approaching general use, an evaluation of its ditching characteristics has been made. Particular emphasis has been placed on rough-water behavior and on ditching aids. Ditching is a hazardous operation at best and a reasonable effort to minimize its dangers seems to be justifiable in light of the large number of passengers that might be involved. The ditching characteristics of an airplane typical of present jet-transport designs were investigated with a dynamic model. The model is shown in figure 1. Various configurations were investigated including the landing gear retracted as shown, the landing gear extended, several ditching aids, and a condition in which the fuselage breaks or separates into two parts. Scale strength parts such as bottom sections, flap attachments, and wheel and engine struts were used throughout the investigations to determine danger points with regard to behavior and to safety. These parts are designed so that they break under loads which are the best estimates available of the strength of the airplane.

DISCUSSION

The effectiveness of damage simulation is the key to the model investigations since indications are that it usually is not the accelerations that personnel must take during a ditching but rather the water rushing into the fuselage through the damaged areas during the high-speed portion of the run or the airplane sinking before personnel have time to evacuate that cause the loss of life. Consequently, ways of minimizing the damage in a ditching are desired. The landings to be discussed are typical landings from a number of runs and simulate a weight of 225,000 pounds, a landing attitude of 12° , and a horizontal speed of 120 knots with flaps full down. The data were obtained from visual observation, motion pictures, and accelerometer records. When the model was ditched in calm water with the landing gear retracted, the run was fairly smooth, 4g accelerations occurred, and some damage resulted to the scale-strength bottoms. Typical damage in a calm water ditching is shown in figure 2. A large hole was torn in the bottom of the fuselage but the damage was mostly confined to the aft fuselage. Some of the engines were lost and the landing flaps failed. The engines frequently

break off and the flaps fail in a ditching but these engine and flap failures are not usually detrimental. In landings in waves 4 feet high (full scale) with the gear retracted, the run was relatively short, the model was buffeted heavily by the waves, accelerations were fairly high, and considerable damage to the fuselage bottom resulted. Typical bottom damage is shown in figure 3. Almost the entire bottom was torn away and much more damage occurred than in a calm water landing. Under slightly different approach conditions or sea conditions less damage might occur but even much less damage would still be serious.

Another possibility of damage which has been mentioned frequently in recent months is the case in which the fuselage breaks apart, that is, separates into two sections. In order to simulate such a condition (fig. 4), the model was cut apart just aft of the wing and then held together with approximately scale-strength attachments. It was difficult to get a meaningful reading on the strength required to break the attachments because, if the model landed very slightly yawed, one side attachment would break and the other attachment would lose effectiveness. In landings at this condition the aft fuselage broke off and sank quickly while the nose and wing section continued on for a short run. It is possible that such an airplane would break apart and typical behavior would be as shown in the model tests but it is difficult to predict the possibility of breakage from the model tests. Breakage would depend to a large extent on how much bottom damage occurred, and how the landing was made; that is, a swerve in landing would increase the chances of breaking the fuselage apart. The precise strength of the full-scale airplane is also hard to obtain.

What may be expected in a rough-water ditching of a large jet transport has been seen and it is not very encouraging. A procedure or device is needed to prevent the severe damage to the airplane during rough-water ditching. A possible procedure that has always had some advocates is the extension of the landing gear. (See fig. 5.) In the model tests the gear was attached with a scale-strength shear pin in the drag link so that the gear would pivot about the upper end of the strut but would not tear completely off when the shear pin failed. The strength of the main gear was found to be marginal; that is, sometimes the gear failed and sometimes it did not but the nose gear always failed in the model tests. The data are, therefore, divided into two parts depending on whether the main gear failed. In a ditching when the extended main gear did not fail, a dive always resulted. Accelerations of 4 or 5g were experienced and the landing run was very short. The damage that occurred is shown in figure 6. A large hole was torn under the nose portion of the fuselage. This would result in the entire fuselage being flooded in the dive even though there was little damage to the aft fuselage. The wing and upper fuselage are overstrength in the model tests but in a full-scale ditching the wing might tear off or the fuselage break apart or the airplane submerge and stay down. A dive is

the worse thing that can happen in a ditching and is indicative of a catastrophe. In a landing in which the landing gear failed, the model did not dive but ran deeply. The accelerations were about 5g and the run was fairly smooth. Figure 7 shows that considerable damage occurred to the bottom in the aft fuselage as well as in the forward fuselage. There is also a fairly large hole in the midsection.

The wheels-down landings were made to see whether ditching behavior could be improved by this method. The damage may have been lessened but the possible motions in a ditching were worsened. In other words, the airplane might dive with the accompanying hazards to pilots and passengers and, even though the aft fuselage might not be damaged as severely as when the wheels are retracted, the large inflow of water through the damaged nose during the dive would be very hazardous. When the landing gear failed, the motions were not so severe but the damage was about as dangerous as when the gear was retracted. Consequently, there appears to be little to gain and much to lose in a wheels-down landing.

Indications are that there is no easy way to take care of the rough-water ditching problems of the large jet transports of today. For a safe ditching, bottom damage must be minimized. Slight increases in strength are not enough to prevent excessive damage; a higher order of strength over the entire fuselage bottom is necessary and this increase in strength would result in large weight penalties. The ditching aid certainly is not an easy solution either, but it is a solution since adequate bottom strength is not feasible. Some small, and therefore highly loaded, hydrofoils and hydro-skis have been investigated. The aids to be discussed have been minimized in size; that is, the size is the minimum acceptable from the standpoint of behavior or damage. Figure 8 shows a supercavitating hydrofoil installed on the bottom of the model. The foil is relatively small, being about 27 square feet in area. The outstanding physical characteristics of the foil are a sharp thin leading edge and a highly cambered bottom, and in this installation dihedral has been used to reduce the impact forces since tests without dihedral indicated a tendency to bounce. In a landing with this hydrofoil the run was fairly long and very smooth, and the accelerations were low. Figure 9 shows the damage for this condition. Moderate damage occurred just aft of the hydrofoil due to the wake from the foil. This damage is considered to be moderate in spite of the size of the hole because the stringers and bulkheads are intact and only the skin is broken. It is believed that the floor of the passenger compartment would retain its integrity with this skin damage since the water force is apparently relatively small and not from solid water. Damage with the hydrofoil was less than that in the wheel-up or -down conditions but was not completely eliminated. If the damage elimination is necessary, it could be accomplished with a larger hydrofoil or longer strut but the retraction problem would be greater.

Figure 10 shows a twin hydro-ski installation. The loading of the ski has been greatly increased in recent work, and in the present installation an area of about 45 square feet for each ski worked very well. In a landing with the skis the model made a very smooth run, the accelerations were low, and the behavior was good. The skis held the model clear of the waves until a low speed was reached. Typical damage is shown in figure 11. Very little damage occurred but there are small holes here and there.

Table I is a summary chart which gives a quick comparison of the data presented. The normal accelerations vary from about 4 to 6g in conditions at which major failures occurred to about 3g with the hydrofoil or hydro-skis installed. The longitudinal accelerations vary from about 6g with major failures to about $3/4$ g with the ditching aids. The length of landing runs varies from about 300 feet or 2 fuselage lengths when the extended landing gear caused a dive to about 1,200 feet or 10 fuselage lengths with the ditching aids. And, most important of all, the damage varied from most of the bottom being torn away in the gear-retracted configuration to very little damage with hydro-ski-installed configuration. As pointed out previously, accelerations of the order obtained are not as important with regard to ditching survival as the amount or the location of damage or the behavior when violent.

CONCLUDING REMARK

Thus, the ditching characteristics of a large jet transport can be very severe in waves of moderate size but are acceptable if suitable equipment is used.

TABLE I
SUMMARY CHART

CONFIGURATION	MAXIMUM ACCELERATION, g UNITS		LENGTH OF RUN, FT	REMARKS
	NORMAL	LONGITUDINAL		
GEAR RETRACTED	4-6	6	575	DEEP RUN MOST OF BOTTOM TORN AWAY
GEAR EXTENDED- DID NOT FAIL			300	DIVED LARGE HOLE UNDER NOSE
GEAR EXTENDED- FAILED			460	DEEP RUN SEVERAL LARGE HOLES
DIHEDRAL HYDROFOIL	3	$\frac{3}{4}$	1,100	SMOOTH RUN MODERATE HOLE AFT OF FOIL
TWIN HYDRO-SKIS			1,280	SMOOTH RUN VERY LITTLE DAMAGE

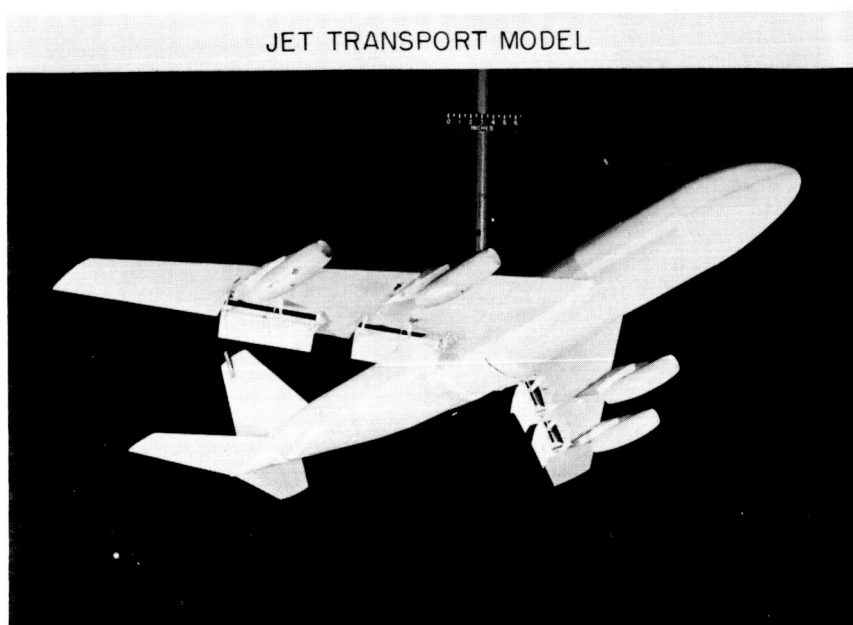


Figure 1



Figure 2



Figure 3

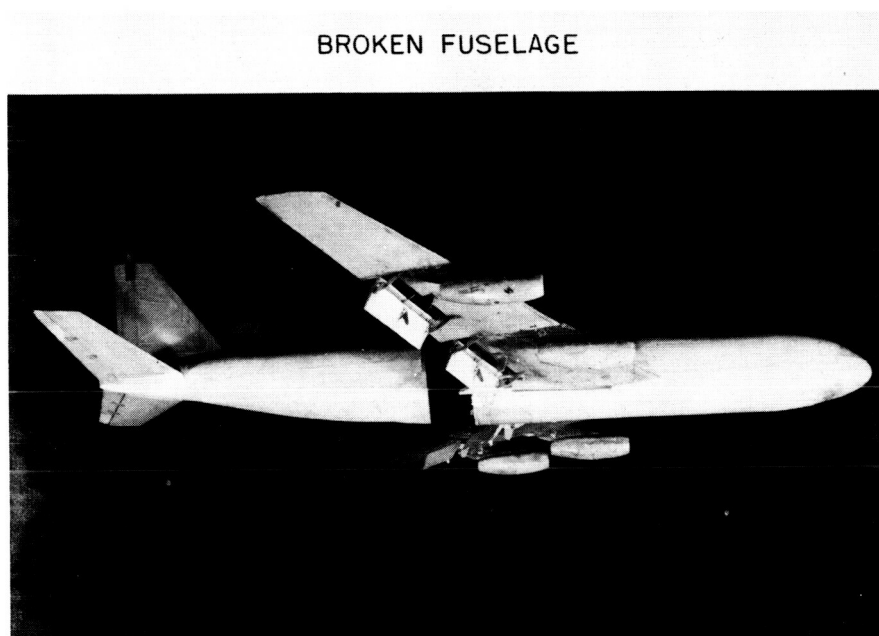


Figure 4

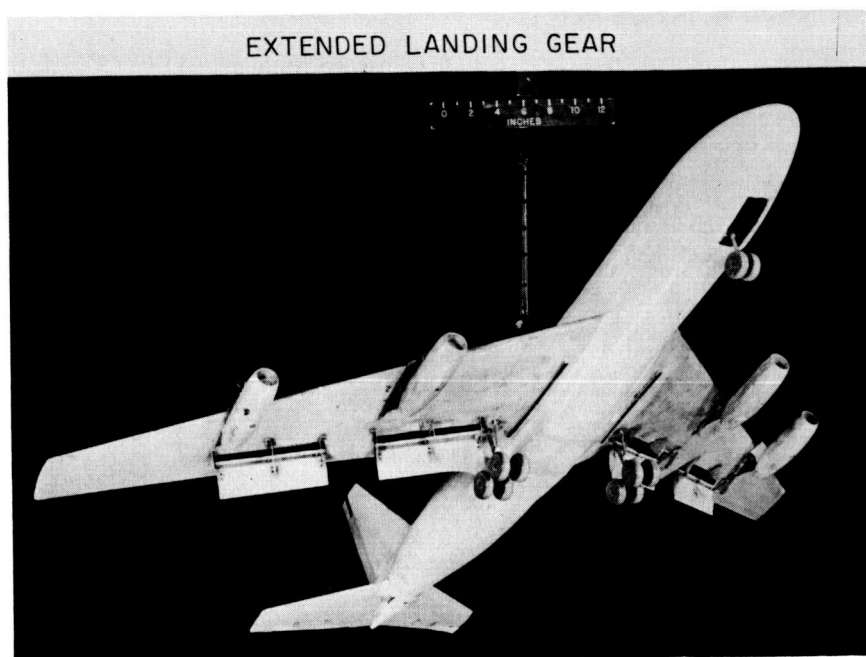


Figure 5



Figure 6



Figure 7

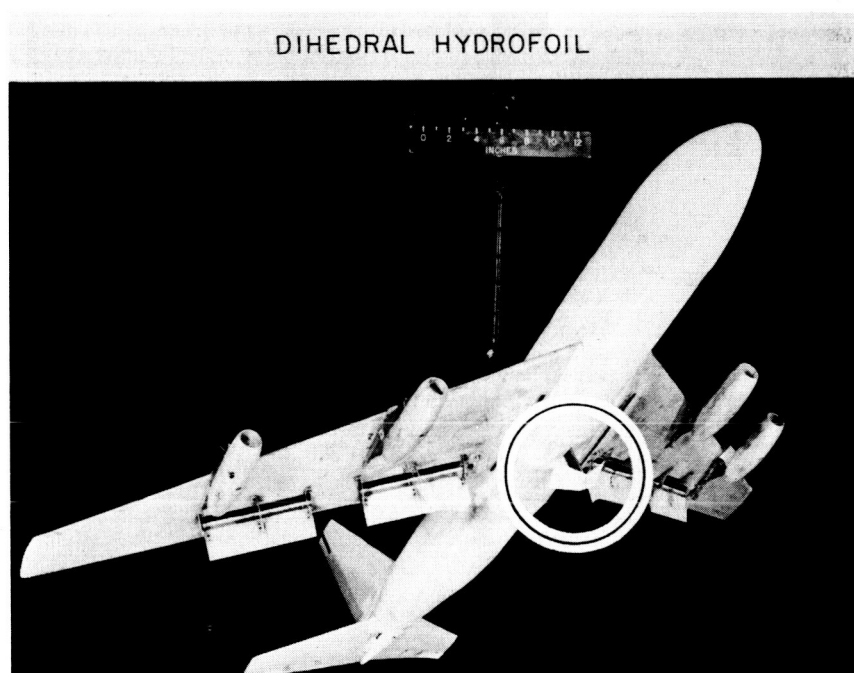


Figure 8

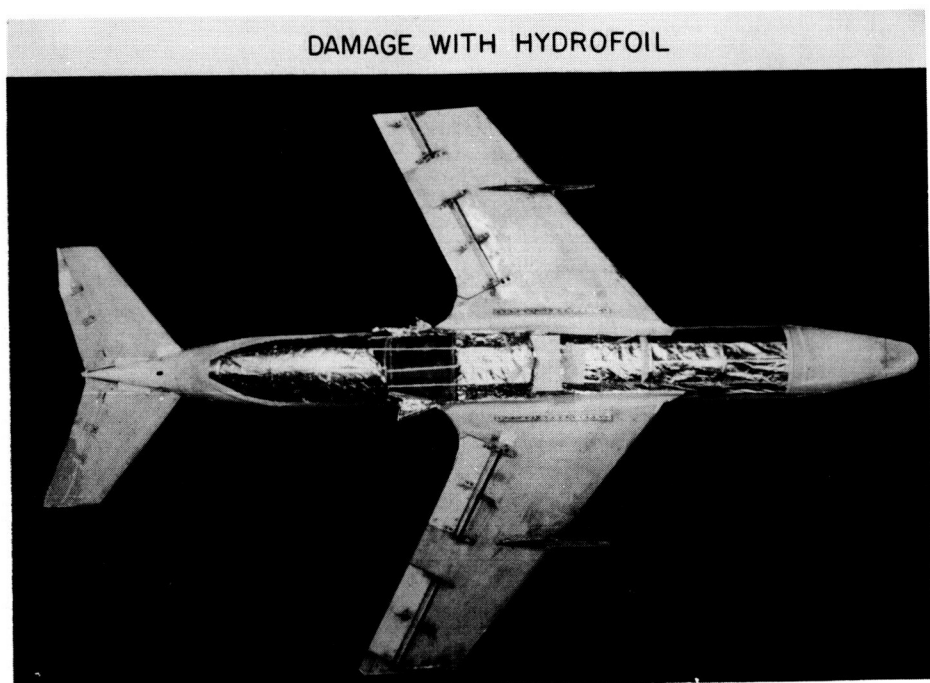


Figure 9

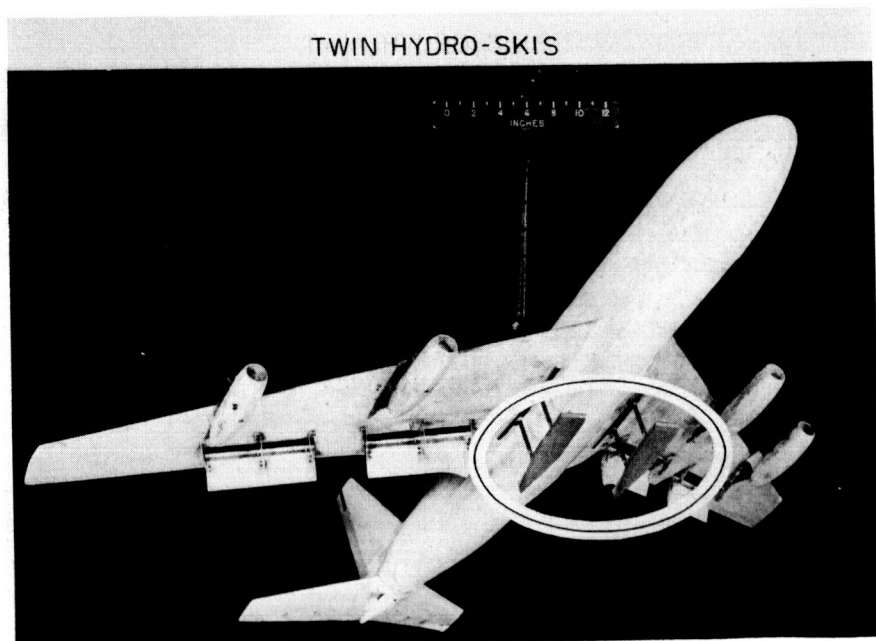


Figure 10



Figure 11

AIRCRAFT MAINTENANCE AS A POSSIBLE FACTOR IN SOME TYPES OF FLUTTER

By Dennis J. Martin

Langley Research Center

INTRODUCTION

There has been an intense effort by the airframe manufacturers to design airplanes which are free from flutter. In this paper some of the hidden factors involved in the flutter solutions are reviewed and the importance on flutter of some of the factors that might be affected by maintenance is indicated. For example, some of the factors are loose or missing balance weights, slack cables or free play within a control system, an inoperative or defective damper, condensation or ice formation in a control, fuel distributions, and others.

DESCRIPTION OF FLUTTER

Flutter may be considered to be an oscillation that arises when the damping in a mode of vibration vanishes and becomes negative. Figure 1 illustrates a typical way in which the damping in a mode of vibration varies with airspeed. In most cases there will be an increase in the damping as the velocity is first increased. As indicated by the decrement plots, as the velocity is increased an oscillation, if started, will die out more quickly until the velocity is reached where a reduction in the stable damping is found. As indicated by the decrement plot at that velocity, an oscillation, if started, will persist for a longer time. At the flutter point the damping has decreased to zero and an oscillation is self-excited; with a very slight increase in velocity the oscillation will start by itself and grow in amplitude until the structure is destroyed. The flutter point exists for all aircraft; however, aircraft are designed so that the flutter point is above the maximum operating conditions. As transonic speeds are approached, the margins between the maximum operating conditions and the flutter point decrease and closer attention must be directed to certain factors or quantities that can be altered as a result of extended operation or maintenance by an amount that might lower the flutter point into the range of operation of the aircraft and result in a flutter accident.

It is of interest to indicate the relation of figure 1 to flight flutter testing. The test flight of an aircraft rarely extends to the

flutter point. The attempt is usually made to examine a significant flutter variable, for example, the damping in the various modes of vibration as the speed is increased toward the flutter speed. It is hoped that the damping data can be extrapolated to obtain the neutral damping point and that the tests can be terminated prior to reaching the point where the damping vanishes. The damping may be measured, for example, by inducing oscillations by means of a shaker or a sharp pulse on a control member. The oscillations and the decrements are measured by a wide range of methods ranging from complex instrumentation to estimates obtained from vibrations felt through the seat of the pants or through the control column. The damping trend shown in figure 1 is for a well-behaved case. The danger is always present that a type of flutter will occur that cannot be accurately extrapolated and that the flutter point will be inadvertently reached with probably disastrous results.

IMPORTANCE OF FLUTTER

The flutter-problem areas of present-day transports are closely related to the flutter troubles that have plagued recent military aircraft, the forerunners of transports. Figure 2 shows the reported number of military-aircraft types that have had flutter incidences in two recent 4-year periods (ref. 1). The data for this figure are incomplete since many flutter incidences are known that are not reported. There may have been more than one incidence on any one type of aircraft; however, it is given only one entry in figure 2. This figure does not necessarily reflect flutter troubles that were related to maintenance. The flutter incidences occurred during aircraft development and were subsequently corrected. The totals for the number of incidences indicate that flutter problems are becoming more severe and that controls are particularly troublesome. Some characteristics of controls can be affected by maintenance; hence, this paper will deal mainly with controls. The quantities affecting tab and tail flutter are similar to those affecting control-surface flutter and, in general, the maintenance rules will be found to be similar. Wing flutter is not generally affected by maintenance, since an airplane wing that initially was designed with characteristics that provided an adequate margin of safety from flutter is unlikely to undergo changes later as a result of extended service or maintenance that would not first be critical from aspects other than flutter. Some effects on wing flutter of fuel distributions and added masses will be given.

FLUTTER OF CONTROL SURFACES

Fortunately, control-surface flutter is not always destructive. Frequently, the oscillations can be endured for a few seconds while the aircraft is being slowed so as to depart from the flutter condition. There are two types of flutter in which a control surface plays a dominant role. One is a coupled flutter in which the control surface interacts strongly with a motion of the fixed surface. This type is frequently destructive. The second is a flutter in which the control oscillates by itself, usually at transonic speeds. This latter type is often called "buzz" and is frequently not destructive.

Some of the variables which are important in control-surface flutter are listed in table I. Four important flutter factors that may be affected by maintenance are given as follows:

- (1) The control natural frequency
- (2) The control mass balance
- (3) The free play or "slop"
- (4) The damping

Frequency and Balance

An example of some of the effects of the first two factors given in table I, natural frequency and mass balance, upon the flutter characteristics is shown in figure 3. (See ref. 2.) The curves are flutter boundaries calculated for a case involving three degrees of freedom: wing bending, wing torsion, and control-surface rotation. A lower flutter speed is indicated when the control-surface natural frequency is near the wing torsional frequency for both the underbalanced and overbalanced control. As an example, if the maximum velocity of an airplane were at a value indicated by point A, the underbalanced control would not be safe from flutter for a range of control natural frequencies near wing torsion. For the same velocity, the frequency of the overbalanced control would not be critical. On the other hand, if the velocity were at a value indicated by point B, the overbalanced control would be acceptable only if the control natural frequency were held at a relatively low value or at a value well above wing torsion. It is difficult to acquire unpowered controls with natural frequencies as high as wing torsion; hence, the operating point would usually be on the lower portion of the curve. A failure of any part of the control system would result in a free-floating control and its frequency would decrease toward zero; however, the control would remain flutter free. For higher

velocities, powered systems may be used and the frequencies are usually higher than wing torsion. Failure of the control system in this case would be unfavorable; hence, parallel powered systems are usually used so that the control surface will be flutter free even though one system completely fails. A study of figure 3 indicates that the factors that determine the flutter of control surfaces combine in a complex manner. Under some conditions a specific quantity may have only a small influence, whereas under similar circumstances the same quantity may exert a critical influence.

Table I lists some of the factors that may change the control natural frequency or mass balance. The control stiffness strongly affects the frequency and may be changed because of slack cables and weakened or loose push rods or brackets. Air entrapped in the servo or hydraulic system may be particularly troublesome since it is difficult to detect without a ground vibration test. Air in the servo may cause an appreciable reduction in the natural frequency before a softening of the control can be detected. Failure of any link in the control system will cause a large reduction in frequency. Added weights affect the frequency as well as the mass balance, and flutter accidents have occurred because of condensation inside a control which had clogged drain holes. Ice formation not only affects the controls aerodynamically but may cause large changes in the mass balance as well as the frequency. Collection of dust has not only been responsible for clogged drain holes but there are cases where crop dusters have accumulated enough dust within the controls to change the mass balance sufficiently to cause flutter. Balance weights are usually designed with very large safety factors; however, the supporting brackets, bolts, and so forth have fatigued because of, for example, engine vibration, and the loss of one balance weight or even a loose balance weight has caused flutter. As a matter of interest, private owners of light aircraft have induced flutter by applying several coats of paint to a control without checking the mass balance. Although there are no reported incidences in the case of metal controls, there are many cases where the addition of several patches on the old fabric-covered controls has brought about a flutter condition. The addition of any weight to a control surface should be treated with caution and the mass balance should be carefully checked to see that it remains within the manufacturers' tolerances.

Free Play

Free play or "slop" is an important parameter of controls and tabs. Figure 4 illustrates one effect of free play on a case of flutter involving three degrees of freedom: control-surface rotation, wing bending, and wing torsion. (See ref. 3.) In figure 4 the flutter speed is plotted against disturbance level (e.g., such as might be encountered while flying through a gust or very rough air). For the simple linear system without free play, the diagram indicates that, as a moment is

applied to the control surface tending to rotate it, a small deflection results which is proportional to the moment applied. The slope of the line is a measure of the stiffness of the control system. For the system with free play, when the control surface is near neutral, a small amount of control motion is possible without requiring appreciable change in moment. The amount of motion possible is the free play or "slop." The flutter speed of the linear system is unaffected by the disturbance level; however, for a system with free play there is a reduction in the flutter speed as the disturbance level increases. For this particular research case, a mild flutter was first encountered and, at large disturbance levels, a violent and destructive flutter was found. Free play may develop gradually as a result of wear in bolts, bearings, or any of the fittings. (See table I.) Loose bolts, arising either from wear, from wrong diameter initially, or from not being tightened properly, have introduced sufficient free play to cause flutter. Loose brackets, balance weights, or certain types of servo troubles may introduce effects of free play. Frequent checks to prevent the free play from becoming greater than the amount specified by the manufacturer may prevent a possible flutter accident.

Damping

The effect of increased damping is usually favorable on any type of flutter; however, for most components, wings, for example, the natural damping value is fixed by the materials and methods of construction. In the case of controls the damping can be increased by the addition of an artificial damper. In figure 5 a case is illustrated in which the total damping of a control without a damper becomes negative over a small range of Mach numbers, the amount depending upon the altitude. This is typical of the single-degree-of-freedom flutter called buzz. As an example, if a damper is designed for the control and provides the amount of artificial damping indicated, it will counteract the unstable damping and the entire speed and altitude range may be traversed without flutter. The failure or weakening of a damper may permit a flutter oscillation if flight is attempted over the entire speed range at the lower altitudes. It is seen in table I that the effectiveness of a damper can be changed because of weak connections or free play between the damper and the control, loss of oil, air entrapped in the damper, and leaking orifices. Dampers have lost oil while exposed to very high temperatures and there have been instances where someone forgot to put oil in the damper initially. Methods of determining the effectiveness of a damper require specialized vibration and measuring equipment and it is difficult to propose a simple procedure for determining whether a damper is functioning properly; however, damping is obviously important and the best protection is to maintain the damper carefully and to inspect it at frequent intervals.

FLUTTER OF WINGS

As a matter of interest, a few factors involved in wing flutter will be briefly discussed. Although not generally affected by maintenance, the wing frequencies and the wing center of gravity can be affected by the fuel distributions. Some effects of wing natural frequency and wing center of gravity will be illustrated.

Wing Natural Frequency

A case of wing bending-torsion flutter is illustrated in figure 6. (See ref. 4.) A large reduction in flutter speed occurs when the torsional frequency is near the bending frequency. Usually the torsional frequency is considerably greater than the bending frequency; thus, increasing the torsional stiffness and hence the torsional frequency is a rule of thumb for increasing the flutter speed. Here again a case can be illustrated in which the rules might change. For an airplane with a large external store, the torsional frequency may be less than the bending frequency and the reverse effect is found. A case has been recorded where sway braces were added to a fuel tank to reduce the tank motion due to buffeting and this resulted in flutter. It was found that the braces increased the torsional stiffness without changing the bending frequency and this resulted in a lowered flutter speed. This case illustrates the rule that built-in stiffness or flexibility should not be changed because it may be necessary to prevent flutter.

Wing Center of Gravity

Figure 7 illustrates the way in which the flutter speed can be affected by the center-of-gravity location of an external store. (See ref. 5.) As the weight or center of gravity of the store is moved rearward, a large reduction in the flutter speed is noted. For different types of flutter and for different frequency ratios, there are cases where the reverse effect may be found. The sequence of removal of fuel from wing tanks, as well as from external tanks, strongly affects the center of gravity of the store and may produce large changes in both the bending and torsional frequencies of the wing and, hence, in the flutter speed. The fuel utilization schedule for some present military aircraft is necessary to avoid frequencies or center-of-gravity locations that would produce a lowered flutter boundary. Added masses, if not placed in prescribed locations, may also adversely affect the frequencies as well as the center-of-gravity locations and, hence, the flutter characteristics.

CONCLUDING REMARKS

Effects on control-surface flutter of control natural frequency, mass balance, free play, and damping have been illustrated. Some of the maintenance details that might alter these factors have been listed. Effects of fuel distributions or added masses on wing center of gravity and wing natural frequency and their effect on wing flutter have been presented. Although this paper probably has not outlined any new checks or inspection procedures, it is hoped that there will be a better awareness of some of the factors that have an important effect on an aircraft's flutter characteristics.

REFERENCES

1. Rainey, A. Gerald: Interpretation and Applicability of Results of Wind-Tunnel Flutter and Control Surface Buzz Investigations. Presented to Joint Meeting of Wind Tunnel and Model Testing Panel and Structures and Materials Panel of AGARD (Copenhagen, Denmark), Oct. 20-21, 1958.
2. Walter, F.: Flutter Tests on the Influence of the Aerodynamic Balance of Ailerons. Library Translation No. 301, British R.A.E., Apr. 1950.
3. Woolston, Donald S., Runyan, Harry L., and Andrews, Robert E.: An Investigation of Effects of Certain Types of Structural Nonlinearities on Wing and Control Surface Flutter. Jour. Aero. Sci., vol. 24, no. 1, Jan. 1957, pp. 57-63.
4. Theodorsen, Theodore, and Garrick, I. E.: Flutter Calculations in Three Degrees of Freedom. NACA Rep. 741, 1942. (Supersedes NACA ARR, Oct. 1941.)
5. Sewall, John L., Herr, Robert W., and Igoe, William B.: Flutter Investigation of a True-Speed Dynamic Model With Various Tip-Tank Configurations. NACA RM L54I19, 1955.

TABLE I

FACTORS AFFECTING FLUTTER OF CONTROL SURFACES

NATURAL FREQUENCY	MASS BALANCE	FREE PLAY	DAMPING
SLACK CABLES	CONDENSATION	WEAR IN BOLTS	EFFECTIVENESS
WEAK SUPPORTS	ICE	WEAR IN BEARINGS	WEAK CONNECTIONS
AIR IN SERVO	DUST OR DIRT	WEAR IN FITTINGS	FREE PLAY
SYSTEM FAILURE	BALANCE WEIGHTS	LOOSE BOLTS	LOSS OF OIL
ADDED WEIGHTS	PAINT	LOOSE BRACKETS	AIR IN DAMPER
		LOOSE WEIGHTS	ORIFICES
		FAULTY SERVO	

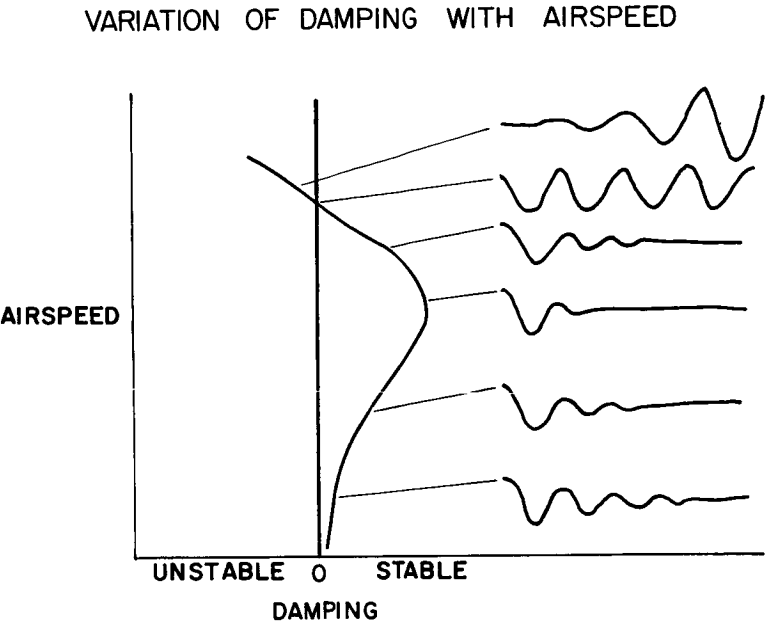


Figure 1

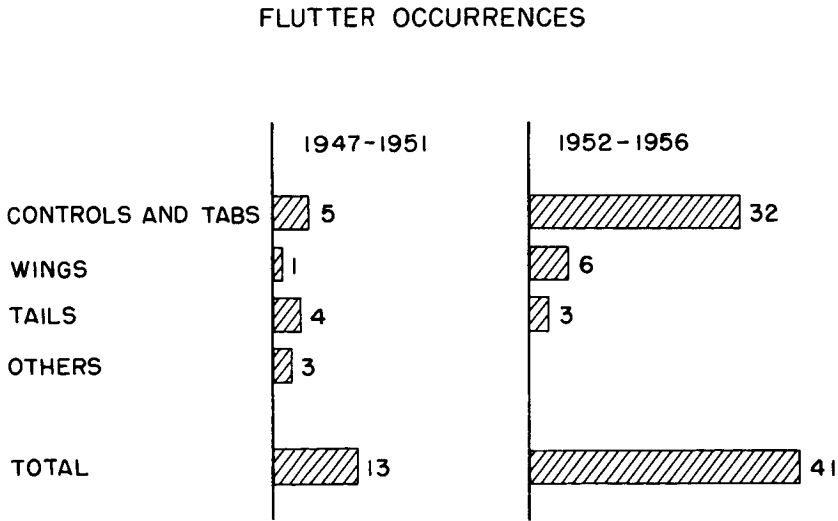


Figure 2

EFFECTS OF FREQUENCY AND BALANCE ON FLUTTER OF CONTROL SURFACES

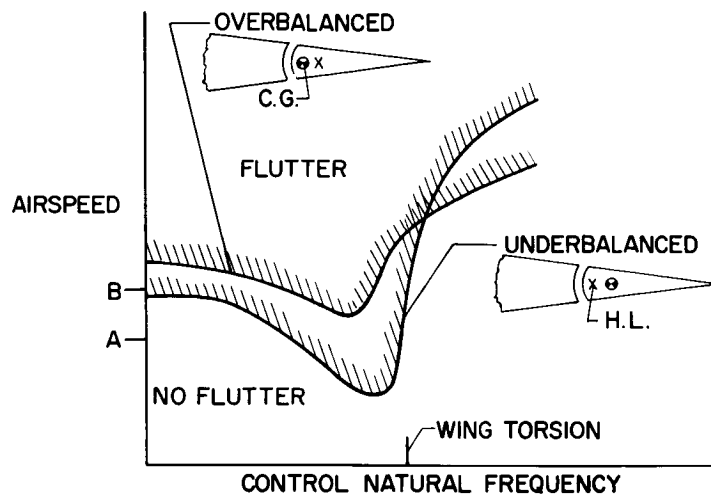


Figure 3

EFFECTS OF FREE PLAY ON FLUTTER OF CONTROL SURFACES

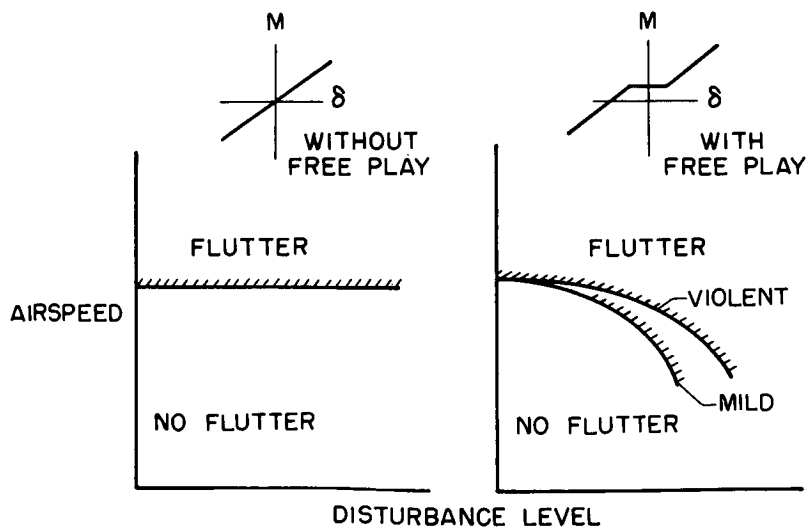


Figure 4

EFFECTS OF DAMPING ON FLUTTER OF CONTROL SURFACES

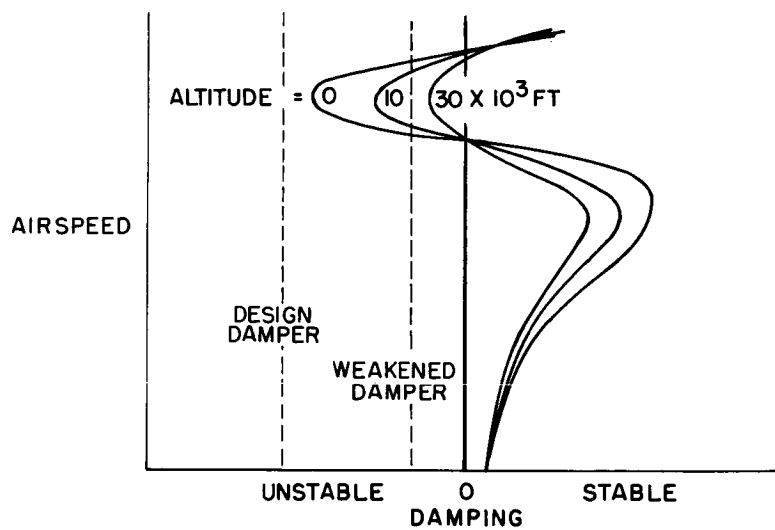


Figure 5

EFFECT OF FREQUENCY ON WING FLUTTER

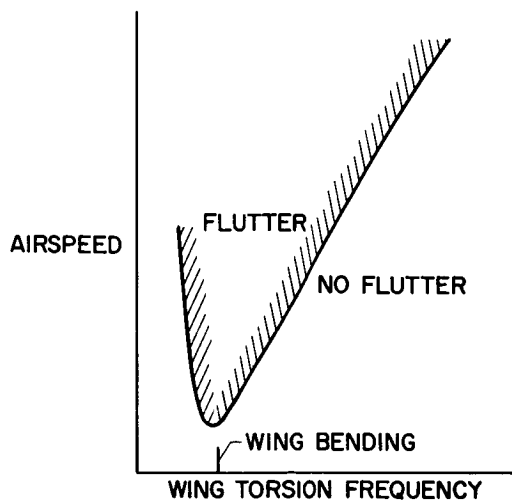


Figure 6

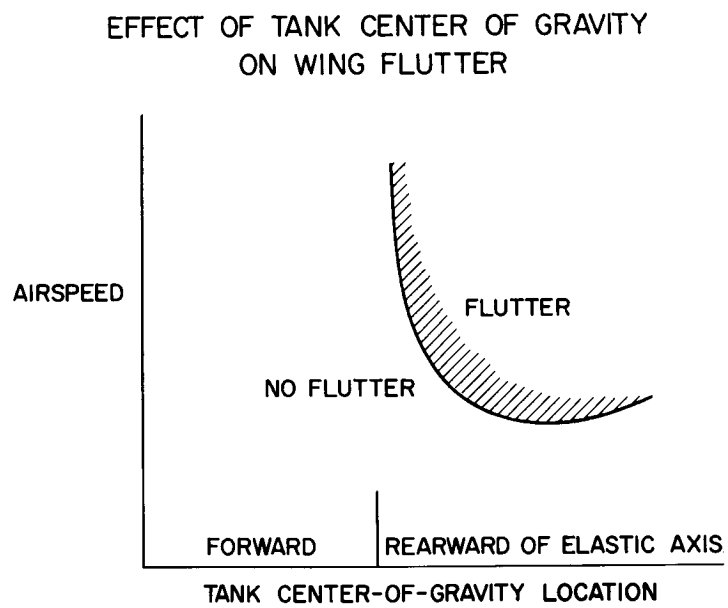


Figure 7

SOME ASPECTS OF COMPRESSOR AND TURBINE BLADING RELIABILITY

By Richard H. Kemp and John W. Weeton

Lewis Research Center

INTRODUCTION

The compressor and turbine blades of a turbojet engine represent one of the more serious problem areas with respect to the overall reliability of the engine. Failure of the blading usually results in loss of power and often produces catastrophic results. This discussion includes three specific aspects of the problem area. These aspects are as follows:

- (1) Criteria for replacing and reworking compressor blades damaged by foreign-object ingestion
- (2) Reduction of turbine-bucket vibration through the use of modified stator-vane assemblies
- (3) Operating conditions leading to thermal fatigue cracking of turbine buckets, including the effects of overtemperaturing.

Each of these areas is introduced and discussed separately.

CRITERIA FOR REPLACING AND REWORKING COMPRESSOR

BLADES DAMAGED BY FOREIGN OBJECT INGESTION

One of the major problems in the maintenance of axial-flow jet engines is impact damage to the compressor blades caused by foreign-object ingestion. The damage is usually in the form of small nicks and dents which do not measurably affect the aerodynamic performance but could possibly result in premature failure by notch fatigue. Examples of typically damaged blades are shown in figure 1. When blades such as these are found during routine inspections, a decision must be made regarding blade replacement. In the absence of factual data, the natural tendency in drafting inspection specifications is to be cautious and reject an excessive proportion of the blades.

As evidence that this lack of data results in more blade replacement and reworking than is necessary are the many engines wherein blade

damage is first discovered at normal overhaul; some of the blades in these engines have undoubtedly operated many hours after sustaining the damage. A good basis for inspecting blades could provide substantial savings of money spent every year for overhauling engines and rejecting damaged blades that either represented no danger to the aircraft or could have been reworked without complete disassembly of the engine.

An attempt was, therefore, made to determine both the fatigue strengths of damaged blades, while taking into account the location, size, and stress-concentration effect of the damage, and the fatigue strength of the material. In reference 1 it was shown that the nicks on the leading and trailing edges were most damaging to the life of the blades; dents could be straightened and most of the lost fatigue strength restored. It was further shown that nicks on the pressure surface, away from the edges, did not adversely affect the fatigue life because of the fact that the pressure face was relatively close to the neutral axis. Damage on the suction surface was found to be extremely rare. It was, therefore, possible to limit this study to nicks commonly found on the edges (up to 1/16 inch depth).

The study of leading- and trailing-edge nick damage was considerably simplified by experimental evidence (ref. 1) indicating that the stress-concentration factor for nicks is essentially independent of the nick depth and location along the span. It was shown that when the depth of a nick exceeded approximately 0.020 inch, the stress-concentration factor was in the range of approximately 1.6 to 1.8. Depths of 0.008 to 0.020 inch produced factors as low as approximately 1.4. The stress-concentration factor can be considered constant at approximately 1.8 for determining the maximum probable damage; thereby, a variable is eliminated from the determination. From additional related data it was shown that the stress-concentration factor was approximately the same regardless of the position of the nick along the span. The data presented in reference 1 were determined for a specific blade configuration and a specific material, and a similar determination should be made if a different configuration and material are employed.

The determination of inspection curves to use as a basis for blade rejection by utilizing the foregoing two assumptions is given as a seven-step procedure in reference 2. This procedure can be summarized as follows: Data are obtained concerning the fatigue life, failure location, endurance limit, and stress distribution for undamaged blades when the blades are vibrated in the mode which has previously been determined as the critical mode during engine operation. The assumption is made that a number of engines have been suitably instrumented with strain gages in order to determine not only the critical vibratory mode of the blades but also the maximum vibratory stress to be expected under the various possible engine operating conditions. In those cases which have been examined at the Lewis Research Center, the first bending mode

has always been the critical mode. If the S-N curve does not show an endurance limit, then a pseudoendurance limit at a given number of cycles (that is, 10^8) must be specified. Strain gages are used to measure the stress at the critical section as determined from the fatigue tests and also the stress distribution along both sides of the leading and trailing edges.

A number of artificially nicked blades with the nicks located at the same span position as the critical section in the endurance tests of undamaged blades are then fatigued in the same vibratory mode. The data are plotted in a standard S-N form, and a curve is drawn at the lower limit of the scatter in order to allow for the worst possible conditions. The fatigue limit or safe stress level for blades nicked at this span position is then the flat portion of the curve or some pseudofatigue limit at a given number of cycles.

An allowable stress curve, as shown in figure 2, is then established for nicks at any span location that shows the permissible vibratory stress at the critical section as a function of the damage location. Higher vibratory stresses at the critical section would result in premature blade failure at the damage location. The allowable vibratory stress at the critical section (failure point in undamaged blades) is plotted against the span location of the damage. A horizontal line is drawn at 27,000 pounds per square inch, which represents the maximum vibratory stress obtained at the critical point in the blade during engine operation. This value has been corrected with the aid of a Goodman diagram to take into account the fact that the fatigue tests were made without a centrifugal load on the blades. Those points along the curve which lie below the engine vibratory stress level represent damaged blades which are a threat to the safety of the engine. Blades having nicks up to $1/16$ inch deep above the 52-percent-span point will not fail.

The effect of reworking nicks up to $1/16$ inch deep by filing and polishing can be determined in the same manner as just described for the unworked nicks. Again, a curve can be established for the reworked blades, and a sample of such a curve is shown in figure 2. In this case all reworked blades would represent safe operation.

In order to check the assumed relation between the endurance limit due to a nick at the critical section and the endurance limit due to nicks at other span points, 68 blades with nicks at various edge locations were fatigued. The fatigue data were then compared with endurance-limit calculations based on the measured endurance limit due to a nick at the critical section and on the measured stress distribution along the leading and trailing edges. In all cases except one, the computed life reductions were on the conservative side. The one

case which was not resulted in a failure at a stress level only 2 percent below the computed limit curve. It was, therefore, indicated that the experimental damage determination need be carried out with nicks at the critical section only on the leading and trailing edges.

It should be remembered that the allowable stress curve must be redetermined every time a change is made to either the blade shape or the material, largely because of changes that occur in the endurance limit, stress distributions, and notch sensitivity. For certain non-ferrous materials (such as aluminum) that generally have no sharply defined endurance limit, an alternate method must be used in which a pseudoendurance limit for a finite number of cycles is employed. The use of the method just given places the damage-assessment determination on a more scientific basis and should reduce overhaul costs materially by permitting continued service of blades having damage which represents no threat to the safety of the engine.

REDUCTION OF TURBINE-BUCKET VIBRATION THROUGH THE USE OF MODIFIED STATOR-VANE ASSEMBLIES

In the previous section, it was pointed out that the proximity to failure by vibratory fatigue is a function not only of the degree of damage that the blade may have suffered, but also of the vibratory stress encountered during service operation. It is obvious that one way of reducing the vibratory-stress level is to reduce the excitation forces to which the blades or buckets are subjected. The turbine bucket is representative of a vibratory system having an infinite number of degrees of freedom. This simply means that it is possible for a bucket to take on many different deflection shapes during vibration, with a different frequency associated with each shape or mode. For a simplified illustration of this fact, see figure 3 in which the turbine-bucket deflection associated with the first bending mode is shown on the left and the second bending mode on the right, with a representation of the stress distribution below each mode form. The height above the base plane is an indication of the relative stress magnitude at any given location. In passing from the first mode to the higher modes, the natural frequency of vibration increases. The same thing occurs in the case of the torsional modes, and, in addition, other new and still more complex modes arise from a combination of the bending and torsional modes.

In order to reduce the vibratory-stress level of the buckets in the engine, it is obvious that one method might be to reduce the excitation forces which cause the buckets to vibrate. One of the main sources of the excitation force is the periodic variation in air flow over the

bucket as it passes through the wake behind each turbine stator vane. The number of pulses received per revolution of the turbine is simply the number of vanes in the stator. If the number of pulses per unit time received by the bucket equals the frequency of one of its natural modes of vibration, then resonant vibration will result. In most conventional turbojets, the number of stator vanes is such that the bucket vibratory modes which are excited by the stator vanes are the high-frequency complex modes. These are the modes which are often associated with vibration failures in the tip regions of the buckets.

In order to reduce the excitation forces caused by the stator vanes, it is necessary to interrupt the regularity with which the individual pulses strike the buckets. This interruption can be thought of roughly in terms of the old story about the soldiers breaking step when crossing a bridge in order to eliminate the possibility of bridge failure by resonant vibration at a frequency equal to the cadence of their marching. In the case of the stator vanes it is necessary to move some of the vanes in a circumferential direction and, thereby, interrupt the regularity of the pulses. There are many ways of accomplishing this interruption and figure 4 illustrates several of these ways. A standard stator-vane assembly having all vanes equally spaced is shown on the left in figure 4 for reference purposes. This configuration is used in most jet engines today. In the figure, however, the number of vanes have been reduced for illustrative purposes. In the center of the figure is shown one possible variation in which the assembly is divided into three segments. In the first segment, the vane spacing is the same as in the standard assembly on the left. In the second segment the spacing has been decreased between the vanes, and in the third segment the spacing has been increased between the vanes. In the configuration on the right, the same procedure has been used and, in addition, each segment has been rotated relative to the other segments by a small amount. This rotating is called phasing. As a result of theoretical and experimental analyses, it has been shown that the configuration on the right will provide the greatest reduction of excitation force of any of the configurations studied. The excitation reduction provided by this configuration and the amount of vane-spacing change required is shown in figure 5. The spacing change within the segments, in terms of percent of the standard spacing, is plotted on the abscissa against the relative exciting force on the ordinate. A standard vane assembly with 48 equally spaced vanes was chosen as the basis for the calculations, and the configuration represented is merely a modification of this assembly. For the equally spaced assembly, there would be 48 pulses per revolution, and the excitation force of these pulses was arbitrarily given a value of 1. For the modified assembly, it was determined that the excitation force of the 48 pulses per revolution was decreased. However, because of the phasing and spacing, other pulse frequencies were introduced. The pulses having the highest excitation force are shown in figure 5; these pulses are

47, 48, 49, and 50 per revolution. The excitation force of these pulses is shown in this figure relative to the force of 1 for the equally spaced assembly. It will be noted that when the spacing is changed only 8.5 percent of the standard spacing, the excitation-force level drops to 0.32. In other words, the excitation level has been decreased 68 percent compared with the equally spaced assembly. A detailed description of this investigation is presented in reference 3.

It would, therefore, appear desirable to incorporate a modified stator-vane arrangement in all engines and thereby reduce the probability of dangerous vibration of the turbine buckets in the higher frequency modes. The modification of the stator-vane assembly must, of course, be carried out with proper attention to the aerodynamics of each of the nozzle passages that is altered in order to prevent a decrease in the stage efficiency. For the small changes in spacing that have been indicated, however, it should not be necessary to change the vane shape but merely to alter the vane setting angle slightly.

THERMAL FATIGUE CRACKING OF TURBINE BUCKETS

Often, cracks on the leading edges of turbine buckets are the equivalent in turbine-bucket failures of nicks and dents in compressor-blade failures. Where a multiplicity of cracks occur on the leading edges of turbine buckets, they are not caused by foreign-object ingestion but rather by a process called thermal fatigue in references 4 and 5. Experience has shown that turbine-bucket failure by stress rupture or fatigue may be greatly accelerated by thermal-fatigue cracks. Typical leading-edge cracks caused by thermal fatigue are shown in figure 6 (from ref. 4). The cracks appear to be wide because of the bleeding of the inspection oil from the cracks. In this case, cracks have formed up and down the leading edges of the bucket. If leading-edge cracks such as those shown in figure 6 are observed during inspection procedures, buckets are removed from the engine and discarded, and, in fact, are termed "bucket failures." Tests have been conducted on many different types of alloys in turbojet engines, and thermal-fatigue cracks have been produced in both cast materials and forged materials. (See ref. 6.) Many alloys exhibited leading-edge cracks after they had been operated at rated-speed or full-power conditions for time periods less than 50 hours.

Since any thermal-fatigue crack is thought to be potentially detrimental to good engine reliability, the National Aeronautics and Space Administration undertook a study of the mechanics of fatigue-crack formation and the phase of engine operation that promotes its occurrence. It would be suspected that a cold turbine bucket suddenly exposed to hot gases from the combustion chamber during a start would be thermally

shocked. Similarly, when an engine is shut down by suddenly cutting the fuel flow, it would be expected that further thermal shocking of a bucket would take place. In order to learn more about the temperature changes in a turbojet engine, an extensive series of temperature surveys were made of engine components while the engine was being operated, and an example of the data obtained is shown in figure 7. In this figure the temperature profile of a turbojet-bucket leading edge is shown for the starting of the engine in a normal fashion. This profile is established within approximately 10 seconds after the engine is started. Two things are evident: First, there is a large change in temperature from the leading-edge skin to the midchord. In this case, the temperature difference was 840° F. The second fact is that the temperature decrease from the leading edge is very rapid. From the total temperature difference and from the slope of the curve, it has been calculated that on starting, stresses well in excess of the elastic limit of the material are obtained. As a result, plastic flow of the edge material would occur upon starting. As the temperature of the bucket is stabilized, the colder inner portions would expand and put the outer portions in tension or, in other words, cause the outer edges to elongate. Additional tensile stresses would be induced in the bucket edge when the engine is stopped. It is this type of induced tensile stress which fluctuates upon starting, running, and stopping the engine that would be expected to account for the thermal-fatigue cracks at the leading edges of the bucket.

Some conclusive evidence that shows that leading-edge thermal-fatigue cracks are caused largely by starting an engine is presented in table I. This table represents a series of full-scale-engine tests with turbine buckets made from the alloy M-252. (See ref. 7.) This alloy is a nickel-base alloy similar to many in use in turbojets today. The data presented in table I relate the mode of engine operation with the appearance of the first thermal-fatigue cracks. The results of testing M-252 in a cycle designed to simulate service conditions is shown in table I as the first type of test. This cycle consisted of starting, running the engine at idle for 5 minutes, running at full-power conditions for 15 minutes, and then returning to the idle condition. For various reasons, a start and stop was averaged for every 3 hours of rated speed. Under these operating conditions, the buckets exhibited cracks after 18 starts or 55 hours of operation at rated speed. To determine whether steady-state operation at rated speed could produce leading-edge cracks, a second test was made. The engine was run on a three-shift basis, and the engine was started as few times as possible. After 360 hours of operation at rated speed, no cracks had formed.

To determine whether the portion of the cycle between idle- and rated-speed conditions could cause cracks, the third test was made (table I). After cycling the engine 1,984 times between idle and rated speed, no cracks had formed. This number of cycles is considerable and was believed to more than adequately permit the conclusion that this portion of the cycle did not produce leading-edge cracks. In the fourth test, the engine was started, was brought to idle, and stopped. At this point, cracks were produced in the leading edges. During this test the engine never reached rated-speed or full-power conditions. In the fifth test the engine was started, was brought to idle, increased to rated-speed conditions, and then stopped. This procedure reduced the number of starts necessary to cause cracking and showed that full-power conditions could reduce the number of engine starts that produced cracks. Finally, the engine was started slowly by igniting one burner, then another, and then more burners so that the buckets would not be shocked on starting. The engine was started in this manner 900 times, and it was found that no cracks formed. The conclusion was reached, therefore, that normal starting caused cracks and that gradual starting of the engine could prevent crack formation. Results of the thermal-fatigue studies may be stated as follows:

(1) Thermal-fatigue cracks may be induced in many different types of alloys.

(2) Starting the engine did more to cause thermal cracks than any other portion of the cycles.

(3) Operation of the engine at full-power conditions reduced the number of starts necessary to cause cracks.

(4) It may be possible to prevent or reduce cracking completely by starting the engine by lighting the combustors one at a time as the engine accelerates.

It is evident from the discussion of thermal-fatigue cracks that hot starts, a form of overtemperaturing, will aggravate crack formation because temperature gradients at the edges are greater during hot starts than during normal starts. Overtemperaturing of buckets may also occur, of course, under other circumstances. (See, for example, refs. 4 and 5.)

A separate study of the useful life of turbine buckets that were subjected to overtemperaturing in actual airplane service is discussed in reference 4. Data were obtained with one set of turbine buckets subjected to an overtemperature of 500° F as measured in the tailpipe and another set subjected to an overtemperature of 200° F caused by operation at 4 percent above the rated engine speed.

These data showed no well-defined decline in crack resistance of either set of turbine buckets as a result of the single overtemperature experience. Several other investigations have been conducted in order to better understand the effects of overtemperaturing. Such investigations are discussed in references 8 to 10. Further work is necessary to better define the tolerance of turbine buckets to engine overtemperature as functions of engine design and materials.

REFERENCES

1. Kaufman, Albert, and Meyer, André J., Jr.: Investigation of the Effect of Impact Damage on Fatigue Strength of Jet-Engine Compressor Rotor Blades. NACA TN 3275, 1956.
2. Kaufman, Albert: Method for Determining the Need To Rework or Replace Compressor Rotor Blades Damaged by Foreign Objects. NACA TN 4324, 1958.
3. Kemp, Richard H., Hirschberg, Marvin H., and Morgan, W. C.: Theoretical and Experimental Analysis of the Reduction of Rotor Blade Vibration in Turbomachinery Through the Use of Modified Stator Vane Spacing. NACA TN 4373, 1958.
4. Signorelli, Robert A., Johnston, James R., and Garrett, Floyd B.: Effect of Prior Air Force Overtemperature Operation on Life of J47 Buckets Evaluated in a Sea-Level Cyclic Engine Test. NACA TN 4263, 1958.
5. Lewis Laboratory Staff: Factors that Affect Operational Reliability of Turbojet Engines. NACA RM E55H02, 1956.
6. Signorelli, R. A., Johnston, J. R., and Weeton, John W.: Thermal Fatigue Cracking of Turbine Buckets Operated in a Turbojet Engine at 1700° F. Part I - Frequent Starts and Stops. (Prospective NASA paper.)
7. Johnston, J. R., Weeton, J. W., and Signorelli, R. A.: A Study of Engine Conditions Which Cause Thermal Fatigue Cracks in Turbojet Engine Buckets. (Prospective NASA paper.)
8. Signorelli, R. A., Garrett, F. B., and Weeton, J. W.: Engine Performance of Overtemperature Heat-Treated S-816 Buckets. NACA RM E55L06a, 1956.
9. Floreen, S., and Signorelli, R. A.: Survey of Microstructures and Mechanical Properties of Overtemperated S-816 Turbine Buckets From J47 Engines. NACA RM E56K30, 1957.
10. Robins, Leonard: Evaluation of the Use of Electrical Resistance For Detecting Overtemperated S-816 Turbine Blades. NACA RM E57A29a, 1957.

TABLE I

SUMMARY OF THERMAL-FATIGUE ENGINE TESTS

TYPE OF TEST	CRACKS FIRST OBSERVED AFTER -	
	NUMBER OF STARTS	TIME AT RATED SPEED, HR
NORMAL TEST	18	55
STEADY STATE	NO CRACKS - 360 HRS	
IDLE-RATED-IDLE	NO CRACKS 1984 CYCLES	
START-IDLE-STOP	85	0
START-RATED-STOP	40	10
GRADUAL START-IDLE-STOP	NO CRACKS AFTER 900 STARTS AND STOPS	

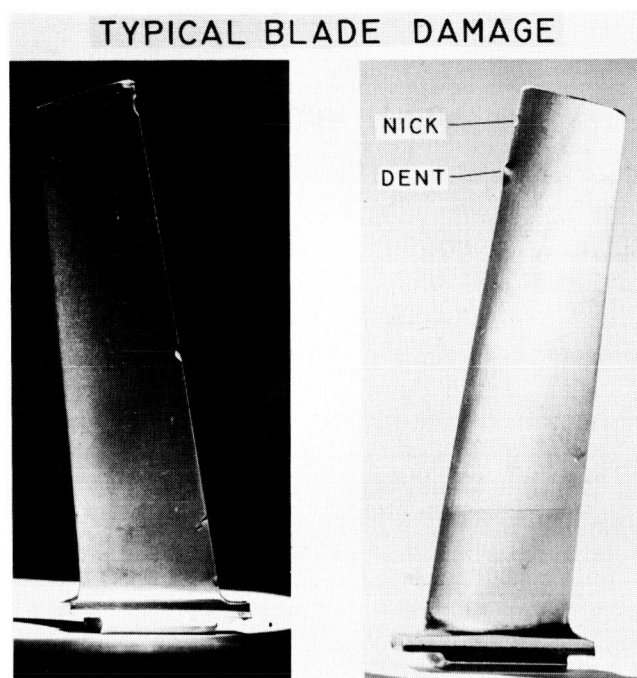


Figure 1

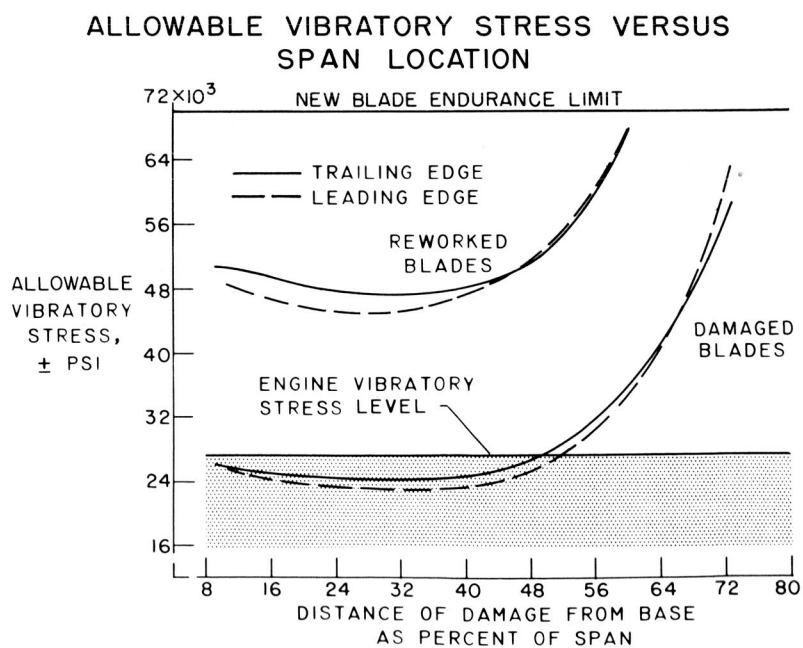


Figure 2

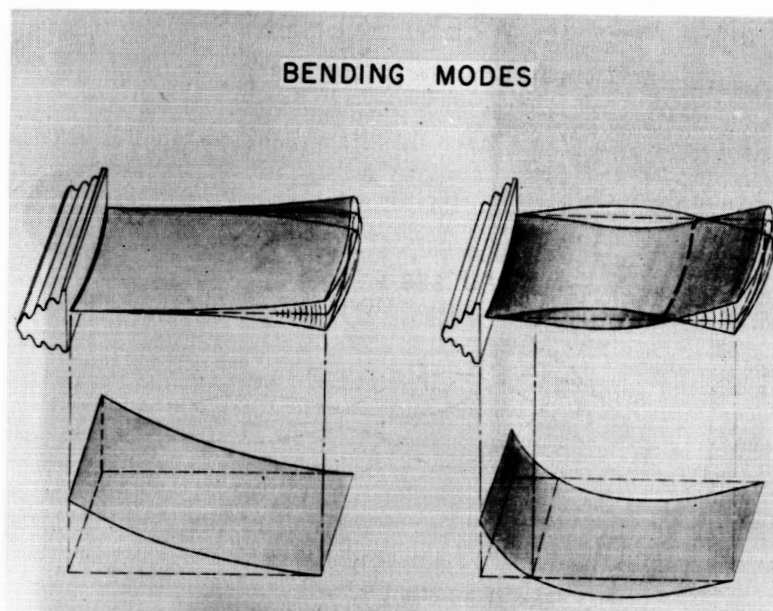


Figure 3

STATOR VANE MODIFICATIONS

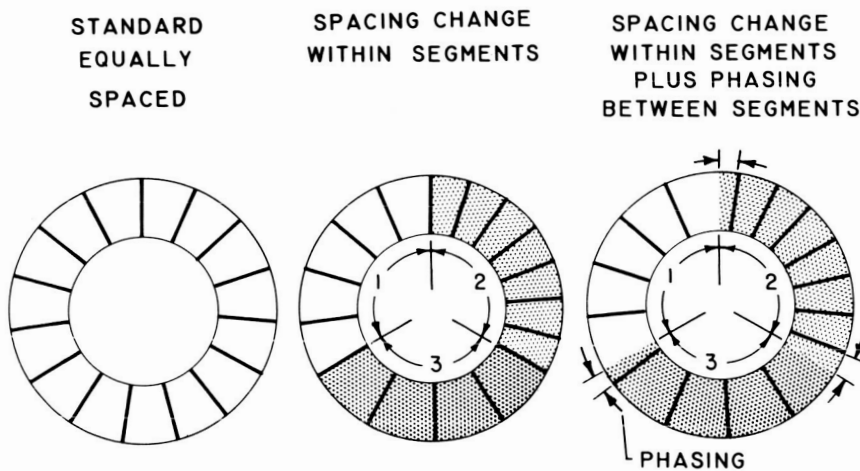


Figure 4

THREE-SEGMENT ASSEMBLY WITH VARIABLE SPACING BETWEEN SEGMENTS

2.5° PHASING BETWEEN SEGMENTS

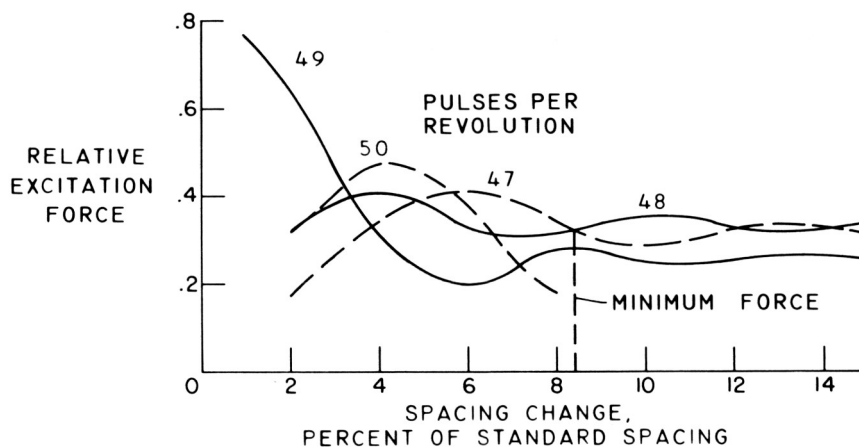


Figure 5

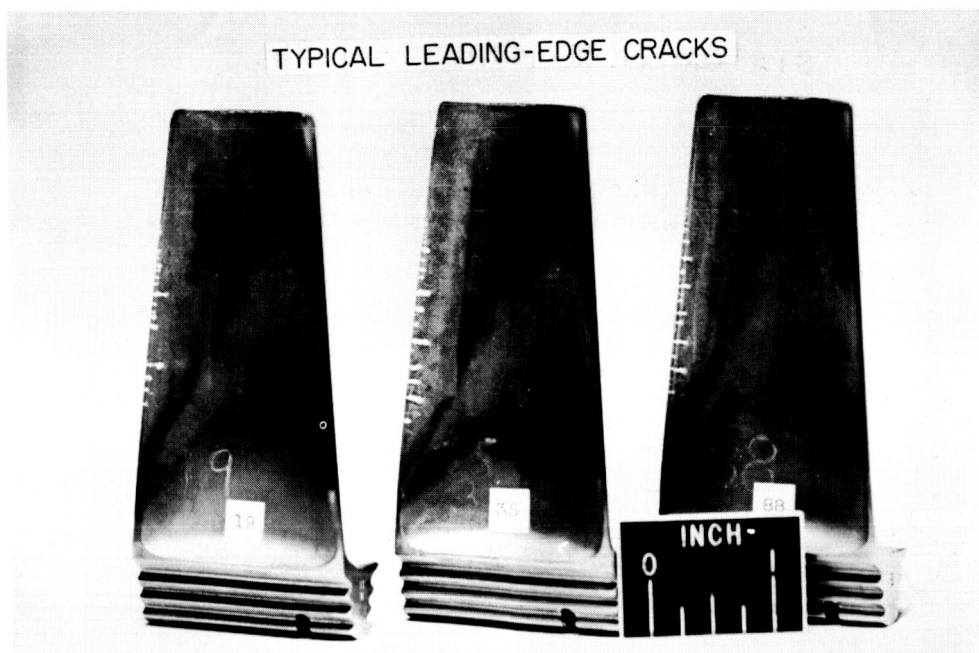


Figure 6

TURBINE BUCKET TEMPERATURE PROFILE
DURING START OF J47 ENGINE

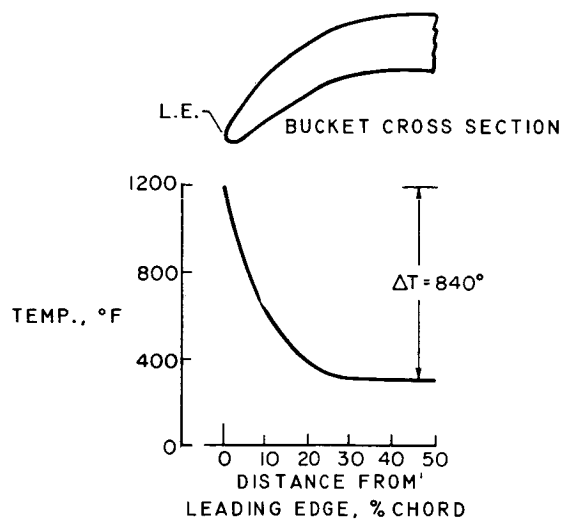


Figure 7

BOUNDARY-LAYER NOISE AT SUBSONIC AND SUPERSONIC SPEEDS

By Gareth H. Jordan and Norman J. McLeod

NASA High-Speed Flight Station

INTRODUCTION

The limited amount of data available on the noise environment of an aircraft in flight makes it difficult to formulate proper design specifications based on the noise environment to be experienced by the aircraft. The noise environment of aircraft has increased through the use of more powerful jet engines and the boundary-layer noise has increased with increase in flight speeds. Boundary-layer noise as used in this paper is defined as wall pressure fluctuations in the turbulent boundary layer.

The purpose of this paper is to present the results of flight surveys of boundary-layer and engine noise levels in an attempt to establish the contribution and relative importance of boundary-layer and engine noise on the noise environment of aircraft in flight. These data are the preliminary results of an investigation of boundary-layer noise and the noise environment of aircraft being conducted by the NASA High-Speed Flight Station. (See ref. 1.)

RESULTS AND DISCUSSION

Two airplanes were used in this investigation and neither of the airplanes contained insulation. The Boeing B-47A airplane, shown in figure 1, is a swept-wing bomber, similar in configuration to commercial jet transports, and is powered by six General Electric J47 jet engines. Microphones were located inside the fuselage at positions A, B, and C. Positions A and B are in the bomb bay and position C is in the heater compartment beneath the dorsal fin. Each of the internal microphones were located approximately in the center of the fuselage and facing forward. In addition, an external noise measurement was obtained at position B with a flush-mounted microphone equipped with a sintered wind-screen. This external microphone was located on the side of the fuselage and approximately on the fuselage center line.

Data were obtained during engine ground runs, acceleration and deceleration flights at 100 percent rated engine rpm (7,800 rpm) and 50 percent rated engine rpm, and during constant-speed flights at altitudes of 10,000 and 20,000 feet.

Overall noise levels obtained during acceleration and deceleration flights at an altitude of 20,000 feet are shown in figure 2. In this figure, the overall noise level, in decibels, is shown as a function of Mach number for positions A, B, and C. The data for 100 percent engine rpm are indicated by the circular test points and the data for 50 percent engine rpm are indicated by the square test points. All data show an increase in overall noise level with increase in Mach number. The measurements at positions A and B, which are located in the bomb bay, show approximately the same internal noise level, as might be expected. At position C, which is farther rearward, the noise level is about 5 decibels higher than at position A or B as a result of a higher engine noise environment and a thicker boundary layer. Since the internal noise levels show a small to negligible effect of engine rpm at Mach numbers greater than about 0.6, the boundary layer becomes the predominant source of noise inside the fuselage at the higher speeds.

The external noise level at position B indicates a noise level from 20 to 30 decibels higher than the internal noise level. It should be pointed out that this is a point measurement of noise and since the microphone was located close to the inboard engine, the measurement was greatly influenced by engine rpm as evident by the 15-decibel increase in noise level with increase in engine rpm from 50 percent to 100 percent throughout the Mach number range. Other areas of the fuselage would be in a less intense engine noise environment and thus would not show a large effect of engine rpm at high airspeeds.

It is interesting to compare the maximum overall noise levels measured in flight with those measured during engine ground runs at 100 percent engine rpm. The maximum internal overall noise level measured in flight at position B was 118 decibels whereas that measured during ground runs was 126 decibels. The maximum external overall noise level measured in flight at position B was 146 decibels compared with 143 decibels during ground runs. It may be seen that engine noise at high engine rpm and high airspeed may impose noise levels on local areas of the aircraft in flight as high as during engine ground runs.

Overall noise level and frequency spectrum at position B is shown in figures 3 and 4. In these two figures the internal and external noise levels in various octave bands from 75 to 10,000 cps are shown for engine settings of 50 percent engine rpm, the engine rpm required for constant speed, and 100 percent engine rpm. Gross thrust F_j produced by each engine is shown for the test conditions. Figure 3 is for a Mach number of approximately 0.45 and figure 4 is for a Mach number of approximately 0.65. The overall noise levels are shown on the left portion of the figures for reference.

For a Mach number of 0.45 at 50 percent engine rpm, the engine produces only 400 pounds of thrust and the engine noise would be expected to be small. (See fig. 3.) Increasing engine rpm from 50 percent to 100 percent raises the noise level throughout the frequency range whereas increasing engine rpm from 50 to 75 percent has a negligible effect on the noise level except at the highest octave band. The abrupt increase at the higher frequency at 75 percent engine rpm resulted in an increase in the overall noise level of about 7 decibels; however, the internal overall noise level was not affected appreciably by this increase. At a Mach number of 0.65 (fig. 4), the increase in noise level due to increasing engine rpm from 50 percent to 100 percent is less than that shown for $M \approx 0.45$ except for the 300-to-600-cps and the 600-to-1,200-cps octave bands for the external noise. In the case of the internal noise, the only increase evident occurs in the 300-to-600-cps and the 600-to-1,200-cps octave bands. From the results shown in these two figures, it is concluded that the data obtained at 50 percent rpm is boundary-layer noise both for the external and internal noise levels.

All the data shown in the previous figures have been for subsonic Mach numbers less than 0.80. An indication of the trend of boundary-layer noise at supersonic speed has been obtained from tests made with the Douglas D-558-II research airplane. The D-558-II research airplane shown in figure 5 is a swept-wing rocket-powered airplane. It is powered by a Reaction Motors rocket motor rated at 6,000 pounds of sea-level static thrust. An internal measurement of the overall noise level in the rear part of the fuselage was obtained during accelerating flight with rockets on and during decelerating flight with rockets off at Mach numbers up to 1.4 at an altitude of 47,000 feet.

The overall noise levels obtained in the D-558-II are shown in figure 6 as a function of Mach number. The noise level shown for the rocket-off condition or the glide portion of the flight is the noise level inside the fuselage due to boundary-layer noise. The noise level is seen to increase to the highest Mach number shown; however, at supersonic speeds the rate of increase of noise level in decibels with Mach number is less than at subsonic speeds. When the noise level for the rocket-off condition is compared with that for the rocket-on condition, it is seen that at subsonic speeds the rocket noise determines the noise level in the rear part of the fuselage. The rocket noise is produced downstream, and at supersonic speeds does not contribute to the noise environment of the aircraft.

The data presented in the previous figures have indicated that boundary-layer noise increases with increase in Mach number and, at Mach numbers greater than about 0.6, was the predominant source of noise inside the fuselage for the B-47A airplane. Noise levels and trends obtained during this investigation have shown the need for

adequate methods of predicting noise environment of high-performance aircraft in the design stage. Theoretical and experimental investigations of boundary-layer noise (refs. 2 and 3) have indicated that the pressure fluctuations in the turbulent boundary layer vary as the velocity squared and with density or with dynamic pressure. These experimental investigations have indicated that the pressure fluctuations are about 0.006 times the dynamic pressure. Estimates of the boundary-layer noise levels have been made by use of the equation for sound pressure level. The equation for sound pressure level in which the measured effective sound pressure has been replaced with 0.006 times the dynamic pressure is as follows:

$$\text{Sound pressure level} = 20 \log_{10} \frac{0.006q}{p_{\text{ref}}} \quad (1)$$

where p_{ref} is equal to 4.177×10^{-7} lb/sq ft. The reference pressure p_{ref} is expressed in pounds per square foot instead of the more usual dynes per square centimeter so that the dynamic pressure q may be expressed as pounds per square foot. This equation has been used to estimate the external boundary-layer noise level in decibels.

Comparison of the overall noise levels obtained during this investigation with those estimated values from equation (1) are shown in figure 7. In this figure, the overall noise level is shown as a function of free-stream dynamic pressure. The faired line represents the estimated level, and the experimental results are shown for external and internal noise levels at position B for the B-47A airplane and internal noise levels for the D-558-II airplane. The external boundary-layer noise level for the B-47A airplane is felt to be in good agreement with the estimated boundary-layer noise level. The constant used in the prediction of the boundary-layer noise (0.006) was based on flat-plate investigations and it is expected that this constant would vary with location on the airplane. If the constant varies by a factor of 2 (from 0.003 to 0.012), however, it would result in a band of ± 6 decibels from the estimated level shown. The external microphone on the B-47A airplane was located on the relatively flat portion of the side of the fuselage, and local dynamic pressure did not vary appreciably from the free-stream dynamic pressure. As mentioned previously, theoretical and experimental studies have shown that the pressure fluctuations in the turbulent boundary layer vary as the velocity squared V^2 . These flight results vary as $V^{2.3}$. This difference may be a result of changes in angle of attack with Mach number and corresponding changes in boundary-layer thickness. The angle of attack varied from 12° at the low speeds to 0° at the high speeds.

The internal noise levels (fig. 7) show the same trend as the external noise and indicate a level about 20 decibels less than the external level. The internal level for the D-558-II airplane shows

essentially the same general trend up to a Mach number of 1.4. The level of the boundary-layer noise inside the fuselage is somewhat higher than that for the B-47A airplane; however, this increase may result from turbulence created by the wing-fuselage juncture and by the blunt base of the D-558-II airplane. The results of this investigation are limited to Mach numbers less than 1.4 and dynamic pressures less than 600 lb/sq ft. Proposed supersonic transports designed to operate at Mach numbers as high as 3.0 will probably operate within this range of dynamic pressure. Estimation of boundary-layer noise at higher Mach numbers will probably require consideration of local dynamic pressure and boundary-layer characteristics. An additional flight investigation is under way to extend these results to a Mach number of 2.0 and to dynamic pressures of about 1,300 lb/sq ft.

CONCLUDING REMARKS

From the preliminary results of an investigation of boundary-layer and engine noise, the following results were noted:

1. At Mach numbers greater than about 0.6, the boundary-layer noise was the predominant source of noise inside the fuselage of the B-47A airplane.
2. The experimental results are felt to be in good agreement with the estimated values within the limits of this investigation.
3. Engine noise at high engine rpm and high airspeeds may impose high noise levels on local areas of the aircraft in flight and should be considered in the design.

REFERENCES

1. McLeod, Norman J., and Jordan, Gareth H.: Preliminary Flight Survey of Fuselage and Boundary-Layer Sound-Pressure Levels. NACA RM H58B11, 1958.
2. Phillips, O. M.: Surface Noise From a Plane Turbulent Boundary Layer. Rep. No. 16,963, British A.R.C., Aug. 4, 1954.
3. Willmarth, William W.: Wall Pressure Fluctuations in a Turbulent Boundary Layer. NACA TN 4139, 1958.

B-47A AIRPLANE

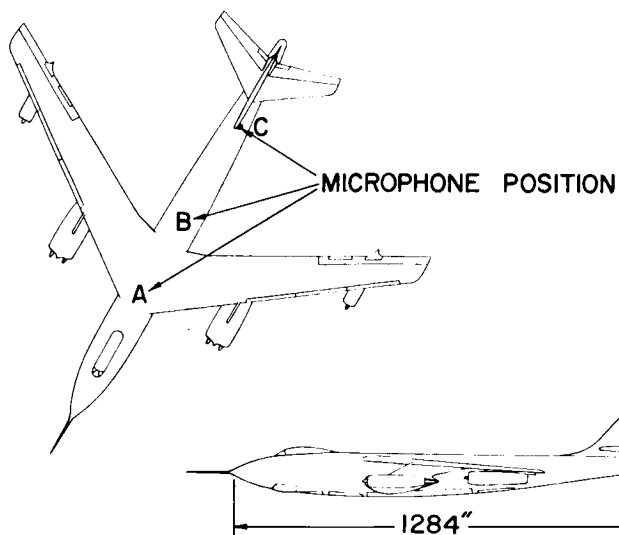


Figure 1

OVERALL NOISE LEVELS B-47A AIRPLANE
ALTITUDE = 20,000 FT

- 100% RPM
- 50% RPM

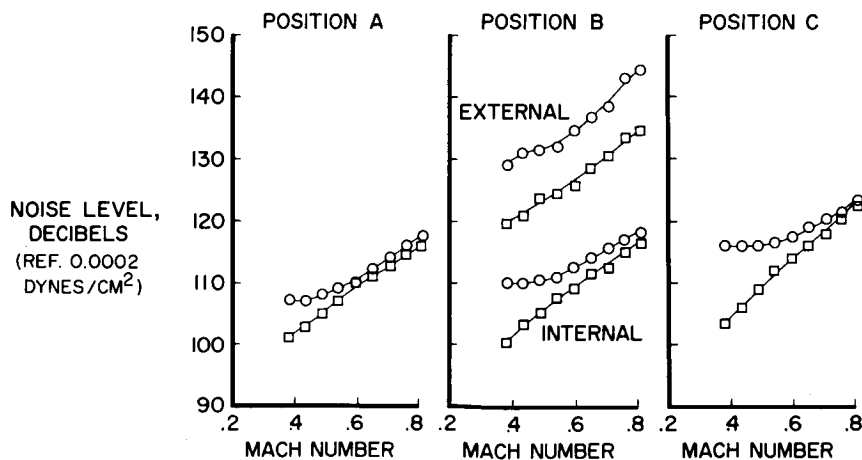


Figure 2

FREQUENCY SPECTRUM POSITION B

M ≈ 0.45 ALTITUDE = 20,000 FT

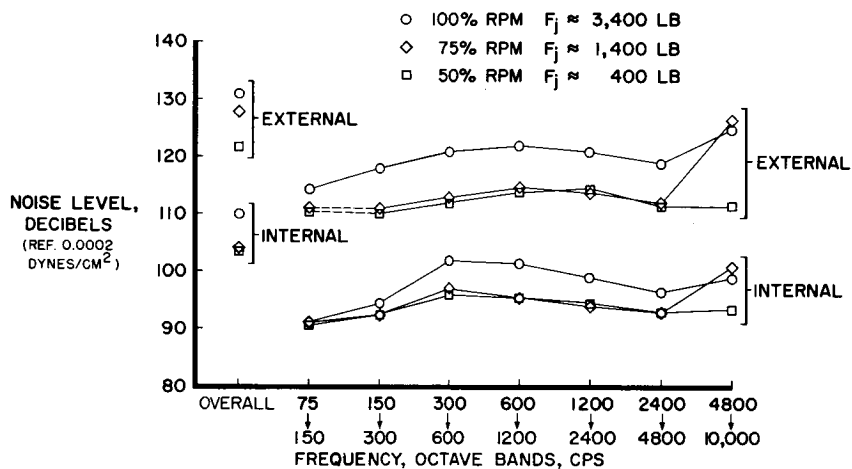


Figure 3

FREQUENCY SPECTRUM POSITION B

M ≈ 0.65 ALTITUDE = 20,000 FT

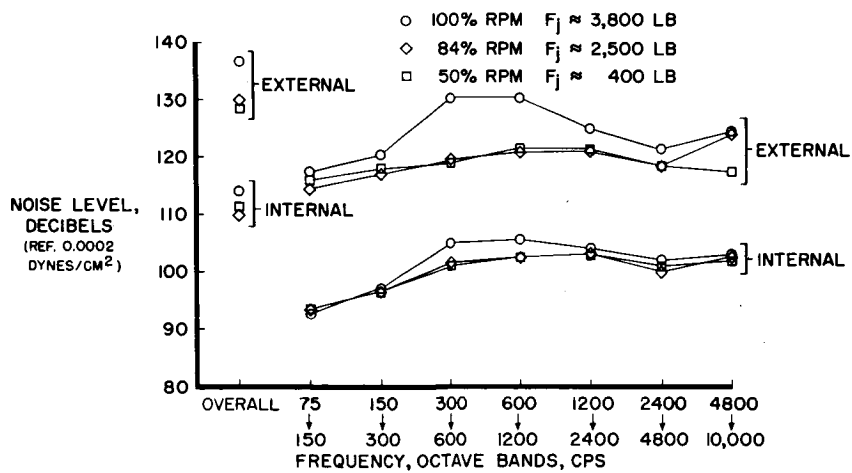


Figure 4

D-558-II RESEARCH AIRPLANE

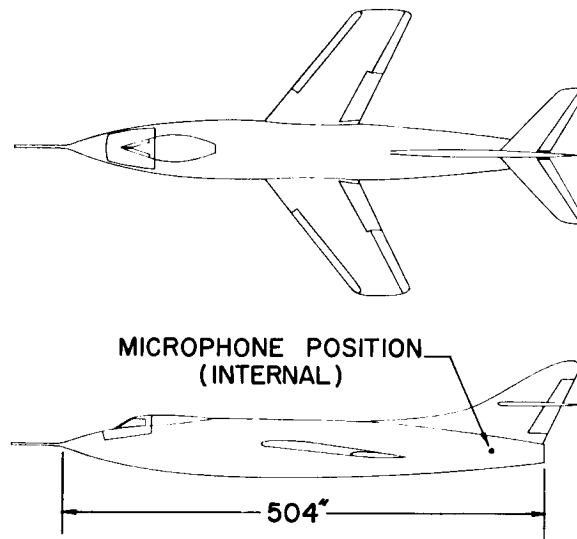


Figure 5

OVERALL NOISE LEVEL D-558-II AIRPLANE

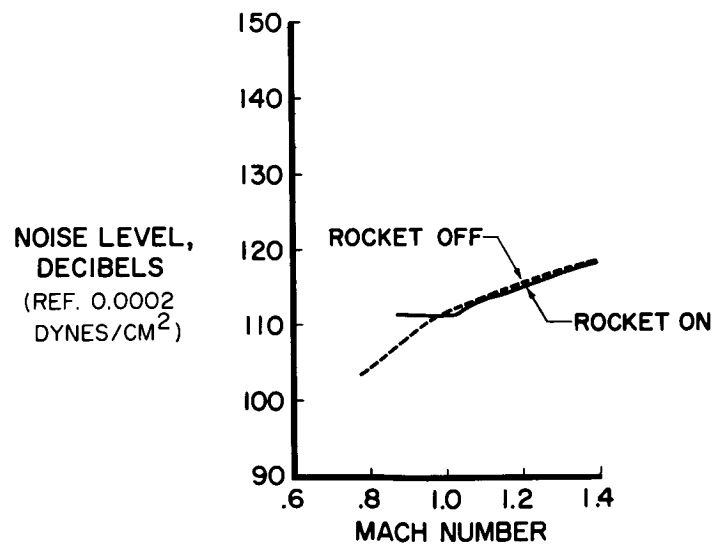


Figure 6

COMPARISON OF MEASURED AND ESTIMATED BOUNDARY-LAYER NOISE

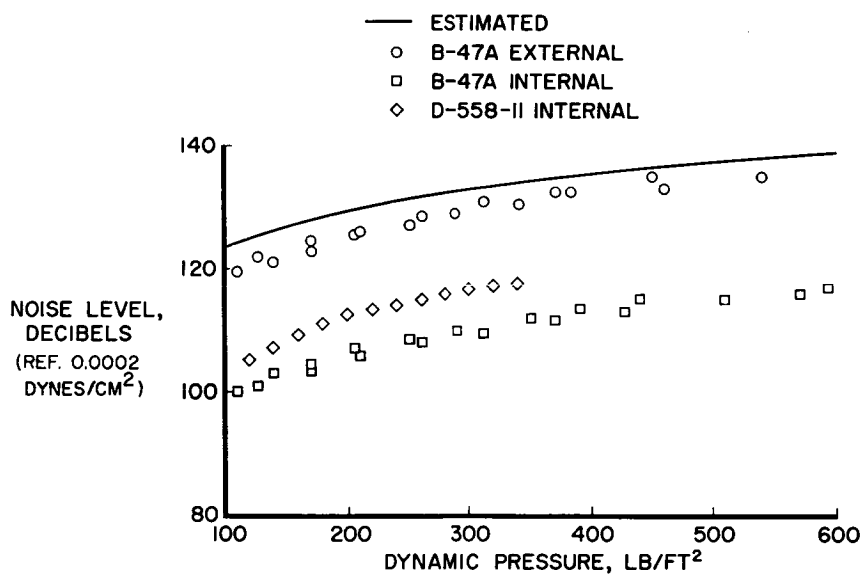


Figure 7

JET-ENGINE-NOISE REDUCTION

By Warren J. North

Lewis Research Center

SUMMARY

The acoustic and aerodynamic characteristics of several jet-noise suppressors are presented. The best sound reduction and propulsive thrust are obtained with a configuration having a corrugated nozzle and retractable ejector. Additional noise reduction under the flight path will result from modified climb techniques. Future commercial transports may be equipped with engines which are designed with lower jet velocities and, consequently, will produce lower noise levels.

INTRODUCTION

Noise problems introduced by the jet airplane will be magnified as the military makes use of higher performance engines and as the jet transports come into widespread use by the airlines. The engines currently used in jet transports are basically the same as those designed for military applications wherein high thrust and small frontal area were major considerations. Unfortunately, these design concepts are not compatible with modest noise generation.

Some measure of solution to the noise problems can be achieved by insulating passenger cabins, enclosing waiting passengers on the ground in sound-reducing enclosures, and providing ground crews with protective helmets. The airplane-noise nuisance in communities near airports, however, appears to be a much more difficult problem.

The airframe designer is also concerned with high noise levels because intense noise produces pressure fluctuations which can cause structural fatigue.

The purpose of this paper is to discuss briefly some of the jet noise parameters and then describe recent developments in noise-reduction techniques. A bibliography of related papers is presented.

SYMBOLS

P	sound power
ρ_0	density of surrounding medium
A	cross-sectional area of jet
V	efflux velocity of jet
a_0	speed of sound in surrounding medium
K	dimensionless constant
S	spacing
W	width
D_2/D_1	diameter ratio
L/D_1	length-diameter ratio
M	Mach number

DISCUSSION

The turbojet engine has several noise sources; however, the majority of the noise is caused by the high-velocity exhaust jet. The exhaust jet creates noise by three mechanisms:

- (1) The turbulent fluctuations within the jet mixing region
- (2) Oscillating shock waves within the jet
- (3) Interaction between shock waves and turbulence

During take-off and climb, jet noise is predominantly caused by turbulent fluctuations. The exhaust-nozzle pressure ratio is sufficient during high-speed flight to cause strong shock waves in the jet. However, because of the importance of reducing the noise nuisance in communities near airports and because this nuisance is caused by low-speed flight at take-off and climb, the major research effort has been directed toward reduction of noise created by turbulence in jets.

An outstanding contribution to the theory of noise created by jet turbulence was made by Lighthill in references 1 and 2. Lighthill predicted the effect of jet velocity on the sound radiated from a jet. The following equation shows the relation which was derived by Lighthill:

$$P = K \frac{\rho_0 A V^8}{a_0^5}$$

Numerous experiments have shown that this "eighth power" expression reasonably predicts the noise for the range of turbojet-exhaust velocities of interest.

Most of the jet noise is generated within 10 nozzle diameters downstream of the conventional nozzle. In order to reduce the noise, the jet velocity should be reduced as quickly as possible. One method of accomplishing this is by mixing the low-energy surrounding air into the jet stream. Figure 1 shows how the region downstream of the standard nozzle has a high-velocity core surrounded by large-scale noise-producing turbulence. In the same figure is a sketch of a multiple nozzle which is designed to produce rapid mixing of the surrounding air and jet. Low-energy air is induced into the spaces between the individual nozzles and then mixes with the high-velocity flow. In order to determine how the mixing-nozzle geometry affected noise production, tests were undertaken with rectangular mixing nozzles.

During the tests it was of interest to find the optimum ratio of the spacing S to the width W . In figure 2 the sound-power ratio is shown as a function of spacing ratio for a pressure ratio of 2.0. Current jet transports have a nozzle pressure ratio of approximately 2.0 during take-off. The sound-power ratio is the total acoustic power of the mixing nozzle divided by the acoustic power of the standard nozzle. As the spacing-width ratio increases, the sound-power ratio decreases rapidly; and for a nozzle pressure ratio of 2.0, the sound-power ratio reaches a minimum of about 0.25 for spacing-width ratios between 2 and 3. A sound-power ratio of 0.25 should greatly reduce the structural fatigue stresses. The equivalent sound reduction would be 6 decibels and represents a significant improvement to an observer. This type of nozzle was used for static tests only and was not intended for use in flight because of high base drag.

In an effort to improve the aerodynamic characteristics, the three nozzles shown in figure 3 were investigated. The first has 12 corrugations or lobes around a small circular exit and is similar to a nozzle originally suggested by Greatrex in reference 3. This configuration was designed to induce low-energy air between the lobes with minimum

external-drag penalty. The second configuration has a solid center body with larger corrugations. The third model consists of 31 individual tubes. The structural integrity of the tubular nozzle should be better than that of the corrugated nozzle since the flat surfaces of the corrugations tend to distort under pressure. A major difficulty in designing the tubular nozzle is the fairing of the internal flow passages to prevent large total-pressure losses at the entrances to the tubes.

Another possible device for noise reduction is the ejector. An ejector attached immediately downstream of an eight-lobe corrugated nozzle is shown in figure 4. The ejector is a device which is used to pump secondary air, in this case, through the corrugated nozzle and into the ejector where it mixes with the primary jet and decreases the downstream velocity. Polar plots of the sound-pressure levels from the standard nozzle and the lobe-ejector combination are shown in figure 5. The peak sound-pressure level was decreased 12 decibels. The overall sound-power level was reduced 8 decibels. An additional attenuation of about 2 decibels was obtained by lining the ejector with sound-absorbing material. Figure 6 shows the change in sound-power spectrums for the 31-tube nozzle and the two ejector configurations as compared with the spectrum of the standard nozzle. All the suppressors cause moderate sound reductions in the middle frequencies which contain the majority of the sound power; however, the tubular nozzle increases the noise above 400 cps, whereas the lined ejector causes large reductions in this region. In addition to reducing the noise, the ejector static thrust was actually greater than that for the standard nozzle. This thrust gain is expected to be quickly overshadowed by external drag as the forward speed increases.

The external drag of noise-suppressor nozzles is extremely important to cruising flight performance. Consequently, wind-tunnel tests of several nozzles were undertaken. In one of the wind-tunnel tests the drag of full-scale nozzles was investigated on a turbojet engine at Mach numbers up to 0.5. Some of the nozzles used in these tests were the lobe and tubular configurations shown previously. The engine nacelle with one of the nozzles is shown in figure 7. Generally, the increase in external drag was less than 3 percent of engine thrust at a Mach number of 0.5 for all the configurations tested.

The drag studies were extended into the transonic speed range by testing 1/5-scale nozzles in the Lewis 8- by 6-foot transonic and supersonic tunnel. Drag results are shown in figure 8 for the standard nozzle and for the lobe-ejector configuration. At a Mach number of 0.86 the lobe-ejector configuration increased the nacelle drag coefficient by a factor of 2 which is equivalent to about 5 percent of the net thrust. Figure 9 shows a propulsive thrust (thrust minus drag) and a sound-power comparison for five suppressor configurations. The lobe

nozzles and the standard nozzle with ejector caused 3- or 4-percent losses in propulsive thrust and moderate noise reductions. Large internal thrust losses were mainly responsible for the poor performance of the tubular nozzle. The lobe nozzle with ejector produced the greatest sound reduction, 8 decibels, but it also caused a $6\frac{1}{2}$ -percent loss in propulsive thrust. The propulsive-thrust loss was primarily due to drag. This drag may be reduced substantially by retracting the ejector during cruising flight.

The noise nuisance to the community can also be reduced by modifying the take-off and climb procedure. In order to realize maximum climb performance, a jet airplane should attain a climb airspeed of approximately 300 knots as soon as possible after take-off. If, however, the airplane climbs at the lowest speed compatible with directional controllability in the event of engine failure, the flight-path angle will be steeper and will provide more altitude separation which will reduce the noise levels on the ground.

Another method of decreasing jet noise is by reduction of jet velocity through engine redesign. The bypass engine or an engine designed to operate at low turbine-inlet temperature will produce lower jet velocities and, consequently, reduce noise levels.

CONCLUDING REMARKS

It appears that present-day suppressor-equipped jet transports can compromise propulsive thrust and climb performance with noise reduction in order to gain public acceptance. Future commercial transports may be equipped with engines which are designed for low-noise generation.

REFERENCES

1. Lighthill, M. J.: On Sound Generated Aerodynamically. I. General Theory. Proc. Roy. Soc. (London), ser. A, vol. 211, no. 1107, Mar. 20, 1952, pp. 564-587.
2. Lighthill, M. J.: On Sound Generated Aerodynamically. II. Turbulence as a Source of Sound. Proc. Roy. Soc. (London), ser. A., vol. 222, no. 1148, Feb. 23, 1954, pp. 1-32.
3. Greatrex, F. B.: Jet Noise. Preprint No. 559, S.M.F. Fund Preprint, Inst. Aero. Sci., Inc., June 1955.

BIBLIOGRAPHY

- North, Warren J., and Coles, Willard D.: Effect of Exhaust-Nozzle Ejectors on Turbojet Noise Generation. NACA TN 3573, 1955.
- Lassiter, L. W., and Hubbard, H. H.: Some Results of Experiments Relating to the Generation of Noise in Jets. Jour. Acous. Soc. of America, vol. 27, no. 3, May 1955, pp. 431-437.
- Laurence, James C.: Intensity, Scale, and Spectra of Turbulence in Mixing Region of Free Subsonic Jet. NACA Rep. 1292, 1956. (Supersedes NACA TN 3561 by Laurence and TN 3576 by Laurence and Stickney.)
- Coles, Willard D., and Callaghan, Edmund E.: Investigation of Far Noise Field of Jets. II - Comparison of Air Jets and Jet Engines. NACA TN 3591, 1956.
- Howes, Walton L., Callaghan, Edmund E., Coles, Willard D., and Mull, Harold R. (with Appendix B by Conger, Channing C., and Berg, Donald F.): Near Noise Field of a Jet-Engine Exhaust. NACA Rep. 1338, 1957. (Supersedes NACA TN 3763 by Howes and Mull and TN 3764 by Callaghan, Howes, and Coles.)
- Coles, Willard D., and Callaghan, Edmund E.: Full-Scale Investigation of Several Jet-Engine Noise-Reduction Nozzles. NACA TN 3974, 1957.
- Ciepluch, Carl C., North, Warren J., Coles, Willard D., and Antl, Robert J.: Acoustic, Thrust, and Drag Characteristics of Several Full-Scale Noise Suppressors for Turbojet Engines. NACA TN 4261, 1958.
- Coles, Willard D., Mihalow, John A., and Callaghan, Edmund E.: Turbojet Engine Noise Reduction With Mixing Nozzle-Ejector Combinations. NACA TN 4317, 1958.
- North, Warren J.: Transonic Drag of Several Jet-Noise Suppressors. NACA TN 4269, 1958.
- Rollin, Vern G.: Effect of Jet Temperature on Jet-Noise Generation. NACA TN 4217, 1958.

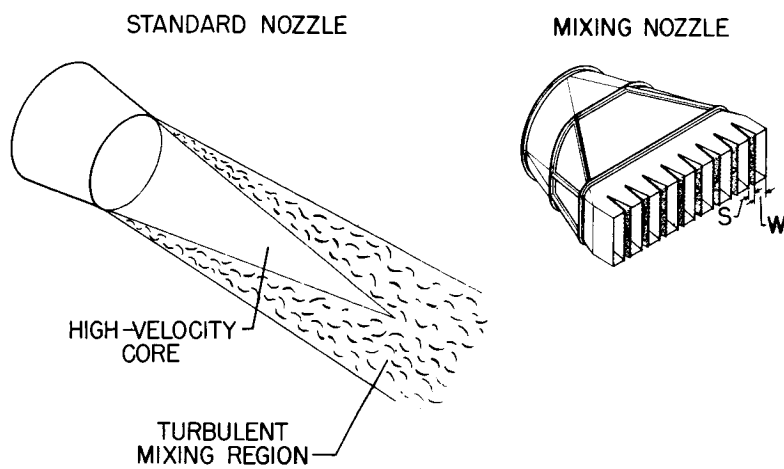


Figure 1

POWER RATIO AS A FUNCTION OF
SPACING RATIO FOR FOUR-
SLOT NOZZLE

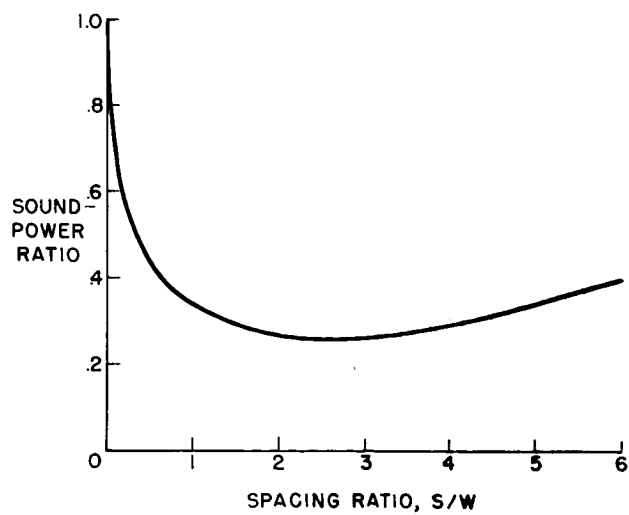
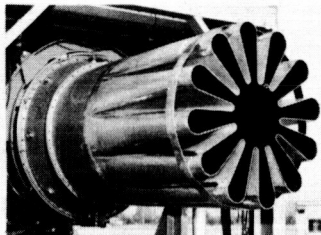
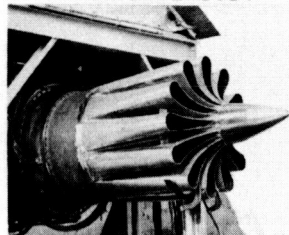


Figure 2

NOISE-SUPPRESSION NOZZLES

CORRUGATED NOZZLE

CORRUGATED NOZZLE
WITH CENTERBODY

31-TUBE NOZZLE

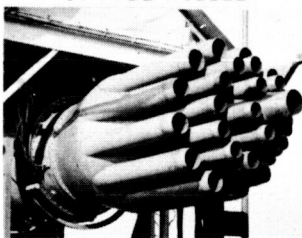


Figure 3

8-LOBE NOZZLE AND EJECTOR

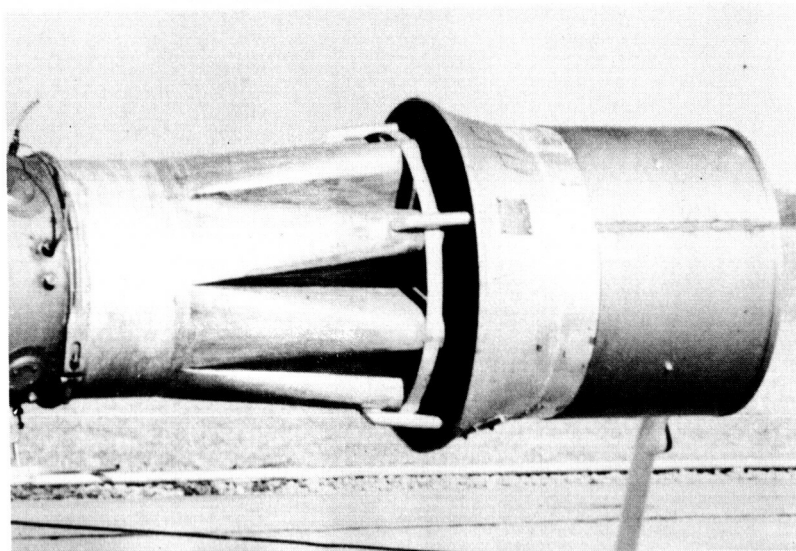


Figure 4

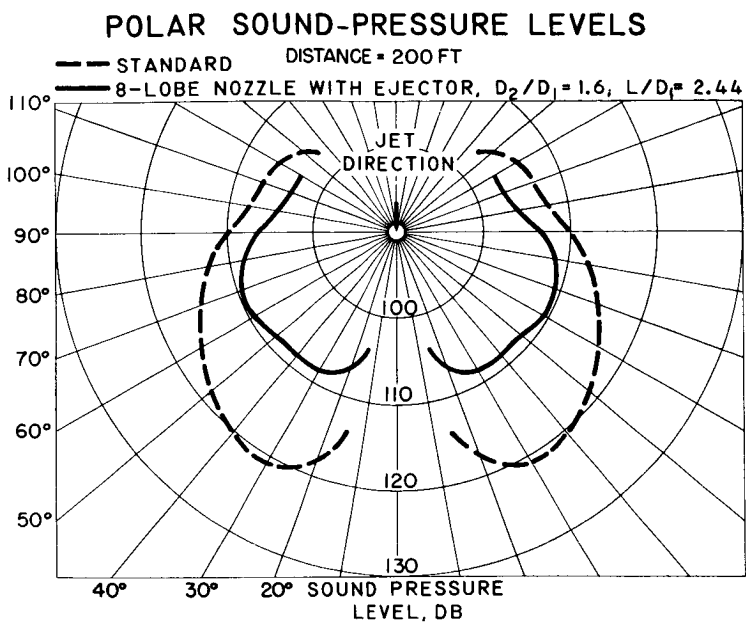


Figure 5

**CHANGE IN SOUND POWER
AS A FUNCTION OF FREQUENCY**

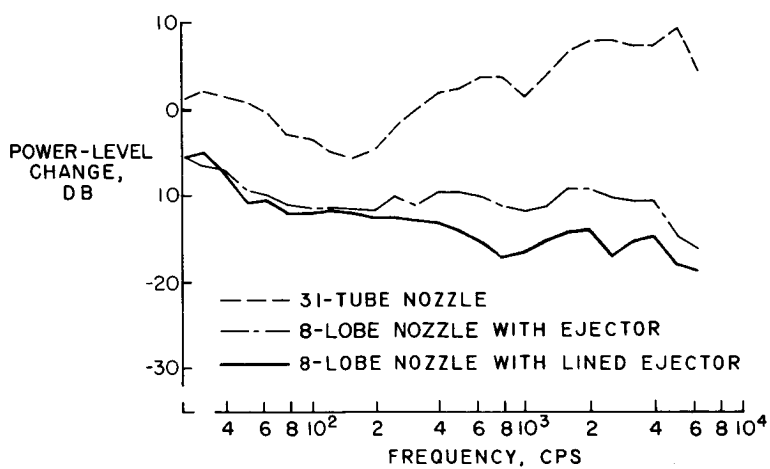


Figure 6

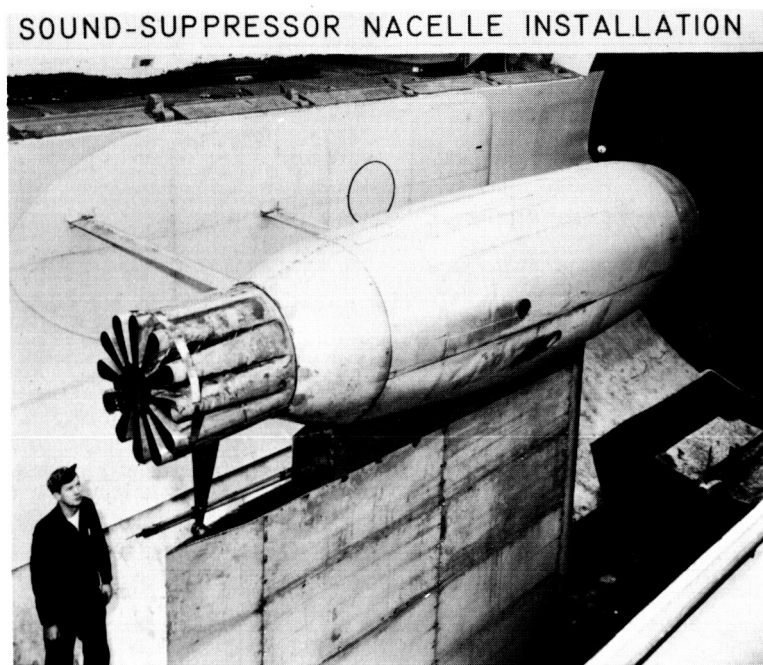


Figure 7

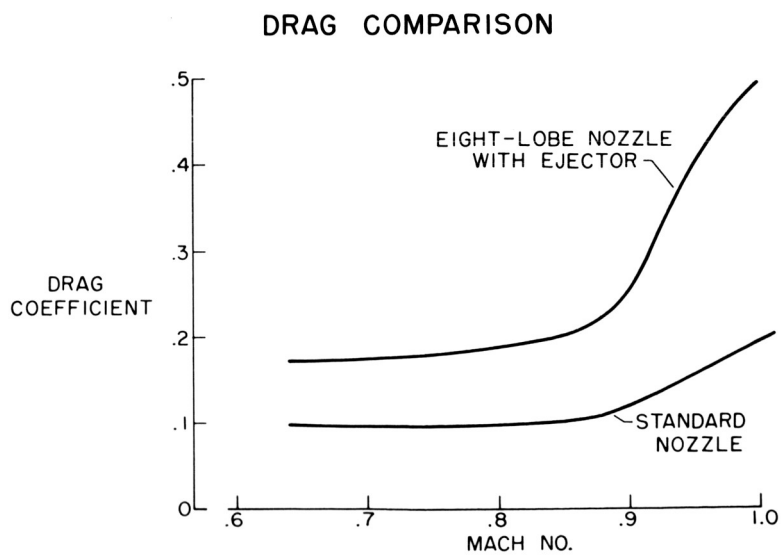


Figure 8

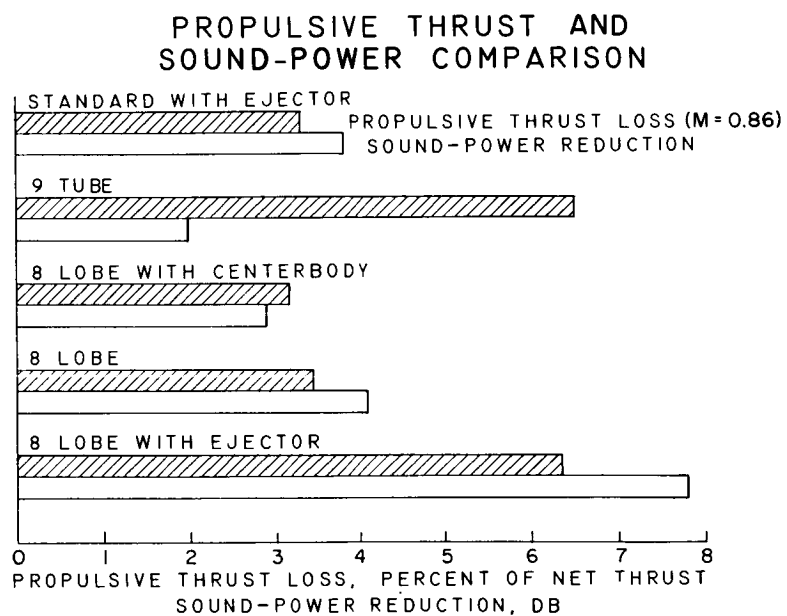


Figure 9

NOISE PROBLEMS ASSOCIATED WITH GROUND OPERATIONS OF JET AIRCRAFT

By Harvey H. Hubbard

Langley Research Center

INTRODUCTION

The noise generated by the engines of jet aircraft during ground runup operation will lead to serious problems, particularly with regard to the ground-crew personnel, the structure of the aircraft, and, to a lesser extent, the surrounding community. The purpose of this paper is to review the nature of these problems and to focus attention on some of the more critical aspects. Brief mention is also made of various devices useful for noise reduction during ground operations. There will be only general discussion of some types of these devices and no attempt is made to include all the very large number currently available for use. (For further information see the bibliography.)

ALLOWABLE NOISE EXPOSURE

Some insight into the noise-exposure problem for humans is given by figure 1. These data were obtained from reference 1 and are based largely on Air Force experience in operating jet aircraft. Noise exposure has two ingredients: the level of the noise and the time of exposure to that noise. It can be seen in the figure that the allowable exposure time is plotted as a function of the overall noise level in decibels. Three general regions are noted: (a) a region where no protection is needed, (b) a region where ordinary personal equipment such as ear plugs, helmets, or muffs would be adequate, and (c) a region to be avoided unless special equipment is provided. This special equipment could be custom-fitted ear-protection devices or devices for protecting the whole body. It was also noted from reference 1 that ear protection alone is not adequate for exposure to noise levels higher than 150 decibels even for a short time. Where no protection is required, it is noted that the average man can be exposed to 100 decibels of random noise for an 8-hour workday without adverse effects. As the noise level increases the allowable exposure time decreases until at a level of 135 decibels an exposure time of only a few seconds is permissible. It should be noted that the data of figure 1 apply directly for random noise and the allowable levels are about 10 decibels higher than they would be for discrete noise under otherwise comparable conditions.

The significance of these levels with regard to an actual engine running up on the ground is illustrated with the aid of figure 2. Shown in the figure are several contour lines of equal overall noise level for an engine with a flight-type muffler attached operating at 10,000 pounds of thrust (ref. 2). Also indicated in the figure are distances radially outward and forward and rearward of the nozzle-exit plane. It can be seen that in a large area where maintenance men might be required during engine runup, the levels range from 110 to about 150 decibels. As indicated in figure 1, it would be permissible to enter any part of the region ahead of the 130-decibel contour line without protection, provided the exposure time did not exceed 1 minute. For the region within the 130-decibel contour line some type of personal-protection device would be required even for short-term exposures.

NATURE OF THE AIRCRAFT-DAMAGE PROBLEM

Because of the very high noise levels in the region behind the engine near the exhaust, there is also a possibility of doing structural damage to the aircraft for long-term exposures. The damage areas on the airplane will occur generally rearward of the engine-exhaust exits (ref. 3). Shown schematically in figure 3 is a bottom view of a multi-engine jet airplane with pod-mounted engines. The shaded areas are those susceptible to damage by engine noise and are noted to be along the wing trailing edges and the rearward part of the fuselage.

Areas of the airplane located close to a given engine will be primarily affected by that particular engine and not significantly affected by the others. There are some areas of the airplane, however, in which excitation from more than one source is significant, as, for example, the rearward part of the fuselage. The damage referred to results from fatigue failures of the skin and other secondary structural members due to the fluctuating noise-pressure loads. These failures are generally not catastrophic in nature but may be costly to repair.

Other experience (refs. 4 and 5) has indicated that the severity of the damage due to noise is very much a function of the noise level of exposure. Of course, ground operation involves a variety of engine conditions with an associated range of noise levels. Some of these are illustrated in figure 4 (from ref. 6) for the take-off, cruise, taxi, and idle conditions of the engines of a four-engine jet airplane with flight-type mufflers. The data are shown in the form of overall noise levels, measured at 200 feet, plotted as a function of azimuth angle measured from the front of the airplane. Unfortunately, near-field data of the type shown previously are not available for engine conditions other than the 100-percent-rpm condition shown in figure 2. It

is believed, however, that the near-field data for these power conditions would be in the same order of rank and have about the same differences as those shown in figure 4. Of particular interest are the data at azimuth angles toward the rear where the noise levels are the highest. In this orientation it can be seen that the noise levels associated with take-off power are higher than those for any of the other engine conditions.

The significance of these data with reference to the damage problem is illustrated schematically with the aid of figure 5. Hours of structural life are shown as a function of noise level in decibels. The resulting curve is similar to a conventional S-N diagram. Its shape will thus depend on the stress level in the structure and the type of construction used. If it is assumed that a certain part of the airplane is designed for a satisfactory life of 100 hours of take-off time, then the usable life in the cruise condition might be of the order of 1,000 times that long because of the lower noise levels. The take-off condition is thus very important with regard to structural life and, for many parts of the aircraft, is a controlling factor in design. The noise levels associated with the taxi and idle conditions would, of course, be below the cruise noise level and would have essentially no effect on the life of the airplane. On the other hand, if a ground operator became careless and unknowingly operated the engines in such a way that the noise levels were higher than those at the take-off condition, the usable life of the airplane would then be greatly reduced. One point that can be made in connection with figure 5 is that operation at take-off power on the ground will directly affect the life of some parts of the airplane. With regard to those parts of the structure which receive excitation from more than one engine, it would be helpful if only one engine at a time were operated for the routine operational and maintenance checks that are performed, since that would tend to fix the operations on the lower segment of the curve.

NOISE-REDUCTION DEVICES

Of course, another method of operating on the lower segment of the curve (fig. 5) is to use some noise-reduction devices in addition to those installed on the airplane. Schematic illustrations of some of these, along with an indication of the main principle of operation, are shown in figure 6.

The top diagram shows a nozzle shroud which is fitted to the flight-type suppression nozzle and extends behind it. Additional air is entrained by this method which results in more rapid mixing and additional noise reduction of about 5 decibels (ref. 7). A longer shroud

than shown here would give larger noise reduction (ref. 8) and would thus be more effective in shielding the rearward part of the airplane.

Another possibility is to cause the exhaust gases to enter a perforated sleeve from which they would exit in a radial direction from many small jets (ref. 9). The total jet kinetic energy would be reduced and a reduction of 10 to 20 decibels might be obtained. It should be noted that skirt-type deflectors are provided to turn the exhaust flow away from the structure and also from the direction of the engine inlet.

The bottom sketch in figure 6 shows an enclosure containing absorbing materials arranged in such a manner as to absorb a large part of the noise energy before the exhaust reaches the free air. Many such devices are now commercially available for noise reductions of 20 decibels or more (ref. 10). Some proposed inlet silencers also operate on the principle of absorbing the noise energy, which in the case of the compressor is in a frequency range where many acoustic absorbing materials are very effective.

No attempt is made here to include discussions of all available or proposed noise-reduction devices; however, a bibliography is provided for those interested in the technical details. Some of the above studies indicate that the most practical ground-noise-reduction devices may very well incorporate more than one of several basic principles of operation.

Devices of the types illustrated in figure 6 would be suitable for both ground-crew personnel and structural problems and even for protection of the community. In some cases where protection is desired mainly for the community it may be possible to take advantage of the existing terrain features to reduce the noise at a distance as indicated in figure 7. As an illustration, if 1 mile separated the runup area and the community to be protected, noise reductions due to intervening terrain might vary from about 8 to 32 decibels in addition to normal spreading, depending on the type of terrain, foliage, and so forth (ref. 11). For a practical solution, a noise reduction of about 20 to 30 decibels due to terrain would be needed. Reductions comparable to these could be obtained by the use of a shielding wall about 40 feet high and comparable to the wing span in length (ref. 12). To be most effective, the aircraft during runup would have to be located close to the wall. This would cause reflections back onto the aircraft and would result in higher noise levels at some locations than would ordinarily exist in an area free of reflections. Thus, care should be used in the case of ground running of engines close to shielding walls or buildings. As a word of caution, it is particularly undesirable to run up engines while the airplane is located between buildings or walls in such a manner that parts of the airplane are in a reverberant space.

CONCLUDING REMARKS

In conclusion, it has been pointed out that the ground runup operation of jet engines at full power with flight-type mufflers can present a hazard to the ground-crew personnel and can be detrimental to the airplane by reducing its usable fatigue life. Care should be taken to keep to a minimum all full-power engine operation for which additional noise reduction is not provided. Additional muffling can be obtained by conventional methods, and, if these are used properly, protection may be obtained for both the personnel and the structure of the airplane.

REFERENCES

1. Parrack, Horace O.: Effects of Noise on Ground Personnel Who Support Air Operations. Presented at Flight Safety Foundation Industry Advisory Committee Meeting, June 5, 1958.
2. Greatrex, F. B.: Jet Noise. Preprint No. 559, S.M.F. Pub. Fund Preprint, Inst. Aero. Sci., Inc., June 1955.
3. Regier, Arthur A., and Hubbard, Harvey H.: Response of Structures to High Intensity Noise. National Advisory Committee for Aeronautics. (Presented at 55th Meeting of Acous. Soc. of America, Washington, D. C., May 7-10, 1958.)
4. Edson, John R.: Review of Testing and Information on Sonic Fatigue. Structural Dev. Note No. 38 (Doc. No. D-17130), Boeing Airplane Co., Mar. 7, 1957.
5. Belcher, Peter M.: The High Intensity Siren as an Instrument for Fatigue Testing of Aircraft Structure. Douglas Aircraft Co., Inc. (Presented at Specialists' Meeting of Inst. Aero. Sci., Los Angeles, Feb. 26, 1957.)
6. Miller, Laymon N., and Hoover, Robert M.: The Noise Characteristics of Some Commercial Jet Aircraft During Ground Operations. Bolt Beranek and Newman, Inc., Cambridge, Mass. (Presented at 55th Meeting of Acous. Soc. of America, Washington, D. C., May 7-10, 1958.)
7. Coles, Willard D., Mihalow, John A., and Callaghan, Edmund E.: Turbojet Engine Noise Reduction With Mixing Nozzle - Ejector Combinations. NACA TN 4317, 1958.
8. Burton, J. T., Oddo, E. T., and Smith, P. H.: Jet Noise Suppressors - Ejectors. Rep. No. SM-19694, Douglas Aircraft Co., Inc., May 2, 1956.
9. Tyler, John, and Towle, George: A Jet Exhaust Silencer. Noise Control, vol. 1, no. 4, July 1955, pp. 37-41, 54.
10. Tully, Barry: Airlines Shop for Portable Jet Silencers. Aviation Week, vol. 69, no. 17, Oct. 27, 1958, pp. 119-123.
11. Hubbard, Harvey H., and Maglieri, Domenic J.: An Investigation of Some Phenomena Relating to Aural Detection of Airplanes. NACA TN 4337, 1958.

12. Hayhurst, J. D.: An Investigation Into the Acoustic Screening of Aircraft on the Ground. Aircraft Branch Tech. Note 10, Ministry of Civil Aviation, Mar. 1952.

BIBLIOGRAPHY ON JET MUFFLING DEVICES

- De Rosen, A.: The Silencing of Test Houses for Turbo-Jet Engines. Reprinted From Aircraft Engineering, Aug. 1949.
- Young, C. J. T., and Snow, W. B.: Acoustical Redesign of the Forest Grove Burner Laboratory. Bumblebee Ser., Rep. No. 105, Contract NOrd 7386, Bur. Ord., U. S. Navy and Appl. Phys. Lab., The Johns Hopkins Univ., Nov. 1949.
- Bolt, R. H., Lukasik, S. J., Nolle, A. W., and Frost, A. D., eds.: Handbook of Acoustic Noise Control - Volume I: Physical Acoustics. WADC Tech. Rep. 52-204 (Contract No. AF 33(038)-20572), U. S. Air Force, Dec. 1952, p. 285.
- Hardy, Howard C.: Design Characteristics for Noise Control of Jet Engine Test Cells. Jour. Acous. Soc. of America, vol. 24, no. 2, Mar. 1952, pp. 185-190.
- Westley, R., and Lilley, G. M.: An Investigation of the Noise Field From a Small Jet and Methods for Its Reduction. Rep. No. 53, College of Aero., Cranfield (British), Jan. 1952.
- Hayhurst, J. D.: An Investigation Into the Acoustic Screening of Aircraft on the Ground. Aircraft Branch Tech. Note 10, Ministry of Civil Aviation, Mar. 1952.
- Callaway, D. B., and Lemmerman, R. D.: A Comparison Between Model Study Tests and Field Measurements on an Aircraft Test-Cell Silencer. Jour. Acous. Soc. of America, vol. 25, no. 3, May 1953, pp. 429-432.
- Lemmerman, Richard D.: Materials and Structures Problems in Aircraft Noise Control. Jour. Acous. Soc. of America, vol. 25, no. 3, May 1953, pp. 438-441.
- Veneklasen, Paul S.: Noise Control for Ground Operation of the F-89 Airplane. Jour. Acous. Soc. of America, vol. 25, no. 3, May 1953, pp. 417-422.
- Hardy, Howard C.: Noise Control Measures for Jet Engine Test Installations. Jour. Acous. Soc. of America, vol. 25, no. 3, May 1953, pp. 423-428.
- Callaghan, Edmund E., Howes, Walton, and North, Warren: Tooth-Type Noise-Suppression Devices on a Full-Scale Axial-Flow Turbojet Engine. NACA RM E54B01, 1954.

- Fogle, Robert E. L., and Withington, Holden W.: An Airplane Manufacturer's Progress With Noise Suppression Devices. SAE Trans., vol. 63, 1955, pp. 303-307.
- Beranek, Leo L., Labate, Samuel, and Ingard, Uno: Acoustical Treatment for the NACA 8- by 6-Foot Supersonic Propulsion Wind Tunnel. NACA TN 3378, 1955.
- Callaghan, Edmund E., and Coles, Willard D.: Investigation of Jet-Engine Noise Reduction by Screens Located Transversely Across the Jet. NACA TN 3452, 1955.
- North, Warren J., and Coles, Willard D.: Effect of Exhaust-Nozzle Ejectors on Turbojet Noise Generation. NACA TN 3573, 1955.
- Stubbs, S. B.: Preliminary Noise Tests on Cullum Muffler Type H/B. Exp. Dept. Rep., Rolls-Royce, Ltd., Oct. 28, 1955.
- Greatex, F. B.: Jet Noise. Preprint No. 559, S.M.F. Pub. Fund Preprint, Inst. Aero. Sci., Inc., June 1955.
- Ward, J. K.: Acoustic Evaluation of Corrugated Nozzle Noise Suppressor No. 1. Boeing Airplane Co.
- Callaghan, Edmund E., Sanders, Newell D., and North, Warren J.: Recent NACA Investigations of Noise Reduction Devices for Full-Scale Engines. Preprint No. 515, S.M.F. Pub. Fund Preprint, Inst. Aero. Sci., Inc., Jan. 1955.
- North, Warren J.: Summary Evaluation of Toothed-Nozzle Attachments as a Jet-Noise-Suppression Device. NACA TN 3516, 1955.
- Tyler, John, and Towle, George: A Jet Exhaust Silencer. Noise Control, vol. 1, no. 4, July 1955, pp. 37-41, 54.
- Withington, Holden W.: Silencing the Jet Aircraft. Aero. Eng. Rev., vol. 15, no. 4, Apr. 1956, pp. 56-63, 84.
- Burton, J. T., Oddo, E. T., and Smith, P. H.: Jet Noise Suppressors - Ejectors. Rep. No. SM-19694, Douglas Aircraft Co., Inc., May 2, 1956.
- Lassiter, Leslie W., and Hubbard, Harvey H.: The Near Noise Field of Static Jets and Some Model Studies of Devices for Noise Reduction. NACA Rep. 1261, 1956. (Supersedes NACA TN 3187.)

- Lemmerman, Richard D., and Calloway, Daniel B.: Aircraft Run-Up Silencing Design. Noise Control, vol. 2, no. 1, Jan. 1956, pp. 10-14, 65.
- Anon.: The Development of Silencing Equipment for Ground Running of Jet Aircraft. ME/A2/1041/DJD, Ministry of Supply, Aircraft Noise Suppression Comm.
- Christian, George L.: Scientists Tackle Jet Noise Problem. Aviation Week, vol. 65, no. 10, Sept. 3, 1956, pp. 50-56.
- Miller, M. M.: Sound and Furor - The Jet Noise Suppression Age. SAE Trans., vol. 65, 1957, pp. 595-607.
- Doelling, N., and Staff of Bolt Beranek and Newman Inc.: An Acoustical Evaluation of Two Durastack Ground Run-Up Muffler Systems. WADC Tech. Note 57-392, Dec. 1957.
- Von Gierke, Henning E.: Aircraft Noise Control. Handbook of Noise Control, ch. 34, Cyril M. Harris, ed., McGraw-Hill Book Co., Inc., 1957.
- Coles, Willard D., and North, Warren J.: Screen-Type Noise Reduction Devices for Ground Running of Turbojet Engines. NACA TN 4033, 1957.
- North, Warren J.: Transonic Drag of Several Jet-Noise Suppressors. NACA TN 4269, 1958.
- Ciepluch, Carl C., North, Warren J., Coles, Willard D., and Antl, Robert J.: Acoustic, Thrust, and Drag Characteristics of Several Full-Scale Noise Suppressors for Turbojet Engines. NACA TN 4261, 1958.
- Dyer, Ira, Franken, Peter A., and Westervelt, Peter J.: Jet Noise Reduction by Induced Flow. Jour. Acous. Soc. of America, vol. 30, no. 8, Aug. 1958, pp. 761-764.
- Hoover, Robert M., and Staff of Bolt Beranek and Newman Inc.: Acoustical Evaluation of General Sound Control Model N-400 Jet Aircraft Noise Suppressor. WADC Tech. Note 57-391, ASTIA Doc. No. AD 142162, U. S. Air Force, Apr. 1958.
- Coles, Willard D., Mihalow, John A., and Callaghan, Edmund E.: Turbojet Engine Noise Reduction With Mixing Nozzle-Ejector Combinations. NACA TN 4317, 1958.

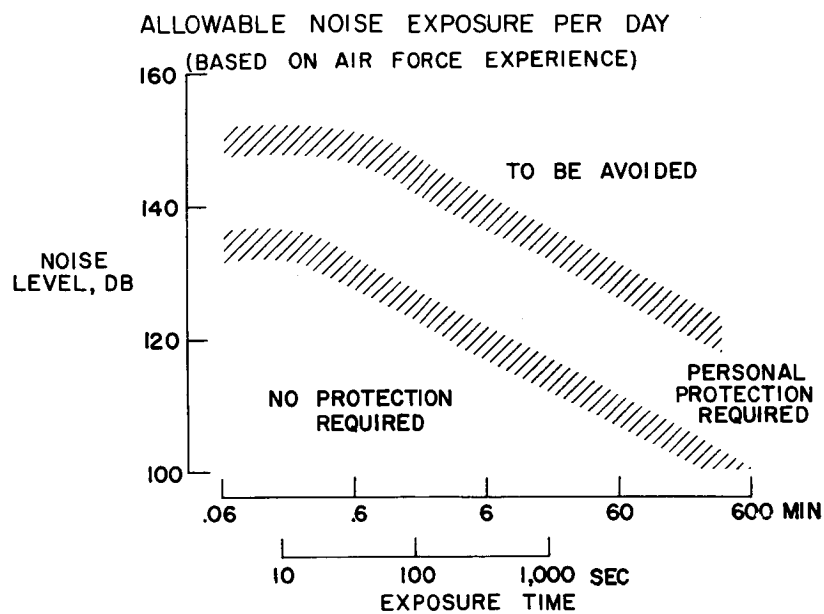


Figure 1

NEAR-FIELD ENGINE-NOISE CONTOURS
THRUST, 10,000 LB

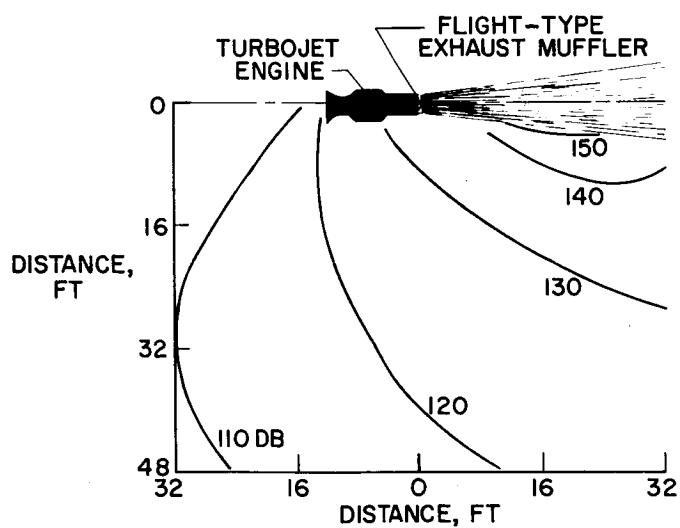
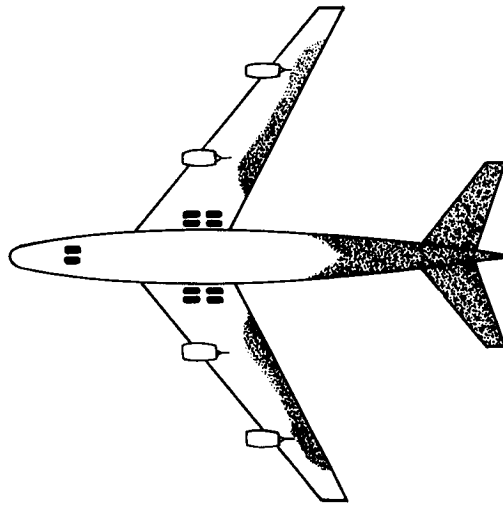


Figure 2

AREAS OF POSSIBLE DAMAGE



BOTTOM VIEW

Figure 3

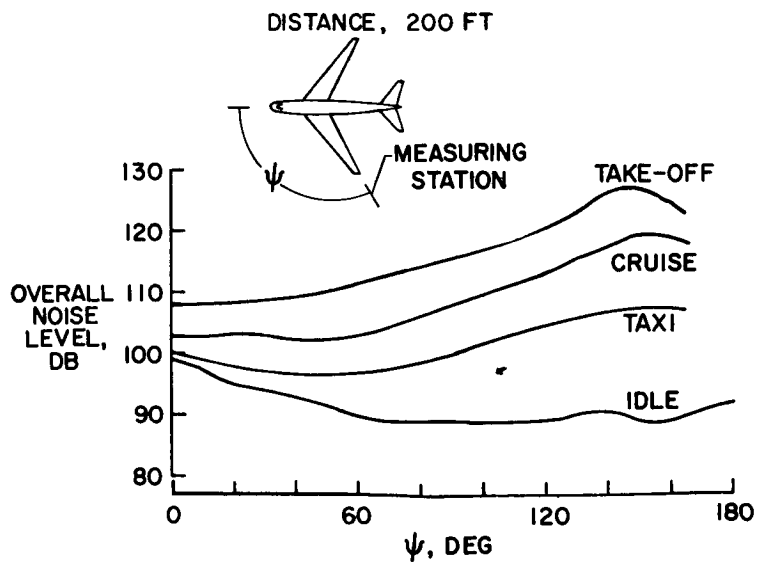
OVERALL NOISE LEVELS FOR JET AIRPLANE WITH
FLIGHT-TYPE MUFFLERS

Figure 4

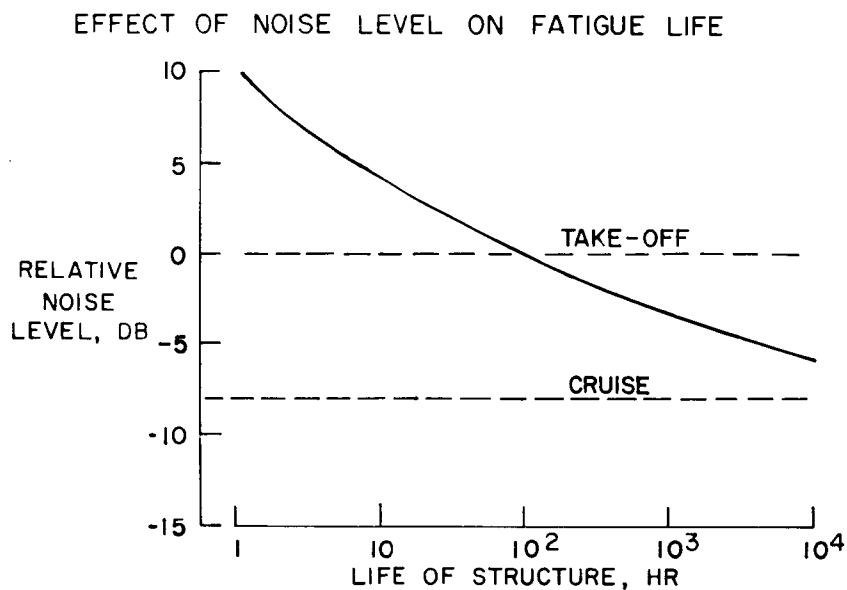


Figure 5

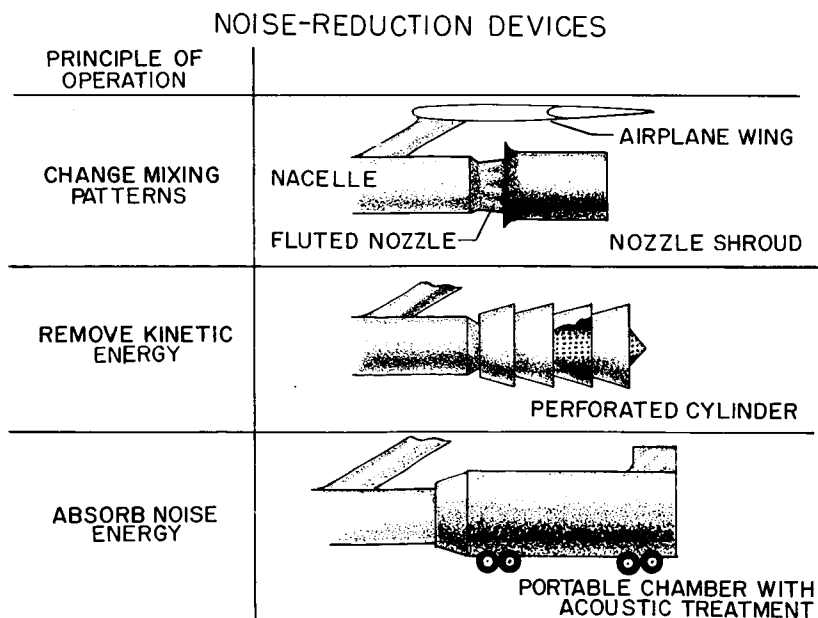


Figure 6

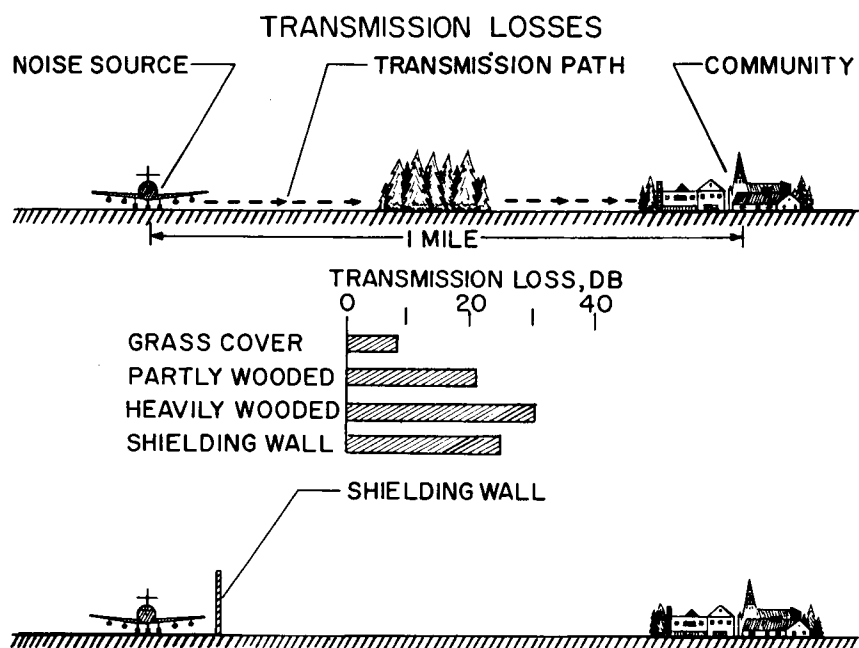


Figure 7

THE SHOCK-WAVE NOISE PROBLEM OF SUPERSONIC

AIRCRAFT IN STEADY FLIGHT

By Domenic J. Maglieri and Harry W. Carlson

Langley Research Center

SUMMARY

Data are presented which provide an insight into the nature of the shock-wave noise problem, the significant variables involved, and the manner in which airplane operation may be affected. Flight-test data are also given, and a comparison with the available theory is made. An attempt is also made to correlate the subjective reactions of observers and some physical damage associated with the pressure amplitudes during full-scale flight.

It is indicated that for the proposed supersonic transport airplanes of the near future, booms on the ground will most probably be experienced during the major portion of the flight plan. The boom pressures will be most severe during the climb and descent phases of the flight plan. During the cruise phase of the flight, the boom pressures are of much lesser intensity but are spread laterally for many miles. It is indicated by wind-tunnel studies made thus far that only small changes in the boom pressures will result from changes of the aerodynamics of the airplane; however, the manner in which the airplane is operated does appear to be significant. For example, the boom pressures during the climb, cruise, and descent phases can be minimized by operating the airplane at its maximum altitude consistent with its performance capabilities.

INTRODUCTION

In order to operate supersonic aircraft, it will be necessary for the commercial operator to recognize not only the noise problems associated with power plants and the aerodynamic boundary layer, but also the problem of the so-called sonic boom. Accordingly, data are presented which provide some insight into the nature of this shock-wave noise problem, the significant variables involved, and the manner in which airplane operation may be affected. An attempt is also made to correlate the subjective reactions of observers and some physical damage associated with the pressure amplitudes during full-scale flight.

SYMBOLS

K_1	ground-reflection constant
K_2	body-shape constant
l	body length
l/d	body fineness ratio
M	airplane Mach number
p_a	ambient pressure at altitude
p_0	ambient pressure at ground level
Δp	pressure rise across shock wave
x	distance to maximum thickness along body length
y	distance normal to flight path
Subscript:	
MAX	maximum

NATURE OF THE PROBLEM

As an aid in understanding the nature of the problem, a schlieren photograph of a small airplane model is shown in figure 1. This is a profile view taken at a Mach number of 2.0 during wind-tunnel tests. The figure shows that there are strong shock waves attached to the bow and tail of the body, with additional shock waves emitting from other airplane components such as the wing. As these shock waves extend outward, they coalesce into the bow and tail waves which are gradually spreading apart or diverging. This divergence results from the difference in propagation velocities of the bow and tail waves which are, respectively, higher and lower than ordinary sonic velocity. The main reason for these differential velocities of propagation is, as indicated by reference 1, due to the longitudinal particle velocity or streaming velocity of the air which is always associated with shock waves. This same general shock-wave pattern is observed, whether lift is present or not, for bodies of various sizes and shapes and for full-scale airplanes.

In figure 2 is shown a schematic diagram for the test condition of figure 1. A slice through the wave pattern, as indicated by the horizontal line, would yield the pressure distribution shown by the heavy line. At the bow wave a compression occurs in which the local pressure rises to a value Δp above atmospheric pressure. Then a slow expansion occurs until some value below atmospheric pressure is reached, and then there is a sudden recompression at the tail wave. Again it is seen that the bow and tail waves are diverging, and, if the airplane were at an altitude of 40,000 feet, the time between these peaks would be about 0.2 second, which corresponds to a distance of the order of two to three times the length of the airplane.

If these waves were sweeping past an observer on the ground, the ear would respond as shown schematically in the sketch at the bottom of the figure. Since the ear is sensitive only to sudden changes in pressure, it would respond to the steep part of the wave and not to the portion which is changing slowly. If the time interval between these two rapid compressions is small, as for a bullet, the ear would not be able to discriminate between them and they would seem as one explosive sound. If the time interval were on the order of 0.10 second or greater, as in the case of the airplane, the ear would probably detect two booms.

SIGNIFICANT VARIABLES

There are many significant variables involved in the problem of the boom. These variables include those associated with the shock-wave generation in addition to those associated with the wave propagation through the atmosphere. Some of these variables are involved in the following equation, taken from references 1 to 3, which is used to predict the intensity of the boom:

$$\Delta p = K_1 K_2 \left(\frac{\sqrt{p_a p_0}}{y^{3/4}} \right) (M^2 - 1)^{1/8} \left(\frac{1}{l/d} \right) l^{3/4} \quad (1)$$

A discussion of the relative significance of the terms in the equation follows, but before the discussion, it is necessary to consider the equivalent-body concept. The pressure field at large distances from an airplane can be approximated as that from a body of revolution having the same length and maximum cross-sectional area. As in the "transonic area rule," this area includes not only sections from the fuselage but also from the wing, nacelles, and so forth. In equation (1) the constant K_1 , which is a reflectivity factor varying between 1.0 and 2.0,

depends upon the ground surface, and for the particular tests considered herein it averaged between 1.7 and 1.9. The constant K_2 depends upon the equivalent body shape, and a theoretical variation of the constant is shown in figure 3.

The data of figure 3 are for three bodies of revolution having their maximum areas occurring at about 0.3 and 0.5 body length and at the tail of the body. It can be seen that for this extreme variation in the location of the maximum thickness, the constant K_2 varies from about 0.55 to about 0.80. In addition, wind-tunnel tests have indicated that bodies having the same longitudinal area development but widely different shapes give about the same value of Δp at large distances from the body or in the far field. These tests also indicate that changes of the aerodynamics of the airplane result in only small changes in the boom pressures in the far field.

Figure 4 shows the theoretical variation of Δp with the remaining variables in the equation: altitude, Mach number, fineness ratio, and body length. Initial conditions indicated by the arrows are $l/d = 14.0$, $l = 190$, $M = 2.0$, and an altitude of 40,000 feet.

It should be noted that altitude has a twofold effect; namely, that of distance and of ambient pressure. It is obvious from figure 4 that the pressure decreases very rapidly with altitude. The pressure increases as Mach number increases but at a very slow rate above $M = 1.1$. Increasing body fineness ratio is beneficial in that the pressure varies inversely with the fineness ratio. Increasing the body length while maintaining the same fineness ratio is detrimental.

Equation (1) has been successfully used by many investigators to predict the pressures in the near field, as for the case of close passes of airplanes, where the distances involved are relatively small. (See refs. 4 and 5.) In this case the variables accounted for by the equation appear to be of primary importance. Equation (1) accounts for thickness only and does not include any effects of lift. The effects of lift in the downward direction are believed to be in phase with, and should add to, the effects of thickness and result in increased shock strength. The contribution of the lift is believed to be small at moderate altitudes but may become of greater importance for high-altitude operations. (See ref. 6.) In the present discussion an attempt is made to extend the use of this equation to the case of the observer on the ground, or in the far field, wherein the distances involved are relatively large. For this case, variables such as wind direction, wind velocity and temperature gradients, airplane flight path, and atmospheric losses may be of importance.

As an introduction to the far-field noise problem, or the exposure of people and structures on the ground to the shock front, it is helpful to review briefly the phenomena of shock-wave propagation. In general, a shock wave will not extend to the ground (and, consequently, no boom will be heard) unless the airplane local free-stream Mach number is greater than unity and the airplane velocity at altitude is greater than the velocity of sound at the ground. Thus, depending on the effects of existing temperature and wind conditions on shock-wave propagation, a boom may or may not be heard when the airplane is operated at supersonic Mach numbers. By assuming the conditions of a standard atmosphere, these propagation phenomena are illustrated in figure 5 for two steady-flight conditions where, for simplicity, only the bow waves are considered.

At a Mach number of 1.1 the bow wave does not extend all the way to the ground. If the temperature were constant at all points between the airplane and the ground, the bow wave would take the position of the dashed line and would intersect the ground. There is, however, a temperature gradient present; the ambient temperature at ground level is higher than at altitude. This temperature gradient affects the shape of the wave because the lower extremities propagate faster than the upper extremities and, thus, result in a "bending forward" of the wave as shown. This temperature effect is beneficial since, in some cases at low supersonic Mach numbers, it causes the wave to miss the ground completely. In the second case, where the local airplane Mach number is 2.0, the speed of the airplane exceeds the speed of sound at ground level and the wave front reaches the ground despite its curving because of the temperature gradient. Wind gradients have similar effects on the wave propagation and may either increase or decrease the curvature of the wave.

In connection with the pressures on the ground, therefore, it is recognized that there is a flight regime at low Mach numbers where the shock wave may not reach the ground. This condition is significant with regard to operations at low supersonic speeds in acceleration and deceleration near airports. However, in the steady-flight condition of higher supersonic Mach numbers, it is apparent that the shock wave will reach the ground, and this condition is the one primarily discussed herein.

OPERATIONAL FACTORS

The data of figure 6 show the pressure changes associated with the booms experienced near the flight track from some practical steady-flight operations of a supersonic airplane at various altitudes. The theoretical curve shown was calculated for a McDonnell F-101J airplane by using equation (1) and assuming $K_1 = 2.0$, $K_2 = 0.645$, $M = 1.3$,

and $l/d = 7.7$ where $l = 67$ feet. The four experimental data points shown were recently measured for the airplane in the Mach number range from 1.25 to 1.4 and an altitude range of 25,000 to 45,000 feet. The circled data points were taken under different atmospheric conditions than were those designated by the square symbols. Examination of atmospheric-sounding data for the circled data points indicated that there were moderate headwinds of from 0 to 30 feet per second at altitude. Atmospheric-sounding data represented by the square symbols indicated a very similar temperature gradient, closely simulating that of the standard atmosphere, but a tailwind of from 60 to 100 feet per second existed at altitude. The data seem to fall into two groups, both of which show the same relative decrease with altitude as the theory predicts. It will be noted that the data fall on each side of the calculated curve for these two widely varying atmospheric conditions. Although not enough data are available for definite conclusions to be drawn, it does appear that equation (1) should be used with caution to predict pressures in the far field in cases of extreme variations in atmospheric conditions.

So far, only the observer on or near the flight track has been considered. From practical considerations an investigation of the extent to which the boom spreads outward from the track is also of interest. Some insight into this phenomenon is given in figure 7 in which both calculated and experimental data are again given for the F-101J airplane at an altitude of 35,000 feet traveling at a Mach number of 1.3. In this figure the pressures are shown as a function of lateral distance from the track in miles. The theoretical curve is given by equation (1), where y represents the slant distance from the airplane to the observer station. This calculation of equation (1) indicates a maximum pressure along the flight track, a decreasing pressure with increasing lateral distance, and a sudden "cutoff" due to refraction effects. The refraction effects arise from the previously discussed temperature gradients. (See fig. 5.) As indicated schematically in the sketch in figure 7, the ray paths emitting from the airplane are turned upwards as they approach the ground. The experimental data confirm, in general, the trends predicted by equation (1) and, in particular, the extent to which the boom spreads laterally. In that the terrain between observer stations was fairly flat and the surface winds quite low, it is believed that the effects of terrain and surface winds on the results indicated were minor.

Equation (1) has also been used to predict the pressure along the flight track of a possible future Mach number 3.0 transport airplane with fineness ratio l/d of 12.8 and a fuselage length l of 208 feet. These results are presented, along with similar calculations for the F-101J airplane at a Mach number of 1.3, for comparison in figure 8. Perfect reflection was again assumed in both cases, and a value of K_2 of 0.61 was taken for the Mach 3.0 transport airplane. At a given altitude, the difference in the calculated pressures is mainly due to the

size and shape of the two airplanes; the other factors are secondary. (See fig. 4.) It is apparent that the pressures associated with the future transport airplane are higher, but it should be remembered that this airplane will cruise at much higher altitudes.

The following table, which is based on the material of reference 7 and the present tests, attaches some significance to the order of magnitude of pressures to be expected.

Shock-noise phenomena			
Δp , lb/ft ²	Δp , decibels	Resulting physiological reaction	Associated physical phenomena
0.1 to 0.3	108 to 118	Not objectionable	Barely audible explosion
0.3 to 1.0	118 to 128	Tolerable	Distant explosion or thunder
1.0 to 3.0	128 to 138	Objectionable	Close-range thunder and some window damage
3.0 to 10.0	138 to 148		Damage to large plate-glass windows
10.0 to 30.0	148 to 158		Definite damage to small barracks- type windows

This table presents some shock-noise phenomena for various pressures along with the equivalent decibel values. Also indicated in the table are some observations by people who have experienced this type of noise along with some well-known physical phenomena that occur at the same pressure values. For the particular tests of this investigation where the ground pressures did not exceed 1.0 pound per square foot, the observers did not consider the booms objectionable and likened them to a distant thunder or explosion. For pressures exceeding 1.0 pound per square foot the observers considered the boom objectionable and, in addition, a large plate-glass window in the test area was broken at a pressure of about 2.0 pounds per square foot. For higher pressures of from 3.0 pounds per square foot to 30.0 pounds per square foot it was indicated in reference 7 that definite damage to large plate-glass windows and smaller barracks-type windows would occur.

With regard to the window breakage noted during the test, it is believed to be significant that similar windows on either side of the broken window did not break. This result would indicate that the pressures in this test were near the magnitude where damage would begin to occur for commercially installed plate-glass windows.

With an appreciation established for the mechanism of generation of the boom, for the operational and atmospheric factors that affect it, and for the associated physical phenomena, an examination was made of how the shock-wave noise problem may influence future airplane flight plans.

Proposed altitude profiles are shown in figures 9 and 10 for the previously discussed Mach 3.0 transport airplane on a cross-country flight, along with an indication of the intensity and lateral speed of the boom pressures. The nominal flight plan of figure 9 can be associated with optimum performance and the plan of figure 10 with having taken into consideration the "boom" problems. In both plans the same amount of fuel is consumed, but in the optimum-performance plan the distance is covered in about 13 minutes less time. The only difference between the two plans is in the climb and descent phases, as shown. In the optimum-performance plan the climb and descent are made at maximum allowable indicated airspeed, which results in high supersonic speeds at low altitudes and, therefore, produces pressures of about 5 pounds per square foot along the flight track. During the cruise portion of the flight plan, which begins about 300 miles from take-off, the pressures are of much lesser intensity (0.5 pound per square foot) but extend laterally about 60 miles. In an attempt to minimize the pressures during the critical phases of climb and descent, the alternate flight plan of figure 10 which results in the same fuel consumption but requires a longer flight time has been proposed. In this plan the climb and descent phases are made at subsonic speeds to some intermediate altitude of perhaps 35,000 feet at which time the airplane is about 80 miles from the point of take-off, and then the Mach number is increased at constant altitude to about 2.0. A supersonic climb is then made to the cruise altitude of 70,000 feet, and the airplane has attained a distance of about 400 miles from the point of take-off. For this alternate flight plan, pressures of about 2.5 pounds per square foot are experienced during the climb and descent phases, as compared with 5.0 pounds per square foot for the previous plan of figure 9. Since both flight plans are similar during the cruise phase, similar pressures result. It is obvious from the results that the boom will be experienced for a major portion of the flight plan.

CONCLUDING REMARKS

It has been pointed out that for the proposed supersonic transport airplanes of the near future, booms on the ground will most probably be experienced during the major portion of the flight plan. The boom pressures will be most severe during the climb and descent phases of the flight plan. During the cruise phase of the flight, the boom pressures are of much lesser intensity but are spread laterally for many miles. Wind-tunnel studies thus far indicate that changes of the aerodynamics of the airplane will result in only small changes in the boom pressures; however, the manner in which the airplane is operated does appear to be significant. For example, the boom pressures during the climb, cruise, and descent phases can be minimized by operating the airplane at its maximum altitude consistent with its performance capabilities.

REFERENCES

1. DuMond, Jesse W. M., Cohen, E. Richard, Panofsky, W. K. H., and Deeds, Edward: A Determination of the Wave Forms and Laws of Propagation and Dissipation of Ballistic Shock Waves. Jour. Acous. Soc. of America, vol. 18, no. 1, July 1946, pp. 97-118.
2. Whitham, G. B.: The Flow Pattern of a Supersonic Projectile. Communications on Pure and Appl. Math., vol. V, no. 3, Aug. 1952, pp. 301-348.
3. Randall, D. G.: Methods for Estimating Distributions and Intensities for Sonic Bangs. Tech. Note No. Aero. 2524, British R.A.E., Aug. 1957.
4. Mullens, Marshall E.: A Flight Test Investigation of the Sonic Boom. AFFTC-TN-56-20, Air Res. and Dev. Command, U. S. Air Force, May 1956.
5. Daum, Fred L.: The Theory and the Problems of the Sonic Boom. Aero. Res. Lab., Wright Air. Dev. Center, U. S. Air Force, Oct. 6, 1954.
6. Busemann, Adolf: The Relation Between Minimizing Drag and Noise at Supersonic Speeds. Proc. Conf. on High-Speed Aeronautics, Antonio Ferri, Nicholas J. Hoff, and Paul A. Libby, eds., Polytechnic Inst. of Brooklyn, c.1955, pp. 133-144.
7. Cox, Everett F., Plagge, H. J., and Reed, J. W.: Meteorology Directs Where Blast Will Strike. Bull. Am. Meteorological Soc., vol. 35, no. 3, Mar. 1954, pp. 95-103.

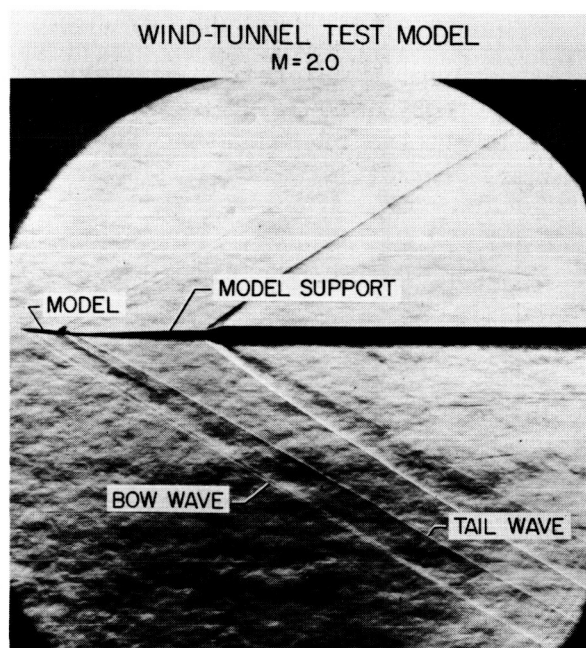


Figure 1

NATURE OF THE PROBLEM

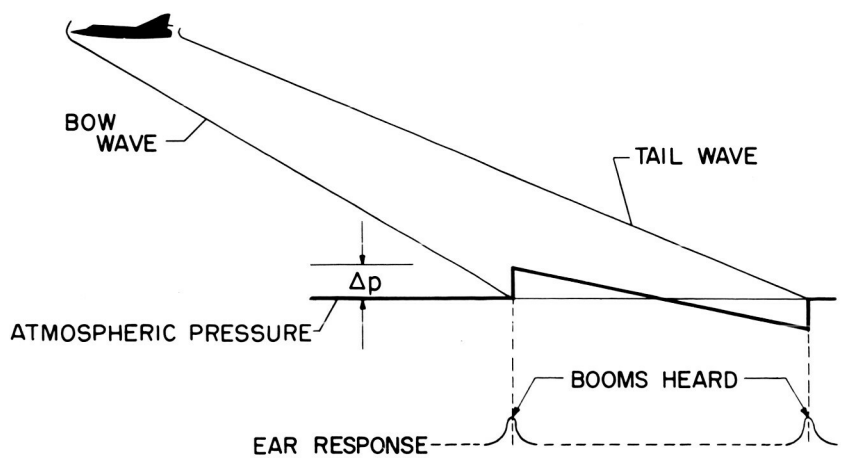


Figure 2

CALCULATED EFFECT OF BODY SHAPE

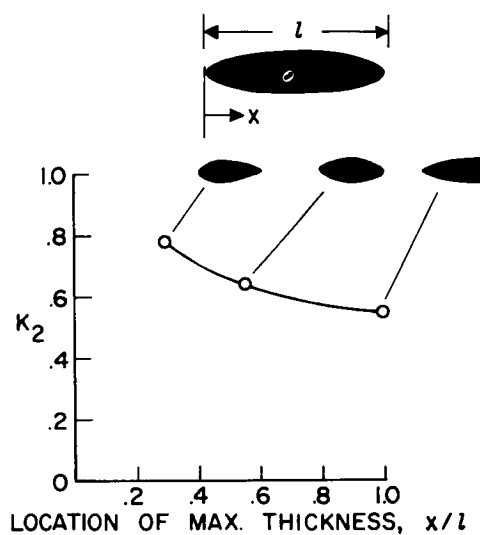


Figure 3

CALCULATED EFFECTS OF THE VARIOUS VARIABLES

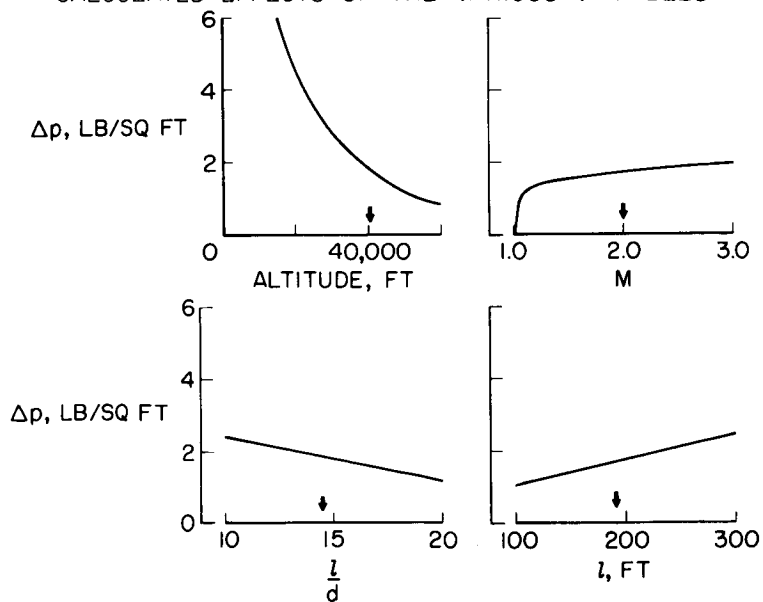


Figure 4

EFFECT OF TEMPERATURE GRADIENT ON BOW-WAVE PROPAGATION

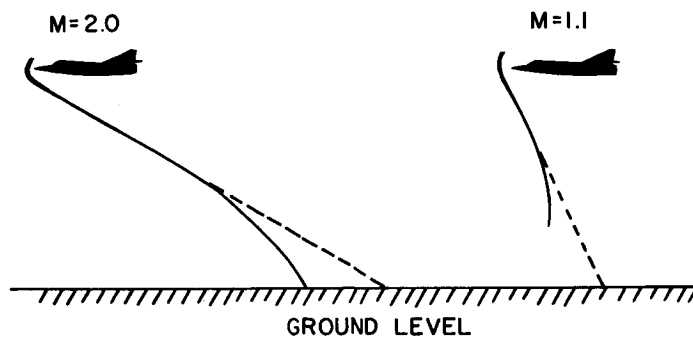


Figure 5

PRESSURES ON GROUND ALONG TRACK

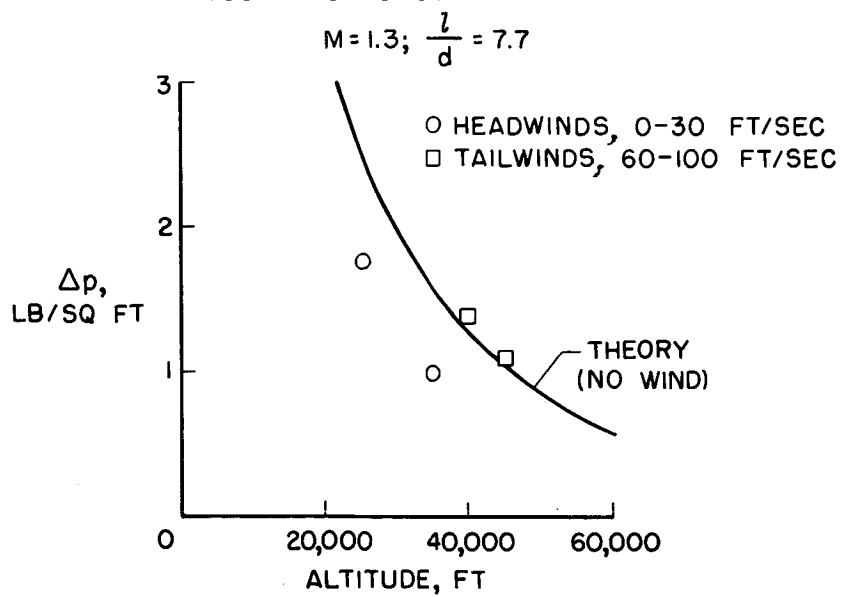


Figure 6

LATERAL SPREAD FROM TRACK

$M=1.3$; ALTITUDE, 35,000 FT; $\frac{l}{d} = 7.7$

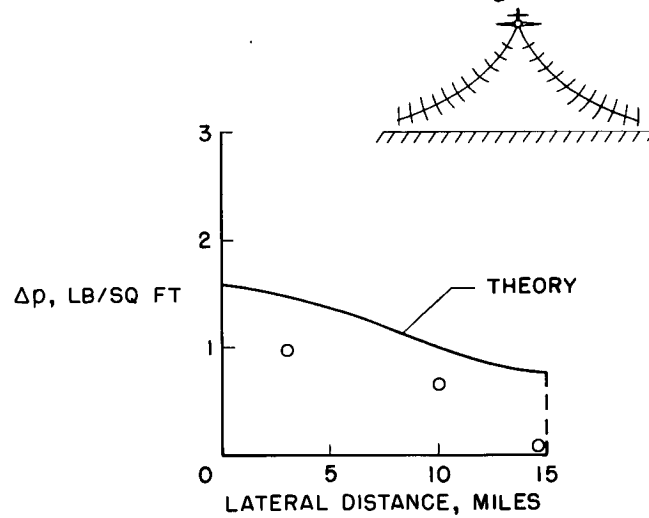


Figure 7

CALCULATED PRESSURES ALONG GROUND TRACK

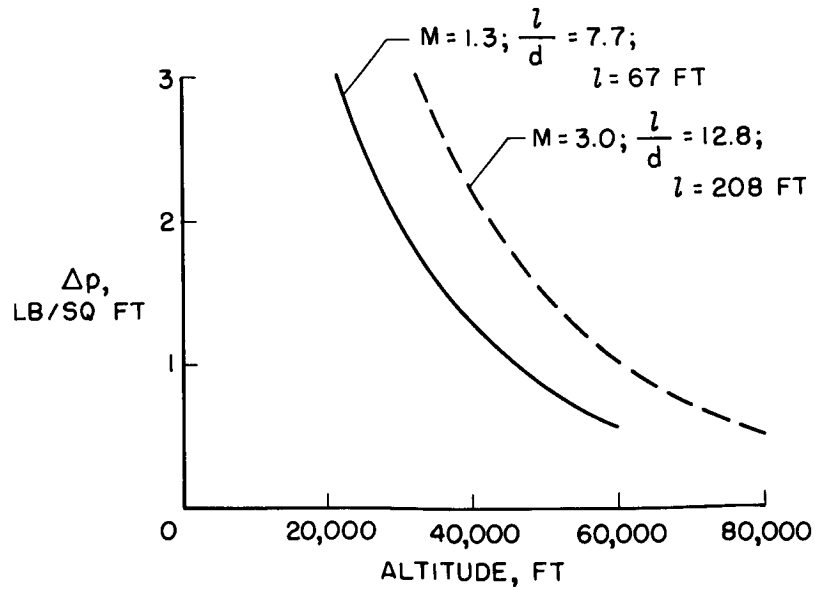


Figure 8

CROSS-COUNTRY FLIGHT PLAN

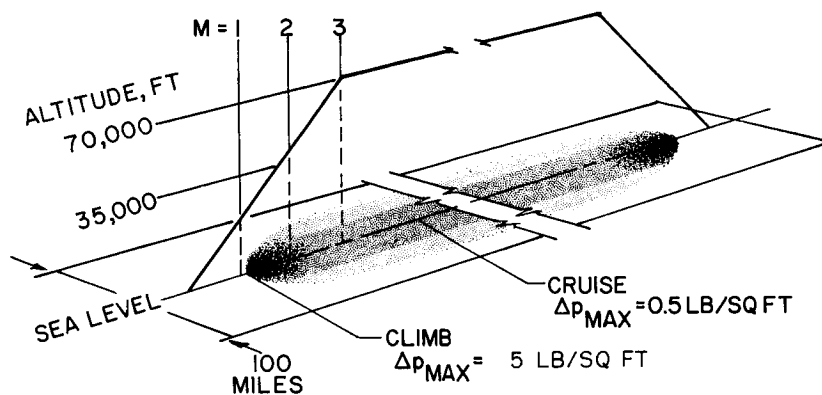


Figure 9

CROSS-COUNTRY FLIGHT PLAN TO REDUCE NOISE

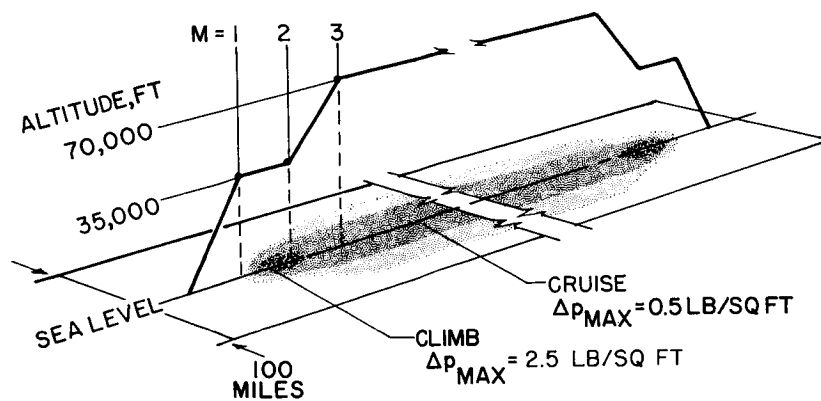


Figure 10

SEVERAL METHODS FOR REDUCING THE DRAG OF TRANSPORT CONFIGURATIONS AT HIGH SUBSONIC SPEEDS

By Richard T. Whitcomb and Atwood R. Heath, Jr.

Langley Research Center

SUMMARY

Results of investigations of several promising methods for alleviating the drag rise of transport configurations at high subsonic speeds are reviewed briefly. The methods include a wing leading-edge extension, a fuselage addition, and additions on the wing. Also, results are presented for a complete, improved transport configuration which incorporates the fuselage and wing additions and show that the improved configuration could have considerably higher cruise speeds than do current designs.

INTRODUCTION

The cruise speeds of the current subsonic jet transports are limited by the severe drag rise of these airplanes as they approach the speed of sound. Numerous design variations for delaying and reducing this drag-rise have been investigated in past years. Also, a number of new variations have been studied relatively recently. To provide an indication of possible future improvements of the performance of subsonic transports, results for some of the more promising of these recent modifications are described in the present paper. The variations discussed include some which might be incorporated in existing transport configurations without excessive redesign or modification and others of more complex nature which could probably be incorporated only in new transport designs.

DRAG-RISE PHENOMENA

An indication of the magnitude of the increase in drag at high subsonic speeds is illustrated by the wind-tunnel results presented in figure 1. Presented in this figure is the variation of drag coefficient C_D with Mach number M for a configuration similar to the current jet

transports. The wing has 35° of sweep and an aspect ratio of 7. The results are presented for a lift coefficient C_L of 0.3, which is near the values for cruise of the current jet transports. As may be seen, the drag coefficient starts to rise at Mach numbers somewhat above 0.80. At a Mach number of 0.92, the drag coefficient is twice that at the lower speeds. For most of the current jet transports, the maximum Mach numbers are limited to approximately 0.88, while the speeds for reasonably efficient cruise are somewhat less than this value.

At the lift coefficients normally utilized for jet transports, the drag rise results primarily from separation of the boundary layer on the upper surface of the wing induced by the presence of a shock wave associated with the development of a local region of supersonic flow above the wing. The boundary-layer separation phenomenon is illustrated in figure 2. Shown in this figure are flow patterns in a thin film of oil on the upper surface of the wing of the configuration shown in the previous figure for a Mach number of 0.88 at a lift coefficient of 0.4. The film of oil is made visible through illumination by ultraviolet light. The flow of oil conforms with the local flow in the boundary layer and provides an indication of the nature of that flow. (See ref. 1.) The sharp change of the oil thickness along the midchord of the sections indicates the initiation of boundary-layer separation. The outward flow of oil on the rearward portion of the wing indicates a boundary-layer flow that is typical of separation on a sweptback wing.

METHODS OF IMPROVEMENT

To provide improvements in the drag at high subsonic speeds, the shock-induced boundary-layer separation on the wing must be reduced. The more significant means for accomplishing this action are as follows:

Direct boundary-layer control

- Fences
- Vortex generators
- Suction or blowing

Reduction of shock strength

- Wing modifications
 - Additional sweep
 - Reduced thickness ratio
 - Redistribution of camber
 - Leading- or trailing-edge extensions
- Fuselage changes
 - Streamline contouring
 - Area-rule shaping
 - Concentrated additions
- Additions on wing

The methods may be divided into two broad groups: First, those which provide a direct action on the boundary layer and, second, those which reduce the strength of the shock wave, with a resulting alleviation of separation. The methods of the first group usually provide only relatively small reductions of shock-induced separation. Therefore, the discussion presented herein will be limited to methods for reducing the strength of the shock wave. Of the various methods listed, results will be presented for the wing extensions, fuselage additions, and additions on the wing.

Wing Modifications

The most powerful means of reducing the shock strength is wing sweep. (See ref. 2.) However, for the wings used for subsonic transports, large amounts of sweep normally result in very severe pitch-up. Thus, the sweep angles used for the current transports have been limited to moderate values. The shock strength may also be reduced by reducing the thickness ratio of the wing (ref. 3) and modifying the camber distribution (ref. 4). Each of these wing changes normally would require a complete redesign of the wing. For existing wing designs, improvements in these wing parameters may be obtained effectively by adding leading-edge and trailing-edge extensions to the basic wing structures. Results obtained for such a leading-edge extension on a wing with 40° of sweep are presented in figure 3. The extension was 20 percent of the chord at the wing-fuselage juncture and tapered to zero at the 50-percent-semispan station. It may be seen that the extension provides a significant delay of the drag rise at a lift coefficient of 0.3. However, such a modification also results in an adverse effect on the pitch-up similar to that obtained for a moderate increase in wing sweepback.

Fuselage Changes

Among the changes of fuselage shape to reduce the shock strength are those which provide a fuselage contour which is aligned with the streamlines of the flow over a sweptback wing (ref. 5) and those which improve the longitudinal area distribution for the airplane on the basis of the area rule (ref. 6). For configurations similar to subsonic transports, these fuselage contours provide moderate delays in the drag rise (refs. 3 and 7); however, these shapes have not as yet been utilized in transport designs, since the improvements have not justified the structural complexity involved. More recently, a fuselage addition for reducing the shock strength which does not involve such severe problems of application has been investigated. (See ref. 8.) This addition, which is concentrated on the forward portion of the top of the fuselage (fig. 4), provides a desired fuselage camber as well as improving the area distribution. The basic configuration is the same as that shown

in figure 1. The fuselage addition results in a delay in drag rise approximately the same as that provided by the more extensive stream-line contouring or normal area-rule shaping.

Additions on Wing

Changes described in the previous section generally provide a significant reduction of separation on the inboard sections of a wing but result in little reduction of separation on the outer regions of the high-aspect-ratio wings normally utilized for subsonic transports. In order to reduce the separation on these regions, special bodies added to the wing, as shown in figure 5, have been proposed. (See ref. 9.) These bodies might be added to an existing configuration or incorporated in a new design. The bodies are entirely above the wing as shown in the cross section in figure 5 and extend from near the leading edge of the wing to beyond the trailing edge. The noses of the bodies decelerate the local supersonic flow ahead of the shock wave standing above the wing and thus reduce the strength of this wave. Results of an investigation of the effect of the bodies on the drag coefficient for the wing-fuselage combination of the configuration shown in figure 1 are shown in figure 5. The additions provide a considerable reduction of the drag at high subsonic speeds at a lift coefficient of 0.3. The reduction of the boundary-layer separation associated with this reduction of drag is illustrated by comparison of the surface oil flow for the configuration with the bodies (fig. 6) with that for the configuration without the added bodies (fig. 2). With the bodies added, the sharp change of oil thickness and the strong outflow of oil associated with boundary-layer separation on the basic wing are essentially eliminated.

The bodies added to the wing (fig. 5) also provide marked alleviation of the pitch-up for swept wings throughout the Mach number range. This effect is illustrated in figure 7, which presents the variation of pitching-moment coefficient C_m with lift coefficient C_L at a Mach number of 0.88 for the configuration just discussed with and without the added bodies. The curve for the configuration without the added bodies has a severe break in the slope near a lift coefficient of 0.3. Such a break would usually result in pitch-up for an actual airplane. With the bodies added, this adverse break is eliminated.

IMPROVED CONFIGURATION

In order to demonstrate the improvements in drag at high subsonic speeds that might be obtained for a new transport design incorporating several of the devices just described, a configuration representative

of such a design has been investigated recently. The test configuration is shown in figure 8. An addition has been attached to the top, forward portion of the fuselage. Six bodies have been added to the wing. The four inner bodies have been made sufficiently large to enclose engines. The air inlets for engines placed in these bodies would be near the leading edge of the lower surface of the wing. However, no inlets are incorporated in the model investigated. Placement of the engines in these fairings, of course, eliminates the drag of the engine installation in the normal underslung location. This drag may be relatively large at the higher subsonic speeds.

The sweep of the improved configuration of figure 8 has been made 45° . The significant alleviation of the pitch-up of sweptback wings provided by the added bodies considerably relaxes the limitation on wing sweep previously imposed by these adverse changes. With the use of these bodies, sweeps considerably greater than the 30° or 35° used for current transports should be practical. The aspect ratio of the configuration is 7, which is approximately the value for most current transports. The thickness of the wing varies from 11.5 percent of the chord at the root to approximately 7.5 percent of the chord at the 50-percent-semispan station with a thickness of 7.5 percent of the chord from that station to the tip. The wing is cambered to obtain a lift distribution which should provide good high-speed characteristics at a lift coefficient of 0.3.

In figure 9, the variation of drag coefficient with Mach number at a lift coefficient of 0.3 for this improved configuration is compared with that for the representative current configuration of figure 1. At high subsonic speeds, the drag characteristics for the improved configurations are markedly superior to those for the current design. These improvements in drag should result in considerably higher cruise and maximum speeds. With the same relative thrust of the current transports, the improved configuration could fly at or very near the speed of sound. The stability characteristics throughout the speed range and the maximum lift at low speeds for the improved configuration are satisfactory. However, although such a configuration offers possibilities for markedly improving aerodynamic characteristics, the design of an actual transport airplane based on such a configuration would, of course, require consideration of a number of other important factors.

CONCLUSIONS

Results have been presented which indicate that a wing leading-edge extension, a localized addition on the fuselage, and additions on the wing can provide significant reductions of the drag rise at high subsonic speeds for configurations similar to current subsonic jet

transports. Such additions possibly could be incorporated into current transports, without excessive redesign, to provide some increases of the cruise speeds for these configurations. Utilization of the fuselage and wing additions in new, improved designs should result in subsonic transports with considerably higher cruise and maximum speeds.

REFERENCES

1. Loving, Donald L., and Katzoff, S.: The Fluorescent-Oil Film Method and Other Techniques for Boundary-Layer Flow Visualization. (Prospective NASA Report.)
2. Sutton, Fred B., and Dickson, Jerald K.: A Comparison of the Longitudinal Aerodynamic Characteristics at Mach Numbers Up to 0.94 of Sweptback Wings Having NACA 4-Digit or NACA 64A Thickness Distributions. NACA RM A54F18, 1954.
3. Carmel, Melvin M.: Transonic Wind-Tunnel Investigation of the Effects of Aspect Ratio, Spanwise Variations in Section Thickness Ratio, and a Body Indentation on the Aerodynamic Characteristics of a 45° Sweptback Wing-Body Combination. NACA RM L52L26b, 1953.
4. Harrison, Daniel E.: The Influence of a Change in Body Shape on the Effects of Twist and Camber As Determined by a Transonic Wind-Tunnel Investigation of a 45° Sweptback Wing-Fuselage Configuration. NACA RM L53B03, 1953.
5. Küchemann, D.: Design of Wing Junction, Fuselage, and Nacelles To Obtain the Full Benefit of Sweptback Wings at High Mach Number. Rep. No. Aero. 2219, British R.A.E., Oct. 1947.
6. Whitcomb, Richard T.: A Study of the Zero-Lift Drag-Rise Characteristics of Wing-Body Combinations Near the Speed of Sound. NACA Rep. 1273, 1956. (Supersedes NACA RM L52H08.)
7. McDevitt, John B., and Haire, William M.: Investigation at High Subsonic Speeds of a Body-Contouring Method for Alleviating the Adverse Interference at the Root of a Sweptback Wing. NACA TN 3672, 1956. (Supersedes NACA RM A54A22.)
8. Whitcomb, Richard T.: A Fuselage Addition To Increase Drag-Rise Mach Number of Subsonic Airplanes at Lifting Conditions. NACA TN 4290, 1958.
9. Whitcomb, Richard T.: Special Bodies Added on a Wing To Reduce Shock-Induced Boundary-Layer Separation at High Subsonic Speeds. NACA TN 4293, 1958.

DRAG RISE FOR REPRESENTATIVE CURRENT JET TRANSPORT
WITH WING SWEEP OF 35°
 $C_L = 0.3$

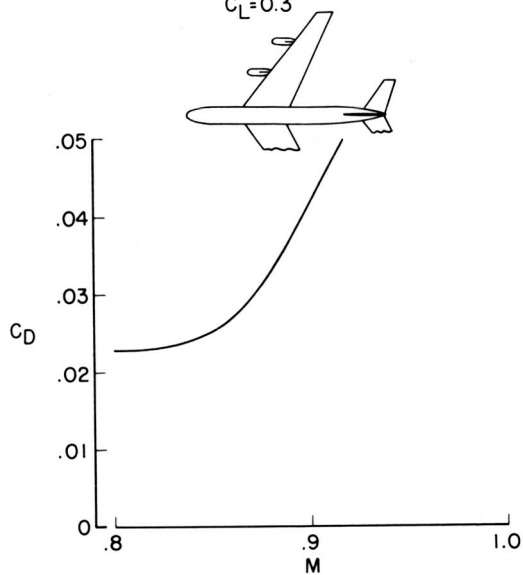


Figure 1

BOUNDARY-LAYER FLOW ON WING WITH 35° SWEEP
 $C_L = 0.4$; $M = 0.88$



Figure 2

EFFECT OF WING LEADING-EDGE EXTENSION ON DRAG RISE
 $C_L=0.3$

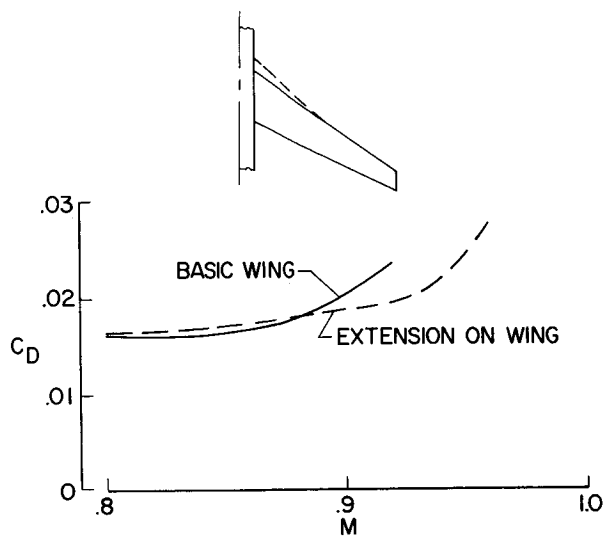


Figure 3

EFFECT OF FUSELAGE ADDITION ON DRAG RISE
 $C_L=0.3$

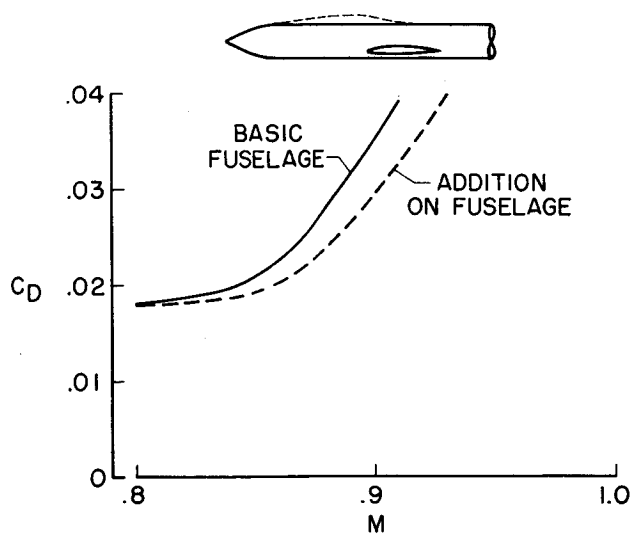


Figure 4

EFFECT OF BODIES ADDED TO WING ON DRAG RISE
 $C_L = 0.3$

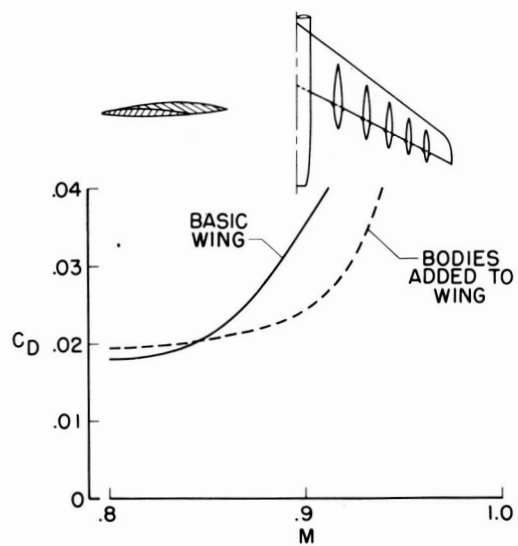


Figure 5

BOUNDARY-LAYER FLOW ON WING WITH SPECIAL BODIES ADDED
 $C_L = 0.4$; $M = 0.88$

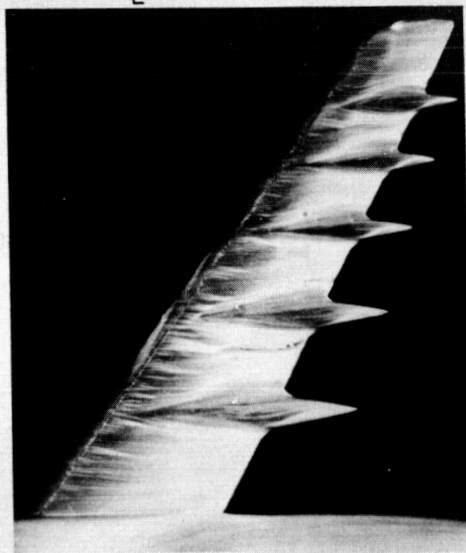


Figure 6

EFFECT OF WING ADDITIONS ON LONGITUDINAL
PITCHING MOMENTS
 $M = 0.88$

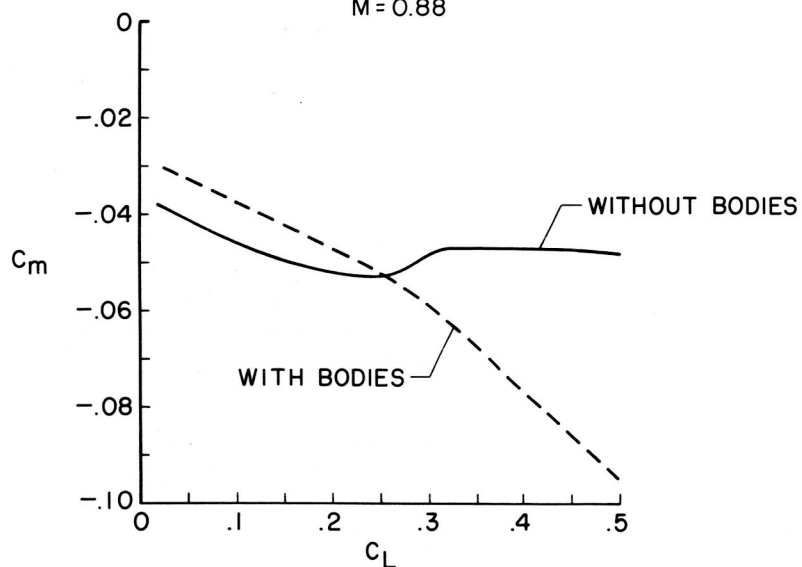


Figure 7

WIND-TUNNEL MODEL OF IMPROVED
JET-TRANSPORT CONFIGURATION

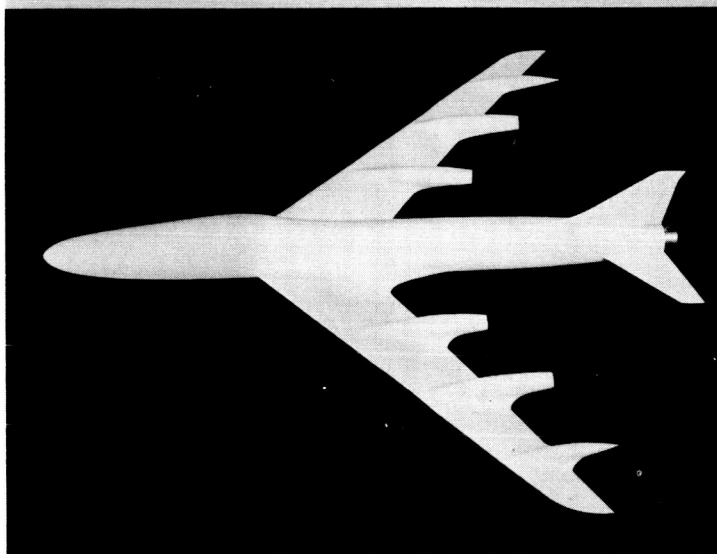


Figure 8

COMPARISON OF DRAG RISE FOR CURRENT
AND IMPROVED JET-TRANSPORT CONFIGURATIONS

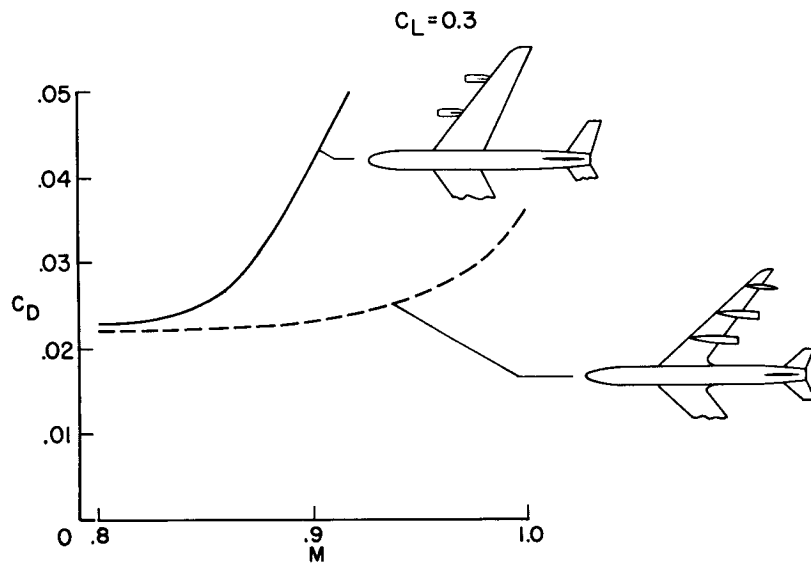


Figure 9

POWERPLANTS FOR SUPERSONIC TRANSPORT AIRPLANES

By Arthur V. Zimmerman

Lewis Research Center

INTRODUCTION

With the introduction of subsonic turbojet transports into airline operation currently taking place, attention is now being focused on the feasibility of supersonic jet transports. The purpose of the present paper is to discuss one of the problem areas that will be encountered in developing a supersonic transport - the propulsion system. A comparison of the performances of several basic turbine-engine types is presented with emphasis on turbojet and turboprop engines suitable for transports cruising in the flight Mach number range from 1.5 to 3.0. Some of the engine component problems that become increasingly important as flight speeds are increased are discussed briefly.

DISCUSSION

Operational military airplanes designed for supersonic flight use turbojet engines, and the turbojet engine is also a suitable choice for a supersonic transport. In order to evaluate the potentialities of turbojet engines, three basic types were analyzed. They are illustrated schematically in figure 1. The engines investigated were a low- and a high-turbine-inlet-temperature nonafterburning engine and an afterburning engine. The low-temperature nonafterburning engine has a turbine-inlet temperature of $1,540^{\circ}\text{F}$ which is a conservative temperature within the present state of the art. The high-temperature nonafterburning engine has a turbine-inlet temperature of $2,040^{\circ}\text{F}$ which represents a possible future temperature capability obtainable through advances in either turbine-blade materials or in the development of turbine-blade cooling. The afterburning engine, of course, provides a means of obtaining high-cycle temperatures without exceeding current turbine temperature limitations. The afterburning engine investigated has a turbine-inlet temperature of $1,540^{\circ}\text{F}$ and an afterburning temperature at cruise of $2,040^{\circ}\text{F}$.

The cruise performances of these engines are compared in figure 2. Cruise performance is presented in terms of specific fuel consumption and specific engine weight - that is, engine weight per pound of thrust at cruise. Each curve represents the performance of a family of engine designs. The engines are designed to cruise at flight Mach numbers

from 1.5 to 3.0. The design compressor pressure ratio (at sea-level static flight condition) was varied from 12 to 1 for the engines cruising at a Mach number of 1.5 down to 6 or 8 to 1 for the engines cruising at a Mach number of 3.0. The specific engine weights shown in figure 2 are based on a variation in cruise altitude from 45,000 feet at a Mach number of 1.5 to 60,000 feet at a Mach number of 3.0.

Making an engine selection involves a compromise between engine weight and specific fuel consumption. For example, at a Mach number of 1.5, the 1,540° F nonafterburning engine provides the best specific fuel consumption but, because of its low thrust, it also results in the highest engine weight. Specific engine weight can be measurably reduced by increasing turbine-inlet temperature to 2,040° F with only a small increase in specific fuel consumption. On the other hand, if a higher turbine-inlet temperature capability does not become a reality and engine specific weight must be reduced by afterburning, then the specific-fuel-consumption penalty becomes severe.

As flight speed is increased, the performance of the 1,540° F nonafterburning engine decreases, as compared with the performance of engines with higher cycle temperatures. At a Mach number of 3.0, the 2,040° F nonafterburning engine, in addition to having a lower specific weight, also has a better specific fuel consumption. Also, at a Mach number of 3.0, the specific-fuel-consumption penalties of using an afterburning engine are substantially more acceptable than at the lower flight speeds. A large reduction in specific engine weight can be obtained by afterburning with only a moderate increase in specific fuel consumption.

Because of the compromises that must be made among engine weight, thrust, and specific fuel consumption, an overall evaluation of the three engine types requires a mission analysis. The mission selected was that of a supersonic transport with a gross weight of 300,000 pounds and a payload of 37,000 pounds. In a comparison of engine types, several figures of merit can be used. For the present analysis, the gross weight and payload of the transport were held fixed, and the transport range was used as a measure of engine performance capability. As in all mission studies, the absolute results are strongly dependent not only on engine performance but also on the aircraft aerodynamic and structural weight assumptions. Therefore, the results to be presented are useful primarily for comparing propulsion systems rather than for defining overall aircraft capability. The results of the mission study are shown in figure 3. Relative range is presented as a function of cruise flight Mach number for transports powered by the three turbojet engines under consideration. The ranges shown are relative to the ranges obtained by a transport with 2,040° F nonafterburning engines. This range curve, therefore, appears as a straight line.

As mentioned previously, the afterburning engine has an afterburning temperature of $2,040^{\circ}\text{F}$ during cruise, but for take-off and climb the afterburning temperature was increased to $3,040^{\circ}\text{F}$.

In a comparison of the two nonafterburning engines, the $2,040^{\circ}\text{F}$ engine provides a better range than the $1,540^{\circ}\text{F}$ engine at all flight speeds. This is due to the better specific weight of the $2,040^{\circ}\text{F}$ engine at the lower flight speeds and to both its better specific weight and specific fuel consumption at the higher flight speeds. These results indicate that, for nonafterburning engines, turbine-inlet temperatures should be as high as possible consistent with engine life and reliability requirements. However, if turbine-inlet temperatures cannot be raised much above current levels, the range penalty at the lower supersonic flight speeds is not marked. Up to a flight Mach number of 2.0, the range of the $1,540^{\circ}\text{F}$ engine is 12 percent less than that of the $2,040^{\circ}\text{F}$ engine. When flight speeds are increased above a Mach number of 2.0, the range of the $1,540^{\circ}\text{F}$ engine begins to decrease rapidly. If turbine-inlet temperatures cannot be raised above current levels, then above a Mach number of 2.5 the best range is obtained with an afterburning engine.

In summary, nonafterburning engines with current temperature limitations appear adequate to flight Mach numbers of 2.0, although higher turbine-inlet temperatures are beneficial. As flight speed is increased above a Mach number of 2.0, the use of higher cycle temperatures becomes increasingly desirable, and above a Mach number of 2.5 either a higher turbine-inlet temperature capability or an afterburning engine is required.

For subsonic jet transports, the turbofan engine is a strong competitor to the turbojet. Therefore, consideration of turbofan engines as powerplants for a supersonic transport is also in order. There are many possible configurations for a turbofan engine. A schematic illustration of the particular configuration investigated for this study is shown in figure 4. A representation of the turbojet engine is included for comparison. The turbofan engine shown in the top view is a twin-spool, mixed-jet design. It consists of a fan, a compressor, a primary combustor, and turbines which drive the compressor and fan. The inner spool of the engine consists of the compressor and the compressor-driving turbine and the outer spool consists of the fan and the fan-driving turbine. The configuration of the turbofan shown in figure 4 works as follows: The engine air flow is compressed by the fan and part of the air is delivered to the compressor. The remainder of the air is bypassed around the compressor and turbines to the tailpipe. The portion of the air entering the compressor is compressed, heated in the primary combustor, and expanded across the turbines. For the mixed-jet configuration shown, the turbine discharge gases are then mixed with the bypassed air flow prior to expansion through the exhaust nozzle. Insofar as performance is concerned, the essential difference between the turbojet and

turbofan engines is in their exhaust-gas temperatures. The exhaust-gas temperature of the turbofan engine, due to the bypass flow, is significantly lower than that for the turbojet engine. The lower exhaust-gas temperature of the turbofan engine accounts for its better specific fuel consumption at subsonic speeds. The lower exhaust-gas temperature, however, also results in a lower thrust per pound of engine air flow.

The cruise performances of the nonafterburning turbofan and turbojet engines are compared in figure 5. Again, performance is presented in terms of specific engine weight and specific fuel consumption. The turbofan engine shown has a design fan pressure ratio of 1.8, and at sea-level static conditions approximately 40 percent of the fan air flow is bypassed to the tailpipe. Both the turbojet and the turbofan engines have turbine-inlet temperatures of $1,540^{\circ}\text{F}$. The resulting exhaust-gas temperature for the turbojet engine is approximately $1,100^{\circ}\text{F}$, whereas the exhaust-gas temperature of the turbofan engine is only approximately 700°F .

At the lower supersonic flight speeds, the turbofan engine has a better specific fuel consumption than the turbojet engine. However, due to its lower exhaust-gas temperature the turbofan engine also has a lower thrust per pound of engine air flow and this is reflected in a higher specific engine weight. As flight speed is increased, the performance of the nonafterburning turbofan engine deteriorates because of its lower exhaust-gas temperature, and both specific fuel consumption and specific engine weight rise rapidly.

When afterburning configurations of the turbofan and turbojet engines are compared, the result is different, since afterburning engines can achieve the same exhaust-gas temperature. The cruise performances of afterburning versions of the turbojet and turbofan engines are compared in figure 6. Both engines have turbine-inlet temperatures of $1,540^{\circ}\text{F}$ and afterburning temperatures of $2,040^{\circ}\text{F}$. When afterburning engines are compared, the specific weight of the turbofan engine investigated is better than that of the turbojet engine. On the other hand, at the lower flight speeds, the specific fuel consumption of the turbojet is superior to that of the turbofan. However, at the higher flight speeds, where the afterburning engine might be of interest, the specific fuel consumption of the two engines is virtually the same.

In order to evaluate the overall potentialities of turbofan engines as powerplants for supersonic transports, a mission study similar to the one for the turbojet engine was made. The gross weight of the transport was 300,000 pounds, the payload was 37,000 pounds, and the transport range was used as a measure of engine performance capability. The results of the mission study are shown in figure 7. Some of the turbojet data shown previously are included for reference. As in figure 3, the ranges shown are relative to the ranges obtained by a transport with

2,040° F nonafterburning turbojet engines. This range curve, if indicated in figure 7, would be a straight line with a value of 1.0. The engines compared in figure 7 have turbine-inlet temperatures of 1,540° F.

Consider the two nonafterburning engines first. As has been indicated by the engine-performance comparison, the range capability of the nonafterburning turbofan is inferior to the capability of the nonafterburning turbojet, particularly as the flight Mach number is increased above 1.5. Therefore, the nonafterburning turbofan engine does not appear to be as attractive as the nonafterburning turbojet engine for supersonic transport application. However, when afterburning configurations are considered, the turbojet and turbofan engine capabilities are comparable over the entire flight speed range. Again, the turbojet engine might be the better choice since it is simpler and would tend to have fewer development problems.

Aside from flight performance, other factors influence engine selection. Two important ones that are related to engine type are engine noise level at take-off and take-off distance. Engine noise level at take-off can be related to the engine jet velocity which, in turn, is a function of exhaust-gas temperature. Clearly, if engines with higher exhaust-gas temperatures are used, the problem of engine noise during take-off will be aggravated. This problem will be particularly severe if afterburning engines are used. If the noise problem dictates take-off and climb with the afterburner inoperative, the resulting propulsion system penalty is severe and the take-off distances become prohibitive. Therefore, until effective means of noise suppression are developed, the use of either afterburning turbojet or turbofan engines from presently located airports appears unlikely.

The major component problems that will be encountered in developing an engine for supersonic flight are those associated with the inlet and exhaust nozzle. As design flight Mach numbers are increased, inlets and exits will become both larger and heavier portions of the engine. In addition, efficient operation over wider ranges in flight speed may require variable geometry designs. For example, to obtain efficient cruise performance, inlets will be sized for the cruise flight condition. For the high Mach number designs, this will require relatively large inlet capture areas. During climb at the lower supersonic flight speeds, this capture area is excessive and the inlet will spill air flow. This air flow spillage gives rise to large inlet spillage or additive drags. One method for reducing the additive drags is to use variable-geometry inlets capable of passing higher amounts of air flow at low supersonic flight conditions. This method also requires an efficient system to bypass the increased inlet air flow around the engine.

In order to obtain efficient performance, the exhaust nozzles, will have to be supersonic designs such as the convergent-divergent nozzle

shown in figure 1. This type of nozzle may require both variable throat and exit areas. This requirement is complicated by the fact that turbine engines for a transport application will also require thrust-reversing devices and noise suppressors installed in the exhaust section of the engine.

CONCLUDING REMARKS

Particular turbojet- and turbofan-engine configurations have been investigated for supersonic transport application. There are, of course, many variations of these two basic engine types. However, it is believed that the data shown are characteristic of the differences that exist. It appears that the nonafterburning turbojet engine will continue to be a suitable transport powerplant as flight speeds are increased from subsonic to supersonic. The major engine requirement will be the development of a higher turbine-inlet temperature capability. In addition, there will be a significant increase in inlet and exhaust nozzle complexity as flight speeds are increased.

TURBOJET ENGINES

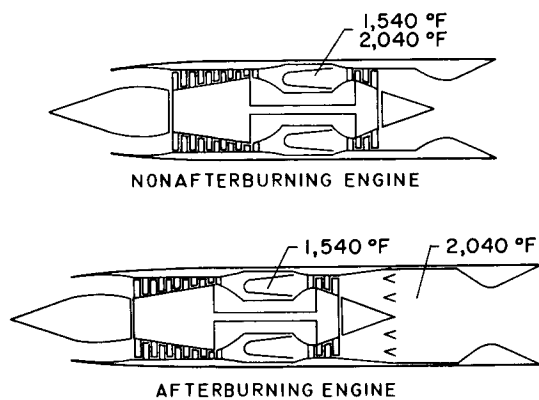


Figure 1

TURBOJET-ENGINE CRUISE PERFORMANCE

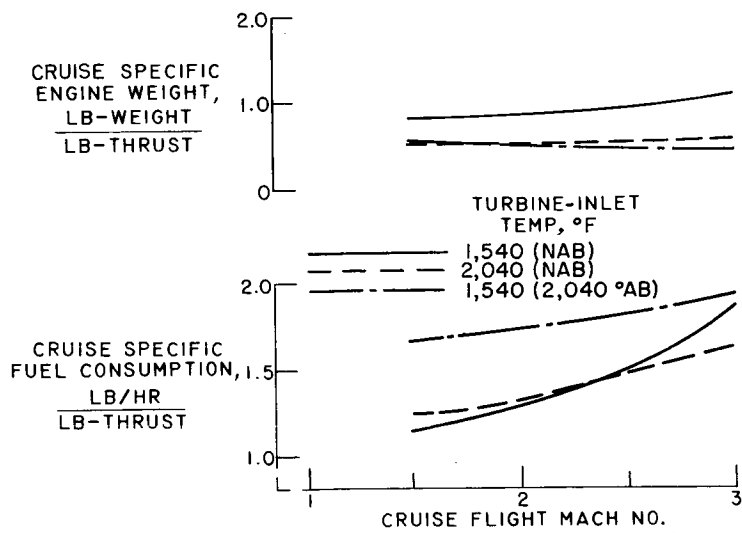


Figure 2

SUPERSONIC-TRANSPORT PERFORMANCE
TURBOJET ENGINES

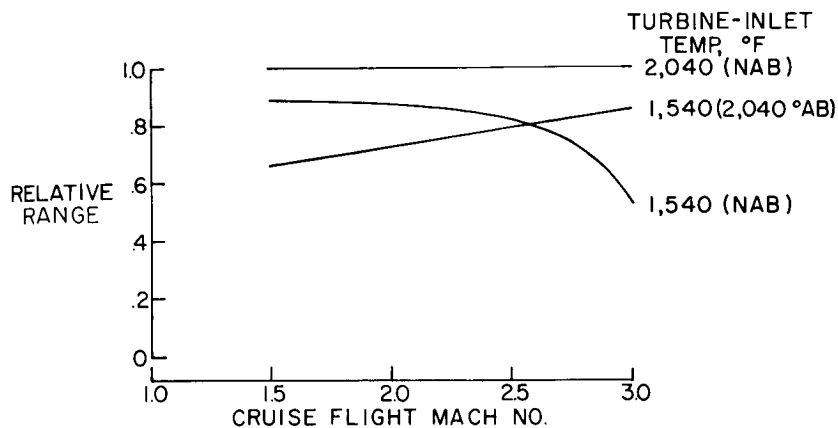
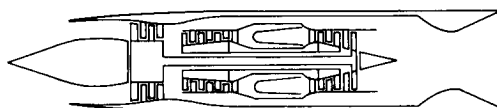


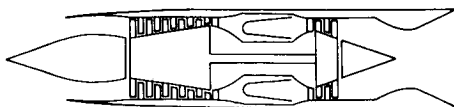
Figure 3

TURBOFAN AND TURBOJET ENGINES

NONAFTERBURNING



TURBOFAN ENGINE



TURBOJET ENGINE

Figure 4

COMPARISON OF NONAFTERBURNING TURBOJET AND TURBOFAN ENGINES

TURBINE-INLET TEMP, 1540° F

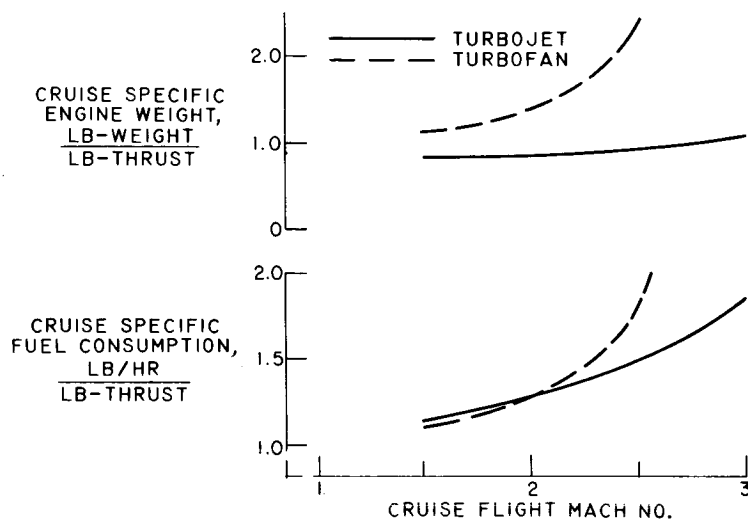


Figure 5

COMPARISON OF AFTERBURNING TURBOJET AND TURBOFAN ENGINES

TURBINE-INLET TEMP, 1,540 °F

AFTERBURNING TEMP, 2,040 °F

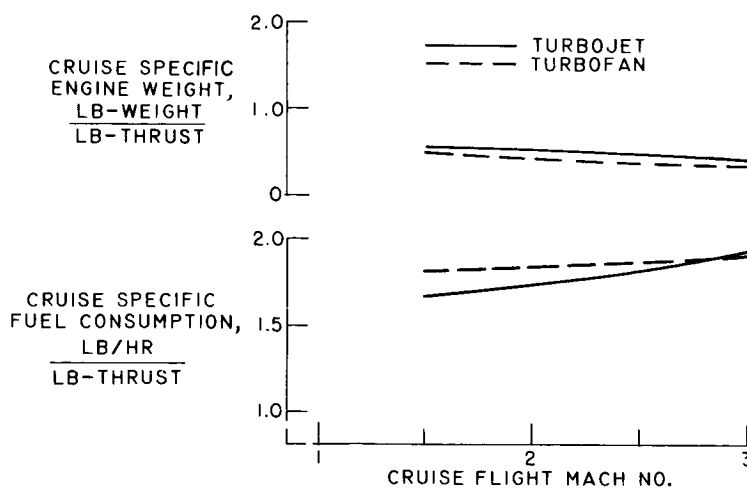


Figure 6

COMPARISON OF TURBOJET AND TURBOFAN
TRANSPORT PERFORMANCE

1,540 °F TURBINE-INLET TEMP.

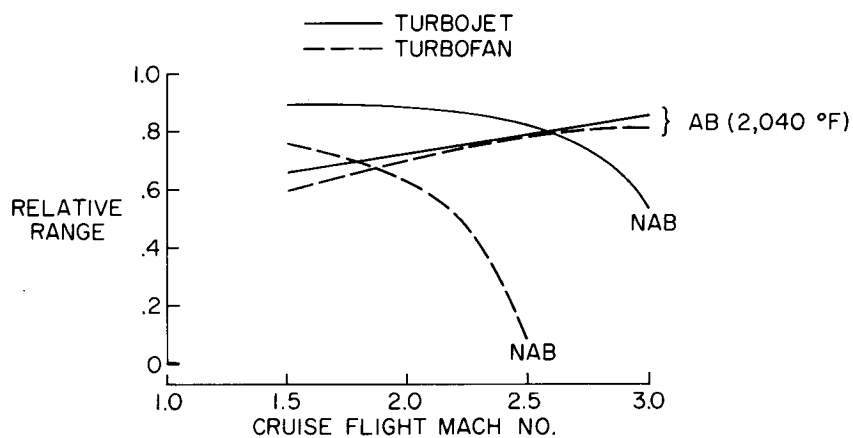


Figure 7

SOME CONSIDERATIONS OF SUPERSONIC AND HYPERSONIC
AIRPLANES AS COMMERCIAL TRANSPORTS

By J. Lloyd Jones and David H. Dennis

Ames Research Center

INTRODUCTION

This paper, which is based upon present knowledge and upon the assumption of reasonable state-of-the-art advances, attempts to examine the feasibility of achieving economical flight at supersonic and hypersonic speeds with commercial transport aircraft. It should be made clear that this paper contains no new data; it is rather a survey of the present status and of what developments might be expected of transports in the foreseeable future.

The undeniable desire of man to "get there faster" is, of course, a prime impetus to achieve ever higher travel speeds. It is, thus, good business for the commercial airline to be the "first with the fastest." Higher flight speeds are, of course, attractive from the standpoint of economics, because the faster an airplane flies the more passenger-miles or ton-miles it will yield in a given period of time.

SYMBOLS

I	specific impulse, $\frac{\text{Pounds of thrust}}{\text{Pounds of fuel per hour}}$
V	velocity, mph
L/D	lift-drag ratio
W	weight
M	Mach number
T	temperature, °F
S	wing area

Subscripts:

e effective
s satellite

DISCUSSION

Supersonic or hypersonic transport aircraft seem best suited to the intercontinental and long-range domestic routes. For the purposes of this discussion, an ultimate range of 5,000 statute miles has been assumed. The ultimate range is used as being the best basis for comparison of the capabilities of aircraft having given empty weights. In 1957, the total long-haul traffic of United States airlines on both domestic and international routes amounted to about 1 billion ton-miles. Herein, 3 billion ton-miles will be used arbitrarily as a future long-haul annual traffic volume for the time period that the supersonic or hypersonic transport might be in service.

Figure 1 shows the relative number of aircraft required to provide this traffic capability as a function of cruise Mach number. A 36,000-pound payload has been assumed with a utilization of 8 hours per day. The number of aircraft, although plotted against cruise Mach number, is based on an average speed which has been calculated to include a 1/4-hour allowance for taxi, take-off, approach, and landing with acceleration limited to 0.2g and deceleration determined according to aerodynamic drag. Variation of the traffic, payload, or utilization would affect the absolute number of airplanes required at a given speed but would not change the relative requirements. A significant reduction in the size of fleet required at supersonic speeds is indicated. No attempt has been made to consider route structure or scheduling. There is, of course, a practical minimum number of aircraft compatible with the number of routes to be serviced.

Although fewer aircraft are required at supersonic speeds, each will undoubtedly cost more to buy and to operate. As a basis for estimating relative costs, it is necessary to know something of the size of the aircraft being considered and its fuel requirements. For consideration of the latter, reference may be made to the Breguet range equation, one form of which is given as

$$\text{Range} = (IV) \left(\frac{L}{D} \right)_e \log_e \frac{W_{\text{INITIAL}}}{W_{\text{FINAL}}} \quad (1)$$

where

$$\left(\frac{L}{D}\right)_e = \frac{L/D}{1 - \frac{v^2}{v_s^2}}$$

For most efficient performance, or for the greatest range with a given ratio of initial weight to final weight, it is desirable to have both (IV) and $(L/D)_e$ of equation (1) as large as possible. The effective lift-drag ratio is seen to contain a term to account for centrifugal force in a curved flight path around the earth. This force is opposed to the gravitational pull on the airplane and reduces the aerodynamic lift required to sustain the weight. The effect is noticeable at a Mach number of 5.0, at which a $3\frac{1}{2}$ -percent increase in effective L/D is obtained, and grows in importance until at satellite speed ($M \approx 27$) no aerodynamic lift at all is required.

The effect of Mach number on maximum obtainable effective lift-drag ratio is illustrated in figure 2. The increase at the higher Mach numbers results from the effect of centrifugal force. Maximum values of L/D for research configurations have been obtained in the shaded-band range (see fig. 2) in wind-tunnel tests. It must be pointed out that many of these were idealized configurations and, in general, were not representative of complete airplanes; also, the addition, in various instances, of such components as stabilizing fins, engine inlets, or pilot's canopy would reduce the measured values below this range. However, the reduction in the value of turbulent skin friction in extrapolating these data to full-scale flight Reynolds numbers would, in general, have a compensating effect. Actually, higher maximum lift-drag ratios are theoretically possible. For instance, for a planar all-wing configuration of optimum plan form for its design cruise Mach number, theory predicts maximum values of L/D as indicated by the dashed-line curve. In tests, these values have not yet been realized. The range of maximum values of L/D indicated by the shaded band, however, is used for the purposes of this study as being representative of what might reasonably be expected to be obtained in flight by more conventional wing-body configurations. Of greatest importance here, however, is the relatively small variation in maximum values of L/D beyond Mach numbers of approximately 1.5 as compared with the large reduction through the transonic speed range.

The factor of the Breguet equation involving specific impulse and velocity is, of course, affected by the type of propulsion system used. This factor is plotted as a function of flight Mach number in figure 3 for the turbojet, the ram-jet, and the rocket engines with the range of values for the piston engine shown for comparative purposes at subsonic

speeds. A logarithmic scale has been used for clarity. This comparison of engine characteristics is an extension of that presented in reference 1. A rather wide range of values is shown in figure 3 for a given Mach number.

To realize the maximum values shown in figure 3 for ram-jet, turbo-jet, and rocket engines will require considerable advances over present systems. If, through future development, certain of the high-energy fuels can be utilized with transport-aircraft propulsion systems, additional increases in specific impulse might be realized. Different types of propulsion systems are seen to be desirable in different speed ranges. Each propulsion system has, of course, its own limitations, advantages, and disadvantages, but time does not permit a detailed discussion of these factors. Penalties for off-design performance would be greater for the higher cruise-speed aircraft using ram-jet systems, and take-off and landing would require special considerations. It may be necessary, for instance, to develop compound systems to permit operation over wider speed ranges. Of primary interest here, however, is the fact that values of specific impulse times flight velocity at least as high as have been dealt with at subsonic speeds may be realized at nearly all supersonic speeds depending upon the propulsion system used.

By using average values of lift-drag ratio and the ranges of specific impulse times flight velocity which were just presented, the variation with Mach number of the ratio of initial weight to final weight, for a range of 5,000 miles, has been computed and is shown in figure 4. Reference 2 has defined an effective lift-drag ratio and an effective product of specific impulse and velocity which permit the performance of boost-glide and ballistic vehicles to be represented by the Breguet equation. The ratios of initial weight to final weight for these vehicles (fig. 4) were determined on this basis and have been used as end points in establishing the trend of weight ratio with Mach number shown in figure 5. Shown also in figure 4 are representative values of the ratio of initial weight to final weight for subsonic piston, turboprop, and turbojet transports. This ratio is indicative of the efficiency of transporting a given load over the specified range. This means that if the upper value of $W_{\text{INITIAL}}/W_{\text{FINAL}}$ of approximately 2.7 is used for Mach numbers from 1.5 to 5, 1,700 pounds of fuel is required for every 1,000 pounds of final or landing weight. This is of little significance, however, unless it is known how much of the final weight is payload and how much is the operational empty weight of the aircraft, or, in other words, what empty weight of airplane is required to perform a given ton-mile mission.

Unless detailed designs of specific aircraft are available, these weights are exceedingly difficult to predict accurately. It is possible, however, to indicate trends in the empty weight of aircraft required to

perform a given mission by consideration of the primary factors which are expected to affect the weight. Expected trends are illustrated in figure 5 in terms of empty weight per ton-mile of mission. At speeds up to those of the current jet transports, the weights of airplanes capable of performing a 5,000-mile mission, presented herein as the ratios of empty weight to the product of range and payload, show little effect of design speed. This parameter would be expected to increase markedly through the transonic speed range because the higher drag associated with these speeds would require greater thrust, which would mean increased weight to provide for carrying larger amounts of fuel and increased engine weights. At the low supersonic speeds, up to a Mach number of about 3, only slight additional increases would be expected.

Of course, with increasing speed in this range, aluminum will become inadequate for many structural members because of its poor strength and fatigue properties at elevated temperatures. There remains some question as to whether the use of heavier, though higher strength, materials will result in significant increases in airframe weight for aircraft designed for these flight speeds. Beyond this speed the effect of elevated temperatures, due to aerodynamic heating, in reducing the strength of structural members and the requirements for special construction to insulate the structural members from the hot skin will in all probability cause increases in structural weights. The weight of the cabin cooling system would also be expected to increase significantly. As flight speed is increased further, critical areas such as leading edges will attain temperatures that are sufficiently high enough for the area to require cooling. The provision of a coolant and a circulatory system will add considerable weight to aircraft designed for these high flight speeds.

If the trends shown can be indicative of the empty weights of aircraft having the same payload and range capabilities and if certain necessary assumptions are made, an estimate can be developed of the relative annual costs of fleets of aircraft designed to cruise at various Mach numbers. This has been done for an assumed long-haul traffic volume of 3 billion ton-miles and is summarized in figure 6. The subsonic jet airplane has been used as a basis of comparison. The relative number of airplanes was obtained from the variation shown in figure 1. Relative initial cost was based on \$40.00 per pound of empty weight for all speeds and on the empty weight obtained with the Mach numbers shown in figure 5 by using a payload of 36,000 pounds. The same amortization period was assumed for all airplanes. The fuel costs were developed from the ratios of initial weight to final weight shown in figure 4 and from the empty-weight variations for airplanes having equal payload-range capabilities shown in figure 5. Airframe and engine-maintenance costs were scaled in proportion to airplane weight. Crew and indirect

costs per ton-mile were considered to be independent of cruise speed, and indirect costs were taken as being 51 percent of the total operating costs for the reference airplane. Costs were computed by the 1955 revised method of the Air Transport Association. From the results of this comparison, as illustrated in figure 6, it appears that the supersonic airplane designed for cruise at Mach numbers up to about 5 may be developed as a transport having a profit potential comparable with that of the subsonic jet. At a Mach number greater than about 5, however, the costs appear to rise rapidly.

Some of the assumptions made in this comparison are certainly questionable, and the validity of these assumptions cannot be verified without making much more detailed studies or possibly without actual construction and operating experience. However, considerable latitude is possible without greatly changing the resultant trends shown. The airplane cost per pound, for instance, may well be much greater for the supersonic airplane. If, for example, the assumed cost of \$40.00 per pound were doubled, the relative fleet costs per year for an airplane designed for a Mach number of 3 would increase by about 30 percent; and the fleet costs per year for an airplane designed for a Mach number of 5 would increase by about 25 percent. It is heartening to reflect upon the development of the subsonic jet transport when it is realized how the total costs have been trimmed over early estimates to the point where it is competitive with the piston-engine transport.

Utilization, of course, affects the relative annual fleet costs greatly. Recent estimates indicate that utilization of the subsonic jet transports may have to be as high as 10 to 11 hours per day if they are to show a profit. A change from 8 hours to 10 or 11 hours for the purpose of this comparison, if constant for all Mach numbers, would result in only minor changes, because the costs shown are relative. However, with the increased number of flights that the supersonic airplane could make per day, there would be more turn-around periods, and the shorter flight times would make scheduling for use of the early morning period more difficult. Thus, it may not be possible to hold the utilization of the supersonic airplane up to that of the subsonic jet. If, for example, the utilization were only half as great, the relative fleet costs per year would be roughly doubled.

Although the development of supersonic commercial transport airplanes designed for flight at Mach numbers up to approximately 3 may logically follow the development of military airplanes such as the B-58 and the B-70, it should not be inferred that answers to all the problems to be encountered are now known. A considerable amount of research remains to be done before solutions to the problems to be encountered by these as well as by higher speed aircraft are well in hand. All the various operational problems and safety considerations associated with the high-subsonic-speed transport, which have been discussed in some

detail in other papers presented, will be present, and in many cases aggravated, in the supersonic transport.

Many aerodynamic problems will be encountered in the design of commercial transport airplanes for flight at supersonic speeds. In general, these problems resolve into the basic requirement of providing adequate longitudinal, directional, and dynamic stability and adequate control capabilities. The main difference is that the aerodynamic phenomena which dictate the design of supersonic airplanes are different from those which govern the subsonic designs. For instance, different aerodynamic-load distributions, reduced lift-curve slopes, and different influences of aerodynamic interference between airplane components are encountered at supersonic speeds. The phenomena which govern the design at subsonic and supersonic speeds are not necessarily compatible, and many more compromises will have to be made for the supersonic airplane. Considerable ingenuity and developmental effort will be required on the part of the designer to produce an airplane with satisfactory aerodynamic characteristics at both subsonic and supersonic speeds.

At the higher supersonic speeds the problems encountered because of aerodynamic heating will become progressively the major obstacles. Such items as maintaining structural strength, avoiding skin buckling due to thermal expansion and aerodynamic load, cumulative distortion resulting from creep, protection of passengers and crew, fuel, auxiliaries and instrumentation, and, as previously discussed, the provision of a structural coolant system will all require much attention in design and much research is needed in these fields.

Because this is a relatively new area in airplane design, the temperatures which might be encountered by the supersonic transport will be considered briefly. Figure 7 presents leading-edge equilibrium surface temperatures as a function of Mach number that are calculated for a wing having a leading-edge diameter of 3 inches and loadings of 30 and 100 pounds per square foot with no cooling. Equilibrium temperatures for the lower surface are also shown which were calculated by using flat-plate considerations. These lower surface temperatures are representative of average skin temperatures and are not excessive for the materials which would be used for a given Mach number design. For the leading edge, however, it is obvious that cooling will be required above a Mach number between 5 and 6 if the temperature is to be held below a temperature between $1,700^{\circ}\text{F}$ and $2,000^{\circ}\text{F}$; however, even these are high temperatures. Leading-edge surfaces heated to a temperature between $1,700^{\circ}\text{F}$ and $2,000^{\circ}\text{F}$ would have the appearance of an element of an electric range.

CONCLUDING REMARKS

It can be concluded that there is a good possibility of achieving economical commercial flight at supersonic Mach numbers up to approximately 5. However, the design of transport airplanes for flight at these speeds must follow continued advancements in technology and experience gained from the development and operation of supersonic military aircraft. On the other hand, it has been shown that, for speeds greater than a Mach number of about 5, relatively small reductions in fleet size can be realized. It has also been shown that large increases in airplane and fuel weights are to be expected; hence, the long-haul missions considered, of which current transports are capable, can be achieved only by aircraft having very much larger gross weights and with accompanying large increases in cost. For commercial flight at speeds greater than a Mach number of approximately 5, then, the prospects do not look promising unless revolutionary developments in the fields of propulsion and structural materials occur.

REFERENCES

1. Allen, H. Julian: Hypersonic Flight and the Re-Entry Problem. Jour. Aero. Sci., vol. 25, no. 4, Apr. 1958, pp. 217-227; Discussion, pp. 228-229, 262.
2. Eggers, Alfred J., Jr., Allen, H. Julian, and Neice, Stanford E.: A Comparative Analysis of the Performance of Long-Range Hypervelocity Vehicles. NACA TN 4046, 1957. (Supersedes NACA RM A54L10.)

INCREASED SPEED MEANS FEWER AIRCRAFT

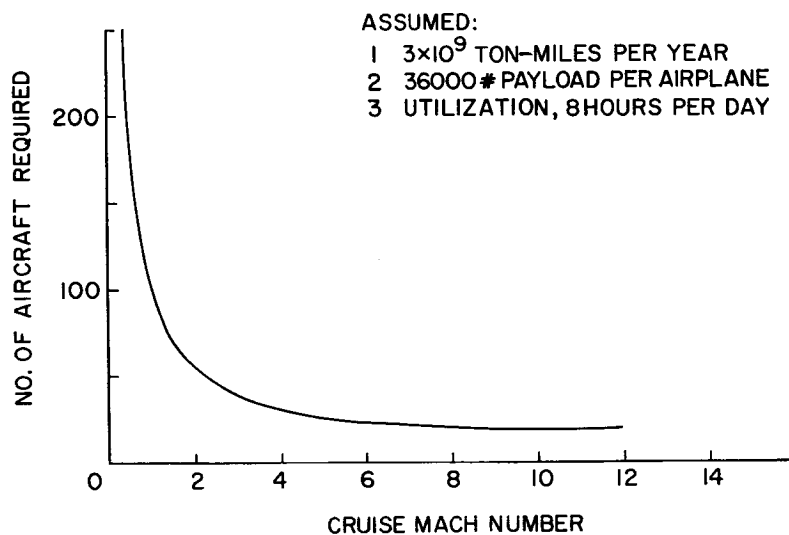


Figure 1

EFFECTIVE LIFT-DRAG RATIO

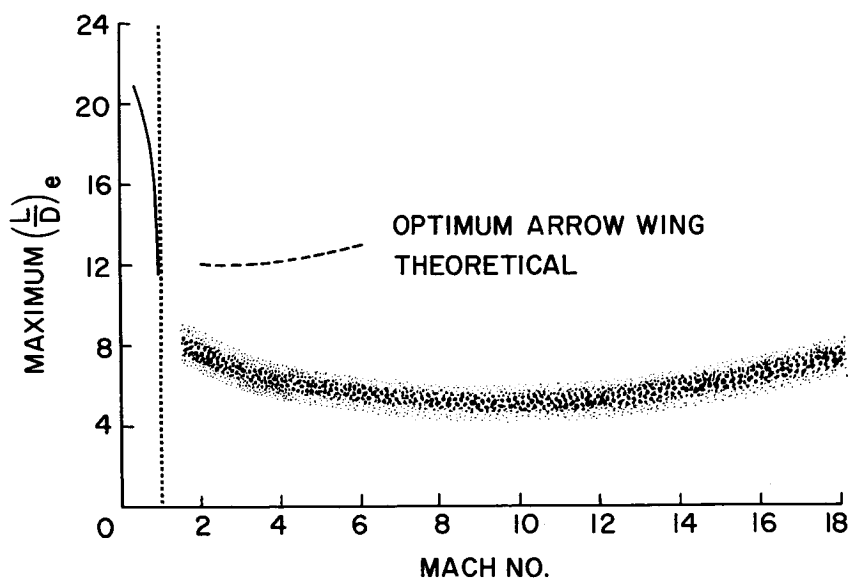


Figure 2

PRODUCT OF SPECIFIC IMPULSE AND VELOCITY

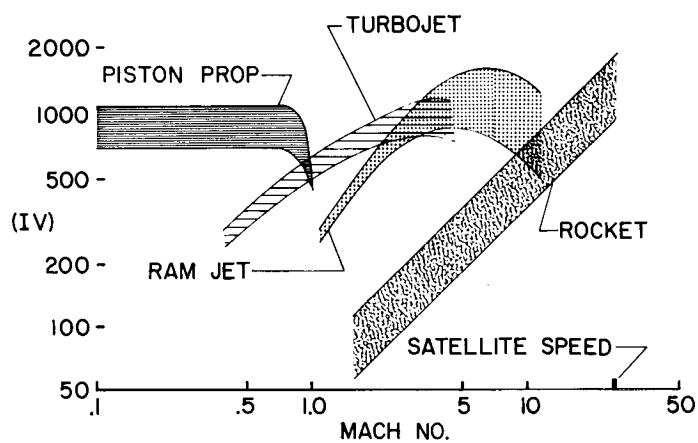


Figure 3

RATIO OF INITIAL TO FINAL WEIGHTS

ULTIMATE RANGE, 5000 MILES

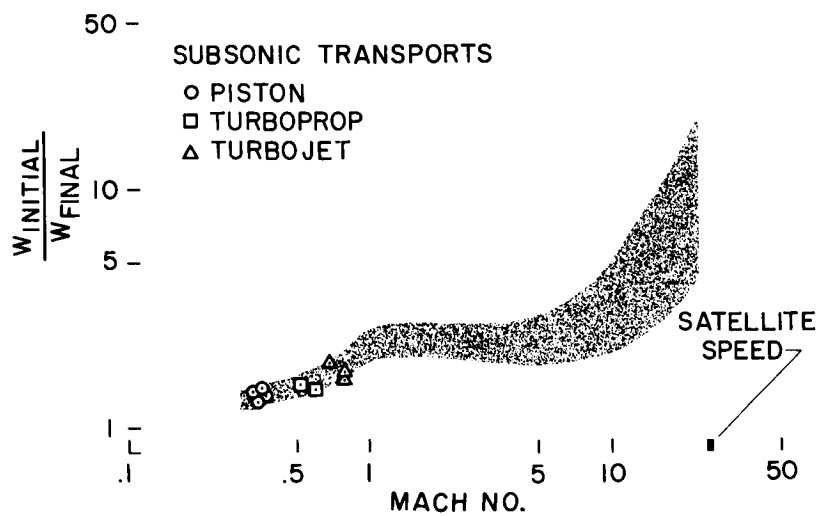


Figure 4

TREND OF EMPTY WEIGHT WITH MACH NUMBER

ULTIMATE RANGE, 5000 MILES

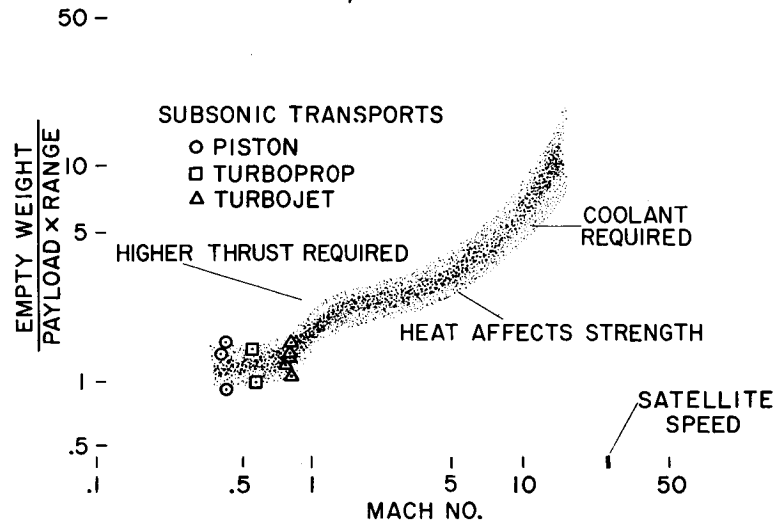


Figure 5

RELATIVE FLEET COST PER YEAR FOR GIVEN ANNUAL TRAFFIC

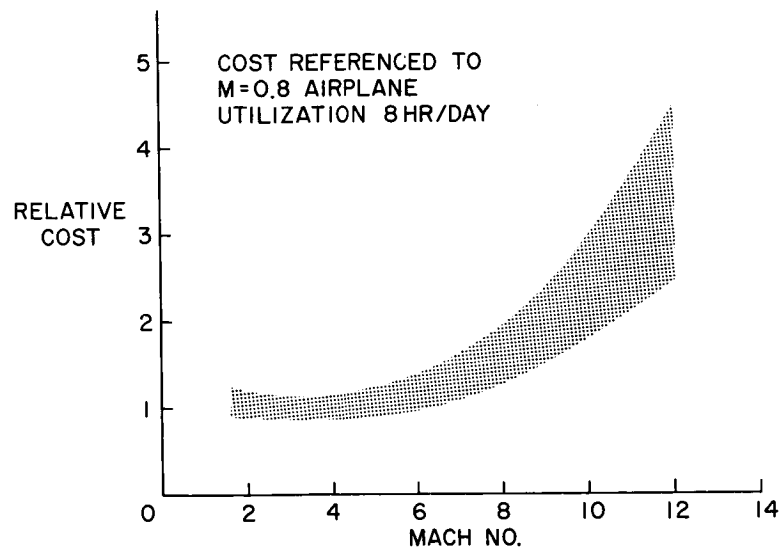


Figure 6

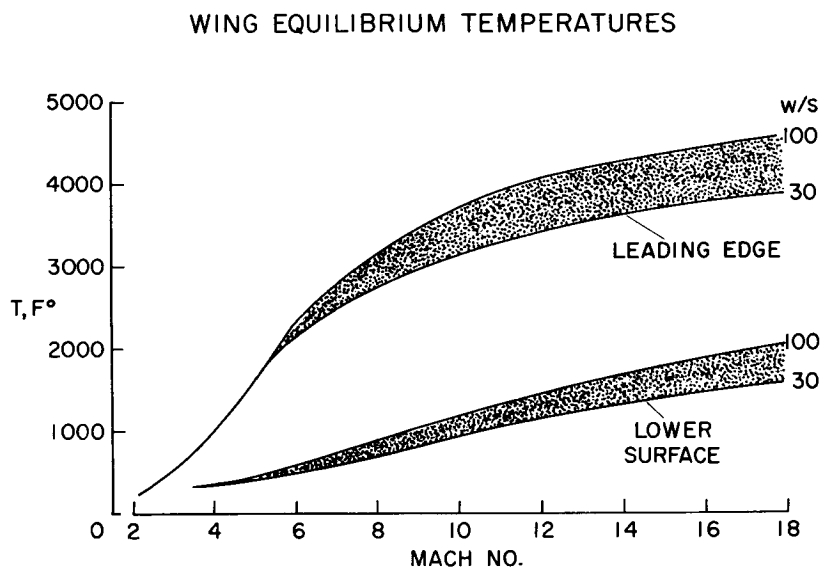


Figure 7